An Investigation of the Effects of Submarine Groundwater Discharge on the Coastal Carbon and Nutrient Cycles of a Karstic Aquifer, Kinvara Bay, Co Galway, Ireland

By Tara Kelly B.SC. (Chemistry)

A Thesis submitted to the University of Dublin for the degree of Doctor of Philosophy

Department of Geography,

School of Natural Sciences,

University of Dublin

Trinity College

Dublin

Declaration

I hereby declare that the work contained in this thesis is my own work, and has not been submitted as an exercise for a degree at this or any other university.

I also give the library permission to lend or copy this thesis, upon request, for academic purposes. This permission covers only single copies made for study purposes, subject to normal conditions of acknowledgment.

_____

Tara Kelly November 2018

Summary

Submarine Groundwater Discharge (SGD) is an important pathway of terrestrial nutrients to the coastal ocean. The influence of SGD on the carbon cycle in coastal zones and the relationship between SGD-borne carbon and other macronutrients remains uncertain. I used a combination of *in-situ* sampling techniques, experiments with defined conditions and modelling to identify, quantify and characterise SGD-derived carbon and nutrients and assess their biogeochemical importance within coastal zones, using Kinvara Bay, Western Ireland as a case study.

Firstly, I used the LOICZ water/salt budget models, and radon analysis where possible, to determine the seasonal SGD rates into the bay. Quantitative nutrient (nitrogen, phosphorus and silica) and carbon budgets were then closed in Kinvara Bay for four sampling campaigns (July 2013, January 2015, June 2015 and January 2016). Across all campaigns, of the three allochthonous carbon and nutrient sources (SGD, raw sewage and wet deposition), SGD was the largest source of carbon and oxidised nitrogen but the lowest source of ammonium and phosphorus into Kinvara bay. Dissolved organic nitrogen (DON) fluctuated significantly from season to season but was highest during the wettest campaign (January 2015). A portion of DON is bioavailable and the DON delivered via SGD contributed to productivity within Kinvara Bay. In terms of whole-system N metabolism, the bay was net autotrophic during July 2013, June 2015 and January 2016 but net heterotrophic during January 2015 (the wettest campaign).

SGD was the major allochthonous contributor of C to Kinvara Bay. Freshwater SGD delivered elevated concentrations of DIC and comparable concentrations of DOC in comparison to seawater. Whole core sediment incubation experiments confirmed sediment acted as a sink of DOC and as a source of DIC to the bay during June 2015. Closure of the nutrient and carbon budgets confirmed higher primary productivity during July 2013, June 2015 and January 2016 regarding N and C metabolism. Kinvara Bay was net autotrophic and sink for carbon during July 2013, June 2015 and January 2016 but net heterotrophic during January 2015, which was the wettest month and acted as a source of CO_2. Ocean acidification is one of the most serious consequences of rising CO_2 levels in the atmosphere. The pH of SGD was consistently lower (7.07 – 7.47) than that of oceanic waters (8.1). The role of SGD and its influences on acidification within coastal zones has remained an open question. SGD in karst regions transports large quantities of total alkalinity, which may buffer against acidification but also contains high levels of DIC, which may accelerate acidification. Quantification of the DIC and total alkalinity delivered via SGD to Kinvara Bay indicated that SGD buffered against ocean acidification in Kinvara Bay due to the higher TAlk loading in each sampling campaign. During June 2015, the biological to geochemical ratio was 2.03, calculated from the equation of the line from the plot of TAlk versus DIC. Therefore, SGD may buffer against ocean acidification due to higher TAlk levels in combination with increased metabolism associated

with high DIN influxes. Closure of the nutrient and carbon budgets confirmed a productivity-respiration annual cycle in Kinvara Bay, with primary productivity dominating in July 2013, June 2015 and January 2016. Kinvara Bay is currently mesotrophic, however, as future scenarios may lead to eutrophic conditions, continual monitoring of the system is vital as many people rely on it for their livelihoods.

SGD delivered a substantially higher N:P ratio than the Redfield Ratio of 16 whilst sewage inputs, although volumetrically small (286 m^3 d^{-1}) accounted for 74% of allochthonous P inputs. Mitigation plans for removal of raw sewage may, therefore, further alter the molar and nutrient availability ratios within the bay. As a result, I investigated a future 'what-if' scenario whereby the suspended particulate matter structure within Kinvara Bay changes. A land use change resulting in increased N:P imbalances may lead to a change in the suspended particulate matter within the bay as algae adapt. Species that survive better at altered N:P ratios would be expected to dominate. In this study, *Fucus vesiculosus* was the dominant macroalgae species at the SGD springs, followed by *Enteromorpha intestinalis*. Near the sewage outflow point, *Ascophyllum nodosum* was the dominant species, and both *Ascophyllum nodosum* and *Fucus vesiculosus* were found to be significant at the mouth of the bay. These species had high N:P ratios suggesting that they have adapted to survival in an SGD disturbed area. In future scenarios, particularly when *Enteromorpha* dominated, there was an increased flux of labile materials from the sediment to the water column. As algae function as high-quality food for consumers, productivity within Kinvara Bay would be expected to rise as a result. Increased population and tourism pressures were investigated through increased plastic pollution but did not produce increased refractory or labile components within the water column. This may be due to the types of compounds present in plastic, long organic polymers, which may not be susceptible to degradation or due to the incubation time of five days. Thus, plastic pollution may pose greater influence in the open ocean.

A combination of Excitation-Emission Matrix Fluorescence coupled with Parallel Factor Analysis (EEMF-PARAFAC) and Fourier-Transform Ion Chromatography Mass Spectrometry (FT-ICR-MS) was employed to characterise chromophoric dissolved organic matter (CDOM) delivered via SGD and its subsequent degradation processes within the coastal zone. SGD was responsible for the delivery of predominately humic-like substances, which were highly refractory. Peak T, a protein-like component, was validated as a secondary component in the 3-component model but with low intensity (0.005 R.U.) This bioavailable component corresponded to spring and was attributed to fertiliser use. In fact, approximately 1% of SGD-borne DOM transported to Kinvara Bay was typically labile, and SGD-borne DOM mainly contributed to C storage within the coastal ocean or was exported to the wider Galway Bay. This pathway may relocate C stocks on land to the sea over time.

Acknowledgements

I would like to thank my supervisor, Prof. Carlos Rocha, for his support and guidance during the course of this research. Also, I would like to express my gratitude to Dr. Hannelore Waska for her co-supervision. Financial support was gratefully received from the Irish Research Council (IRC) as an Embark Research Initiative funded Postgraduate Scholarship.

Special thanks goes to Mr. Mark Kavanagh (TCD) for all his hard work in the lab and always being there to give advice.

Many people helped me conduct research, often involving 24-hour sampling in not so nice weather conditions, so in particular I would like to acknowledge Dr. Shan Jiang, Dr. Laura Foley, Dr. Jean Wilson, Dr. Alexandra Oppelt, Manaswi Raghurama and Linh Trieu.

I would like to thank all members of the Biogeochemistry Research Group and some non-members for making the time spent in 'The Centre" so rewarding and enjoyable. I must mention in particular my once gym and now my hand in buddy, Louise.

I could not have completed this thesis without the constant support and encouragement from my parents. Not only did they always believe in me but they provided me with a sense of hard work, dedication and achievement. Without them, this Ph.D. would not have been possible.

So many friends have supported me, both near and far, not only over the years of this research but throughout my life and I can't thank them enough for their friendship. In particular, I must mention my lifelong friends, Tara and Cassie.

And a special mention to my Husband, Conor Harris.

Table of Contents

Declaration i

Summary iii

Acknowledgements v

Table of Figures xvii

Table of Tables xxi

1. General Introduction 1

1.1 Coastal zones 1

1.1.1 Functions of the coastal zone 1

1.1.2 Pressures facing the coastal zone 1

1.2 The coastal zone hydrologic cycle 1

1.3 SGD inputs into the coastal zone 2

1.3.1 Modes of SGD 2

1.3.2 Method of measurement 4

1.3.3 Global estimates of SGD 5

1.3.4 Comparison of riverine and SGD hydrological inputs 7

1.3.5 SGD in karst regions 7

1.4. The role of SGD in coastal biogeochemical budgets 8

1.4.1 The subterranean estuary 8

1.5 SGD-borne nutrients 9

1.5.1 SGD flow path 9

1.5.2 Sources of nutrients 10

1.5.3 Eutrophication 11

1.5.4 Molar ratios 11

1.6. Carbon cycle and the coastal reaction node 12

1.6.1 Dissolved organic matter (DOM) 13

1.6.1.1 SGD-borne DOM 14

1.6.1.2 Chromophoric DOM (CDOM) 15

1.6.1.3 CDOM classification 16

1.6.1.4 Properties of CDOM 17

1.6.2 DOC 19

1.6.3 The importance of SGD-borne dissolved inorganic carbon (DIC) 21

1.6.3.1 SGD-borne DIC 21

1.6.3.2 SGD-borne CO_2 22

1.6.3.3 Ocean acidification (OA) 24

1.7 Impacts and management issues **26**
1.8 Synopsis **27**
1.9 Study Site – Kinvara Bay, Co. Galway, Ireland **27**
1.9.1 Choice of study site 27
1.9.2 Irish karst aquifers 28
1.9.3 The Gort Lowlands 30
1.9.4 Hydrogeology and climatology 30
1.9.5 Kinvara Bay 33
1.9.6 Human ecological and economic importance 35
1.9.7 Previous studies 37
1.9.7.1 Hydrological studies 37
1.9.7.2 SGD studies 37
1.9.7.3 Carbon and nutrient studies 38
1.10 Research questions and hypotheses **40**
1.11 Chapter summaries **41**
Chapter 2 – Quantitative nutrient budgets 41
Chapter 3 – Evaluation of the importance of SGD-borne carbon in the coastal zone 42
Chapter 4 – Determination of SGD-borne CDOM in Kinvara Bay 42
Chapter 5 – Future scenarios of CDOM efflux 42
Chapter 6 – Characterisation of SGD-borne DOM using FT-ICR-MS Analysis 43
2. Determining Submarine Groundwater Discharge (SGD)-borne Nutrients and their Fate in Kinvara Bay, Co. Galway **45**
2.1 Introduction **47**
2.1.1 Submarine groundwater discharge-borne nutrients 47
2.1.2 LOICZ biogeochemical modelling approach 48
2.2 Research aims **48**
2.3 Sampling strategy **49**
2.4 Methodology **49**
2.4.1 Water collection 49
2.4.2 Sediment analysis 50
2.4.3 Dissolved inorganic nutrients 50
2.4.4 Phosphate 51
2.4.5 DON measurements 51
2.4.6 Mass balance calculations 52
2.4.7 Primary productivity (PP) 55
2.4.8 Propagation of uncertainty 56
2.5 Results **56**

2.5.1 SGD inflows....56
2.5.2 Nutrient analyses....58
2.5.2.1 SGD....58
2.5.2.2 Sewage....60
2.5.2.3 Wet deposition....61
2.5.2.4 Allochthonous loads....62
2.5.3 Sediment analyses....62
2.5.4 Nutrient budgets....62
2.6 Discussion....65
2.6.1 SGD volumes....65
2.6.2 Allochthonous nutrient transport....66
2.6.3 Autochthonous nutrient inputs....68
2.6.4 Nutrient budgets....69
2.6.4.1 Exchange at Parkmore Pier....69
2.6.4.2 DIN....70
2.6.4.3 DON....71
2.6.4.4 DRSi....72
2.6.4.5 TDP....72
2.7 Synopsis....73
3. Investigation of Submarine Groundwater Discharge-borne Carbon (DIC, DOC and TAlk) and their Circulation in Kinvara Bay, Co. Galway....75
3.1 Introduction....77
3.2 Sampling plan....78
3.3 Aims and hypotheses....78
3.4 Methods....78
3.4.1 DOC/DIC measurements....79
3.4.2. Sediment....79
3.4.3 Total alkalinity (TAlk)....79
3.4.4. pCO_2 calculations....80
3.5 Results....81
3.5.1 SGD-derived inputs....81
3.5.2 Sewage inputs....82
3.5.3 Wet deposition....83
3.5.4 Allochthonous loads....84
3.5.5 Sediment analyses....84
3.5.6 Fate of carbon species within the bay....84
3.5.7 pCO_2 calculations....89

3.6 Discussion **90**
3.6.1 Allochthonous carbon transport 90
3.6.2 Autochthonous carbon transport 92
3.6.3 pCO_2 93
3.7 Synopsis **96**

4. Characterisation of Submarine Groundwater Discharge (SGD)-borne Dissolved Organic Matter (DOM) in a Karstic Aquifer, Ireland **97**
4.1. Introduction **99**
4.2. Sampling site and strategy **100**
4.2.1 Sampling site 100
4.2.2 Sampling procedure 101
4.3. Methodological principles **101**
4.3.1 Principles of fluorescence 101
4.3.2 Methodology employed 103
4.4. Results and discussion **106**
4.4.1 Hydrochemical parameters 106
4.4.2 SGD-borne DOC 107
4.4.3 SGD-borne DOC seasonal variation 107
4.4.4 EEMF-PARAFAC 108
4.4.5 CDOM absorbance in Kinvara Bay 113
4.4.6 Modelled CDOM scores in Kinvara Bay 113
4.4.7 Relationship of CDOM optical properties and salinity 116
4.4.8 Spectral indices 117
4.4.9 Anthropogenic pressures and CDOM components in Kinvara Bay 120
4.4.10 Further statistical analysis 121
4.5 Synopsis **121**

5. The Potential Effects of Increased Anthropogenic Pressures on the Inferred Dissolved Organic Matter (DOM) Concentrations in Kinvara Bay **123**
5.1 Introduction **125**
5.1.1 Future scenario 1: land use alteration 126
5.1.2 Future scenario 2: biodegradable microplastic pollution 126
5.2 Specific hypotheses of this experiment **128**
5.3 Sampling procedure **128**
5.4 Methodology **129**
5.4.1 Sediment flux analysis 129
5.4.2 Water analysis 130

5.4.3 Flux estimation 130
5.4.4. Statistical analyses 130
5.5 Results 131
5.5.1 Current status of Kinvara Bay 131
5.5.2 DOC 131
5.5.3 CDOM 132
5.6 Discussion 137
5.6.1 Justification of future scenario predictions 137
5.6.2 Macroalgae cover 138
5.6.3 DOC 140
5.6.4 CDOM 141
5.7 Conclusion 143
6. Identification of Dissolved Organic Carbon (DOC) Complexes in an Incubation Study of Submarine Groundwater Discharge (SGD) using Solid-Phase Extraction (SPE) and Fourier-Transform Ion Cyclotron Resonance Mass Spectrometry (FT-ICR-MS) 145
6.1 Introduction 147
6.1.1 DOM lability 147
6.1.2 Photodegradation 148
6.1.3 Biodegradation 148
6.2 Research aims 149
6.3 Sampling protocol 150
6.3.1 *In-situ* samples 150
6.3.2 Incubation experiments 150
6.4 Methodology 152
6.4.1 DOC analysis 152
6.4.2 EEMF-PARAFAC analysis 152
6.4.3 FT-ICR-MS 152
6.4.3.1 Extraction of DOM 152
6.4.3.2 FT-ICR-MS protocol 153
6.4.3.3 Data analysis 153
6.5 Results and discussion 156
6.5.1 Hydrological parameters 156
6.5.1.1 SGD seasonal impacts 156
6.5.2 DOC 157
6.5.3 EEMF-PARAFAC 158

6.5.4 FT-ICR-MS analysis 160
6.5.4.1 Seasonal SGD-borne DOM loading 162
6.5.4.2 Molecular ratios 163
6.5.4.3 Organic nutrients 165
6.5.4.4 Incubation differences 166
6.6 Fate of terrestrial DOM 167
7. General Discussion 169
7.1 Karst-channelled SGD in Kinvara Bay 171
7.2 SGD-derived nutrient loading 172
7.3 Carbon inputs and circulation in Kinvara Bay 174
7.4 Further studies 178
7.4.1 CNP budgets 178
7.4.2 Component identification 178
7.4.3 Future CDOM scenarios 179
7.4.4 FT-ICR-MS 179
References 181
Appendix A – Important Hydrological Data - Raw Data measured *in-situ* 219
Appendix B – Measured Nutrient Concentrations for Budgetary Analysis (Chapter 2) - Raw Data 231
Appendix C: Examples of Calculations 243
Appendix D: Measured Carbon Species (DOC, DIC, TAlk) Concentrations for Budgetary Analysis (Chapter 3) - Raw Data 249
Appendix E: CDOM 3-Component Model for Kinvara Bay (Chapter 4) – DOC Concentration, CDOM Scores and Indicator Parameters, where recorded 261
Appendix F: EEMF-PARAFAC 3-Component Model for Kinvara Bay, n = 333 273
Appendix G: EEMF-PARAFAC 5-Component Model for Kinvara Bay Sediment Incubation Experiment, n = 338 277
Appendix H: Whole Core Sediment Incubation DOC fluxes 281
Appendix I: Sediment Incubation Setup 287
Appendix J: FT-ICR-MS Spectrum of SGD 291

List of Abbreviations

A	Absorbance
^{12}C	Carbon-12 isotope
^{13}C	Carbon-13 isotope
^{222}Rn	Radon 222 isotope
^{226}Ra	Radium 226 isotope
3D EEMF	Three dimensional excitation-emission matrix fluorescence
Ag	Silver
AI_{mod}	Aromaticity index (FT-ICR-MS)
Anammox	Anaerobic ammonium oxidation
ANOVA	Analysis of Variance
BC	Black carbon
BDL	Below Detection Limit
BOD	Biochemical Oxygen Demand
BRG	Biogeochemistry Research Group
C	Carbon
C Cycle	The Carbon Cycle
cm	Centimeters
CNP	Carbon, Nitrogen, Phosphorus
CO	Carbon monoxide
CO_2	Carbon dioxide
CSO	Central Statistics Office
DBE	Double bond equivalence
denit	Denitrification
DIC	Dissolved Inorganic Carbon
DIN	Dissolved Inorganic Nitrogen
DIP	Dissolved Inorganic Phosphorus
DO	Dissolved Oxygen
DOC	Dissolved Organic Carbon
DOM	Dissolved Organic Matter
DON	Dissolved Organic nitrogen
DRSi	Dissolved Reactive Silica
EC	Electrical Conductivity
EEMF	Excitation-Emission Matrix Fluorescence
EEMs	Excitation-Emission Matrices
Em	Emission wavelength
EPA	Environmental Protection Agency
ESI	Electrospray Ionisation
E.U.	European Union
Ex	Excitation wavelength
FDOM	Fluorescent Dissolved Organic Matter
FI	Fluorescence Index
FIA	Flow Injection Analysis
FT-ICR-MS	Fourier transform ion cyclotron mass spectrometry
FW	Freshwater
GFF	Glass Fibre filters
GHG	Greenhouse Gas
GSI	Geological Survey of Ireland
Gt	Gigatonnes
GWDTE	Groundwater Dependent Ecosystems

H	Hydrogen
HABs	Harmful Algal Blooms
HCl	Hydrochloric Acid
HDPE	High density polyethylene
HF	High Flow
HIX	Humification Index
HMWDOM	High Molecular Weight DOM
HS	Humic Substances
HSD	Honest Significance Difference
HTCO	High Temperature Catalytic Oxidation
K	Potassium
L	Litres
l	Path Length
LDOM	Labile dissolved organic matter
LF	Low Flow
LOD	Limit of Detection
LOD	Limits of detection
LOICZ	Land-Ocean Interactions in the Coastal Zone
LOQ	Limit of quantification
m	Meters
m/z	Mass-to-Charge ratio
MDL	Method Detection Limit
mg	milligrams
mL	Millilitres
mM	millimole
N	Nitrogen
NDIR	Near-Dispersive Infrared
NEM	Net Ecosystem Metabolism
NEP	Net Ecosystem Production
nfix	Nitrogen fixation
NH4+	Ammonium
NO2-	Nitrite
NO3-	Nitrate
NOM	Natural Organic Matter
NPP	Net primary Production
O	Oxygen
OA	Ocean Acidification
P	Phosphorus
PARAFAC	Parallel Factor Analysis
pCO_2	Carbon dioxide partial pressure
PLA	Poly(lactic acid)
POPs	Persistent Organic Pollutants
PP	Parkmore Pier
PPHF	Parkmore Pier High Flow
PPLF	Parkmore Pier Low Flow
ppmV	ppm by volume
ppt	parts per thousand
psu	Practical Salinity Units
QC	Quality Control
R.U.	Raman Units
RDOM	Recalcitrant Dissolved Organic Matter

S	Sulphur
S (DOM)	Spectral Slope
S/N	Signal-to-noise ratio
SAC	Special Area of Conservation
SE	Standard Error
SGD	Submarine Groundwater Discharge
SGR	Submarine Groundwater Recharge
Si(OH4)	Silicate
SLDOM	Semi-labile dissolved organic matter
SOM	Sedimentary Organic Matter
SOP	Standard Operating Procedure
SPA	Special Protection Area
SPE	Solid phase extraction
SPM	Sedimentary Particulate Matter
Sr	Slope ratio
SRP	Soluble Reactive Phosphorus
SS	Spectral Slope
STE	Subterranean Estuary
SUVA	Specific absorbance at 254 nm
T.D.	Teachta Dala - A member of government
TAlk	Total Alkalinity
TDC	Total Dissolved Carbon
TDIC	Total Dissolved Inorganic Carbon
TDP	Total dissolved phosphate
TDS	Total Dissolved Solids
TNb	Total bound nitrogen
TOC	Total Organic Carbon
UNFCCC	United Nations Framework Convention on Climate Change
URDOC	Ultra-refractory dissolved organic carbon
UV	Ultra-violet
UVR	Ultraviolet Radiation
W	Watts
WFD	Water Framework Directive
WWTP	Wastewater Treatment Plant
Xe	Xenon
α	Absorption coefficient
$\delta^{13}C$	Carbon-13 isotope
ε	Molar Absorptivity
µm	Micrometer/micron (cm^{-6})

Table of Figures

Figure 1.1: Schematic depiction of submarine groundwater discharge and recharge processes at the land-sea boundary. Terrestrial and oceanic forces influence the movement of SGD. Arrows represent fluid movement (Moore, 2010) 3

Figure 1.2. Schematic of submarine groundwater discharge flow, illustrating fresh intertidal SGD transported from land and brackish SGD from recirculated seawater, taken from Cook (2005). 4

Figure 1.3: Schematic box model of processes affecting the aquatic DIC pool, including inputs from land and atmosphere and outputs to the atmosphere (after Atekwana and Krishnamurthy, 1998) 21

Figure 1.4: Relationship of DIC species with pH. Modern seawater has a pH of approximately 8.1, as highlighted in the figure. At this pH, HCO_3^- is dominant (after Holmén, 2000). 24

Figure 1.5: 35 potential SGD sites around the coast of Ireland identified using thermal infrared imagery (Wilson and Rocha, 2012). Kinvara Bay is located above site 13 on this map. 27

Figure 1.6: Distribution of Carboniferous limestones in Ireland (Drew, 2008). Kinvara Bay is situated in the major city of Galway, highlighted on map. 28

Figure 1.7: Total rainfall (mm) and potential evapotranspiration (mm) for the year 2015, measured at the closest Met Eireann weather station, Athenry, 26.2 Km north of Kinvara town (http://www.met.ie/climate/monthly-data.asp?Num=1875). 31

Figure 1.8: Tracer tests in the Gort Lowlands catchment showing the groundwater flows underground and its exit at Kinvara Bay carried out as part of the Gort Flood Studies Report (Drew, 2003) 32

Figure 1.9: Map of Kinvara Bay highlighting the main sampling sites. These sampling locations were selected as a continuum of groundwater from land discharging into Kinvara Bay and exiting into the open ocean at Parkmore Pier. Kinvara Bay is a semi-enclosed system, and these sampling locations represent the boundaries of the system in terms of box model studies. These sites are represented by stars on the map, Loughcurragh South (inland borehole) represented by the yellow star, Dunguaire Castle (the major spring for SGD) represented by red star, the sewage outfall point represented by the green star, the sediment collection points in the intertidal zone represented by the blue star and Parkmore Pier (exit point for waters discharging to Galway Bay) represented by the orange star. 34

Figure 1.10: A photograph of Kinvara Bay taken from the entrance to Dunguaire Castle highlighting the main SGD and intertidal sampling sites. These sampling locations were selected as the main SGD springs and an undisturbed location to take sediment samples. These sites are represented by circles on the map, Dunguaire Castle (the major spring for SGD) represented by a green circle, the Arch SGD springs represented by a red circle and the sediment collection points in the intertidal zone represented by the purple circle. 34

Figure 2.1: Bar chart of total precipitation (mm) recorded at the Met Eireann station in Athenry, 26.1 km North of Kinvara Bay over the course of 2013 – 2016, including the times in which sampling took place (June 2013, January 2015, June 2015 and January 2016). 49
Figure 2.2: Water budget box model for Kinvara Bay representing freshwater inputs from SGD, tributaries, runoff and sewage, outputs as residual flow (exchange at Parkmore Pier) and evaporation losses and precipitation addition within the bay. 53
Figure 2.3: Salinity budget box model for Kinvara Bay representing salinity inputs from SGD, tributaries, runoff and sewage, outputs as residual flow while evaporation and precipitation are expected to be zero within the bay. The difference between system salinity and ocean salinity determines the residual salt flux. 53
Figure 2.4: Non-conservative materials (Y) box model. Inputs of materials to Kinvara Bay due to runoff, SGD, sewage and tributaries. Within the bay, evaporation may remove materials while precipitation adds materials. The residual flux of materials is determined as the mean exchange at Parkmore Pier over two sequential tidal cycles. 54
Figure 2.5: Bar chart of percentage of allochthonous loading associated with each input: SGD, Sewage and Wet Deposition into Kinvara Bay annually. TDP and DON concentrations were not measured in wet deposition values, and therefore these values are only represented by SGD and sewage. 62
Figure 3.1: A plot of DOC versus salinity for samples taken at the SGD point, sewage point and within the bay over all sampling campaigns, n = 253, SGD (n = 42), sewage (n = 42), Parkmore Pier (n = 169) 85
Figure 3.2: A plot of DIC versus salinity for samples taken from the SGD point, sewage outflow point and within the bay over all sampling campaigns, n = 206, castle (n = 34), sewage (n = 32), Parkmore Pier (n = 140) 85
Figure 3.3: A plot of TAlk versus salinity for samples taken at the SGD point, sewage point and within the bay over all sampling campaigns, n = 167, SGD (n = 24), sewage (n = 23), Parkmore Pier (n = 119) 85
Figure 3.4: DOC concentration (μmol L^{-1}) versus salinity (ppt) measured at Parkmore Pier over two sequential tidal cycles every 30 minutes during January 2015 (n = 45) and January 2016 (n = 47). 86
Figure 3.5: DOC concentration (μmol L^{-1}) versus salinity (ppt) measured at Parkmore Pier over two sequential tidal cycles during July 2013 (n = 73, samples every 20 minutes) and June 2015 (n = 49, samples every 30 minutes). 87
Figure 3.6: DIC concentration (μmol L^{-1}) versus salinity (ppt) measured at Parkmore Pier over two sequential tidal cycles every 30 minutes during January 2015 (n = 45) and January 2016 (n = 47). 87

Figure 3.7: DIC concentration (μmol L^{-1}) versus salinity (ppt) measured at Parkmore Pier over two sequential tidal cycles during July 2013 (n = 73, samples every 20 minutes) and June 2015 (n = 49, samples every 30 minutes).....87
Figure 3.8: Mixing plots of pH versus salinity at Parkmore Pier during all sampling campaigns Samples were taken every 20 minutes in July 2013 (n = 72) and every 30 minutes during January 2015 (n = 51), June 2015 (n = 46) and January 2016 (n = 48).....88
Figure 3.9: A graph of TAlk versus DIC for time-series sampling at Parkmore Pier over the course of two sequential cycles during January 2015 (n = 47), June 2015 (n = 48) and January 2016 (n = 23) sampling campaigns. TAlk data was not available for the July 2013 sampling campaign 90
Figure 4.1: A simplistic Jablonski Diagram.....102
Figure 4.2: EEM Components from the validated annual three-component EEMF. Component 1, 2 and 3, n = 305, measured over ten sampling campaigns. Samples were collected based on a continuum of water flow which includes inland, the SGD springs, sewage outflow location within the bay, Parkmore Pier and Galway Bay. 108
Figure 4.3: Pie chart of the percentage of each component (C1, C2 and C3) in the overall validated annual three-component EEMF model, measured over ten sampling campaigns, n = 305. Samples were collected based on a continuum of water flow which includes inland, the SGD springs, sewage outflow location within the bay, Parkmore Pier and Galway Bay. 110
Figure 4.4: An annual mixing curve of CDOM absorbance values (aCDOM) vs. salinity (ppt) measured at all locations, inland, SGD springs, sewage outflow location within the bay, Parkmore Pier and Galway Bay over the course of the sampling campaigns, n = 216 113
Figure 4.5: An annual mixing curve of CDOM Scores (R.U.) vs. salinity (ppt) measured at all input locations and through Kinvara Bay over the course of the nine sampling campaigns, n = 335. Samples were collected based on a continuum of water flow which includes inland, the SGD springs, sewage outflow location within the bay, Parkmore Pier and Galway Bay. 117
Figure 4.6: Measured Fluorescence Index (F.I.) variability with salinity fluctuations measured in the SGD, sewage and marine endmembers and throughout the bay, over the course of the sampling campaigns (n = 333). An F.I. of 1.4 represents terrestrially-borne CDOM and of 1.9 represents microbially-derived CDOM.....119
Figure 4.7: Mixing curve of Humification Index (HIX) and Salinity (ppt) . Samples were collected based on a continuum of water flow which includes inland samples, the SGD springs, sewage outflow location within the bay, Parkmore Pier and Galway Bay, n = 201.....120
Figure 5.1: Pie chart of the percentage of each component (C1-C5) in the validated annual 5-component EEMF model, measured over all treatment groups, n = 338.....133
Figure 5.2: Bar chart of the EEMF-PARAFAC model output component 1-5 scores for each treatment group. C = control, CMP = Microplastics only, MA = *Fucus* treatment, MAMB =

Fucus plus microplastics, MB = *Enteromorpha* treatment, MBMP = *Enteromorpha* plus microplastics 134
Figure 6.1: Incubation study sampling strategy for SGD collected from the Kinvara Springs in September 2014 151
Figure 6.2: Bar chart of DOC concentrations taken at T0 (n =4) and the end (n = 4) of the incubation experiment for all treatment groups including error bars (Standard Error). Units are μmol L^{-1} 158
Figure 6.3: Component 1 and 2 EEM surface plots of the incubated SGD samples. 159
Figure 6.4: A pie chart outlining the relative abundance of compound classes (CHO, CHON, CHOS, CHOP, CHONS) in SGD endmember, measured at Kinvara Springs in September 2014. 161
Figure 6.5: Van Krevelen plot of DOM, presenting molecules identified in the SGD endmember (n = 2), taken from Kinvara Springs September 2014. 164
Figure 6.6: Van Krevelen plot of DOM, presenting molecules identified in seawater samples only (n = 4), in September 2014. 164

Table of Tables

Table 1.1: SGD rates examples from across the word, detailed in the relevant literature referenced in the table. Modes of measurement and units of SGD differ between studies. 6

Table 1.2: Mean DOC concentrations found in the main rivers in Europe and DOC concentrations found in groundwater samples globally, as referenced in the cited literature..... 20

Table 1.3: Summary of measured water nutrient concentrations in SGD endmember (mean salinity = 0.61 ppt), measured at the Kinvara Springs located within the bay over the course of four sampling campaigns during summer. Data are the result of the mean of several replicates plus or minus the standard error of the mean (± SE) (Rocha et al., 2015). 39

Table 2.1 Summary of measured water parameters in the SGD endmember, measured at Castle Springs over the four sampling campaigns and meterological conditions obtained from Met Eireann. Data is the result of an average of several replicates ($11 < n < 15$) plus or minus the standard error of the mean (± SE). See Appendix A for raw data measured *in-situ*. Meteorological information during the survey periods was obtained from the averages of Met Éireann weather stations Athenry, 26.2 Km north of Kinvara town, and Oranmore, 14.4 Km north of Kinvara town (http://www.met.ie/climate/daily-data.asp). 57

Table 2.2: SGD/FW ratios for all sampling campaigns. The proportion of SGD to other freshwater sources is represented by SGD/FW ratios. Aside from SGD, freshwater (FW) sources to Kinvara Bay enter by sewage, small tributaries and runoff. --- represents data not measured. *This value was determined using FW/SGD ratios determined using Rn^{222} for a period with similar rainfall in the 14-day period before sampling published in Rocha et al., (2015). 58

Table 2.3: Summary of nutrient concentrations in SGD endmember, measured at Castle Springs. Data is the result of an average of several replicates ($11 < n < 15$) plus or minus the standard error of the mean (± SE), units are μmol L^{-1}. BDL = Below Detection Limit. July 2013 results have been published in Rocha et al., (2015). DON concentration was calculated by subtracting DIN from TNb. Refer to Appendix B for raw data measured *in-situ*. 59

Table 2.4: Summary of SGD nutrient loads measured at the Castle Springs over the four sampling campaigns calculated by multiplication of the nutrient concentration in SGD by the SGD volume. Data is the result of an average of several replicates ($11 < n < 15$) plus or minus the standard error of the mean (± SE). Units are mol per day. Negligible values are the result of concentrations that are close to or below the detection limit. July 2013 results have been published in Rocha et al., (2015). 59

Table 2.5: Estimates of SGD-borne nutrients in mass terms for winter (January 2015 and 2016) and summer (July 2013 and June 2015), measured at Kinvara Springs. Units are kg d^{-1}, to the closest kg. 60

Table 2.6: SGD molar ratios of DIN:P, TN:P and DRSi:DIN using measured parameters (DIN, TDP and DRSi) from SGD at Kinvara Springs for the four sampling campaigns, January 2015 and 2016, July 2013 and June 2015..... 60

Table 2.7: Sewage composition determined for sewage discharge to Kinvara Bay using values published in the literature (Henze, 2008). Units are μmol L^{-1} for absolute concentrations and mol d^{-1} for sewage fluxes. Fluxes were calculated using an average flow rate of 286 m^3 d^{-1} as determined in EPA (2010). * Measured as NO_3^- + NO_2^-..... 61

Table 2.8: Wet deposition values calculated for DIN in Kinvara Bay for each sampling timepoint. Fluxes were calculated for the surface area of the Bay using the concentration of DIN determined by Aherne and Farrell, (2002) for the closest stations, Cloosh and The Burren, and the seasonal rainfall that occurred during the 14-day period prior to sampling divided by 14 to determine the flux per day. Units of wet deposition are mol d^{-1}. See example in Appendix C. 61

Table 2.9: Mean nutrient exchange at Parkmore Pier, the mouth of the bay over all sampling campaigns, negative values represent nutrient concentration flux out of the system, whereas, positive values equal nutrient fluxes into the system. Units are mol d^{-1}. Time series every 30 minutes except July 2013 (20 minutes) analysis determined the nutrient concentration at Parkmore Pier over two full tidal cycles. The difference between the flood and ebb fluxes represents the nutrient exchange at Parkmore Pier. See Appendix B for nutrient concentrations measured *in-situ* and Appendix C for an example of the calculation of tidal exchange. 62

Table 2.10: July 2013 net retention within Kinvara Bay was measured and used to calculate the projected concentration of the measured nutrients in the water column in the absence of assimilation by primary producers. The primary producer's transfer of nutrients was then estimated as the difference between the projected concentration and the actual measured concentration of the relevant nutrient within the bay as per calculations shown in Rocha et al., (2015)..... 63

Table 2.11: January 2015 net retention within Kinvara Bay was measured and used to calculate the projected concentration of the measured nutrients in the water column in the absence of assimilation by primary producers. The primary producer's transfer of nutrients was then estimated as the difference between the projected concentration and the actual measured concentration of the relevant nutrient within the bay as per calculations shown in Rocha et al., (2015)..... 64

Table 2.12: June 2015 net retention within Kinvara Bay was measured and used to calculate the projected concentration of the measured nutrients in the water column in the absence of assimilation by primary producers. The primary producer's transfer of nutrients was then estimated as the difference between the projected concentration and the actual measured concentration of the relevant nutrient within the bay as per calculations shown in Rocha et al., (2015)..... 64

Table 2.13: January 2016 net retention within Kinvara Bay was measured and used to calculate the projected concentration of the measured nutrients in the water column in the absence of assimilation by primary producers. The primary producer's transfer of nutrients was then estimated as the difference between the projected concentration and the actual measured concentration of the relevant nutrient within the bay as per calculations shown in Rocha et al., (2015). 64

Table 3.1: Summary of measured water parameters and carbon concentrations in the SGD endmember, measured at Castle Springs over the four sampling campaigns. Data are the result of the mean of several replicates (11 < n < 15) plus or minus the standard error of the mean (± SE). Meteorological information during the survey periods was obtained from the averages of Met Éireann weather stations Athenry, 26.2 Km north of Kinvara town, and Oranmore, 14.4 Km north of Kinvara town (http://www.met.ie/climate/daily-data.asp). N/A represents samples not analysed for this parameter. See Appendix D for *in-situ* measurements. 81

Table 3.2: Summary of SGD DOC, DIC and TAlk loads measured at the Castle Springs over the four sampling campaigns calculated by multiplication of the carbon specie concentration in SGD by the fresh SGD volume. Data are the result of the mean of several replicates (11 < n < 15) plus or minus the standard error of the mean (± SE). N/A represents samples not analysed for this parameter. 82

Table 3.3: Estimates of SGD-borne carbon (DIC and DOC) and alkalinity in mass terms annually and for winter (January 2015 and 2016) and summer (July 2013 and June 2015), measured at Kinvara Springs. . --- data not measured 82

Table 3.4: SGD molar ratios of TDC:TDP, DOC:TDN, DIC:TDN and TDC:TDN using measured parameters (DIN, DOC and DIC) from SGD at Kinvara Springs for winter (January 2015 and 2016) and summer (July 2013 and June 2015). --- sample not measured. *TDC:TDP ratio calculated using DOC only as DIC was not measured at the SGD springs during July 2013. . 82

Table 3.5: Summary of relevant water parameters and solute (DOC, DIC and TAlk) concentrations associated with sewage inputs. Data are the result of the mean of several replicates (11 < n < 15) plus or minus the standard error of the mean (± SE), adjusted for dilution with seawater back to the salinity of an inland borehole of 0.3 ppt. --- represents samples not analysed for this parameter. See Appendix D for *in-situ* values 83

Table 3.6: Wet deposition values calculated for DOC and DIC in Kinvara Bay for each sampling time point. Fluxes were calculated for the surface area of the Bay using the concentration of DOC in precipitation determined by Iavorivska et al., (2016) for European coastal/island locations and the DIC calculated by Worrall et al., (2003) for a British upland peat catchment, the North Pennines. This was scaled using the seasonal rainfall that occurred during the 14-day period prior to sampling divided by 14 to determine the flux per day. See example in Appendix C. 83

Table 3.7: Percentage of allochthonous loading associated with each input: SGD, Sewage and Wet Deposition into Kinvara Bay over the course of the four campaigns. --- represents parameters not analysed in this study..... 84
Table 3.8: Measured sediment DIC and DOC exchange fluxes by incubation core experiments measured in June 2015, close to Kinvara Springs. 84
Table 3.9: Mean DOC and DIC exchange at Parkmore Pier, the mouth of the bay over all sampling campaigns, negative values represent carbon flux out of the system, whereas, positive values equal carbon fluxes into the system. Time series analysis every 30 minutes except July 2013 (20 minutes) determined the DOC and DIC concentration at Parkmore Pier over two full tidal cycles. The difference between the flood and ebb fluxes represented the nutrient exchange at Parkmore Pier. See Appendix D for DOC and DIC concentrations measured *in-situ* and Appendix C for an example of the calculation of tidal exchange. 84
Table 3.10: pCO_2values calculated using CO2SYS software for allochthonous sources using inputs of TAlk, pH and DIC; submarine groundwater discharge, sewage water and Parkmore Pier, collected across all sampling campaigns. --- Represents data not analysed..... 89
Table 3.11: CO_2 concentrations (µmol L^{-1}) ranges calculated using the CO2SYS software for submarine groundwater discharge collected across each sampling campaign. 89
Table 3.12: pCO_2 fluxes calculated using equation (1) and CO_2 fluxes determined by CO2SYS software for allochthonous sources; submarine groundwater discharge, sewage point and Parkmore Pier, collected across all sampling campaigns. --- Represents data not analysed.... 90
Table 4.1: Ranges of *in-situ* monitoring parameters at input locations (SGD and Sewage) and the mouth of Kinvara Bay (Parkmore Pier), over all sampling campaigns, includes seasonal variability during high and low flow conditions 106
Table 4.2: Summary of measured DOC concentration in SGD endmember, measured at Castle Springs over the nine sampling campaigns. Data are the result of the mean of several replicates ($11 < n < 15$) plus or minus the standard error of the mean (± SE). 107
Table 4.3: ANOVA results after testing the null hypothesis that H0: Mean DOC concentration , measured at Castle Springs, over eight sampling campaigns is the same for all seasons. 107
Table 4.4: Summary *p* values based on Tukey's Honest Significance Difference (HSD), following ANOVA analysis, for DOC concentrations in the SGD endmember, measured at Castle Springs over the eight sampling campaigns. Highlighted results are significant as $p<0.05$ at significance level, $\alpha = 0.05$..... 108
Table 4.5: Fluorescence characteristics of validated annual three-component EEMF model: excitation and emission maxima, compared with previously identified components. Bold Q components indicative of Quinone-like moieties (Cory and McKnight, 2005), n = 305 over ten sampling campaigns. Samples were collected based on a continuum of water flow which includes inland, the SGD springs, sewage outflow location within the bay, Parkmore Pier and Galway Bay. 112

Table 4.6: Summary of measured indicator parameters in SGD and sewage endmembers, measured at the sewage outfall pipe located within the bay and Kinvara Springs compared to the mouth of the bay, Parkmore pier over the course of the ten sampling campaigns. Data is provided as a range of the lowest to highest measured data as the result of several replicates ($20 < n < 100$). 118
Table 5.1: Experimental Design of core incubation experiment conducted in June 2015 from cores collected in the intertidal zone at Kinvara Springs. 130
Table 5.2: Summary of measured DOC concentration flux (μmol cm^{-1} hr^{-1}) from the incubation sediment cores from each treatment type. See Appendix H for raw data. 132
Table 5.3: ANOVA results after testing the null hypothesis that H0: Mean DOC concentration measured at Castle Springs over eight sampling campaigns is the same for all seasons. 132
Table 5.4: *p* values based on Tukey's Honest Significance Difference (HSD), following ANOVA analysis, evaluating differences between each treatment type values in bold indicate a significant difference between two values ($p < 0.05$) at significance level, $\alpha = 0.05$. 132
Table 5.5: Fluorescence characteristics of validated 5-component EEMF model: excitation and emission maxima, compared with previously identified components. n = 338 for all treatment groups. See Appendix G for model output. 133
Table 5.6: Summary of measured CDOM score in each treatment group, measured from each core flux over the course of the incubation study. 134
Table 5.7: ANOVA results after testing the null hypothesis that H0: Treatment groups for each component of the validated 5-component model is identical. 135
Table 5.8: *p* values based on Tukey's Honest Significance Difference (HSD), following ANOVA analysis, of treatment groups for each component of the validated 5-component model. Values in bold indicate a significant difference between two values ($p < 0.05$) 136
Table 6.1: Summary of measured water parameters and DOC concentrations in each sample group, measured *in-situ* throughout Kinvara Bay in September 2014 and at the Castle Springs in January 2015 156
Table 6.2: Summary of measured water parameters in the SGD endmember, measured at Castle Springs during autumn (September 2014) and winter (January 2015), taken as T0 of the incubation study. 156
Table 6.3: Incubation DOC concentrations taken at T0 and the end of the SGD incubation experiment for all treatment groups in September 2014. Units are μmol L^{-1} 157
Table 6.4: Fluorescence characteristics of validated annual two-component EEMF model: excitation and emission maxima, compared with previously identified components. Bold Q components indicative of Quinone-like moieties (Cory and McKnight, 2005), n = 113 over the incubation period. 159

1. General Introduction

1.1 Coastal zones

1.1.1 Functions of the coastal zone

The coastal ocean is the intersection between land, ocean and atmosphere and is defined as the area between the tidal limits as well as the continental shelf and coastal plain (Viles and Spencer, 2014). Coastal zones are areas of particular interest in carbon and nutrient studies globally as they act as connecting zones between land and the open ocean (Sabine et al., 2004). In this capacity, they serve as filters, as natural and anthropogenic inorganic and organic material transported from the continents is trapped here before it can reach the ocean (Ortega et al., 2008).

The world coastline extends over 350,000 km and exhibits a broad range of geomorphological types and ecosystems (Bianchi 2006) including bays, lagoons, estuaries, beaches, and wetlands. The biogeochemical and physical characteristics of these regions vary significantly as they are strongly affected by their surrounding bodies, continents, oceans and the atmosphere (Ortega et al., 2008). This zone is shallow, <200 m, and covers an approximate area of 26 x 10^6 km^2, accounting for approximately 7% of the surface of the global ocean (Gattuso et al., 1998). Although relatively small, it is a critical area of the Earth's surface due to the supply of terrestrial organic matter and nutrients and accounts for as much as 10 – 15% of global primary production and greater than 40% of carbon sequestration in the ocean (Muller-Karger et al., 2005). Therefore the coastal zone plays an important part in determining heterotrophy or autotrophy in the ocean as a whole (Smith and Hollibaugh, 1997).

1.1.2 Pressures facing the coastal zone

It is a challenge to manage this spatially and temporally dynamic area and to measure and model its function due to its heterogeneous nature (Bianchi, 2006), which may vary daily, seasonally, annually, and over decadal or even on glacial-interglacial scales (Buddemeier et al., 2002). As 50% of the world's human population live near the coast, and growing by 1.5% each year, there is a great strain on the natural functioning of coastal regions due to anthropogenic pressures (Golberg 1994; Buddemeier et al., 2002). Many people rely on the coastal zone for their livelihoods. 25% of global biological production and 90% of fisheries are within this area (Buddemeier et al., 2002). Coastal oceans and their respective ecosystems are subject to further anthropogenic pressures through riverine inputs, runoff, sewage inputs and submarine groundwater discharge (SGD). These influxes can carry significant levels of terrestrial materials including nutrients and carbon.

1.2 The coastal zone hydrologic cycle

The hydrologic cycle describes the continuous movement of water above and below the surface of the Earth. When precipitation occurs over land, it can follow three routes. Firstly, it can evaporate returning to the atmosphere; secondly, it can become surface water and travel to the ocean via rivers and streams; and thirdly, it can seep into the ground and travel to the ocean via submarine

groundwater discharge. Therefore, freshwater can flow above or below land for great distances before discharging to the coastal ocean (Zektser and Loaiciga, 1993; Vörösmarty et al., 2000).

Freshwater inputs have long been recognised as an important pathway for nutrients to the coastal zone. Nutrient contamination of freshwater has been shown to cause a reduction in aquatic biodiversity, food web alteration, eutrophication, and increased respiration rates in response to rapid organic matter production (Moyle and Leidy, 1992; Capriulo et al., 2002). Much is known about the precise quantitative nutrient loadings from surface flow and atmospheric deposition globally due to ease of sampling. However, less is known about subterranean sources due to difficulty in detection and quantification of such sources as they emerge in the coastal ocean (Moore et al., 2006; Burnett et al., 2008; Moore, 2010; Porubsky et al., 2014). Among the components of the hydrologic cycle, groundwater is perhaps the most difficult to quantify (Zektser and Loaiciga, 1993).

1.3 SGD inputs into the coastal zone

SGD has long been recognised with accounts dating back to the Roman period. However, it remained a hydrologic ‘curiosity' and was widely understudied as a result (Kohout, 1966). This perception has changed over the last two decades with more and more studies conducted in recognition that SGD is almost ubiquitous in coastal zones throughout the globe (Johannes, 1980; Moore, 1999) and can transport significant terrestrial loads to the coastal ocean (Corbett et al., 1997; Moore, 1999; Burnett et al., 2003; Moore, 2010).

SGD is consensually described as any and all flow of water on continental margins from the seabed to the coastal ocean (Figure 1.1), regardless of fluid composition or driving force (Burnett et al., 2003), acting on scale lengths of meters to kilometres (Moore, 2010b). It, therefore, represents a direct discharge to the ocean wherever the coastal aquifer is connected to the sea and hence transports water and associated constituents from land to sea.

1.3.1 Modes of SGD

Water moves through permeable rocks and sediments in response to pressure and density gradients. Hydraulic gradients on land result in groundwater seepage near shore and may even extend beyond the shoreline from confined aquifers (Burnett et al., 2003). While hydrothermal vents and coastal submarine springs represent visible discharge to the sea, the exchange through permeable coastal sediments is subtle and occurs in response to weaker gradients (Burnett et al., 2003). With these complexities in mind, the main modes of SGD may be divided into (1) shoreline flow, in which fresh groundwater is driven by an inland hydraulic gradient to the sea causing water to flow through the aquifer, and (2) deep pore water upwelling, in which advection of water through permeable shelf sediments and rocks occurs beyond the shoreline (Moore, 2010).

Bratton, (2010) defined the scale to three distinct spatial scales for consideration, (1) The nearshore scale, approximately 0 - 10m offshore including the unconfined surficial aquifer, (2) The embayment scale from 10m as far as 10 km offshore and includes the first confined aquifer and its terminus, and (3) The shelf: a decline that spans the width and thickness of the aquifers of the entire continental shelf.

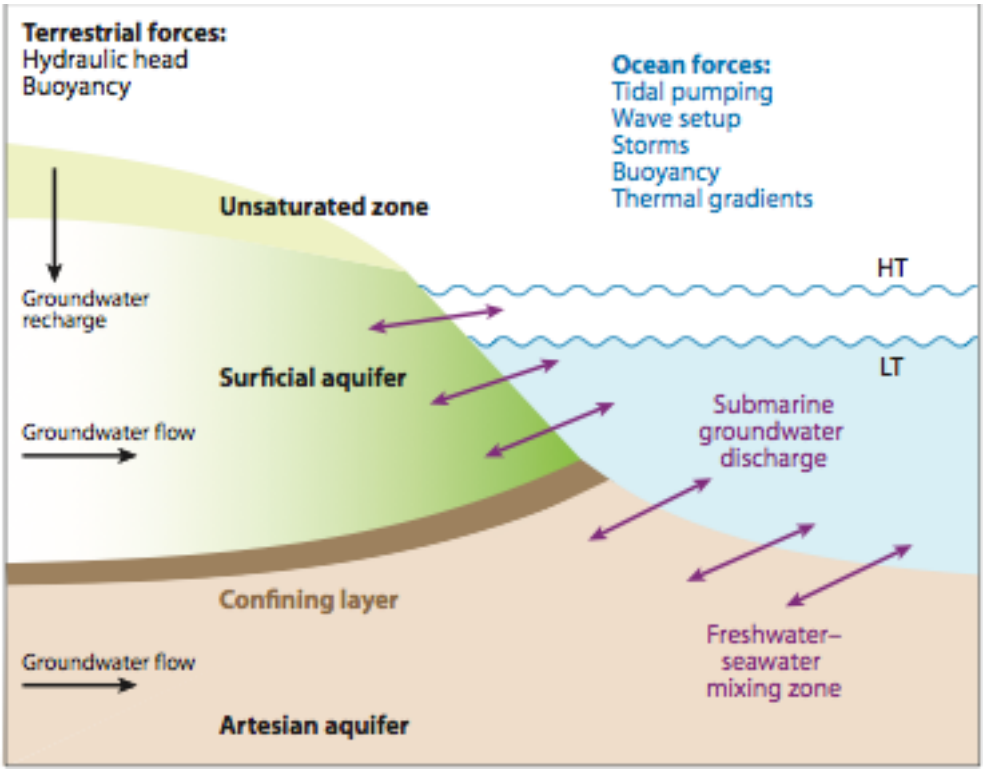

Figure 1.1: Schematic depiction of submarine groundwater discharge and recharge processes at the land-sea boundary. Terrestrial and oceanic forces influence the movement of SGD. Arrows represent fluid movement (Moore, 2010)

Figures 1.1 and 1.2 highlight the movement of groundwater from land to sea. Groundwater from unconfined aquifers in the littoral zone tends to discharge close to the shore due to salt wedge intrusion beneath the freshwater aquifer (Johannes, 1980). On the other hand, submarine groundwater recharge (SGR) can occur in marine environments due to oceanic processes, such as tides, waves, currents, sea level fluctuations, and density differences, which may cause negative potential and force sea water into the sea floor. These two processes do not necessarily balance volumetrically as SGD often contains a portion of terrestrially recharged water, and also, SGR may penetrate the aquifer and raise the water table as opposed to discharging as SGD (Burnett et al., 2003). As a result, SGD can comprise of fresh groundwater, re-circulated seawater or a brackish mixture of the two with varying salinity (Burnett et al., 2003).

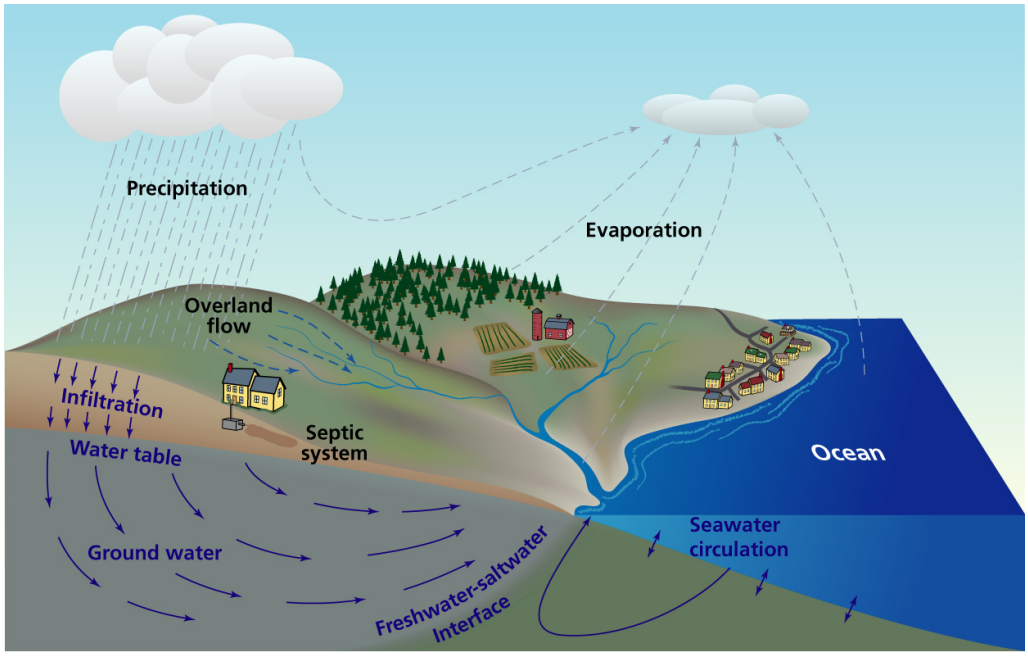

Figure 1.2. Schematic of submarine groundwater discharge flow, illustrating fresh intertidal SGD transported from land and brackish SGD from recirculated seawater, taken from Cook (2005).

1.3.2 Method of measurement

In contrast to rivers, SGD often has low flow rates that make source detection more difficult (Burnett et al., 2003). SGD is spatially and temporally variable, making quantification an arduous task often incurring significant errors (Moore et al., 2006; Burnett and Dulaiova, 2003; Moore, 2010). There have been a number of methods employed to quantify SGD inputs including direct measurements using seepage meters have been employed worldwide (Taniguchi et al., 2002). However, this method is labour intensive and only practical over small scales (Leote et al., 2008).

Water balance approaches have been a traditional method for determining freshwater influxes to the coastal zone due to the simplicity of sampling (Gordon et al., 1996). However, the magnitude of fresh SGD is often within the uncertainty of the water balance parameters, resulting in SGD estimates being incorrect by several orders of magnitude (Burnett and Dulaiova, 2003; Moore, 2010). Therefore these methods are often shown to be unreliable, and justification for their use must be examined (Corbett et al., 1997; Schubert et al., 2015).

Modelling approaches have been undertaken to examine SGD (e.g., McCormack et al., 2014). These models often incorporate Darcy's Law to describe interfacial flow dynamics and therefore usually fail to include seawater recirculation into total SGD (Rocha et al., 2016).

Naturally occurring radionuclides from the uranium decay series have been successfully employed as SGD tracers. These estimates provide a spatially integrated flux and are therefore useful in SGD studies that vary both spatially and temporally (Burnett et al., 2006). Radon (^{222}Rn) in particular, has proven to be an excellent tracer as it is highly enriched in groundwater relative to surface water

(typically 1000-fold or greater), is chemically inert (a noble gas), and has a short half-life ($t_{1/2}$ = 3.83 days) (Cable et al., 1996; Corbett et al., 1997; Burnett and Dulaiova, 2003; Burnett et al., 2006; Cook et al., 2008; Schubert et al., 2015). Radon is produced from the radioactive decay of ^{226}Ra in the subsurface. When SGD discharges into the coastal ocean, radon activities begin to decrease due to atmospheric gas exchange and radioactive decay. Hence, a mass balance approach can be employed to account for all inflows and outputs of radon in the system, permitting calculation of the groundwater inflow (Cook et al., 2008), which increases the accuracy associated with SGD quantification (Corbett et al., 1997).

Radium isotopes, namely ^{226}Ra, are also employed in SGD studies to determine brackish SGD (Webster et al., 1995) and to quantify the residence time of groundwater within the coastal ocean, using mass balance approaches (Moore and Wilson, 2005; Moore et al., 2006). Ra isotopes are continuously produced by the decay of their thorium parents that are bound onto sediment. Radium isotopes are separated into both long-lived (^{228}Ra $T_{1/2}$ = 5.75 y; ^{226}Ra $T_{1/2}$ = 1600 y) and short-lived (^{224}Ra $T_{1/2}$ = 3.66 d; ^{223}Ra $T_{1/2}$ = 11.4 d) isotopes. Radium is not generally present in groundwater or seawater. As seawater recirculates in the aquifer, Ra isotopes desorb and are mobilised from sediment particles into the recirculated seawater compartment. Ra isotopes mix conservatively once released and thus the residence time of SGD can be calculated by comparison of the short and long-lived isotope activities (Rodellas et al., 2017).

A combination of several tracers, particularly the use of naturally occurring tracers, such as radon, silicate, and salinity (Schubert et al., 2015) allows detection of SGD with reduced errors.

1.3.3 Global estimates of SGD

The length of coastline over which SGD may occur is vast and thus may deliver large quantities of freshwater to the marine environment, especially in the littoral zone (Taniguchi et al., 2002a; Burnett et al., 2003). Global SGD rates have been hard to quantify due to the variability and limitations of SGD data from country to country, with limited data from India, South America or Africa (Zektzer et al., 1973; Taniguchi et al., 2002a; Moore, 2010b). Globally, direct terrestrially derived fresh groundwater discharge is said to account for between 6 (Zektser and Loaiciga, 1993) and 10 % (Johannes 1980) of surface water inputs into coastal waters, although this is evaluated with low precision (Burnett et al., 2003). However, the total SGD, incorporating the recycled seawater component, accounts for a much larger proportion. This portion may be 3 to 4 times higher than river water fluxes to the Atlantic and Indo-Pacific Oceans (Kwon et al., 2014).

Table 1.1: SGD rates examples from across the world, detailed in the relevant literature referenced in the table. Modes of measurement and units of SGD differ between studies.

Name	Location	SGD Rate	Method	Reference
Fukae	Osaka Bay, Japan	$9.62 \times 10^{-5} – 4.04 \times 10^{-4}$ cm s^{-1}	Seepage Meter	Taniguchi, 2002
Cockburn Sound	Australia	0.92 – 3.6 cm d^{-1}	Seepage meter	Taniguchi et al., 2003
Northeast Gulf of Mexico	Florida, USA	5 – 50 cm d^{-1}	Radon	Lambert and Burnett, 2003
Ubatuba	Brazil	1 – 29 cm d^{-1}	Radon	Burnett et al., 2008
Kinvara	Ireland	10.4×10^{4} m^3 d^{-1}	Radon	Rocha et al., 2015
South-eastern Sicily	Sicily	60 m^3 s^{-1} km^{-1}	Radium	Povinec et al., 2006
Northeast Gulf of Mexico	Florida, USA	1.5 m^3 min^{-1}	Radionuclides/ Seepage meter	Moore, 2003
South Sea	Korea	50 – 300 m yr^{-1} 1.5×10^{9} m^3 yr^{-1}	Radionuclides	Kim et al., 2003
Indian River Lagoon streams	Florida, USA	117 m^3 d^{-1} m^{-1} of shoreline (marine) 0.02 – 0.9 m^3 d^{-1} m^{-1} of shoreline (terrestrial)	Seepage meters	Martin et al., 2007
Chesapeake Bay	USA	1×10^{6} m^3 d^{-1}	Radon	Charette and Buesseler, 2004
Mediterranean Sea		0.3-4.8 x 10^{12} m^3 yr^{-1}	Radium	Rodellas et al., 2015
Marine Cove	Cape Cod	4.3 – 5 m^3 d^{-1}	Seepage Meter	Giblin and Gaines, 1999

Measurement units of SGD vary between studies based on the parameters available and the requirements of each study (Table 1.1). Measurement units include (1) volume per unit time (m^3 d^{-1}), (2) volume per unit time per unit length of shoreline (m^3 d^{-1} m^{-1}), and (3) volume per unit time per unit area (m^3 s^{-1} m^2). For many studies the areal extent of SGD offshore is unknown (Taniguchi et al., 2002a), therefore making these values incompatible. This is a confounding factor in integrative studies to understand the impact of SGD globally. A lack of consensus of SGD terms, acronyms and discharge units causes difficulty in comparing studies, likely due to the fast growing nature of the field (Bratton 2010).

1.3.4 Comparison of riverine and SGD hydrological inputs

Because locally SGD may act as a point or diffuse source to the coast (Burnett et al., 2003), discharge rates may vary spatially and temporally and are known to vary widely depending on many factors including location, weather and aquifer type (Taniguchi et al., 2002a). Within the nearshore scale, which is the most often reported (Bratton, 2010), SGD might account for anything from an insignificant contribution to almost 100 % of the total water influx to a particular coastal zone (Taniguchi et al., 2002). Total SGD has been shown to be a major contributor to coastal seas worldwide. For example, Rodellas et al., (2015) compared SGD inputs into the Mediterranean Sea to those of atmospheric deposition and riverine flow and found that SGD inflows (0.3 - 4.8 x 10^{12} m^3 yr^{-1}) were equal to or are indeed larger by a factor of 16 than riverine inputs depending on the section of coastline studied. The annual SGD fluxes associated with the South Atlantic Bight have been shown to be three times higher than that of rivers (Moore, 2010a). Moore et al., (2008) estimated the SGD flux into the Atlantic Basin accounts for 80 - 160 % of riverine inputs in the entire Atlantic Ocean using a ^{228}Ra tracer approach. Moore (1996) documented that SGD contributed 40 % of the river flow into the southeast coast of the US. SGD contributed up to 56.9% of riverine inputs and up to 77 % of nutrient inputs in the Jiulong River Estuary (Guo et al., 2011). Martin et al., (2007) studied both the fresh and marine sources of SGD and concluded that marine SGD represented inputs that were four times greater than surface inflows.

Using freshwater SGD measurements only, Taniguchi et al., (2008) identified SGD as contributing 4.5 - 7 % of the river discharge in the Yellow River Delta. Karstic and alluvial aquifers are expected to have the highest potential for SGD due to their high permeability. Additionally, karst aquifers have a large hydraulic conductivity, and therefore large volumes of groundwater discharge can be expected under the right hydraulic gradients (Taniguchi et al., 2002a). For example, SGD accounts for up to 100% of freshwater inputs in Kinvara Bay, Ireland during summer (Rocha et al., 2015).

1.3.5 SGD in karst regions

Karst and carbonate systems, which have a higher propensity to transport large fluxes of fresh groundwater and dissolved constituents compared to other hydrogeological settings, account for

25% of the world's coastline (Ford and Williams, 2007). Pathways created by limestone dissolution allow rapid infiltration and relatively unrestricted conduit flow of groundwater in karst aquifers. These natural channels provide focused, defined coastal entry points rendering karst-channelled SGD a 'point' rather than 'diffuse' delivery mode of SGD. Large volumes of fresh SGD can be rapidly transported to the coastal zone via these point entries (Drew, 2008), varying the effectiveness of tidal dilution in the receiving environment.

Furthermore, surface-groundwater interactions dominate in karst catchments. Karstic features promote contaminant transport more than other hydrogeological settings (Coxon, 2011). Karst aquifers typically have thin soils and subsoils, and rapid conduit groundwater flow. Conduit flow results in a short residence time and fast transport of groundwater to the sea. Additionally, karst aquifers commonly exhibit well-oxygenated conditions which reduce the capacity for nutrient modification and removal during transit (Slomp and Van Cappellen, 2004). These characteristics minimise opportunities for attenuation via absorption, ion exchange, chemical breakdown, microbial die-off, or removal processes. Contamination may derive from both diffuse (fertiliser spreading) and point (leaking of stored animal waste and septic tank effluent) sources (Coxon, 2011).

1.4. The role of SGD in coastal biogeochemical budgets

SGD has been shown to influence the geochemical cycles of major and minor elements either through direct discharge of fresh groundwater or by seawater recirculation through coastal aquifers (Moore 1999). Although SGD is a natural phenomenon, it has become of concern due to anthropogenic pressures. SGD provides an additional pathway for terrestrial contaminants, including carbon (Wassenaara et al., 1991; Fiebig 1995; Pabich et al., 2001), metals (Christensen and Christensen, 2000; Kim and Kim, 2014; Rodellas et al., 2014) and nutrients (Slomp and Van Cappellen, 2004; Hwang et al., 2010; Lee et al., 2012; Ibánhez et al., 2013; Ji et al., 2013) to marine ecosystems. Other environmental factors such as pH, temperature, turbidity and substrate also influence the receiving coastal ecosystem (Bulger et al., 1993). Hence, SGD is a major player in the solute budgets of the world's oceans (Zektser and Loaiciga, 1993).

1.4.1 The subterranean estuary

Moore (1999) coined the term 'Subterranean Estuary' (STE) to highlight the importance of the mixing zone between groundwater and the coastal ocean. He describes it as an area where groundwater derived from recharge on land measurably dilutes seawater that has invaded the aquifer through a free connection to the sea. Freshwater inputs, the permeability of the aquifer, sea level, and tidal dynamics determine the location and width of this mixing zone. These vary both on geological and shorter timescales due to seasonal effects, sea level changes and groundwater extraction inland (Slomp and Van Cappellen, 2004).

SGD composition differs from that of rivers due to this subterranean pathway, which results in slower flows, and chemical reactions occurring in the STE. Chemical reactions occur between the mixed waters and aquifer solids within the aquifer (Burnett et al., 2003) often mediated by bacteria, modifying the chemistry of the discharging water. Hence, the composition of water in the STE will differ from that predicted by simple mixing (Rocha et al., 2009) and will be chemically distinct from the groundwater and seawater endmembers (Beck et al., 2007; Santos et al., 2008; Santos et al., 2009). The most important chemical reactions occurring at this reactive node include (1) desorption of ions from adsorbed sites (Dulaiova et al., 2008) due to increases in ionic strength, (2) dissolution and precipitation of carbonates (Cyronak et al., 2013), (3) remineralisation of organic matter leading to carbon, metal and nutrient release (Santos et al., 2009), and (4) redox reactions that produce and consume metal oxides (Beck et al., 2010; O'Connor et al., 2015), which may release or sequester other ions (Moore, 2010). The recirculated compartment can transport oxygenated seawater, dissolved substances, fine particles, bacteria, viruses and phytoplankton into sediments, and release previously bound nutrients, refractory particles, and organisms from sediments (Boehm et al., 2006; Moore, 2010; Santos et al., 2012). Consequently, this may lead to the release and regeneration of nutrients, carbon and metals (Moore 1999) and mixing of elements is therefore more likely in the coastal ocean compared to riverine inputs (Moore and Shaw, 1998).

1.5 SGD-borne nutrients

Many studies conducted to date highlight the importance of SGD-derived nutrient loading to coastal zones worldwide (e.g. Burnett et al., 2003; Slomp and Van Cappellen, 2004; Leote et al., 2008; Lee et al., 2012; Hwang et al., 2010; Ibánhez et al., 2013a; Ji et al., 2013; 2014; Ibánhez and Rocha, 2014; Rocha et al., 2015). Anthropogenic pressures, such as the use of fertilisers, industrial waste and sewage disposal, have led to an increase in concentrations of inorganic nutrients, carbon and suspended matter being transported via SGD to the coastal ocean (Burnett et al., 2003). In fact, groundwater may have nutrient concentrations several orders of magnitude greater than those of corresponding surface waters (Beck et al., 2007; Moore et al., 2008; Null et al., 2012; Porubsky et al., 2014). Thus SGD has the potential to alter the chemical balance of the receiving surface water and may cause the ecosystems to which they discharge to deteriorate (Corbett et al., 1997). Indeed, many studies emphasise the importance of SGD as a driver for eutrophication (Hwang et al., 2005; Kim et al., 2005; Lee et al., 2009; Lee et al., 2012).

1.5.1 SGD flow path

Due to the subterranean nature of the flow path, the concentration of nutrients delivered by SGD may differ from that of surface flow. The main difference is the presence of nutrient assimilating primary producers in surface estuaries and their absence in subterranean estuaries and the influence of the aquifer on nutrient attenuation/removal for SGD-borne nutrients. In river systems, primary producers remove nutrients, particularly nitrogen and phosphate along the flow path, substantially

reducing nutrient concentrations (Paerl, 2009). This mechanism of nutrient removal is absent in subterranean estuaries, leading to elevated nutrient concentrations relative to surface estuaries.

1.5.2 Sources of nutrients

The SGD nutrient fluxes are determined firstly by the nutrient loading to the aquifer from terrestrial sources and secondly by the subterranean transit path and aquifer characteristics. The primary considerations controlling the flux of nutrients to the coastal zone via SGD are (1) the groundwater residence time within the aquifer, i.e., the amount of time the groundwater is in contact with the aquifer solids. This is a result of flow path and discharge rate (2) The types and amount of Si, N and P made available from natural and anthropogenic sources, and (3) redox conditions in the subsurface, which affect the transformation processes in-loco, which in turn control mobility of compounds within the aquifer (Moore, 1999; Bouwman et al., 2013; Slomp and Van Cappellen, 2004).

Contamination of the coastal zone via SGD, therefore, depends on the conditions in which the groundwater has travelled before discharge and the presence of potential contaminants (Kačaroğlu, 1999). Fresh SGD represents a source of biogeochemically important new nutrients to the ocean, especially in the intertidal zone (Burnett et al., 2003). Anthropogenic sources of nutrients to groundwater include fertilisers applied on land, manure and wastewater. Natural sources of these materials are much smaller and may include downward leaching of N and P released from soil organic matter, *in-situ* release from organic matter in the aquifer, and weathering of mineral phases (Lapointe and Clark, 1992; Slomp and Van Cappellen, 2004; Moore, 2010b). Recirculated seawater can release previously bound autochthonous ions in the aquifer including nutrients (nitrate, ammonia, phosphate) and thus can significantly alter the chemical composition of the discharging water (Moore, 1999; Slomp and Van Cappellen, 2004).

Groundwater-borne nutrients, including nitrate, have been shown to have a significant impact on water quality in surface estuaries (Reay et al., 1992). It is unclear how an estuarine or coastal system will respond to nutrient enrichment as different systems exhibit different responses (Bricker et al., 2008). Potential ecosystem responses to coastal nutrient enrichment are complex but include altered nutrient ratios (DRSi:N and N:P), altered structure and composition of the primary producer community and modified sedimentation of organic matter, changes in water transparency, habitat quality and diversity, and community structure (Cloern, 2001).

Horizontal transport determines the residence time of water, and thus nutrients within the coastal environment. The amount of horizontal transport modulates the effect of nutrient enrichment, as the balance between nutrient loading and removal via transport processes controls primary production processes. Coastal systems with slow transport rates and long residence times tend to retain

exogenous nutrients and therefore are less efficient filters than those systems with shorter residence times (Cloern, 2001).

1.5.3 Eutrophication

Nutrient loading via freshwater SGD has been suggested as a driver of potentially significant coastal ecological alterations (Taniguchi et al., 2002) including the onset and development of eutrophication (Valiela et al., 1990; Hwang et al., 2005; Lee et al., 2012), harmful algal blooms (Paerl, 2009) and changes to species diversity (Kamermans et al., 2002). Eutrophication enhances net ecosystem production (NEP) (Gattuso et al., 1998). Nixon (1995) defined eutrophication as 'an increase in the rate of supply of organic matter to an ecosystem'. The European Commission (EC) Nitrates Directive (91/676/EEC) defines coastal eutrophication as 'the enrichment of water with nitrogen compounds causing accelerated growth of algae and higher forms of plant life to produce an undesirable disturbance to the balance of organisms present in the water and the quality of the water concerned'. A comprehensive definition includes both components - increased organic matter supply (either autochthonous or allochthonous), associated nutrient loading, and the subsequent ecosystem effects.

The process of eutrophication is a major concern in Irish waters (EPA 2010). Over half of the coastal and estuarine water bodies assessed in the Irish Water Quality Status Assessment for the period 2007-2009 were impacted by eutrophication (O'Boyle et al., 2015). This issue is not unique to Ireland as many European coastal and estuarine systems exhibit eutrophic characteristics (Newton et al., 2003). In addition to nutrient concentration entering the coastal zone, the C:DRSi:N:P ratio associated with SGD is important, as this may determine the limiting nutrient for primary production. Nitrogen is usually the limiting nutrient in marine systems (Nixon, 1995; Howarth and Marino, 2006). Increases in those nutrients which are present in lower molar concentrations than C:Si:N:P 106:15:16:1 may result in stimulation of primary production and possibly the eventual onset of eutrophication (Howarth and Marino, 2006).

1.5.4 Molar ratios

On a global scale the average molar ratio of DIN:DIP riverine loading is approximately 18:1 (Smith et al., 2003), which is closely linked to the Redfield Ratio of 16:1 (Redfield, 1958). However, N:P ratios may be altered from this ratio in groundwater as nitrogen and phosphorus are removed from groundwater via mechanisms not associated with primary producer assimilation. Microbially mediated groundwater nitrogen removal can occur in anoxic aquifers, mostly via denitrification (Slomp and Van Cappellen, 2004; Rocha et al., 2009), and possibly via dissimilatory nitrate reduction to ammonia (DNRA) and anammox pathways. Well-oxygenated aquifers, such as karstic aquifers, prohibit anoxia-dependent removal processes and favour relatively conservative nitrate transport (Slomp and Van Cappellen, 2004). As groundwater flows toward the coastline, dissolved phosphate may be removed via sorption to iron oxides or co-precipitation with dissolved

aluminium, calcium or iron to mineral phases (Slomp and Van Cappellen,2004). This phosphate removal occurs in both oxic and anoxic aquifers, though less efficiently in the latter (Slomp and Van Cappellen,2004). Thus, there is often near-conservative nitrate transport while phosphate is removed in karst systems (Kamermans et al., 2002; Slomp and Van Cappellen, 2004). Additionally, there is increased terrestrial derived N contamination of aquifers due to fertiliser use (Rocha et al., 2015). The differing behaviour of nitrate and phosphate in oxic groundwater systems typically results in a sharp increase in the N:P ratio along the groundwater flow path (Slomp and Van Cappellen,2004). This altered N:P ratio in groundwater may drive the coastal ocean towards P-limited from the current N-limited primary production state (Slomp and Van Cappellen, 2004).

It is also important to consider dissolved reactive silica (DRSi) in nutrient ratios. DRSi:N:P ratios transport via terrestrial sources for productivity within the coastal zone (Redfield, 1958; Conley and Malone, 1992). DRSi:N ratios have been shown to be decreasing in riverine sources, such as the Mississippi River (Lane et al., 2004). Diatoms require silicon for the construction of their siliceous outer shell during growth. Increases in nitrogen or phosphorus without concomitant increases in silicon can cause a shift from diatom production toward the growth of dinoflagellate and flagellate taxa as these do not require silicon for growth (Sommer 1994; Cloern, 2001). DRSi is often enriched in SGD (Waska and Kim, 2011). In fact, Kim et al., (2005) demonstrated that SGD accounted for 20 – 100% of the riverine Si flux into the Yellow Sea, which represents a significant source of Si to the coastal zone and may be significant on a global scale, particularly in karst regions.

1.6. Carbon cycle and the coastal reaction node

Carbon cycles between the atmosphere, the terrestrial and marine biospheres (Berner, 2004). The carbon cycle is the flux of carbon between reservoirs including inorganic C in rocks, dissolved inorganic carbon (DIC) in seawater, organic C in rocks, organic and inorganic soil carbon. The contribution of any biological system to the global carbon cycle depends upon the balance between organic carbon production and consumption, and the balance between calcium carbonate precipitation and dissolution (Gattus et al., 1998). This cycle interconnects with nutrient cycles due to biological transfer. The link between land and marine systems has been described as an unreactive pipe in the global carbon cycle in the past (Cole et al., 2007). However, carbon budgets in global coastal zones are receiving increased attention, as they are now known to sequester substantial anthropogenic fluxes (Santos et al., 2009; Moore, 2010; Maher et al., 2013). Both biological and chemical pumps can occur in the coastal ocean. These pumps associated with the net uptake of CO_2 by the coastal ocean are (Kempe, 1996):

1. The chemical pump – the net CO_2 uptake in the mixed surface layer by thermodynamic equilibration in response to rising pCO_2 in the atmosphere and subsequent downwelling.

2. The biological pump – organic fixation of DIC by photosynthetic phytoplankton and the export of new primary production to sediments or deeper water. This pump may be enhanced by anthropogenic eutrophication of coastal seas.

Many key studies have called for an improved understanding of carbon fluxes across land-ocean, air-sea, and coastal-open ocean boundaries while gaining an insight into factors that control biogeochemical transformation processes (Gordon et al., 1996; Doney et al., 2004; Denning et al., 2005; Feely et al., 2009; Ramesh et al., 2015). SGD has been shown to be a major contributor of dissolved carbon to the continental shelf (Liu et al., 2012, 2014), intertidal flats (Moore et al., 2011; Kim et al., 2012), bays (Stewart et al., 2015), estuaries (Santos et al., 2012) and lagoons (Cyronak et al., 2014).

Zhang and Mandal, (2012) provided a crude estimate of the global SGD-C flux as 0.23 PgC yr^{-1}. Szymczycha et al., (2013) concluded that the SGD-C load amounts to 25% of the riverine loading on a global scale. As studies in the field are limited, caution must be taken with these estimates (Cai et al., 2003a; Moore et al., 2006; Liu et al., 2012; Szymczycha et al., 2013, 2014), although they support SGD as a significant carbon supply source to the coastal ocean. Still, groundwater influxes are the least constrained components of coastal nutrient and carbon budgets despite significant methodological advances (Porubsky et al., 2014).

Swaney and Giordani, (2011) concluded that ‘efforts must be made to determine site-specific groundwater flux estimates', and also that budgets are needed from a broader range of watershed and catchment basin sizes and in the nearshore coastal zone. This research will help bridge this gap by determining the nutrient and carbon fluxes transported through SGD in a karstic aquifer.

1.6.1 Dissolved organic matter (DOM)

Organic matter (OM) can be broken down into particulate organic matter (POM) and dissolved organic matter (DOM), according to a size threshold of 0.45 μm, by consensus, although this classification is somewhat arbitrary (Zsolnay et al., 1999). DOM is an active and dynamic component of the carbon and nitrogen biogeochemical cycles playing an important role in marine and coastal ecosystems globally (Mopper et al., 1991). DOM is a complex, heterogeneous mixture of organic molecules, derived mainly from terrestrial plant matter, decaying organisms, such as algae, bacteria and higher plant material, or excreted *in-situ* by microorganisms, and is ubiquitous in coastal ecosystems (Baker and Spencer, 2004; Cory and McKnight, 2005; Chen et al., 2010; Nelson and Coble, 2010). DOM inputs into the coastal compartment may occur from multiple sources, including allochthonous inputs such as terrigenous compounds exported from land by rivers and groundwater or marine materials transported through tidal action. Autochthonous materials are produced by excretion from primary producers, cellular lysis, and release from

sediments (Coble, 1996; Rochelle-Newall and Fisher, 2002; Bertilsson and Jones, 2003; Zonneveld et al., 2010).

DOM consists of a continuum of bioavailability within the coastal zone. The labile material may have a turnover period of less than a day compared to refractory DOM that may persist for millennia (Jiao et al., 2010). 95% of the world's oceanic DOM pool is due to autochthonous production (Kowalczuk et al., 2005). However, terrestrially derived DOM has an average marine residence time of between 21 and 132 years compared to DOM in the deep ocean which has a residence time of thousands of years (Hansell and Carlson, 2014). The turnover time of SGD-borne DOM depends on age and composition of groundwater fluxes (Kim et al., 2013). Rapid cycling of terrestrial DOM may enhance primary productivity in the coastal ocean where it is most prominent. Decomposers process significant amounts of bioavailable OM and return inorganic nutrients to ecosystems, which are then taken up by primary producers.

The properties of DOM are diverse and depend on DOM source (terrestrial vs. aquatic) and diagenetic state (Helms et al., 2008). Gaining an understanding of the processes and mechanisms that regulate the amount of DOM entering the sea and the biogeochemistry of the terrestrial fraction is, therefore, critical to better constrain the global carbon cycle of coastal zones. The fate of terrestrial organic matter within the coastal zone and its subsequent delivery to the open ocean is crucial to understanding the global carbon cycle (Hedges et al., 1997). This study aims to characterise terrestrial CDOM transported via SGD in a karstic region to better constrain the types of components delivered via SGD.

1.6.1.1 SGD-borne DOM

Organic matter content in SGD varies widely depending on the geological and hydrological factors defining groundwater catchments (Nelson et al., 2015). SGD passes through the subterranean estuary which modifies DOM (Benner 2002; Tedetti et al., 2011; Nelson et al., 2015). The biogeochemical processes occurring in the STE alters solutes (Kim et al., 2012) while changes in salinity due to mixing influence the local physicochemical conditions through processes such as adsorption, desorption, flocculation, and aggregation which, in turn, affect DOM behaviour in the discharging mixture (Benner, 2002). Furthermore, the increased loads of nutrients associated with SGD, may, in fact, drive carbon loss and increase turnover of DOM in the STE and permeable sediments in general (Ibánhez and Rocha, 2014a).

Considering the ubiquitous nature of DOM and its ability to accumulate in groundwater, studies to determine the SGD-derived DOM characteristics are critical to understanding the potential impact on the coastal C cycle. In this study, DOM delivered to the coastal ocean via SGD will be

determined in Kinvara bay, which has point discharge and minimal surface flow. Thus, SGD-borne DOM can be characterised with minimal interference from surface flow.

1.6.1.2 Chromophoric DOM (CDOM)

The fraction of DOM that absorbs in the UV and the short-wavelength visible range of the electromagnetic spectrum is referred to as chromophoric or coloured DOM, CDOM (Helms et al., 2008; Nelson and Coble, 2010). This pool is used as a precursor for the wider DOM pool (Coble, 1996) and was initially referred to Gelbstoff (yellow substance) (Kalle, 1938, 1949, Kirk, 1976, Bricaud et al., 1981). Traditional methods for DOM characterisation, including extraction and derivatisation, required large sample volumes, which may not be possible in SGD analysis. Additionally, these methods had complicated and lengthy handling procedures, which may increase the uncertainty associated with quantification or even result in chemical alteration of the original sample (Chen and Bada, 1992; Coble, 1996). CDOM is now characterised by multiple spectroscopic methods, including UV-visible absorption spectroscopy and fluorescence spectroscopy (Nelson and Coble, 2010) as DOM includes organic molecules with chromophoric (light absorbing) and fluorophoric (light emitting) moieties (Her et al., 2003). Recent advances in fluorescence spectroscopy allow for the rapid detection of CDOM (approximately one minute) at a wide range of both excitation and emission wavelengths requiring relatively small sample volumes and minimal handling. In particular, the use of Excitation-Emission Matrix Fluorescence (EEMF) is a very useful tool incorporated into DOM studies. EEMF studies are now extensive in the literature (Coble, et al., 1990; Coble, 1996; Baker and Spencer, 2004; Guo et al., 2010; Singh et al., 2010; Tedetti et al., 2011; Bieroza et al., 2012) with each study typically containing more than 3000 fluorescence intensities. Excitation-Emission Matrices (EEMs) can be used to infer the sources, composition, relative concentrations and biogeochemical cycling through transformations of DOM (Murphy et al., 2010).

DOM from marine sources has been shown to be enriched in aliphatic structures causing blue-shifted spectra in fluorescence while DOM from terrestrial sources has higher aromaticity and conjugation of double bonds resulting in red-shifted spectra (Maie et al., 2005). These characteristics have been used to differentiate between terrestrial/higher plant and marine/microbial origins (Coble, 1996; McKnight et al., 2001; Lapworth et al., 2008). CDOM absorbance or fluorescence is variable as a function of DOC concentration. Hence, there is no current definitive expression able to link the CDOM optical properties to the DOC concentration. In fact, a high proportion of the DOC present may not significantly absorb in the UV-Vis range (Ferrari et al., 1996). Any such relationships derived from CDOM optical activity and DOC concentration tend to be localised in space and time due to chemical reactions, source material, diagenetic processes, degradation, which alter DOM structure and composition (Nelson and Coble, 2010). However, clear CDOM:DOC relationships have been found in some large river systems worldwide. For

example, Kowalczuk et al., (2010) determined a significant linear relationship ($R^2 = 0.87$) between fluorescence intensity and CDOM absorption coefficient a_{CDOM} (370 nm) measured in the southern Baltic over different seasons. They also found a significant relationship ($R^2 = 0.76$) between aCDOM (370 nm) and DOC concentration. Del Castillo and Miller (2008) developed a method to estimate DOC transport from large rivers providing there is data available for the relationship of CDOM, DOC and salinity in the plume. Ferrari (2000) found a significant correlation between aCDOM and DOC in river plumes discharging to the North Sea and concluded that 46 – 60% of DOC is non-absorbing in the visible range. Ferrari et al., (1996) showed a good correlation between CDOM optical properties and DOC in the southern Baltic Sea, however, approximately 70% of DOC did not absorb in the UV-visible range.

Fourier-transform ion cyclotron resonance mass spectrometry (FT-ICR-MS) is a powerful technique now employed to characterise DOM on a molecular level (Koch et al., 2008). Currently, only ~25% of DOM is well described on this level, which has been shown to comprise of amino acids, nucleic acids, carbohydrates, hydrocarbons, fatty acids and phenolic compounds (Coble, 1996; Rochelle-Newall and Fisher, 2002; Bertilsson and Jones, 2003; Zonneveld et al., 2010). FT-ICR-MS allows for the elucidation of indicators, such as amino acids and lignin, on a molecular scale (Koch et al., 2005). FT-ICR-MS studies utilise molar ratios, specifically H/C, O/C and aromaticity, to evaluate DOM in terms of its biogeochemical availability. A clear understanding of the composition of the DOM pool within Kinvara Bay will support efforts to better understand the diagenetic status and biogeochemical and degradation processes occurring in the coastal zone as a result of SGD-borne DOM.

1.6.1.3 CDOM classification

Allochthonous DOM transported from the catchment to the water body is derived from and influenced by the geology, nature of the soil, land use and hydrogeology of the region (Hudson et al., 2007; Rochelle-Newall and Fisher, 2002). CDOM is often classified into two broad groups as (1) humic-like components and (2) protein-like (biogeochemically non-humic substances) components (Chen et al., 2010). Protein-like peaks, namely amino acid-like peaks, tryptophan and tyrosine, have been used as biogeochemical tracers (Fellman et al., 2009). These amino acids compose of an indole group and is thus a DON compound (Coble, 1996; Yamashita and Tanoue, 2004). Protein fluorescence has been associated with biological production in surface waters (Determann et al., 1994; ,Coble, et al., 1998). Cammack et al., (2004) identified this fraction as being highly dynamic. They suggested that tryptophan-like CDOM represents a product of bacterial activity and a bioavailable substrate. The protein peaks are common in waters subject to anthropogenic influence (Hudson et al., 2007) as well as areas of high productivity and pore waters (Coble, 1996). Thus, protein-like peaks are derived from products of microbial activity (Cammack et al., 2004; Yamashita and Tanoue, 2004) and constitute bioavailable, labile organic fractions

(Hudson et al., 2007). These are often found in freshwaters of urbanised areas of increasing anthropogenic pressures.

Humic substances are a heterogeneous mixture of high molecular weight aliphatic and aromatic organic compounds, that are often rich in oxygen-containing functional groups, such as the carbonyl functional group (C=O) (Mobed et al., 1996; Hessen, 1998; Sleighter and Hatcher, 2007). These are a key component, accounting for approximately 60 - 70% of total organic carbon (TOC), in soils (Mobed et al., 1996) and can be released from the soil/subsurface matrix, and consequently, may accumulate in groundwater (Artinger et al., 2000; Kim et al., 2012). In natural waters deemed to be non-contaminated, humic and fulvic acids are the most common fluorophores present (Mudarra and Andreo, 2011). Humic substances can be composed of at least three distinct stages of humification, although in reality, a continuum of all three exists. Humification causes the N-containing functional group content, the carboxyl acid content and the total exchangeable acidity to increase, which in turn, may enhance DOM interaction with ionic constituents, protonation, ligand exchange and cation bridging (Ohno, 2002). Therefore, the degree of humification associated with SGD-borne DOM will determine, to a large extent, its effects in the coastal zone. These stages are given as active, passive and intermediate, which are dependent on the turnover time of the organic matter in each pool (Ohno, 2002). The active pool has a turnover time of less than one year, while the intermediate fraction may turnover in years to centuries but the passive OM will persist for millennia (Carlson and Ducklow, 1996). Passive OM is highly refractory and may contribute to oceanic C storage. The microbial C pump regulates recalcitrant DOM through *in-situ* microbial production. The entire recalcitrant C inventory in storage in the ocean is 624 Gt C (Jiao et al., 2010). This store may be an essential mechanism for long-term storage of fixed atmospheric carbon by the ocean.

1.6.1.4 Properties of CDOM

From its initial production within the soil until it discharges as a component of SGD, DOM undergoes physical transport and geochemical reactions within the aquifer, including transport, sedimentation, and reactions with aquifer materials, such as carbonate solids (Mudarra and Andreo, 2011). DOM itself is non-chlorophyllous, but it plays a vital role in allowing photochemically-induced transformations in surface waters (Singh et al., 2010). CDOM is one of the controlling factors for light attenuation. Suspended sediment also acts as a control for light absorption within the water column. Slowly setting particulate organic matter contributes greatly to suspended solids, which greatly increases light attenuation in the water column (Duin et al., 2001). These factors control the extent of photosynthetically active radiation penetrating through the water column and hence, the size of the euphotic zone. The size of the euphotic zone defines the depths of particular wavelength availability to organisms (Chen et al., 2003, 2010; Baker and Spencer, 2004; Cory and McKnight, 2005). Absorption and refraction by water, and dissolved and suspended matter

determine the spectral quality of light within the photic zone (Jerlov, 2014). Solar radiation is removed by absorption within the water column due to the water itself, CDOM, phytoplankton pigments or non-algal particulate matter (Murray et al., 2015). Murray et al., (2015) showed that CDOM was responsible for 6 – 13% of the absorption in a Greenlandic Fjord.

DOM acts as the primary source of energy for heterotrophic bacteria through the microbial loop (Azam et al., 1983) and hence, also has an impact on secondary production (Chen et al., 2010). DOC is returned to higher trophic levels due to its incorporation into bacterial biomass, such as phytoplankton-derived DOM that supports bacterioplankton production, a portion of which may be transferred to the traditional grazing food chain (Hagström et al., 1988). Murray et al., (2007) reported a direct link with the domination of bacterial growth and large shifts in community composition with utilisation of DOC. Linkages between specific organisms and important ecosystem processes such as carbon utilisation. The community composition, for example phytoplankton composition, may shape the structure and function of the microbial loop (Passow et al., 2007). Much of the flux of C, N and P in coastal waters can be attributed to organic matter (OM) production and consumption (Gordon et al., 1996).

The effect of CDOM on primary and secondary productivity continues beyond the microbial loop and light availability controls, as it provides a direct source of carbon and nutrients to the aquatic food web (Qualls and Haines, 1991). It also acts as a pH buffer and can influence metal speciation and bioavailability (Cory and McKnight, 2005) due to the many complexes that may be present in DOM. Some DOM components may act as electron shuttles or as terminal electron acceptors, which can directly or indirectly affect microorganism-catalysed redox reactions. This characteristic has been attributed to quinone moieties of humic and fulvic acids. Quinones are a group of biomolecules which cycle between three redox states (oxidised, the semiquinone radical and reduced) and can be found in living cells, extracellular material, and in detrital organic material (Cory and McKnight, 2005). As a result, the presence of microorganisms may alter the fluorescence characteristics of DOM due to increased biological activity (Parlanti et al., 2000). The interaction of DOM with anthropogenic pollutants, such as pesticides, fertilisers and metals, also influences their bioavailability, transport and fate. Humic materials may have varying sorption capacities for pollutants, and therefore, affect the fate, exposure and potential effects of different pollutants to varying degrees (Thomsen et al., 2002).

DOM is closely linked to the carbon and nitrogen cycles of coastal oceans as it provides a direct energy source to fuel productivity and its chemical characteristics might influence both light availability and electron transfer. Therefore, this could be a factor in determining net ecosystem metabolism (NEM) in coastal regions, which in turn, determines the contribution as a source or

sink of the system within the context of carbon turnover and hence the C cycle in coastal areas (Gordon et al., 1996).

1.6.2 DOC

Fresh SGD has been shown to account for 5 - 10% of the world's DOC influx to the coast, delivering 11 - 22 Tg C yr^{-1} as DOC (Dai et al., 2012). Although this is within the 30% error estimate of total DOC transport, it still represents a significant DOC flux. The DOC flux associated with total (fresh + recirculated seawater) SGD may represent a significantly larger proportion of that reported here. In spite of this, there is limited data quantifying DOC concentrations in subterranean estuaries globally (Dai et al., 2012). Thus, groundwater inputs are often the least constrained components of carbon budgets of coastal oceans worldwide (Porubsky et al., 2014), although a plethora of studies show that groundwater transports high DOC fluxes to the coast (Fiebig and Lock, 1991; Swarzenski et al., 2006; Dai et al., 2012; Ibánhez and Rocha, 2014).

DOC concentrations in groundwater fluctuate depending on location, season, changes in groundwater flow rate (Montluçon and Sañudo-Wilhelmy, 2001; Ibánhez and Rocha, 2014), seawater mixing in the subsurface (Goñi and Gardner, 2003) and with microbial activity (Pabich et al., 2001). Thus, groundwater has variable DOC concentrations both geographically and temporally ranging from 156 to 1,200 μmol L^{-1} (Grøn et al., 1992; Ibánhez and Rocha, 2014). A given groundwater body may support larger DOC concentrations than a given river (Table 1.2). This applies in particular in karst regions, which have the ability to carry relatively large fluxes of groundwater with minimal surface flow (Schubert et al., 2015). Therefore, the local importance of groundwater DOC influxes is dependent on the particular system in question due to discharge magnitude, land use practices, reactivity in the STE, the catchment type amongst others.

Table 1.2: Mean DOC concentrations found in the main rivers in Europe and DOC concentrations found in groundwater samples globally, as referenced in the cited literature.

River	DOC [μmol L^{-1}]	Reference
Scheldt	566	
Rhine	242	
Gironde	258	
Thames	483	
Sado	383	(Abril et al., 2002)
Elbe	566	
Ems	566	
Douro	208	
Loire	325	
Groundwater	DOC [μmol L^{-1}]	Reference
Northern Jylland, Finland	1,200	(Grøn et al., 1992)
Breitenbach, Germany	475	(Fiebig, 1995)
Ria Formosa, Portugal	156 – 500	(Ibánhez and Rocha, 2014a)
Hampyeong Bay, South Korea	185	(Kim et al., 2012)
North Inlet, USA	500-1000	(Goñi and Gardner, 2003)
Kinvara Bay, Ireland	200 - 600	(Smith and Cave, 2012)

Most DOC is derived from soil and can play a significant role in redox processes and solute transport (Stuart and Lapworth, 2016). Global climate change has been linked to an increase in the export of DOC from land due to rising temperatures and land use change (Baker and Spencer, 2004). Therefore, if global temperatures continue to increase, the terrestrial carbon store may partly relocate to the oceans, causing an increase of terrestrial C stored in the ocean (Sabine et al., 2004). Given the ability of DOC to be incorporated into SGD (Maher et al., 2013; Szymczycha et al., 2014; Szymczycha et al., 2016), this unquantified contribution to the DOC transfer flux may become even more important. Therefore, it is essential to evaluate the current fluxes associated with SGD to have a thorough understanding of the processes by which DOC may enter the ocean. This study will contribute to the current knowledge by determining current DOC fluxes associated with SGD in a karstic aquifer.

DOC often displays conservative behaviour in estuaries. However, this is often due to contemporary sources and sinks that result in small net changes in bulk concentration (Cifuentes and Eldridge, 1998). Sinks include microbial utilisation (Raymond and Bauer, 2000), biodegradability and flocculation of humic substances (Abril et al., 2002). These sinks may experience constraints such as temperature and residence time which result in a flux of allochthonous labile DOC transported through the coastal zone to the ocean (Raymond and Bauer, 2000). Sources include tidal flushing and desorption processes (Miller, 1999).

1.6.3 The importance of SGD-borne dissolved inorganic carbon (DIC)

DIC is a biogeochemically important component of estuarine and coastal waters globally. Total DIC (TDIC) is defined as the sum of H_2CO_3* (H_2CO_3 and dissolved CO_2), HCO_3^- and CO_3^{2-} (Cioni, Gambardella and Marini, 2007; Cai et al., 2008), as shown in Eqn (1):

$$DIC = H_2CO_3^* + HCO_3^- + CO_3^{2-} \quad (1)$$

Figure 1.3 provides a box model to illustrate inputs and outputs of DIC in the coastal zone. The major processes contributing to DIC levels within coastal aquatic ecosystems are photosynthesis, *in-situ* respiration (Cole et al., 2001; Cole et al., 2007), driven by organic matter oxidation in soils and sediments (Brunet et al., 2005) inputs of organic matter, pCO_2 exchange between the atmosphere and coastal zone (Zhai et. al, 2005), as coastal zones may act as a sink of anthropogenic CO_2 released into the atmosphere (Sabine et al., 2004a) SGD (Jiang et al., 2008; Dorsett et al., 2011; Atkins et al., 2013), runoff from surface waters (Frankignoulle et al., 1998; Raymond et al., 2000; Hélie et al., 2002) and precipitation of aquifer materials, such as carbonate or silicate minerals (Berner et al., 1983; Berner, 1992).

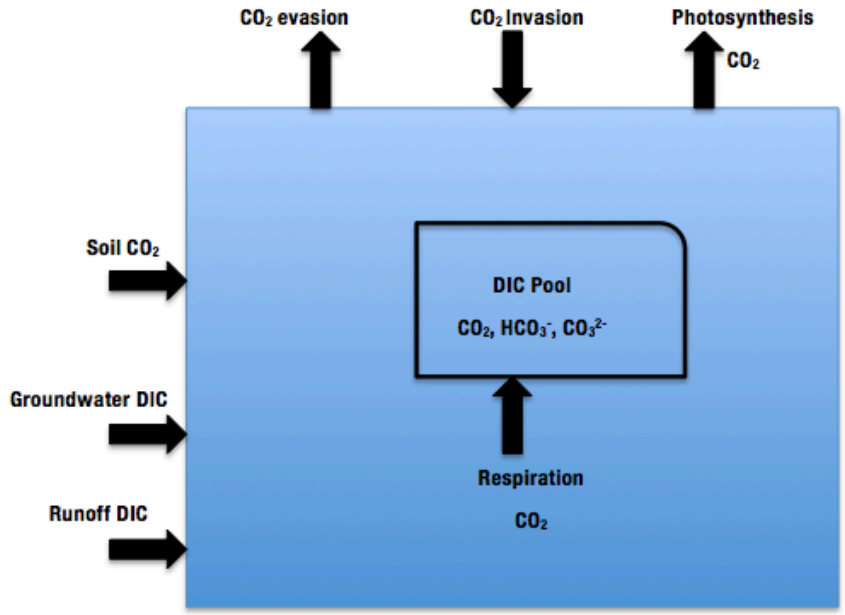

Figure 1.3: Schematic box model of processes affecting the aquatic DIC pool, including inputs from land and atmosphere and outputs to the atmosphere (after Atekwana and Krishnamurthy, 1998)

1.6.3.1 SGD-borne DIC

SGD has been shown to transport large fluxes of dissolved inorganic carbon to coastal zones worldwide (Cai et al., 2003a; Basterretxea et al., 2010; Atkins et al., 2013; Maher et al., 2013). In fact, Dorsett et al., (2011) estimated that 7 – 11 % of global coastal water DIC derives from SGD associated with karst and other carbonate systems alone. SGD accounted for approx. 30% of the DIC load carried by the Pearl River in the South China Sea (Liu et al., 2012). While Moore et al., (2006) concluded that SGD was comparable to riverine inputs regarding DIC in marshes around

the Okatee estuary, USA. In the South Atlantic Bight, SGD-borne DIC and surface waters were also comparable (Cai et al., 2003a). Groundwater transports DIC through $CaCO_3$, CO_2, and DOC production. Reactions between the solutes contained in groundwater and seawater will determine the fluxes of DIC across the boundary to the open ocean. The fluxes of DIC may be subject to modification within the coastal zone through speciation of organic and inorganic compounds, physicochemical gradients, high biological activity, and intense sedimentation and resuspension (Frankignoulle et al., 1998; Gattuso et al., 1998; Abril and Borges, 2005).

Studies have shown that coastal waters, which are SGD influenced, are often a net source of inorganic carbon (Fagan and Mackenzie, 2007; Chen and Borges, 2009; Dorsett et al., 2011). Previous studies have reported SGD to be a significant source of DIC and CO_2 to the coastal zone (Gagan et al., 2002; Cai et al., 2003a; Atkins et al., 2013; Sadat-Noori et al., 2016). As such, SGD may be a primary source to the atmosphere as pCO_2 in groundwater can be three times higher than atmospheric CO_2 (Gagan et al., 2002; Cai, 2011).

1.6.3.2 SGD-borne CO_2

Substantial evidence shows that burning fossil fuels, deforestation and land use change, have increased CO_2 levels in the atmosphere (McCarthy 2001; Chen et al., 2006; IPCC 2007, 2014). Atmospheric CO_2 levels have increased by nearly 40% since preindustrial levels of approximately 280 ppmV (parts per million by volume) to almost 384 ppmV in 2007 (Solomon et al., 2007) and are expected to continue to rise by about 1% per year into the future (Houghton, 2001). As a direct result, global warming has become a serious global issue (McCarthy, 2001). Roughly 30% of anthropogenically produced CO_2 has been absorbed by the oceans. The accumulation of CO_2 in seawater changes the overall composition of DIC species and lowers the pH (Feely et al., 2004; Feely and Doney, 2011). Carbonate and silicate minerals are the major components of karstic aquifers. When CO_2 in water comes into contact with $CaCO_3$ in the aquifer it promotes dissolution of calcite as hydrogen ions are produced (Equation 2). The reverse reaction shows how lower pH in groundwater can promote precipitation by reaction of the hydrogen ions with bicarbonate. This, in turn, contributes to CO_2 in groundwater. As groundwater has been shown to have lower pH, transport through karstic aquifers may lead to higher CO_2 levels as calcium carbonate is precipitated. This is also true for silicate minerals; however, the global silicate-weathering rate is lower than carbonate weathering (Cai et al., 2008).

$$CaCO_3 + CO_2 + H_2O \leftrightarrow H^+ + HCO_3^- \quad (2)$$

It remains uncertain as to whether coastal zones act as a source or sink of atmospheric CO_2 (Chen and Borges, 2009; Cai, 2011). Carbon dioxide is closely linked to the organic carbon pool through metabolism (Cai and Wang, 1998). Photosynthesis in aquatic systems is a fundamental component of the C cycle, acting as a C sink (Gu et al., 2004). Respiration will be the primary metabolic

process if light is limited in the upper part of the water body (Equation 3). The forward reaction represents a simplification of primary production, while the reverse reaction represents aerobic respiration.

$$CO_2 + H_2O \leftrightarrow CH_2O + O_2 \quad (3)$$

Many European estuaries are vulnerable to intense anthropogenic pressure due to high loadings of detrital organic matter which leads to high respiration rates causing pronounced dissolved CO_2 concentrations (Frankignoulle et al., 1998). Terrestrial nutrient loads act as the controlling factor as to whether the coastal zone will be net heterotrophic or autotrophic. Coastal seas can only be heterotrophic if the liberated CO_2 is not subsequently consumed by photosynthesis, which is, fuelled by nutrients (Smith and Mackenzie, 1987). A significant portion of DOC is decomposed and released back to the atmosphere as CO_2 through microbial respiration. Most estuarine systems are net heterotrophic (Smith and Hollibaugh, 1997; Gattuso et al., 1998) and therefore experience an overall increase in pCO_2 within the water column (Abril et al., 2000).

The major processes contributing to CO_2 enhancement in coastal zones are *in-situ* respiration driven by OM inputs, both natural and anthropogenic (Cole et al., 2001b), SGD (Maher et al., 2013), terrestrial surface water runoff (Raymond, Bauer and Cole, 2000), and precipitation of carbonate and silicate minerals (Hagedorn and Cartwright, 2010). Carbonate minerals are more reactive and soluble than silicate minerals. Carbonate and silicate minerals are precipitated by marine organisms, such as coral and molluscs, that need the materials to build their shells (Feely et al., 2009). CO_2 is a by-product of this reaction, as below:

$$Ca^{+} + 2HCO_3^{-} \leftrightarrow CaCO_3 + CO_2 + H_2O \quad (4)$$

Dissolved CO_2 may be highly enriched in groundwater (Macpherson, 2009; Dorsett et al., 2011) due to microbial decomposition of organic carbon (Gagan et al., 2002) and the subsequent build-up of CO_2. In fact, groundwater is often supersaturated with respect to CO_2, only equilibrating upon discharge (Atkins et al., 2013), and ergo, may be a significant source of carbon to the coastal environment and atmosphere (Cai and Wang, 1998; Raymond et al., 2000; Jiang et al., 2008). SGD not only transports DIC to the coastal zone, but SGD also acts as a source of OM and nutrients (Santos et al., 2008; Chen et al., 2010). High productivity stimulated by increased nutrient concentrations may result in increased autotrophy in these regions. Autotrophic activities may utilise DIC that creates an intense but localised sink for atmospheric CO_2 (Chou et al., 2009). A shift towards organic matter with higher C:N ratios at high CO_2 has been shown in mesocosm experiments (Doney et al., 2009) and could degrade the quality of food for consumers. The altered C:N ratio would also make the biological pump more efficient and cause increased carbon export to depth.

In conclusion, SGD-borne DIC transported to the coast is largely understudied and hence, little is known about its effect on the global carbon cycle of coastal areas. pCO_2 can be determined using DIC and TAlk and the first and second dissociation constants of carbonic acid (Dickson and Riley, 1978; Dickson and Millero, 1987; Lueker et al., 2000). Many studies have shown that SGD is an important pathway for DIC in many systems (Johannes, 1980; Cai et al., 2003b; Dorsett et al., 2011; Atkins et al., 2013; Szymczycha et al., 2014). In this study, SGD-borne DIC and TAlk will be studied to draw conclusions about the carbonate system of a karstic aquifer where SGD is the dominant freshwater source.

1.6.3.3 Ocean acidification (OA)

Seawater carbonate chemistry is governed by the below equilibrium reactions:

$$CO_{2(atm)} \leftrightarrow CO_{2(aq)} + H_2O \leftrightarrow H_2CO_3 \leftrightarrow H^+ + HCO_3^- \leftrightarrow 2H^+ + CO_3^{2-} \quad (5)$$

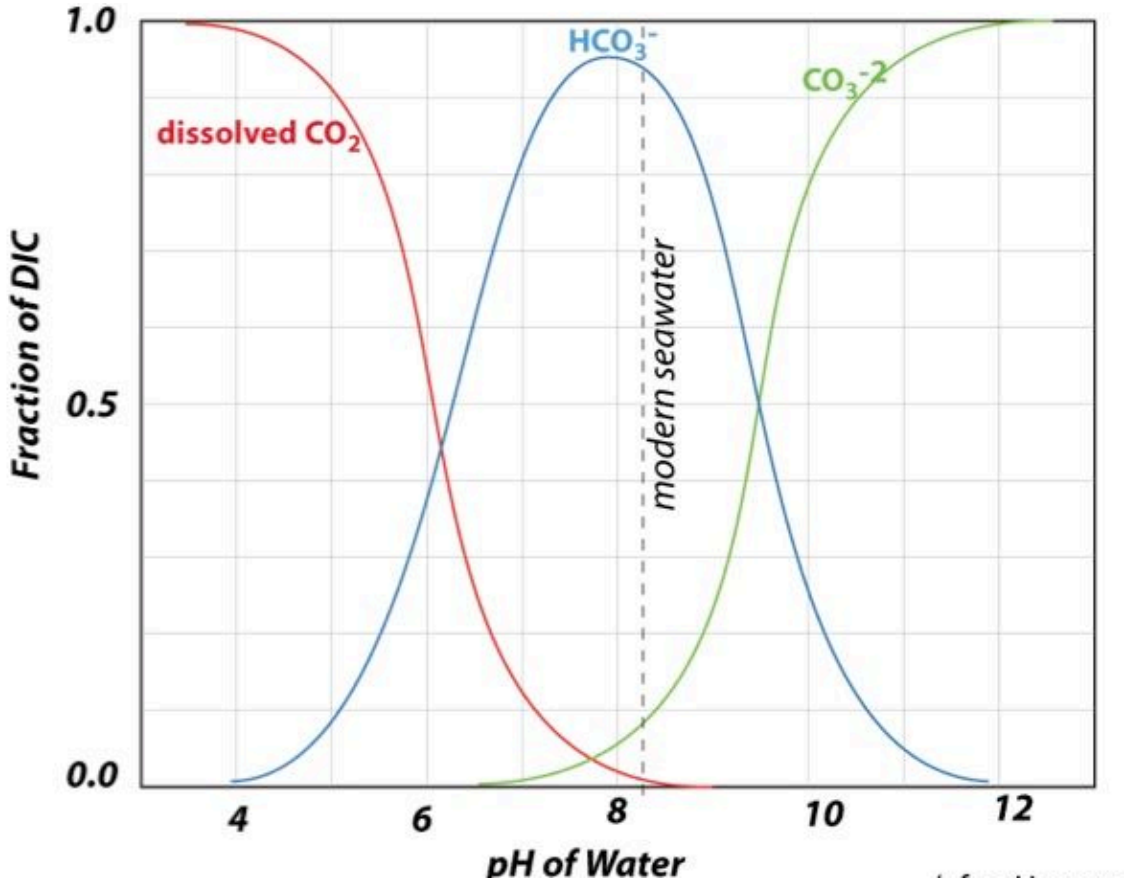

Figure 1.4: Relationship of DIC species with pH. Modern seawater has a pH of approximately 8.1, as highlighted in the figure. At this pH, HCO_3^- is dominant (after Holmén, 2000).

At surface seawater of pH 8.1, these reactions are reversible and near equilibrium (Millero et al., 2002) resulting in approximately 90% of inorganic carbon being in the bicarbonate form with only 9% as carbonate and 1% as CO_2 ions (Dickson, 2010). Physical uptake of anthropogenic CO_2 lowers the pH (Zeebe and Wolf-Gladrow, 2001) as CO_2 is hydrolysed to form carbonic acid. A decrease in pH results in a reduction of carbonate ion concentrations while bicarbonate and carbonic acid are produced (Figure 1.4) (Doney et al., 2009). This is the dominant driver of acidification in the open ocean (Dickson, 2010; Cyronak et al., 2014; Doney et al., 2009) and has

been occurring at a faster rate in recent years due to anthropogenic pressures (Cyronak et al., 2013). Acidification causes a lowering of the pH due to higher hydrogen ion concentration. Increased H^+ promotes $CaCO_3$ dissolution as per equation 6. The pH of the open ocean has decreased by 0.1 pH units since pre-industrialised times (Doney et al., 2009). Further pH reductions of approximately 0.002 pH y^{-1} are predicted to cause further acidification (Feely et al., 2004; Doney et al., 2009).

$$CaCO_3 + H^+ \rightarrow Ca^{2+} + HCO_3^- \quad (6)$$

Acidification can have drastic effects on biological processes and the biogeochemistry of marine ecosystems (Cyronak et al., 2013). High CO_2 concentrations and lower pH promote $CaCO_3$ dissolution (Gonfiantini and Zuppi, 2003). Mineral $CaCO_3$ derives from shells and skeletons of marine organisms. Studies show that some organisms, in particular warm-water corals and coccolithophorid algae, will exhibit reduced calcification in ocean acidified scenarios, (Feely et al., 2004; Kleypas et al., 2005; Doney et al., 2009). These calcifiers need to either adapt to the changing chemistry, migrate to carbonate-rich regions or suffer adverse impacts (Doney et al., 2009). In contrast, some planktonic calcifiers were shown to flourish under acidification conditions (Bown et al., 2004). Specie-specific responses vary as some species of coccolithophores were found not to be sensitive to elevated pCO_2 (Langer et al., 2006). Fabry et al., (2008) reviewed available data at that time and concluded that OA and the synergistic impacts of other anthropogenic stressors has far reaching yet varied specie-specific responses. Understanding the impact of OA on organisms is particularly relevant in areas such as Kinvara Bay where shellfisheries are a source of revenue for the region. The oceans long-term ability to absorb atmospheric CO_2 is dependent on the extent of $CaCO_3$ dissolution in the water column and the sediment.

Alkalinity is an important component of the carbonate system and must be considered in OA studies (Dickson, 2010). Alkalinity is a measure of the water's ability to resist changes in pH, i.e., its buffering capacity (Wong, 1988; Howland et al., 2000; Abril and Frankignoulle, 2001). TAlk can also be described as a measure of the proton deficit of a solution relative to an arbitrary defined zero level of protons (Dickson, 1981). Total alkalinity (TAlk) enhances the ocean's ability to buffer against pH changes while taking up more CO_2 (Zeebe and Wolf-Gladrow, 2001). TAlk in coastal zones can be described by equation (7). TAlk can be altered by the dissolution or precipitation of carbonate minerals. There is also evidence that dissolution rates of carbonates will increase in response to CO_2 forcing.

$$TAlk = HCO_3 + 2CO_3^{2-} + B(OH)_4 + OH^- + HPO_4^{3-} + 2PO_4 + H_3SiO_4 + [NH_3] + HS^- - H^+ - HSO^- - [HF]_4 - [H_3PO_4] - [HNO_2] \quad (7)$$

Total alkalinity responds to calcification, such that TAlk decreases as HCO_3^- is consumed in the ratio $\Delta TA_c = 2\Delta DIC_c$ (Gordon et al., 1996). DIC, however, contributes CO_2 upon discharge to the coastal ocean. Calcification increases CO_2 through changes in carbonate chemistry, as ~0.6 moles of CO_2 are released for each mole of $CaCO_3$ formed (Frankignoulle et al., 1994). Therefore, the rates of production, respiration, and calcification in benthic communities determine their influence on water column pCO_2. Mineral weathering is a primary regulator of atmospheric CO_2 concentrations over geological timescales (Berner et al., 1983), but studies have shown that the weathering rates may change over shorter timescales in response to land use change and global warming (Cai et al., 2003; Raymond and Cole, 2003). In general, carbonate materials have a lower resistance to weathering than silicate materials, and hence, a higher weathering rate under the same environmental conditions (Cai et al., 2008). Biogeochemical reactions have a significant impact on the TAlk in coastal regions. For example, Frankignoulle et al., (1996) observed a significant decrease of alkalinity with nitrification in the water column of the Scheldt basin. Further studies showed that there was highest alkalinity and NH_4^+ associated with the lowest nitrate and oxygen (Abril and Frankignoulle, 2000). Brewer and Goldman (1976) showed that an uptake of nitrate by three marine phytoplankton species caused an increase in alkalinity whereas an uptake of ammonia resulted in a decrease in alkalinity as NH_4^+ assimilation leads to strong acid production. This relationship is very important in nutrient enriched waters, as there is a large influx of these nutrients to the system.

Groundwater, worldwide, contains a broad range of TAlk from 90 to 23,300 mol L^{-1}, which is often higher than corresponding oceanic waters (Moore et al., 2011; Schopka and Derry, 2012) while at the same time providing a source of DIC. High concentrations of TAlk exported from limestone aquifers have been reported in Ireland (McGrath et al., 2015). Factors that contribute to the variations in DIC and TAlk in coastal zones include the mineralogy of the drainage basin, freshwater discharge, weathering intensity, estuarine mixing and biogeochemical reactions (Guo et al., 2010). TAlk is an important parameter for ocean acidification studies as Cyronak et al., (2013) illustrated, in their study at Heron Island, Australia, that enhanced alkalinity can partially buffer against ocean acidification on a local scale. Determining the balance between DIC and TAlk and the subsequent impact on the carbonate chemistry of coastal ecosystems is important in constraining whether groundwater sources act as a positive or negative feedback to OA (Cyronak, 2013).

1.7 Impacts and management issues

Coastal environmental governance should be concerned with SGD contaminant loading. Scientific understanding has increased dramatically in recent years, and this should be incorporated into all coastal management strategies globally, although this has been largely ignored in the United States (McCoy and Corbett, 2009) and elsewhere. The most common concern deals with nutrient loading

due to fertilisers and sewage. However, all forms of contamination are possible (Taniguchi et al., 2002a), particularly in vulnerable karst aquifers (Drew and Coxon, 1988; Coxon, 2011). Ecological effects in the coastal zone depend on water quality, which is affected by the level of terrestrial nutrients, organic matter, and metals, which may contribute to the degradation of surface waters (Corbett et al., 2000; Taniguchi et al., 2002a; Rocha et al., 2015). Management plans should also aim to protect the resource for human use in agriculture and industry as well as for drinking water. Therefore, the use of groundwater, groundwater-surface water interactions, and the chemical input into the coastal ocean via SGD must be researched and implemented into management strategies to establish sustainable strategies that add to the social, economical, environmental and biological fulfilment of coastal systems.

1.8 Synopsis

SGD may deliver substantially elevated material fluxes to the coastal zone (Liu et al., 2012; Szymczycha et al., 2014), including dissolved inorganic and organic nutrients, DOC, DIC and TAlk (Shaw 2003; Burnett et al., 2003; Moore, 2010; Liu et al., 2014; Szymczycha et al., 2014). SGD has been shown, in many cases, to be the dominant pathway of material exchange between terrestrial and oceanic eco-compartments and is widely unquantified and under-represented in the literature (Cai et al., 2003; Moore, 2010). While this introduction highlights the importance of SGD inputs in to the coastal zone, the contributions of SGD to coastal biogeochemical budgets are far from being understood (Moore, 2010).

1.9 Study Site – Kinvara Bay, Co. Galway, Ireland

1.9.1 Choice of study site

Using thermal infrared imagery, research carried out by the Biogeochemistry Research Group (BRG) in Trinity College, Dublin highlighted 35 parts of the Irish coastline, including Kinvara Bay, that are potentially significantly influenced by submarine groundwater discharge (SGD) (Wilson and Rocha, 2012), outlined in Figure 1.5.

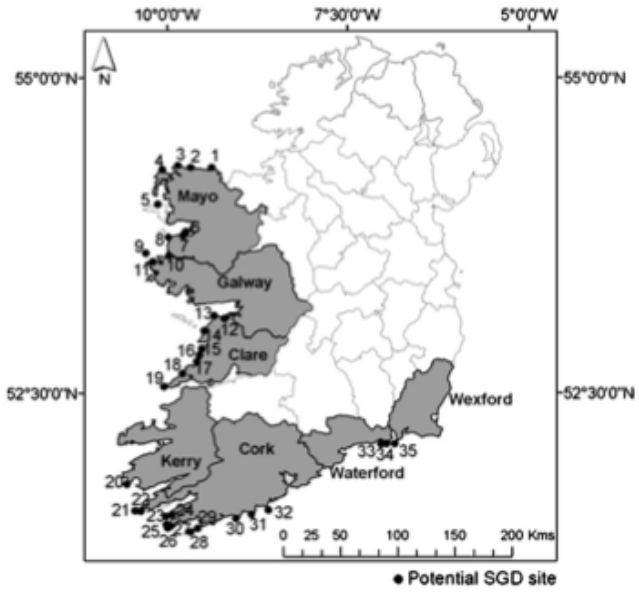

Figure 1.5: 35 potential SGD sites around the coast of Ireland identified using thermal infrared imagery (Wilson and Rocha, 2012). Kinvara Bay is located above site 13 on this map.

Kinvara Bay was chosen as a research site for four primary reasons. Firstly, the karstic nature of the aquifer allows for rapid transport of groundwater and associated constituents to the sea (Drew, 2008). Therefore, attenuation within the aquifer is minimised, and near conservative transport of any contaminants from source to sea might be reasonably assumed. Secondly, SGD is the primary freshwater source to the bay and accounts for the majority of allochthonous nutrients and carbon. Thereby, any inferences drawn in regards to metabolism can be linked to SGD. Thirdly, the bay is easily accessible, and lastly, the land use within the catchment is agricultural. Thus, Kinvara Bay is a natural laboratory for the study of SGD.

1.9.2 Irish karst aquifers

Irish limestones predominantly belong to two geological periods: the Carboniferous (approx. 300-340 million years B.P.) and the Cretaceous (approx. 70-120 million years B.P.). Carboniferous limestone is the most common rock type in Ireland (Karst Working Group, 2000) underlying approximately half the land surface (30,000 km^2) (Figure 1.6). It is composed primarily of calcite (calcium carbonate) and to a lesser extent by dolomite (calcium and magnesium carbonate). Carboniferous limestone is found in almost every county in Ireland (excluding Antrim and Wicklow), these rocks are usually hard and grey/black, whereas, Cretaceous limestones are only found in Ulster (North) and are somewhat softer and usually white (Karst Working Group, 2000).

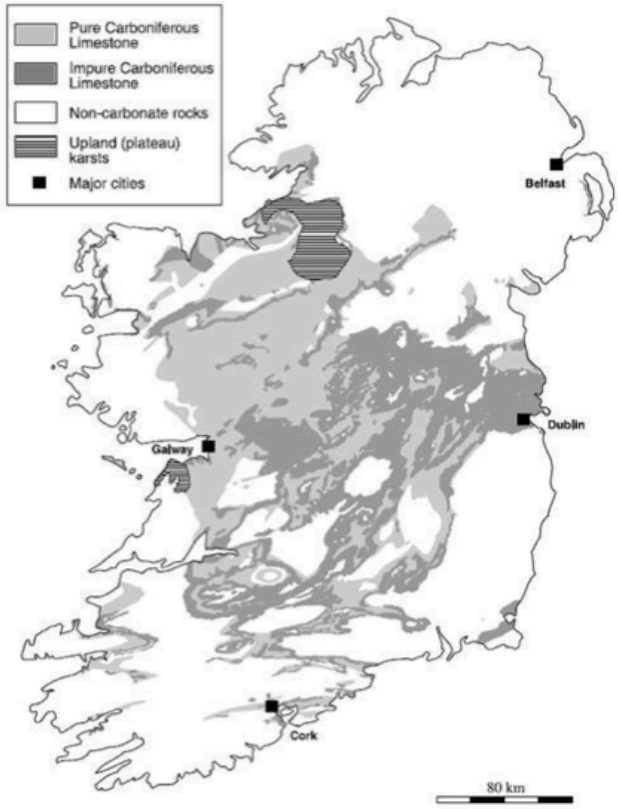

Figure 1.6: Distribution of Carboniferous limestones in Ireland (Drew, 2008). Kinvara Bay is situated in the major city of Galway, highlighted on map.

Limestones in Ireland are often heavily karstified (Drew, 2008). Karstification has been episodic as it was confined to times when base levels were suitable and when limestone was exposed (Drew and Jones, 2000). Accordingly, karst features have been documented in 80-85% of limestone outcrops in Ireland (Drew, 1996), although the degree of karstification is spatially inconsistent as it is dependent upon the purity of the limestone, which is not uniform throughout the country (Drew, 2008). Impure limestones commonly contain sand, clay and chert, which may be distributed throughout the rock or concentrated in distinct beds, such as beds of shale, and may be present in great proportions. Purer limestones are more susceptible to karstification, as they are more brittle allowing for fractures to form (Drew and Jones, 2000).

Irish karst is predominately found in lowland regions. As a result, karst often underlies productive agricultural land as well as major centres of population (Drew, 2008). As a result, the vadose zone can be relatively shallow, and epikarst often develops within the phreatic zone. Hence, a significant portion of diffuse flow occurs through the epikarstic zone and, therefore, horizontal flow can occur within the epikarst as opposed to the more typical vertical flow of other karst systems. Karstic systems thus have the ability to transmit large volumes of groundwater through preferential flow paths, particularly in conduits, to karst springs that can discharge directly to the ocean (Fleury et al., 2007). Consequently, SGD acts as a direct link for terrestrial matter to the coast in these

aquifers. In fact, there is often near conservative transport of constituents such as nitrate through the subterranean path (Kamermans et al., 2002). SGD can have serious implications for the productivity of coastal zones of such regions as a result.

1.9.3 The Gort Lowlands

The Gort Lowlands catchment located in Galway, Western Ireland is categorised as a regionally important karstified aquifer (Drew, 2008). A defining feature of this catchment is that half of it is underlain by impermeable non-calcareous rocks, primarily Devonian sandstone found in the Slieve Aughty Mountains (Coxon and Drew, 1998). Deposits of glacial drift mantle the bedrock over most of the lowland regions of Ireland, but in the Gort Lowlands region glacial deposits tend to be less thick, and bedrock is often exposed (Drew and Coxon, 1988). Lowland systems are characterised by considerable surface-groundwater interactions, evident by the presence of karst features such as sinking and rising streams, swallow holes, estavelles, turloughs and springs. These karst landforms and features are a significant aspect of the Gort-Kinvara landscape.

Turloughs are karst wetland ecosystems found in karst regions that are virtually unique to Ireland, due to the lowland nature of karst aquifers (Skeffington et al., 2006). A turlough is a topographic depression in karst, which is intermittently flooded on an annual cycle as the water table rises (Gill et al., 2013). Generally, turloughs in this region fill due to the insufficient capacity of the underground karst system to transport heavy flows due to increased precipitation. This causes the conduits to surcharge and turloughs then fill and drain through swallow holes, which have a rapid response to rainfall and short hydraulic residence times (Gill et al., 2013). They typically fill and empty once a year and are dry over the late spring/summer period in response to precipitation patterns. However, some turloughs do not follow this pattern and may fill and empty several times in one year (Pereira et al., 2011). This region still contains a significant number of natural turloughs, which have mostly been left untouched (Coxon and Drew, 2000; Karst Working Group, 2000).

1.9.4 Hydrogeology and climatology

Ireland's temperate maritime climate is moderated by the North Atlantic Drift oceanic current, which results in generally warm summers (18–20°C) and mild winters (8°C) (www.met.ie/climate-ireland). In the West of Ireland, annual precipitation is approximately 1500 mm while 980 mm of this is not evapotranspired, thereby, leaving an effective rainfall of c. 520 mm (Drew, 1990). December and January are the wettest and evaporation is assumed to be minimal during winter months. Figure 1.7 shows the total rainfall and potential evapotranspiration for 2015. In this year, 1,575 mm of rain fell with only 502mm of potential evapotranspiration. Rainfall can be rapidly incorporated into groundwater, as infiltration and mixing of surface and groundwater can happen quickly in karstic aquifers (Gill et al., 2013). The limestone aquifer is characterised by rapid

recharge, low storage and rapid transmission of water (Drew, 1990). As such, November-January is expected to have the highest levels of SGD flow.

However, flooding in this region is common due to excessive precipitation events. There were four major flood events between 1989 and 1995. Then, in November 2009 there were record amounts of rainfall, with a monthly total of 329.4 mm. This major flooding event prompted an investigation, known as the Gort Flood Studies. The study concluded that the flow capacity of the underground system was exceeded which caused water levels to rise at Caherglassaun Lough and then Coole Lough. The head differential between Coole and Kiltartan decreased significantly which further reduced the capacity of the underground system (Jennings O'Donovan and Partners, 2011). Then, in 2015, there was more extreme flooding in the region. Rainfall of 297 mm and 437 mm was recorded in November and December 2015, respectively (McCormack and Naughton, 2016).

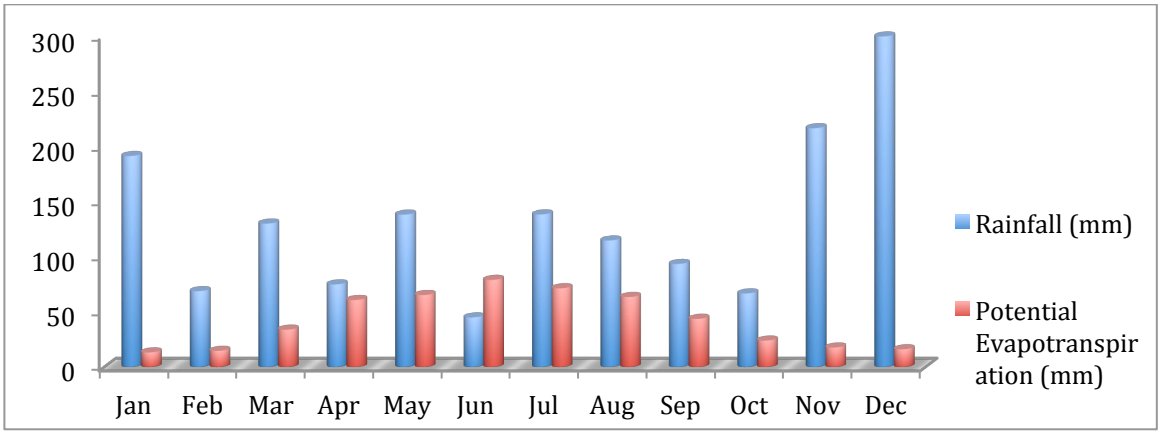

Figure 1.7: Total rainfall (mm) and potential evapotranspiration (mm) for the year 2015, measured at the closest Met Eireann weather station, Athenry, 26.2 Km north of Kinvara town (http://www.met.ie/climate/monthly-data.asp?Num=1875).

The area is bounded by the Slieve Aughty Mountains to the east and the Burren to the west (Drew, 1990). Three rivers, the Owenshree, the Ballycahalan and the Owendullullegh, drain northwest from the mountains and sink underground at the point or close to the point of geological contact and from the non-carbonate catchment to the lowlands, a carbonate aquifer. This allogenic recharge supplies chemically aggressive waters as it is relatively acidic due to the peaty catchment of the mountains and has aided the development of karstic features through the dissolution of calcium carbonate. Locally thick deposits of till may distort the behaviour of the allogenic recharge (Coxon and Drew, 1998).

These three rivers converge at Kiltartan via two large conduits as Coole River. The Coole River flows into Coole Turlough, which is the largest turlough of this system and forms a part of the Coole-Garryland Special Area of Conservation (SAC). As the water drains from the Coole-Garryland complex, it flows into Caherglassaun Turlough. This turlough is small with limited surface inflow and is last in the chain, located 5 km from the sea (Gill et al., 2013). The drainage from this point until Kinvara Bay is entirely subterranean and the landscape is devoid of surface

water. Tracer studies (Figure 1.8) illustrate the complex nature of the underground water flow (Drew, 2003).

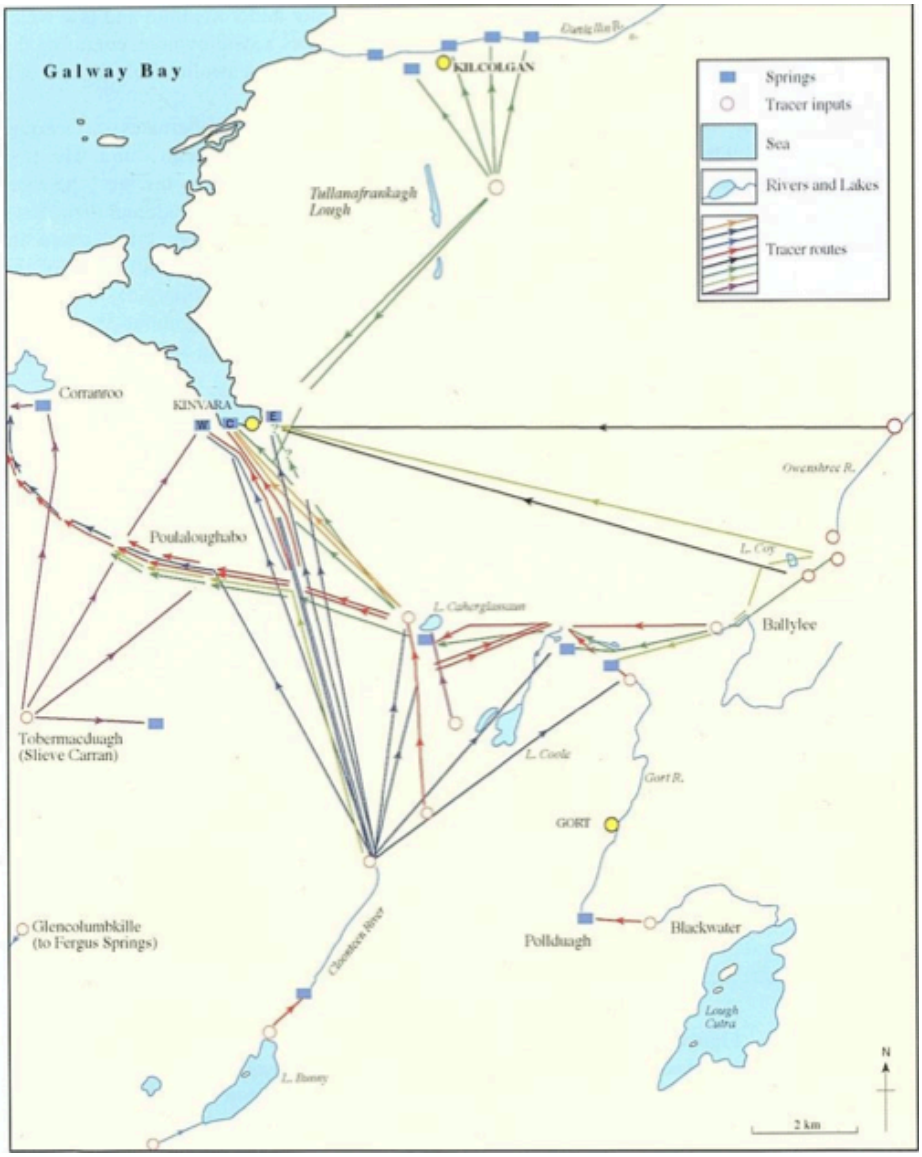

Figure 1.8: Tracer tests in the Gort Lowlands catchment showing the groundwater flows underground and its exit at Kinvara Bay carried out as part of the Gort Flood Studies Report (Drew, 2003).

Water fed by the allogenic streams, in full or part, is generally sediment-rich, acidic, and has a variable temperature by comparison to water fed by epikarst waters (Coxon and Drew, 1998). Deposits are typically thin, patchy, liable to erosion (less than three metres thick) and in some areas rendzina soil overlies the pure limestone bedrock directly (Coxon and Drew, 1998). Glacial deposits, however, several metres thick and basin peats are common in the eastern section of the study site confined to the dolines, which are suitable for cultivation (Karst Working Group, 2000).

The subsoils are predominantly till, covering approximately 50% of the area, with rock outcrop occupying a large proportion of the remainder. Their role is predominantly a local response, as their influence on the overall hydrologic response is low. Locally, they may be essential for groundwater storage and runoff rates. Their effect will depend upon their characterisation as they

may confine the limestone aquifer, or, at the other extreme, function as an aquifer with high storage, feeding water into the highly transmissive aquifer underneath (Drew, 2008).

Karst aquifers are particularly vulnerable to contamination due to their high permeability, which is often found in combination with thin soil layers (Coxon, 2011). In addition to this, groundwater flow velocity is elevated, compared to alluvial aquifers, which doesn't allow sufficient time for self-purification (Kačaroğlu, 1999). Furthermore, sinking streams provide a direct entry point to groundwater and dolines provide a direct entry route through vertical shafts, both with little attenuation capacity (Karst Working Group, 2000) by adsorption, ion exchange, chemical breakdown or microbial interactions (Coxon and Drew, 1998). Conduit flow, thereby, allows rapid transfer of contaminants, resulting in short underground residence times and lack of natural filtration in these systems (Coxon and Drew, 2000).

1.9.5 Kinvara Bay

Kinvara Bay (53° 09' N, 8° 56' W) is elongated in the NNW-SSE direction and connects to the southern edge of Galway Bay, which opens to the Atlantic Ocean (Figure 1.9). The bay is approximately 4.5 km long and has a maximum submerged area of 5.97 km^2, as determined by analysis of LANDSAT imagery, has an average depth of 4.2 m and a mean high tide water volume of approximately 21 x 10^6 m^3 (Rocha et al., 2015). Tides are semi-diurnal with a range of 2 – 4.5 m, with an average height of 3 m. Neap-spring tidal cycling and freshwater inputs can be seen in the bay (Cave and Henry 2011). It is the focal point for waters discharging from the Gort-Kinvara aquifer (Dobson and Laming, 1999; Cave and Henry, 2011; Gill et al., 2013), through the subterranean pathway as SGD and surface drainage in the form of runoff (Figure 1.10). This underground drainage system has a total zone of contribution area of 483.41 km^2 (EPA, 2011), in which two major (located in the SSE limit of the bay) and possibly other minor SGD points discharge land-borne water directly into the coastal zone. Periodically, there may be shallow rivulets entering the bay at times of high discharge. These are fed by seeping groundwater from the karstic subsurface into open wetlands that are attached to the bay's shoreline. Schubert et al., (2015) showed that this water discharge exhibits groundwater characteristics, as indicated by pH and EC data.

At the time of this study, Kinvara Bay did not have a wastewater treatment plant. Instead, sewage is delivered to a collection system which provides approximately 70,000 gallons of untreated sewage to Kinvara Bay daily through a marine outfall pipe (Ciaran Cannon, 2010; Galway County Council, 2013). The discharge point is 100 m northeast of the pier head of Kinvara town (see Figure 1.9). Sewage composition is a combination of ‘dark water' (raw sewage), ‘grey water' (general household bath and cleaning water) and storm water. SGD represents the major freshwater input to the bay, but sewage may deliver significant concentrations of nutrients and carbon.

Therefore, evaluation of both sources, SGD and sewage, regarding biogeochemistry must be conducted.

Figure 1.9: Map of Kinvara Bay highlighting the main sampling sites. These sampling locations were selected as a continuum of groundwater from land discharging into Kinvara Bay and exiting into the open ocean at Parkmore Pier. Kinvara Bay is a semi-enclosed system, and these sampling locations represent the boundaries of the system in terms of box model studies. These sites are represented by stars on the map, Loughcurragh South (inland borehole) represented by the yellow star, Dunguaire Castle (the major spring for SGD) represented by red star, the sewage outfall point represented by the green star, the sediment collection points in the intertidal zone represented by the blue star and Parkmore Pier (exit point for waters discharging to Galway Bay) represented by the orange star.

Figure 1.10: A photograph of Kinvara Bay taken from the entrance to Dunguaire Castle highlighting the main SGD and intertidal sampling sites. These sampling locations were selected as the main SGD springs and an undisturbed location to take sediment samples. These sites are represented by circles on the map, Dunguaire Castle (the major spring for SGD) represented by a green circle, the Arch SGD springs represented by a red circle and the sediment collection points in the intertidal zone represented by the purple circle.

1.9.6 Human ecological and economic importance

The population of Kinvara town itself was 620 and including the surrounding rural areas was 1,351, according to the 2011 Census (CSO, 2012). Kinvara is a mainly rural town consisting of residential and small business properties. The focus for employment has been in the agriculture, fisheries and forestry industries as well as tourism (Galway County Council, 2012). Galway Bay is designated as a Shellfish Water Area under the European Shellfish Water Directive (2006/113/EC) (EPA, 2006). There are numerous commercial shellfisheries including natural oyster beds. Within Kinvara Bay itself, there is a blue mussel (Mytilus edulis) shellfish farm (Cannon, 2010). Therefore, the Kinvara Bay ecosystem is an important socio-economic site as it, directly and indirectly, provides employment, recreation, goods and services to the local population. As highlighted above, the catchment forms a part of a SAC in the form of the turloughs. Additionally, however, the bay also forms part of the Galway Bay Complex SAC, the Inner Galway Bay Special Protection Area (SPA) and is protected under the Ramsar Convention (EPA, 2006).

SGD is responsible for delivering carbon and nutrients and thereby influencing the ecological status of the bay, which may threaten the commercial fish and shellfish activities (Schubert et al., 2015). Any changes in these inputs will affect the composition and productivity of the ecosystem. The ecological status of the Bay has been classified as poor in the past (EPA, 2012) but is currently classified as ‘Good' (EPA, 2015). Periodically the bay has been shown to fail the WFD

requirements for dissolved inorganic nitrogen thresholds in winter and shows moderately high biochemical oxygen demand (BOD) levels (2 - 4 mg L^{-1}), with episodes of low water column oxygen concentration observed in summer (O'Boyle et al., 2009).

The quality of discharged water is dependent on practices within the catchment area (Schubert et al., 2015). Practices including fertiliser spreading, forestry and septic tank discharges influence the chemical input to the coast via SGD and may lead to contamination and in the extreme case, eutrophication. Agricultural sources of pollution include badly maintained farm wastes; unmanaged farm runoff and disposal in swallow holes. Over the last few decades, the use of inorganic fertilisers on agricultural lands has increased globally (Matson et al., 1997). This increase has led to implications for groundwater quality, particularly that of nitrate concentration (Kroeger and Charette, 2008; Ibánhez et al., 2013; Ji et al., 2013). The use of organic materials such as agricultural wastes (manure, slurry, silage effluent and agricultural runoff) has also increased dramatically. In Gort-Kinvara catchment, key swallow holes are overgrown, with floating debris that could potentially block the entrance. Many swallow holes are not secured from animals, which could lead to disturbance of the area and the possible entry of contaminants to the underground system (Southern Water Global, 1998). Dry turloughs provide rich grazing land for domestic livestock during the drier summer months. Different grazing regimes may be utilised as fields are often under different management both between and within turloughs (Skeffington and Gormally, 2007). Grazing may impact the flora and fauna of the turlough but also acts as a source of carbon and nutrients through manure. Turloughs are host to a low number of specialised flora and fauna, which may grow from the turlough edge to its base. Species are divided into two groups, amphibious species that can withstand flooding and those that can quickly colonise after emptying (Goodwillie, 2003).

The catchment has been classified primarily as grassland (agricultural land) with sizeable forest and peat coverage. Therefore, pollution associated with agriculture such as leaching of fertiliser may occur. Other pollution sources include disposal of wastes such as household wastes and dead animals into natural depressions. Leaking fuel storage tanks, both domestic (above ground) and commercial (underground), and septic tank effluent pose a severe water pollution risk (Karst Working Group, 2000; Coxon, 2011). Approximately 6,000 septic tanks are used to store domestic sewage throughout 900 km^2 of Hydrometric Area 29, which is mostly consisted of the Gort-Kinvara aquifer. Many of these tanks have been sited on unsuitable land with thin soil due to poor regulation (Smith and Cave, 2012). This land-borne N and dissolved organic matter (DOM) contamination may be rapidly transferred into the littoral zone with little mitigation available *en route* to discharge in the bay due to the low residence time and well-oxygenated conditions of the karstic aquifer. Theses conditions prevent anoxia-dependent removal processes such as denitrification, DNRA and anammox (Slomp and Van Cappellen, 2004). However, karst systems

favour P removal via sorption to iron oxides. Thus, there is an expected increase in the C:N:P ratio of SGD (Slomp and Van Cappellen, 2004).

The bay is a natural oyster bed (Cannon, 2010), the site of mussel aquaculture industry and the focus of recreational activities vital to tourism in the region. Tourism (~18,000 people per season) is the main tertiary industry in the region and provides the main source of employment (Gallagher et al., 2010) and brings a concomitant influx of pollution to the area, transferred into the bay as sewage. This is seasonally derived as tourism numbers peak during the summer months.

1.9.7 Previous studies

1.9.7.1 Hydrological studies

One of the earliest hydrochemical studies of the region was carried out to determine the hardness of water as it discharges out at Kinvara Bay (Williams, 1964). The region has remained an area of research interest with many studies conducted here throughout the years (Coxon and Drew, 1998; Dobson and Laming, 1999; Deakin, 2000; Einsiedl, 2005; Kilroy and Coxon, 2005; Sheehy Skeffington et al., 2006; Cave and Henry, 2011; Coxon, 2011; Pereira et al., 2011; Petrunic et al., 2012; Naughton et al., 2012; Smith and Cave, 2012; Premrov et al., 2012; Gill et al., 2013; Gill et al., 2013; McCormack et al., 2014; Rocha et al., 2015; Schubert et al., 2015) as the catchment has seen relatively little human impact on the natural drainage system which includes surface to groundwater interactions and many karst features, including several turloughs. Most of these studies have concentrated on the flow and movement of water underground before discharge, with a particular interest in turloughs and their filling/emptying regimes (Skeffington et al., 2006; Coxon, 2011; Pereira et al., 2011; Gill et al., 2013).

1.9.7.2 SGD studies

The two springs, known as the Castle (Kinvara West) and the Arch (Kinvara East) are located in the lower intertidal zone and discharge chemically distinct waters. It is understood that the Castle is the main discharge point for the Gort Lowlands system drawing from a deeper source than the Arch (Cave and Henry, 2011).

Cave and Henry, (2011) estimated SGD flows of up to 80 - 100 $m^3 s^{-1}$ using a whole catchment hydrological balance method. However, this value may exaggerate the true discharge flow, as all freshwater entering the bay was associated with SGD, not accounting for direct precipitation, runoff and sewage inputs, which may also contribute to the freshwater flux to the bay and removal on land through abstraction and evapotranspiration. Other studies aimed at estimating the SGD flow rate may reflect a truer representation; Coxon and Drew, (1998) quote flows typically 5-10 $m^3 s^{-1}$ and increasing beyond 20 $m^3 s^{-1}$ during high winter flow. Drew, et al., (1997) estimated mean water flux through the aquifer as 4–5 $m^3 s^{-1}$ with high winter flows exceeding 15 $m^3 s^{-1}$ and McCormack et al., (2014) estimated an average flow rate of 8.7 $m^3 s^{-1}$. Schubert et al., (2015)

recently used Kinvara Bay as a case study for determining the effectiveness of electrical conductivity (EC), pH and radon as tracers of SGD in the coastal zone. This study revealed that radon was the most sensitive indicator for SGD, but in fact, the combined evaluation of radon, EC and pH can separate the groundwater contribution from that of surface water. SGD has been calculated as $10.4 \pm 6.3 \times 10^4$ m^3 d^{-1} (Rocha et al., 2015) using radon from an average of four summer (low flow) campaigns. However, winter (high flow) SGD rates may be significantly higher.

Discharge into the bay is pulsed and modulated by the tide. Therefore, SGD estimates have been scaled using the tidal cycle to times of peak discharge. Thus, SGD rates of 0.5 – 6.8 m^3 s^{-1} have been calculated for summertime (Rocha et al., 2015). This range has good agreement with the lower end estimates of previous studies (Drew, 2008). Exchange of water between Kinvara Bay and Galway Bay occurs due to tidal flushing. Therefore, the residence time of water within the bay is heavily influenced by wind speed and direction along the wave height, tidal phase and volume of freshwater discharge (Smith and Cave, 2012; Rocha et al., 2015). The measured residence time using radium was found to be 6.8 ± 1.7 days (Rocha et al., 2015). With this, it can be seen that Kinvara is not well mixed horizontally or vertically and there is slow tidal exchange resulting in a portion of groundwater being retained within Kinvara Bay.

1.9.7.3 Carbon and nutrient studies

There have been numerous studies conducted in Kinvara measuring nutrient concentrations (Smith and Cave, 2012; McCormack et al., 2014; Rocha et al., 2015). The nutrient concentrations determined by Rocha et al., (2015) are outlined in Table 1.3. Nitrate was the dominant form of DIN whereas total dissolved phosphate (TDP) concentrations were low.

Table 1.3: Summary of measured water nutrient concentrations in SGD endmember (mean salinity = 0.61 ppt), measured at the Kinvara Springs located within the bay over the course of four sampling campaigns during summer. Data are the result of the mean of several replicates plus or minus the standard error of the mean (± SE) (Rocha et al., 2015).

Parameter	Concentration (μmol L^{-1})
NO_3^-	79.4 ± 5.6
NH_4^+	0.5 ± 0.15
NO_2^-	0.3 ± 0.15
TDP	1.4 ± 0.03
$Si(OH)_4$	75.8 ± 2.61

The EPA monitor groundwater flows and nutrient concentrations at Kinvara Bay from the Kinvara Springs. Their long-term average nutrient values for SGD samples taken at the Springs from 2007-2010 were higher than those recorded by Rocha et al., (2015) but the EPAs period includes a 2009 flood event. Ammonia concentrations were low, close to zero but nitrate concentrations were 112.9 μmol L^{-1} reaching as high as 250 μmol L^{-1}. In addition, three spot samples taken by the EPA in 2009 had an average nitrate concentration of 92.7 μmol L^{-1}. Smith and Cave, (2012) also measured TOxN (total oxidised nitrogen, nitrate plus nitrite) from the two SGD springs (fresh SGD) and found levels of 52.8 μmol L^{-1} at the Castle and 23.6 μmol L^{-1} at the Arch. They concluded that the Castle discharge point draws from a deeper water source and maintains a strong flow year round. The mean N concentration measured by McCormack et al., (2014) was 75 μmol L^{-1} at the Arch and 142 μmol L^{-1} at the Castle.

Phosphate concentrations in SGD were very low amounting to less than 5 μmol L^{-1} at all sampling times (Rocha et al., 2015). N:P availability ratios of 173 and Si:P of 503, greatly exceed the Redfield ratio (Rocha et al., 2015). P limitation of primary producers is a concern in SGD influenced areas across the globe (Slomp and Van Cappellen, 2004) due to this imbalance in concentrations transported via SGD. Smith and Cave, (2012) also determined that SGD is not a source of DIP to Kinvara Bay. Carbon studies are scarce in the region, with only one study of DOC published to date (Smith and Cave, 2012). DOC concentrations of SGD taken during 2009 floods were 200 - 300 μmol L^{-1} compared to higher salinity sample concentrations of 50 - 100 μmol L^{-1}. Concentrations reached as high as 600 μmol L^{-1} during autumn. This agrees well with the TOC concentrations published by the EPA in 2009 of 290 - 400 μmol L^{-1}. There is no study outlining dissolved inorganic carbon (DIC) and alkalinity (TAlk) within the bay. EPA monitoring data recorded alkalinity as 230-344 mg L^{-1} HCO_3 for the period 2007 to 2010 at the SGD springs in the bay. Sources of DIC to groundwater in this region may include meteoric recharge (including

weathering reactions), limestone dissolution, sediment diagenesis and, within the estuary, exchanges with the atmosphere and seawater intrusion (Dorsett et al., 2011). As this is a karst region, concentrations of DIC may be significant.

1.10 Research questions and hypotheses

The overarching research objective of this study was to characterise the sources, quantities and biogeochemical significance of C, in the forms of DOC, DIC, DOM, TAlk, and inorganic nutrients (N, P and DRSi) transported via SGD to the coastal zone in Kinvara Bay. This objective was pursued with a basis on the following research hypotheses:

1. SGD is the main source of nutrients to Kinvara Bay, irrespective of flow regime (i.e., dry, wet). The three allochthonous sources of nutrients to the bay were sewage, atmospheric deposition and SGD at the time of this study. SGD was expected to be the highest contributor of nutrients due to the large daily discharge into the bay.

2. SGD contributes to P limitation in Kinvara Bay irrespective of flow regime. The high fluxes of DIN associated with SGD have been shown to cause P limitation in Kinvara Bay during summer (Rocha et al., 2015). Although DIN concentrations were expected to be lower during winter compared to summer due to seasonal land use within the catchment, it was hypothesised that DIN fluxes were still comparatively larger than P due to the karstic nature of the aquifer and the fresh characteristic of SGD.

3. Nutrients are retained within the bay during summer but are exported to Galway Bay during winter. It was hypothesized that nutrient fluxes delivered via SGD were retained within the bay during low flow (Rocha et al., 2015) due to high productivity fuelled by longer sunlight hours and higher temperatures. Nutrients were expected to be transported to the larger Galway Bay during winter due to lower productivity.

4. Kinvara Bay is eutrophic in summer compared to mesotrophic in winter due to higher nutrient loading and resultant productivity.

5. CDOM delivered via SGD is labile in summer but refractory in winter due to the agricultural land use within the catchment.

6. Increased levels of SPM cause labile CDOM to be effluxed from sediments. It was hypothesised that the presence of high DIN will cause further productivity and fuel labile CDOM to be effluxed from the sediments.

7. Kinvara Bay acts as a net sink of CO_2 in summer due to productivity fuelled by SGD-borne nutrients.

8. SGD contributes to coastal ocean acidification due to the naturally lower pH of discharging waters and high DIC loading, although this is in combination with high TAlk loads.

9. Experiments conducted by Linh Trieu (2015) and Manaswi Raghurama (2015) examined future 'what-if' scenarios of the impact of plastic pollution and a change in suspended particulate matter on the nutrient fluxes in Kinvara Bay. Using these experiments, I examined the impact of CDOM efflux from sediments under these future scenarios. The hypothesis of this experiment was that plastic pollution causes further recalcitrance of the CDOM within Kinvara Bay. Due to the chemical makeup of plastic fragments, it was expected that breakdown processes would contribute refractory CDOM.

1.11 Chapter summaries

Chapter 2 – Quantitative nutrient budgets

The aim of this chapter was to build on work by Rocha et al., (2015), who conducted a summer N, P and DRSi budget over the course of 4 years and Smith and Cave, (2012) who conducted an annual N, P and DOC study in Kinvara Bay. In this study, I developed quantitative N (DIN and DON), P and DRSi budgets based on the two primary flow regimes characteristic of karstic regions, high and base flow. The fluxes associated with terrestrial groundwater were examined by, firstly, determining the SGD volume by use of water/salt budgets and natural tracers (^{222}Rn) where possible, and secondly, determination of N, P and DRSi loading. Internal processes affecting the biogeochemical cycling within the bay and the net export/import of inorganic materials with the open ocean were examined. Furthermore, the molar ratios of DRSi:N:P in SGD were investigated as SGD has been shown to contribute to P limitation of primary productivity in coastal ecosystems.

SGD was the largest source of oxidised nitrogen but the lowest source of ammonium and phosphorus across all campaigns. Dissolved organic nitrogen (DON) fluctuated significantly from season to season but was highest during the wettest campaign (January 2015). SGD delivered a substantially higher N:P ratio than the Redfield Ratio of 16 due to the high dissolved inorganic nitrogen (DIN) flux compared to P. Sewage accounted for 74% of allochthonous P inputs. A wastewater treatment plant came into operation in Spring 2017 and hence raw sewage input has been removed from the bay and now P limitation may become an even more substantial issue. Nutrients were retained within the bay during all sampling time campaigns. The bay was net autotrophic during July 2013, June 2015 and January 2016 but net heterotrophic during January 2015 (the wettest campaign) regarding N metabolism.

Chapter 3 – Evaluation of the importance of SGD-borne carbon in the coastal zone

SGD in karstic systems contribute significant fluxes of DOC, DIC and total alkalinity to the receiving water body. The contribution of pCO_2 associated with SGD inputs was assessed to determine whether Kinvara Bay acted as a sink or a source of CO_2 in the local C budget. Kinvara Bay was net autotrophic and sink for carbon during July 2013, June 2015 and January 2016 but net heterotrophic during January 2015 and acted as a source of CO_2, which corresponded to the wettest month. Elevated CO_2 fluxes could have serious implications for ocean acidification. This is particularly important in regions such as Kinvara Bay that rely on shellfish farms as a source of revenue. Quantification of the DIC and total alkalinity delivered via SGD to Kinvara Bay indicated that SGD buffered against ocean acidification in Kinvara Bay due to the higher TAlk loading. pH within the bay was higher in summer campaigns due to increased seawater mixing but also corresponded to higher dissolved oxygen and temperature.

Chapter 4 – Determination of SGD-borne CDOM in Kinvara Bay

Chapter 4 assessed the SGD-borne CDOM to the coast by use of EEMF-PARAFAC modelling. SGD was responsible for the delivery of predominately humic-like substances, which were highly refractory. Peak T, a protein-like component, was validated as a secondary component in the 3-component model but with low intensity (0.005 R.U.) Groundwater was shown to carry mainly refractory CDOM in relatively pristine conditions due to the humic nature of the aquifer. Anthropogenic pressures can cause pollution of groundwater with more labile materials transported in late spring and autumn through the use of fertilisers and septic tank leakage. The karstic character of the aquifer allows for fast-flowing groundwater with little time for modification in-land. Therefore, any anthropogenic labile material would be expected to be present in the CDOM signature of SGD.

Chapter 5 – Future scenarios of CDOM efflux

Chapter 5 investigated realistic future scenarios of both land-use change (leading to higher N:P ratios) and anthropogenic pressure, regarding plastic litter, in terms of the CDOM fluxes to the water column. The effect of these future scenarios on the relatively pristine CDOM components present in Kinvara Bay was analysed during the summer, as this was considered worst case. *Fucus vesiculosus* and *Enteromorpha intestinalis* were the dominant macroalgae at the SGD outflow and were selected for further analyses. In future scenarios, particularly when *Enteromorpha* dominated, there was an increased flux of labile materials from the sediment to the water column. Plastic pollution was not significantly different from the control for CDOM efflux. This may be due to the types of compounds present in plastic, long organic polymers, which may not be susceptible to degradation or due to the incubation time of five days. Thus, plastic pollution may pose greater influence in the open ocean.

Chapter 6 – Characterisation of SGD-borne DOM using FT-ICR-MS Analysis

CDOM investigated using EEMF-PARAFAC was predominantly refractory in nature (Chapter 4), with minor seasonally derived secondary labile peaks. Therefore, an incubation study was conducted to analyse the possible influences of bio- and photo-degradation on allochthonous DOM in Kinvara Bay. Studies have shown that refractory DOM may become more bioavailable after exposure to light (Moran et al., 2000) or may be susceptible to bacterial degradation at low concentrations (Moran and Hodson, 1990). This study further aimed to obtain a chemical fingerprint of the DOM before and after the incubation experiments in September 2014 using FT-ICR-MS as EEMF-PARAFAC may not be sensitive enough to determine small, yet significant, changes in the DOM pool. 1% of DOM was considered 'typically-labile', while highly unsaturated compounds, polyphenols, unsaturated aliphatics and black carbon accounted for more than 95% of DOM compounds in SGD.

2. Determining Submarine Groundwater Discharge (SGD)-borne Nutrients and their Fate in Kinvara Bay, Co. Galway

2.1 Introduction

Human alteration of nutrient cycles, in particular, the Nitrogen and Phosphorus Cycles, has occurred at a rapid pace in recent times (Vitousek et al., 1997; Bouwman et al., 2009). Anthropogenic pressures including increased population, food production and energy consumption have increased dramatically over the past fifty years. These stresses have caused a massive mobilisation of bioactive nutrients from land (Seitzinger et al., 2005). In fact, N inputs to the coastal zone have increased 9-10 fold since pre-industrial times (Mackenzie et al., 2002).

Anthropogenic nutrient inputs are disproportionately felt in coastal zones (Simpson and Rippeth, 1998) as rivers, runoff and SGD deliver nutrients directly to this zone and are now considered one of the greatest threats to coastal ecosystems (Paerl, 2009). Particularly notable pressures include increased use of fertiliser on land, septic tanks, irrigation, pollution, litter and wastewater leaching into groundwater (Ji et al., 2013). SGD inputs of nutrients have been shown to be a significant factor in the deterioration of coastal zones globally (Paerl, 2009).

2.1.1 Submarine groundwater discharge-borne nutrients

The factors controlling nutrient fluxes associated with SGD are (1) the groundwater flow path through the aquifer, which in turn, controls the length of time that groundwater is in contact with aquifer solids, (2) nutrient sources to groundwater (natural and anthropogenic), and (3) redox conditions that control the transformation and mobility processes of solutes (Slomp and Van Cappellen, 2004). Factor 2 is particularly important in karstic regions, such as Kinvara, as surface-groundwater interactions are prevalent, and therefore, entry to groundwater through sinking streams and turloughs is a natural flow path allowing for increased land-derived contamination through a large number of point sources (Coxon, 2011).

Additionally, high transport rates, low retention times and well-oxygenated conditions in karst aquifers reduce the capacity for biogeochemical reactions and nitrogen removal within the flow path (Slomp and Van Cappellen, 2004) resulting in relatively conservative nitrate transport across the land-ocean boundary. As a result, nutrient concentrations in coastal groundwater may reach several orders of magnitude greater than corresponding surface waters. Thus, even small volumes of SGD can transport comparatively large nutrient fluxes to the coastal ocean and are very important in the oceanic budget of such materials (Moore, 1999; Burnett et al., 2006; Moore et al., 2006; Street et al., 2008; Lee et al., 2009; Ji et al., 2013). SGD-influenced coastal zones, particularly in karstic aquifers, may have altered N:P ratios as P has lower mobility in aquifers compared to N (Fourqurean et al., 1993). This altered N:P ratio associated with groundwater may drive the coastal ocean towards P-limited from the current N-limited primary production state (Slomp and Van Cappellen, 2004) in areas influenced by SGD.

2.1.2 LOICZ biogeochemical modelling approach

Gordon et al., (1996) developed a simple modelling approach for estimating freshwater sources, net ecosystem metabolism (NEM) and nitrogen metabolism. NEM describes the difference between primary production and respiration. Nitrogen metabolism can also be determined and is expressed as the net result of N-fixation and denitrification (nfix – denit) and can be derived by the difference between the non-conservative nitrogen flux and the expected nitrogen removal through biological uptake. In particular, this modelling strategy places a high emphasis on C:N:P stoichiometrically linked budgets (Smith, 2001). The Redfield Ratio of 106:16:1 is most often used to connect these budgets and determine NEM (Redfield, 1958; Gordon et al., 1996; Slomp and Van Cappellen, 2004). Coastal areas influenced by SGD may have altered DRSi($Si(OH_4)$):N:P ratios and thus it is important to use a C:DRSi:N:P ratio suitable to the system under study in these areas (Redfield, 1958; Gordon et al., 1996; Slomp and Van Cappellen, 2004). Using the wrong molar ratio can cause significant errors associated with this calculation as the method is dependent on a stoichiometric link (Gordon et al., 1996).

2.2 Research aims

This study aims to develop quantitative N (DIN and DON), P and DRSi budgets based on two hydrological conditions within Kinvara Bay, expected high (winter) and low (summer) SGD flow. As shown in Figure 2.1, precipitation in winter (November, December and January) was comparatively larger than the corresponding summer (May, June and July) over all years sampled in this study. Hence, SGD would be expected to be higher in winter campaigns in Kinvara Bay due to meteoric recharge during this time. This study will build on information gained by Rocha et al., (2015), who conducted summer N, P and DRSi budgets. This study also aims to determine the fate of SGD-borne nutrients in coastal systems over the course of the year. The analysis was conducted over four sampling campaigns across the two major flow regimes twice (summer: July 2013 and June 2015; winter: January 2015 and 2016) to constrain fluxes better and to assess the influence of SGD in Kinvara Bay fully.

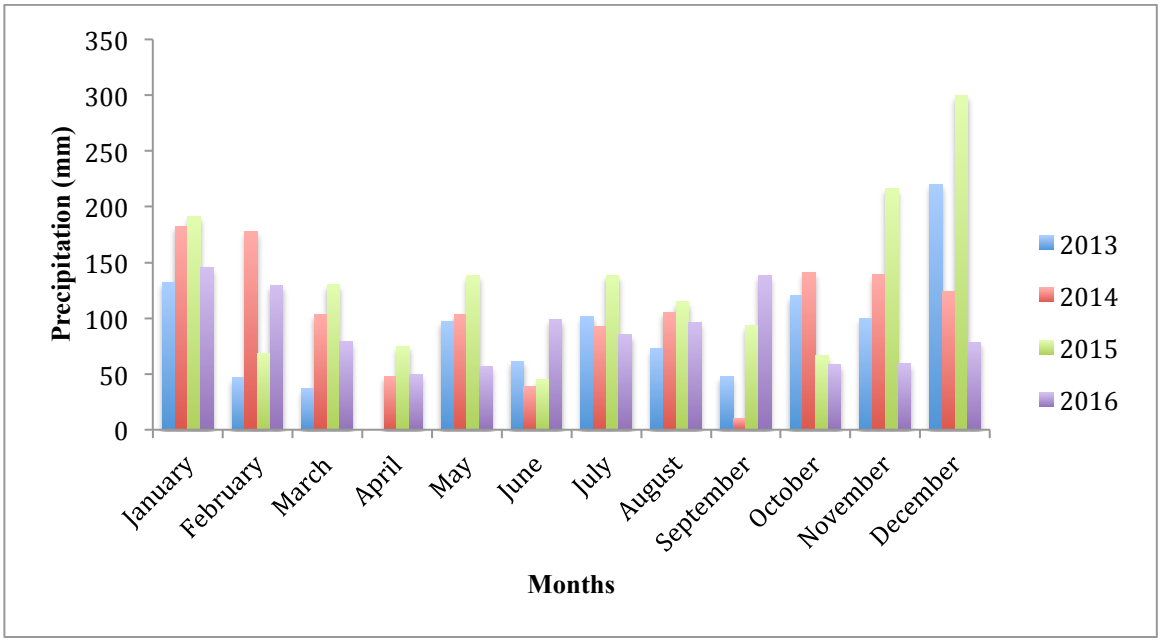

Figure 2.1: Bar chart of total precipitation (mm) recorded at the Met Eireann station in Athenry, 26.1 km North of Kinvara Bay over the course of 2013 – 2016, including the times in which sampling took place (June 2013, January 2015, June 2015 and January 2016).

2.3 Sampling strategy

To close nutrient budgets and to quantify nutrient turnover within the bay, a sampling plan comprising of data acquisition over a representative timeframe was required. Bearing this in mind four sampling campaigns were conducted, two during winter (January 2015 and 2016) and two during summer (July 2013 and June 2015). Time-series sampling was performed at the major allochthonous input locations. Sampling was conducted during low tide at the SGD springs (every 15 minutes) and during high tide at the sewage outflow point (every 15 minutes). Time-series sampling over the full tidal cycle at the inlet of Kinvara Bay, Parkmore Pier (every 30 minutes) was performed to determine nutrient exchange with the open ocean. Sediment cores were collected, and incubation experiments were conducted to determine autochthonous nutrient sources and their role in the biogeochemistry of the bay.

2.4 Methodology

2.4.1 Water collection

Samples were filtered through pre-combusted GF/F filters and collected in pre-cleaned, acid-washed 10 mL amber glass bottles (DON), in 9 mL non-addition Vaccutainer (DIN, DRSi and SRP) and 50 mL autoclavable bottles (TDP). All filters and containers were rinsed several times with the sample before filling. Collected samples were stored on ice in the dark and transported to the laboratory within three days for analysis.

Samples for radon (^{222}Rn) determination were collected after salinity and pH showed constant values. A portable continuous radon-in-air monitor, modified for radon-in-water (Rad7, Durridge; Burnett et al., 2001) was employed. For measuring ^{222}Rn, water from the SGD springs at low tide,

sewage outfall at high tide and 24-hour cycling at the inlet of the bay was continuously pumped through the Rad7. The flowing water is equilibrated with a stream of air that is recirculated through an air-water exchanger and the Rad7. The detection limit was 125 Bq m^{-3} using this setup and had an analytical uncertainty of ± 12 %. Measurements of air temperature, wind speed and atmospheric radon activity concentration were taken to determine atmospheric evasion losses. The radon degassing fluxes were calculated to determine the terrestrial endmember (Burnett and Dulaiova, 2003).

In the field, at the same time water samples were collected, *in-situ* measurements of salinity, conductivity, temperature and pH were obtained using an Aquaread 1000 AP, calibrated prior to use with freshwater conductivity (Varian 12,800 µS cm^{-1}), pH (Varian pH 4.00, 7.00 and 10.00) and ORP (+229 mV) standards.

2.4.2 Sediment analysis

Six undisturbed sediment cores were collected within the bay (Figures 1.9 and 1.10) using an HTH Renberg Corer fitted with 90 mm diameter polycarbonate core liners throughout the Bay in July 2013 and June 2015. Local seawater was acclimatised for 12 hours before it was carefully removed and replaced with 2 L of filtered (GF/C filter) aged seawater. Surface sediment samples (n = 8) were was also taken at each site. Additionally, sediment cores were sliced into 1 cm samples for determination of grain size. Samples were stored frozen until analysed. Sediment size fractions were determined by laser diffractometry (Mastersizer, 2000).

2.4.3 Dissolved inorganic nutrients

Nutrient concentrations (NO_2^-, NO_3^-, NH_4^+, DRSi) were measured using a LACHAT QuikChem 8500 series 2 FIA System. Flow-through analysis is a continuous-flow method, which increases automation and sensitivity. The water sample is injected through a valve into the sample loop connected to the carrier system, containing the appropriate reagents. The sample and reagents react together and pass through the detection system (LACHAT, 2014).

Standards (AccuIon Reference Standard 1000 mg L^{-1} Nitrite as N, Ammonium as N, Nitrite as N and Merck Silicon standard solution 1000 mg L^{-1} as Si) were run to determine the calibration curve. Quality control (QCs) samples (1000 mg L^{-1} nitrite as N made from sodium nitrite, HACH Ammonia Standard solution 1000 mg L^{-1} as NH_3 (N), 1000 mg L^{-1} nitrate-N made from sodium nitrate Rieldel-De Haan AG Ref 13444, Merck silicon standard solution) ensured the accuracy of results. Each sample was run in duplicate, and the average result was taken to reduce analytical error. To facilitate data analysis, Limits of detection (LOD) and limits of quantification (LOQ) for each analyte were calculated using the US EPA method (Clayton et al., 1987). LOD defines the level at which the concentration of analytes can be detected with no guarantee as to the precision and accuracy of this measurement, whereas, the LOQ is the lowest concentration that can be

quantified, and therefore, include accuracy and precision (Shrivastava et al., 2011). A known standard of low concentration was analysed seven times. The standard deviation of this result was multiplied by 3.14 to determine the LOD. Levels recorded below this detection limit were recorded as 'Below Detection Limit' (BDL) and given a zero result. The LOQ was obtained by multiplying the standard deviation of the detection standards by 10. The percentage uncertainty was calculated by dividing the LOQ by the average of all seven readings and multiplying by 100. Blank samples were run every 10-12 samples to account for instrumental shift and experimental error. These were calculated as NO_3^- (1.2 µg N L^{-1}), NO_2^- (0.9 µg N L^{-1}) and NH_4^+ (1.2 µg N L^{-1}). Analytical uncertainties were ± 11% for ammonium (NH_4^+) and silicate as DRSi and ± 12% for nitrate (NO_3^-) and nitrite (NO_2^-).

2.4.4 Phosphate

Total dissolved phosphate (TDP) was determined via a spectro-photochemical method. A digestion solution containing potassium persulphate and sulphuric acid was added and then autoclaved at 121°C for 30 minutes. 5 mL of this solution was taken and added to a clean test tube. 1 mL of the colorimetric solution was added and vortexed. The colour was allowed to develop for approximately 30 minutes (Eisenreich et al., 1975). Samples were measured spectro-photochemically at wavelength 885 nm using a HACH DR5000. Concentration was calculated according to Beers Law:

$$A = \varepsilon Cl \quad (1)$$

Where A is the absorbance (nm), ε is the molar absorptivity coefficient (L mol^{-1} cm^{-1}), in this case, 882 nm, and l measures the path length (5 cm).

QCs were run with every batch to ensure the accuracy of results. The analytical uncertainty for TDP was ± 1% with LOD and LOQ better than 0.2 µM.

2.4.5 DON measurements

Samples were analysed by high-temperature catalytic oxidation (HTCO) using an Elementar Vario TOC cube. Total bound nitrogen (TNb) was measured by injecting the water sample into the cube; it was then aspirated and injected into the combustion tube. High-temperature digestion at 850°C (freshwater) or 680°C (brackish/seawater samples) in an air/O_2 stream takes place. A chemiluminescence detector that determines NO_x gases in the combustion exhaust measured TNb. DIN measurements can be subtracted from TNb results to estimate the organic portion, DON. Standards (Reagecon NO_3^- and NO_2^- standards 1000 ppm as N) were analysed in each run to determine the calibration curve. QCs were run with every batch to ensure the accuracy of results. The LOQ for TNb determination was found to be 0.5mg L^{-1} (14.6 µmol).

2.4.6 Mass balance calculations

The total amount of freshwater flowing into Kinvara Bay was determined by developing mass budgets of salinity (all sampling campaigns) and radon (July 2013 and January 2016). Budget models were then built for nitrogen (DON and DIN = NH_4^+, NO_2^-, NO_3^-), silica (DRSi) and phosphorus (TDP).

Water and salt budgets:

The total freshwater input was estimated by calculating the amount of water with salinity characteristic of terrestrial inputs needed to balance the net outflow of salt at the mouth of the bay (Parkmore Pier). Under steady state, the water balance of a brackish system receiving terrestrial, freshwater inputs and exchanging water with the outer marine system via tidal oscillation can be expressed as (Gordon et al., 1996):

$$V_{in} - V_{out} = V_R = dV_1/dt - V_Q - V_P - V_G - V_O + V_E \quad (2)$$

Where, $V_{in} - V_{out}$ equals V_R, the residual flow, V_Q is runoff flow, V_P is the volume of water associated with precipitation, V_G is groundwater inputs, V_O is any other inputs, such as sewage, and V_E is the water loss due to evaporation. V_E was estimated using equation (3) (Kokya and Kokya, 2008):

$$Qe = f(u) (X_{H2O}e_s - e_a) \quad (3)$$

Where f(u) is the evaporation coefficient as a function of wind speed (υ, km h^{-1}) taken as (1 + υ/16), XH_2O is the water molar fraction for saline waters (0.98), e_s is the saturation vapour pressure (mmHg) and e_a is the gas pressure in air (mmHg).

In general, V_Q is often the largest input term and can be measured to 90 - 95% accuracy. Any term that cannot be estimated within this 5% error bound can be ignored. In this case, the sewage inputs are approximately 286 m^3 per day (EPA, 2010) and are below the 5-10% error bounds of the main freshwater input (SGD) and were not included in the water and salt budgets. This equation can thus be simplified to:

$$V_R = dV_1/dt - V_{Q*} \quad (4)$$

Where, V_{Q*} is all relevant freshwater inputs minus evaporation.

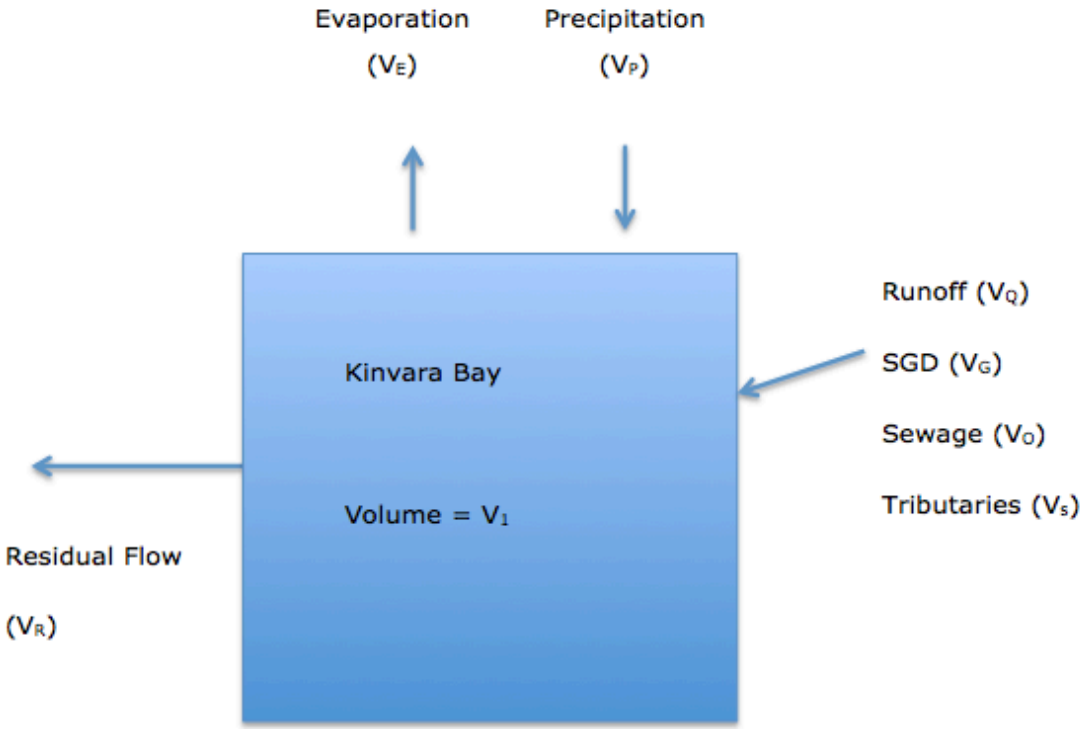

Figure 2.2: Water budget box model for Kinvara Bay representing freshwater inputs from SGD, tributaries, runoff and sewage, outputs as residual flow (exchange at Parkmore Pier) and evaporation losses and precipitation addition within the bay.

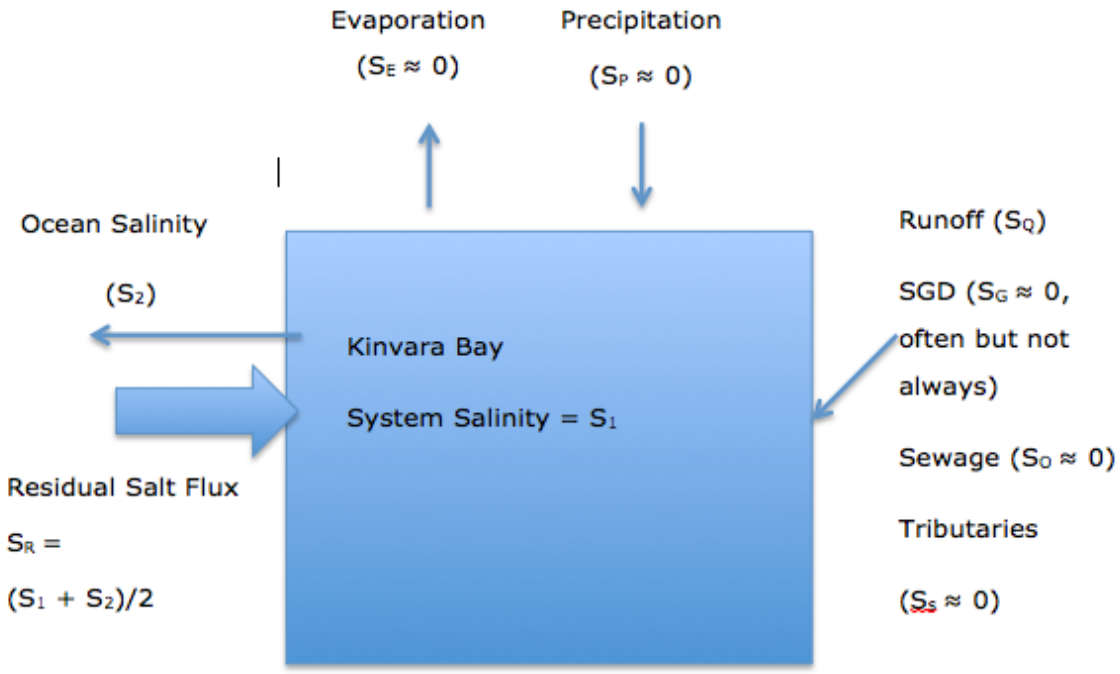

Figure 2.3: Salinity budget box model for Kinvara Bay representing salinity inputs from SGD, tributaries, runoff and sewage, outputs as residual flow while evaporation and precipitation are expected to be zero within the bay. The difference between system salinity and ocean salinity determines the residual salt flux.

The salinity of the residually advecting water is taken at the system boundary (S_2) while the salinity of water within the boundary is S_1. Applying these salinity values to the water balance (Figure 2.2) allows for closure of the salt budget (Figure 2.3). The volume and salinity of terrestrial inputs is represented by V_QS_Q, as below:

$$d(V_1S_1)/dt = V_{Q*}S_{Q*} + V_{in}S_2 - V_{out}S_1 \quad (5)$$

$$\text{Therefore, } S_{land}V_{land} = -S*V_{net} \quad (6)$$

$$\text{And, } V_{land} = -S*V_{net}/S_{land} \quad (7)$$

Where, S_{land} is defined as the salinity of terrestrial water inputs. The salinity of evaporated water is assumed to be equal to zero and is therefore excluded from the salinity box model (Gordon et al., 1996).

Non-conservative materials budgets:

Materials, such as N, P and DRSi may not be conservative with respect to water and salt but can be assumed to have the same hydrological inputs and outputs. The net exchange of dissolved materials between Kinvara Bay and Galway Bay was calculated using data collected periodically over two complete sequential tidal cycles for each of the sampling campaigns. For water/salt budgets, the difference between the two consecutive tidal cycles represents the error of the estimate. Thus, the budgets derived above can be applied to such materials to yield the non-conservative box model (Figure 2.4).

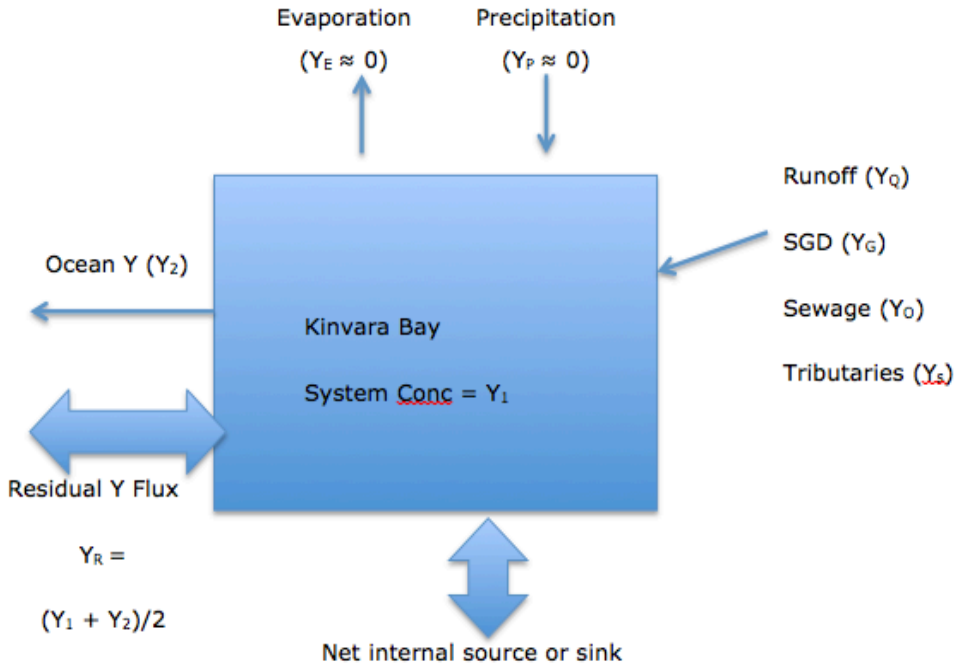

Figure 2.4: Non-conservative materials (Y) box model. Inputs of materials to Kinvara Bay due to runoff, SGD, sewage and tributaries. Within the bay, evaporation may remove materials while precipitation adds materials. The residual flux of materials is determined as the mean exchange at Parkmore Pier over two sequential tidal cycles.

For any material Y, the below equation (8), assuming a steady state, can be derived:

$$\Delta Y = V\,dY/dt + Y\,dV/dt - \Sigma V_{in}Y_{in} + \Sigma V_{out}tY_{out} \quad (8)$$

ΔY may represent a net flux into or out of the system, as either a source or a sink depending on all inputs, outputs and processes within the system. Although sewage inputs can be ignored for water and salt budgets as it is within the 5% error bound, this is not the case for a materials budget as the associated flux may be important in the overall nutrient budget in the bay.

Firstly, the instantaneous directional flux must be calculated, $F_{Sc}(\Delta t)$.

$$F_{Sc}(\Delta t) = (dh/dt)C_{Sc}(\Delta t) \quad (9)$$

Where, $C_{Sc}(\Delta t)$ is the concentration integrated over the sampling interval (Δt). $F_{Sc}(\Delta t)$ was plotted against time, and the total flux of material in both directions can be calculated by integration of the instantaneous directional flux over the full tidal cycle. The net exchange flux and direction can be found for any given material (Rocha et al., 2015).

Radon analysis:

A mass balance approach can be employed to account for all inflows and outputs of radon in the system, thus, allowing for calculation of the groundwater flux (Cook et al., 2008). Full radon calculations for this study are provided in Rocha et al., (2015).

Briefly, the change in inventory of radon in a known reservoir with exchange across one of its boundaries may be expressed as:

$$dI_{Rn}/dt = Rn_{diff} - Rn_{dg} - Rn_{dy} + (Rn_{imp} - Rn_{exp}) + Rn_{adv} \quad (10)$$

where, dI_{Rn} is the radon inventory measured within the domain, t is time, Rn_{diff} is the radon flux across the sediment-water interface due to diffusion, Rn_{dg} is the radon degassing flux, Rn_{dy} is the radon decay within the domain, Rn_{exp} is the export of radon and Rn_{imp} is the import and Rn_{adv} is the advective flux due to groundwater discharge (Burnett et al., 2001).

This equation would equal zero assuming steady state.

Therefore,

$$Rn_{adv} = Rn_{diff} - Rn_{dg} - Rn_{dy} + Rn_{net} \quad (11)$$

Where, $Rn_{net} = (Rn_{imp} - Rn_{exp})$, the residual radon exchange flux with Galway Bay.

2.4.7 Primary productivity (PP)

Nutrient transfer via primary production was estimated based on calculations detailed in Rocha et al., (2015). Nutrient tidal exchange values, determined by the difference of the ebb and flood, were added to the net loading of the particular nutrient in the bay. Allochthonous nutrient inputs to Kinvara Bay include SGD, sewage and wet deposition. Autochthonous fluxes associated with sediment exchange were added to the tidal exchange value. Preserving the sign of each term allowed for the net retention of that nutrient within the bay to be calculated. Negative values

represented decomposition and loss from the water column while positive values represented an addition of that nutrient to the water column. Multiplying the calculated net retention value by the residence time of SGD within the bay and dividing by the volume of the bay at mean tidal level (MTL) estimates the projected concentration of that nutrient in the absence of assimilation by primary producers. The difference between this projected concentration and the mean measured concentration within the bay will yield the transfer of nutrients through primary production. This value needs to be converted to a flux by multiplying it by the volume at MTL and dividing by the residence time within the bay.

2.4.8 Propagation of uncertainty

Uncertainty analysis was carried out by propagation of unknown uncertainties. In short, the standard deviation (±1σ) of an estimated mean value of each independent contributor, X, Y and Z, are $\pm 1\sigma x$, $\pm 1\sigma y$, and $\pm 1\sigma z$, respectively. The relative uncertainty of each term is given as $\frac{\sigma x}{X}$, $\frac{\sigma y}{Y}$, and $\frac{\sigma z}{Z}$, which represents an upper bound of the uncertainty associated with each contributor. For the statistical uncertainty associated with the final result, σR (the combined standard uncertainty) can be calculated as (Taylor and Cohen 1998):

$$\sigma R = (R \times \sqrt{\left[\left(\frac{\sigma x}{X}\right)^2 + \left(\frac{\sigma y}{Y}\right)^2 + \left(\frac{\sigma z}{Z}\right)^2\right]}) \qquad (12)$$

2.5 Results

2.5.1 SGD inflows

As predicted, the salinity of SGD was low under both high and low flow conditions with mean values of 0.52 ± 0.2 ppt (January 2015, 2016, n = 24) and 1.52 ± 0.1 ppt (July 2013 and June 2015, n = 22). An annual long-term average salinity value of 1.02 ± 0.7 ppt is consistent with those recorded by Rocha et al., (2015) of 0.46 – 0.95 ppt and the long-term average of 0.59 ppt recorded by the EPA. Oxygen saturation was moderately low in SGD waters (Table 2.1; 34.4 – 83.5%). Lowest oxygen saturation corresponds to the warmest period (July 2013). Dissolved oxygen (DO) values recorded in each campaign at the SGD point, except July 2013, were higher than those calculated by the EPA of 47.6 ± 12.7 % for the 2007-2012 period. Water temperature showed a clear seasonal pattern, with higher values during summer (13.0 – 15.3°C) and lower temperatures in winter (6.7 – 9.2°C). pH of SGD was relatively uniform (n = 66) over all campaigns, 6.92 – 7.93. ORP was similar between each of the sampling campaigns ranging from +144.0 to +227.4 mV. The annual average ORP was +190.0 ± 48.3 mV.

Table 2.1: Summary of measured water parameters in the SGD endmember, measured at Castle Springs over the four sampling campaigns and meteorological conditions obtained from Met Eireann. Data is the result of an average of several replicates (11 < n < 15) plus or minus the standard error of the mean (± SE). See Appendix A for raw data measured *in-situ*. Meteorological information during the survey periods was obtained from the averages of Met Éireann weather stations Athenry, 26.2 Km north of Kinvara town, and Oranmore, 14.4 Km north of Kinvara town (http://www.met.ie/climate/daily-data.asp).

Parameter	July 2013	January 2015	June 2015	January 2016
Water Temperature (°C)	13.8 – 15.3	6.7 – 8.6	13.0 – 14.1	8.5 – 9.2
Salinity (ppt)	1.84 – 3.67	0.52 – 0.60	0.50 – 0.56	0.51 – 0.56
pH	6.92 – 7.57	7.12 – 7.85	6.96 – 7.93	6.99 – 7.15
ORP (+mV)	144.6 – 207.5	196.1 – 227.4	144.0 - 199.1	193.3 – 216.9
Dissolved Oxygen (%)	34.4 – 44.7	67.6 – 83.5	63.5 – 82.9	62.6 – 72.6
Air temp (°C)	18.9	5.5	15.3	8.0
14-day cumulative precipitation (mm)	16.8	53.2	20.1	35.1

The combined water and salt budgets (see calculation example in Appendix C) suggested that a total of 31.7 ± 8.4 x 10^4 m^3 d^{-1} of freshwater entered the bay during the January 2015 campaign compared to 6.45 ± 6.14 x 10^4 m^3 d^{-1} in the January 2016 campaign calculated from Radon analysis. However, groundwater discharge is modulated by the tide due to the location of the springs within the intertidal zone (Rocha et al., 2015). By scaling the SGD values to times when peak discharge occurs, when the tide is out, the peak outflow rate can be obtained. Kinvara Bay is a semi-diurnal tidal system and a tidal period of 1.91 was used to scale the peak discharge outflow rates. Thus, the peak discharge rate during January 2015 was 4.9 ± 1.4 m^3 s^{-1}. During the January 2016 campaign, SGD was found to represent 5.32 ± 1.92 x 10^4 m^3 d^{-1} of the freshwater flux of 6.45 ± 6.14 x 10^4 m^3 d^{-1} using Rn tracers. Therefore, SGD represents 82.5% of freshwater entering the bay during this period. This flux equates to 1.24 ± 0.4 m^3 s^{-1} during peak discharge.

The SGD/FW ratio (Table 2.2) for the July 2013 campaign (Rocha et al., 2015) was 1.05 ± 0.50. The SGD/FW ratio was assumed to be equal to 1 for the June 2015 campaign as temperatures were relatively high (15.3°C), and precipitation in the 14-day period before sampling was low (16.8mm). SGD was found to contribute 2.43 ± 0.95 x 10^4 m^3 d^{-1} of freshwater to the bay during the July 2013 campaign using radon as a tracer (Rocha et al., 2015). Freshwater flux calculations based on salinity and water budgets for the June 2015 campaign were higher but agreed well with this estimate, given as 4.1 ± 2.7 m^3 d^{-1}, representing an average SGD flux of 3.26 ± 2.5 x 10^4 m^3 d^{-1} during the summer campaigns. This amounts to an SGD discharge rate of 0.28 ± 0.1 m^3 s^{-1} (2013)

and 0.38 ± 0.3 m^3 s^{-1} (2015) representing an average of 0.32 ± 0.3 m^3 s^{-1}. Again, accounting for pulsed modulation within the bay, peak discharges were found to be 0.55 ± 0.2 m^3 s^{-1} (2013) and 0.76 ± 0.6 m^3 s^{-1} (2015), with a seasonal average of 0.65 ± 0.5 m^3 d^{-1} for these two campaigns.

SGD was the major contributor of freshwater to the bay during all sampling campaigns conducted during this study (Table 2.2). A mean annual SGD rate of 10.9 (± 9.6) x 10^4 m^3 d^{-1} was calculated for these campaigns. However, there is a significant error associated with averaging across all campaigns.

Table 2.2: SGD/FW ratios for all sampling campaigns. The proportion of SGD to other freshwater sources is represented by SGD/FW ratios. Aside from SGD, freshwater (FW) sources to Kinvara Bay enter by sewage, small tributaries and runoff. --- represents data not measured. *This value was determined using FW/SGD ratios determined using Rn^{222} for a period with similar rainfall in the 14-day period before sampling published in Rocha et al., (2015).

Date	SGD (x 10^4 m^3 d^{-1})	FW (x 10^4 m^3 d^{-1})	Ratio
July 2013	2.43 ± 0.95	2.32 ± 1.87	1.05 ± 0.44
January 2015	21.4 ± 8.4	31.7 ± 8.4	0.67 ± 0.32
June 2015	4.1 ± 3.90	---	1*
January 2016	5.32 ± 1.92	6.45 ± 6.14	0.83 ± 0.82

2.5.2 Nutrient analyses

Dissolved nutrient budgets were estimated from water/salt budgets and nutrient concentrations in each input term. There were three main allochthonous nutrient influxes within Kinvara Bay at the time of this study; SGD, sewage and wet deposition, each will be discussed in detail below.

2.5.2.1 SGD

SGD-borne nutrient concentrations over the four sampling campaigns are outlined in Table 2.3. For each sampling campaign, nutrient concentrations were uniform per sampling site but differed greatly between sites. For example, the largest standard deviation for nitrate between samples taken on a given day was only 2.3 μmol L^{-1} (n = 12).

Table 2.3: Summary of nutrient concentrations in SGD endmember, measured at Castle Springs. Data is the result of an average of several replicates (11 < n < 15) plus or minus the standard error of the mean (± SE), units are µmol L^{-1}. BDL = Below Detection Limit. July 2013 results have been published in Rocha et al., (2015). DON concentration was calculated by subtracting DIN from TNb. Refer to Appendix B for raw data measured *in-situ*.

Parameter	July 2013 (µmol L^{-1})	January 2015 (µmol L^{-1})	June 2015 (µmol L^{-1})	January 2016 (µmol L^{-1})
NO_3^-	62.27 ± 2.1	157.2 ± 2.3	82.73 ± 1.2	98.35 ± 1.5
NO_2^-	0.24 ± 0.0	1.86 ± 0.0	0.21 ± 0.1	1.85 ± 0.4
NH_4^+	0.63 ± 0.4	1.1 ± 0.1	BDL	0.17 ± 0.1
N–DIN	63.1 ± 5.7	160.2 ± 1.7	82.9 ± 6.1	100.1 ± 24.5
DRSi	58.6 ± 5.3	46.2 ± 0.2	44.83 ± 2.6	50.98 ± 0.5
TDP	0.69 ± 0.1	0.23 ± 0.1	0.24 ± 0.02	1.05 ± 0.3
TNb	88.6 ± 8.8	260.5 ± 2.73	92.7 ± 7.0	159.5 ± 6.9
DON	25.5 ± 3.4	100.3 ± 23.2	9.8 ± 1.0	59.4 ± 14.8

Ammonium results were not included in total DIN as they were close to/below the detection limit and as such associated uncertainty was high (Table 2.3). The variability associated with N-DIN for January 2016 is due to the large error associated with the measurement of both nitrite and ammonium, and therefore these were not included for further analysis.

Nutrient loading for each campaign was calculated by multiplying the nutrient concentration by the SGD volume; as illustrated in Table 2.4.

Table 2.4: Summary of SGD nutrient loads measured at the Castle Springs over the four sampling campaigns calculated by multiplication of the nutrient concentration in SGD by the SGD volume. Data is the result of an average of several replicates (11 < n < 15) plus or minus the standard error of the mean (± SE). Units are mol per day. Negligible values are the result of concentrations that are close to or below the detection limit. July 2013 results have been published in Rocha et al., (2015).

Parameter	July 2013 (mol d^{-1})	January 2015 (mol d^{-1})	June 2015 (mol d^{-1})	January 2016 (mol d^{-1})
NO_3^-	1.5 (±0.2) x 10^3	3.4 (± 0.4) x 10^4	3.4 (± 0.1) x 10^3	5.2 (± 0.1) x 10^3
NO_2^-	5.8 ± 0.6	4.0 (± 0.0) x 10^2	8.6 ± 3.2	88.3 ± 38.4
NH_4^+	15.4 ± 7.6	2.4 (± 0.2) x 10^2	Negligible	8.9 ± 6.5
N–DIN	1.5 (±0.8) x 10^3	3.5 (±0.4) x 10^4	3.4 (± 0.1) x 10^3	5.3 (± 4.5) x 10^3
DRSi	1.1 (± 0.4) x 10^3	9.9 (± 0.1) x 10^3	1.8 (± 0.1) x 10^3	2.7 (± 0.0) x 10^3
TDP	9.0 ± 1.1	99.8 ± 45.2	7.74 ± 0.6	56.1 ± 14.9
TNb	2.1 (± 0.2) x 10^3	5.6 (± 0.1) x 10^4	3.8 (± 0.3) x 10^3	8.5 (± 0.3) x 10^3
DON	6.2 (± 0.1) x 10^2	2.1 (± 0.5) x 10^4	4.1 (± 0.0) x 10^2	3.3 (± 0.3) x 10^3

Nitrate was by far the dominant DIN species in SGD across all sampling campaigns. TDP was present in very low concentrations, close to and in the January 2015 campaign was below the detection limit.

As seen in Table 2.3, January 2015 had the largest nitrate concentrations and as the volume of SGD was also the greatest; the SGD-borne nutrient flux was significantly higher than all other sampling campaigns. In terms of mass loading, there was a substantial increase in the nutrient mass loading of SGD in January 2015 compared to the other three sampling campaigns as shown in Table 2.5.

Table 2.5: Estimates of SGD-borne nutrients in mass terms for winter (January 2015 and 2016) and summer (July 2013 and June 2015), measured at Kinvara Springs. Units are kg d^{-1}, to the closest kg.

	July 2013 (kg d^{-1})	January 2015 (kg d^{-1})	June 2015 (kg d^{-1})	January 2016 (kg d^{-1})
NO_3^-	93	2,101	211	322
NO_2^-	0	18	0	4
NH_4^+	0	4	0	0
DRSi	72	476	87	130
TDP	1	8	1	4
DON	9	294	6	46

Nutrient molar ratios:

P concentrations were low in SGD during all campaigns but were highest during January 2015 and 2016 campaigns. As nitrate concentration in SGD was highly variable and phosphate concentration was very low, the N:P ratios varied widely over the four campaigns, demonstrated in Table 2.6.

Table 2.6: SGD molar ratios of DIN:P, TN:P and DRSi:DIN using measured parameters (DIN, TDP and DRSi) from SGD at Kinvara Springs for the four sampling campaigns, January 2015 and 2016, July 2013 and June 2015.

	July 2013	January 2015	June 2015	January 2016
DIN:P	169.4	440.1	347.1	94.4
TN:P	238.3	493.1	557.5	153.2
DRSi:DIN	1.0	0.3	0.5	0.5

2.5.2.2 Sewage

At the time of sampling, a sewage outfall pipe delivered between 286 m^3 (EPA 2010) and 320 m^3 (Ciaran Cannon, 2010) of untreated effluent to the bay daily at the ebb of high tide. According to the wastewater licence application there is an annual discharge of 104,390 m^3 and discharge occurs 365 days of the year. The licence application does not express the maximum daily discharge (EPA 2010). In this study a figure of 286 m^3 d^{-1} was used as the mean of the annual wastewater discharge over the course of the year. Using this average value introduced error as the population of Kinvara

increases in summer due to a large number of tourists, therefore, sewage discharge would also increase. Solute concentrations measured at the sewage outfall location (Appendix B) were corrected for dilution using the salinity of the public water supply measured at Loughcurragh South, a borehole located 10 km inland (always <1ppt). There was high variability between these samples compared to published values for municipal wastewater (Henze, 2008) and septic tank effluent (Brandes, 1978). To be conservative, published values from municipal wastewater were used for further analysis (Table 2.7).

Table 2.7: Sewage composition determined for sewage discharge to Kinvara Bay using values published in the literature (Henze, 2008). Units are µmol L^{-1} for absolute concentrations and mol d^{-1} for sewage fluxes. Fluxes were calculated using an average flow rate of 286 m^3 d^{-1} as determined in EPA (2010). * Measured as $NO_3^- + NO_2^-$

Parameter	Municipal wastewater (µmol L^{-1})	Fluxes (mol d^{-1})
$NO_3^- + NO_2^-$	35.7*	10.2
NH_4^+	3214	919.2
N–DIN	3229	929.2
DRSi	-	-
TDP	193.7	55.4
DON	1071	306.3

2.5.2.3 Wet deposition

The third and final input term was wet deposition of nitrogen. Aherne and Farrell, (2002) studied wet deposition of nitrogen and other solutes over Ireland for the period 1994-1998. Here, their reported five-year mean concentrations of nitrogen have been analysed for the closest stations, Cloosh and the Burren (Table 1 of their paper) and incorporated into the nitrogen budget of Kinvara Bay. Wet deposition of DIN was calculated based on the precipitation over the 14-day period before sampling (Table 2.8).

Table 2.8: Wet deposition values calculated for DIN in Kinvara Bay for each sampling time point. Fluxes were calculated for the surface area of the Bay using the concentration of DIN determined by Aherne and Farrell, (2002) for the closest stations, Cloosh and The Burren, and the seasonal rainfall that occurred during the 14-day period prior to sampling divided by 14 to determine the flux per day. Units of wet deposition are mol d^{-1}. See example in Appendix C.

	$NO_3^- + NO_2^-$ (mol d^{-1})	NH_4^+ (mol d^{-1})
July 2013	39.3	71.2
January 2015	124.3	225.3
June 2015	45.0	85.1
January 2016	82.0	148.7

2.5.2.4 Allochthonous loads

SGD accounted for the majority, 97.6%, of nitrate (plus nitrite) loading while sewage accounted for the largest proportion of ammonium species (82.2%) over the four campaigns. However, SGD accounted for 75.9% of the total DIN loads within the bay. Regarding DON, SGD was the major contributor, accounting for 97.9% compared to sewage during this study. SGD accounted for only 27.9% of TDP within Kinvara Bay, sewage, thus, accounted for the largest proportion, 72.2%. Wet deposition was a minor contributor of nitrogen species to Kinvara Bay (Table 2.8; Figure 2.5) despite relatively high precipitation (Table 2.1).

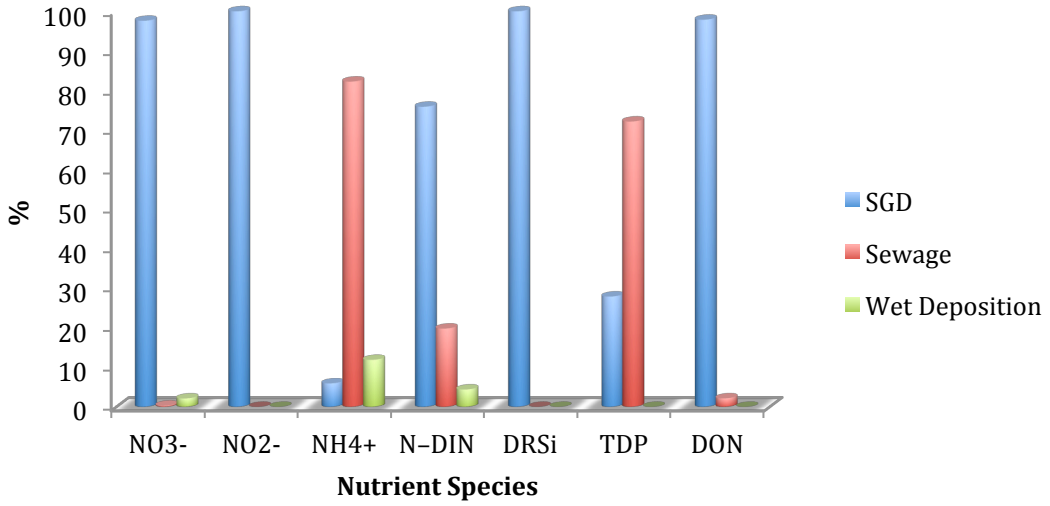

Figure 2.5: Bar chart of percentage of allochthonous loading associated with each input: SGD, Sewage and Wet Deposition into Kinvara Bay annually. TDP and DON concentrations were not measured in wet deposition values, and therefore these values are only represented by SGD and sewage.

2.5.3 Sediment analyses

Kinvara Bay is comprised of two district regions: the intertidal and the subtidal regions. Different sediment typologies exist in both sites reflecting the different hydrological regimes. Sediment taken at the subtidal exhibits grain sizes predominately of very coarse sand (47%) while the intertidal region is dominated by fine (45%) to very fine sand (26%). Silt comprised 12% of the subtidal sand compared to 9% of the intertidal. The SGD springs are located in the intertidal zone. Thus this area receives large volumes of freshwater during low tide. Furthermore, tidal influences are dominant in this zone while they are lessened in the subtidal region.

2.5.4 Nutrient budgets

The mean measured tidal cycle exchange at Parkmore Pier (example provided in Appendix C) was highly variable across all campaigns, shown in Table 2.9. Negative values represent nutrient species exiting the bay through Parkmore Pier while positive values represent nutrients entering the bay from the seaward side.

Table 2.9: Mean nutrient exchange at Parkmore Pier, the mouth of the bay over all sampling campaigns, negative values represent nutrient concentration flux out of the system, whereas, positive values equal nutrient fluxes into the system. Units are mol d^{-1}. Time series every 30 minutes except July 2013 (20 minutes) analysis determined the nutrient concentration at Parkmore Pier over two full tidal cycles. The difference between the flood and ebb fluxes represents the nutrient exchange at Parkmore

Pier. See Appendix B for nutrient concentrations measured *in-situ* and Appendix C for an example of the calculation of tidal exchange.

	July 2013 (mol d^{-1})	January 2015 (mol d^{-1})	June 2015 (mol d^{-1})	January 2016 (mol d^{-1})
NO_3^-	14.7	-213.6	25.3	-6.1
NO_2^-	-2.3	-2.1	-0.9	-14.0
NH_4^+	-24.0	-1.2	9.1	-1.22
DON	-322.0	-799.5	19.2	-863.3
DRSi	10.0	-126.1	12.8	-9.9
P	-	-0.4	37.1	0.5

Projected concentrations were negative for NO_2^- during all sampling campaigns and for NO_3^- during July 2013, June 2015 and January 2016 campaigns reflecting the removal of these species within the bay and therefore transfer via PP was given a value of zero (Rocha et al., 2015).

Table 2.10: July 2013 net retention within Kinvara Bay was measured and used to calculate the projected concentration of the measured nutrients in the water column in the absence of assimilation by primary producers. The primary producer's transfer of nutrients was then estimated as the difference between the projected concentration and the actual measured concentration of the relevant nutrient within the bay as per calculations shown in Rocha et al., (2015).

	Net Retention (mol d^{-1})	Projected conc. (μmol L^{-1})	Measured Mean conc. (μmol L^{-1})	Transfer via PP (mol d^{-1})
NO_3^-	-1.8×10^4	-10.0	1.7	0
NO_2^-	-3.6×10^3	-2.0	0.7	0
NH_4^+	2.1×10^4	11.4	2.4	1.6×10^4
DIN	-6.0×10^2	-0.62	4.8	-9.7×10^3
DON	6.04×10^2	0.003	13.2	-2.4×10^4
DRSi	3.8×10^4	21.2	5.7	2.8×10^4
P	---	---	---	---

Sediment exchange fluxes calculated in July 2013 (Rocha et al., 2015) were used for all sampling time points.

Table 2.11: January 2015 net retention within Kinvara Bay was measured and used to calculate the projected concentration of the measured nutrients in the water column in the absence of assimilation by primary producers. The primary producer's transfer of nutrients was then estimated as the difference between the projected concentration and the actual measured concentration of the relevant nutrient within the bay as per calculations shown in Rocha et al., (2015).

	Net Retention (mol d^{-1})	Projected conc. (μmol L^{-1})	Measured Mean conc. (μmol L^{-1})	Transfer via PP (mol d^{-1})
NO_3^-	1.6×10^4	8.6	3.6	9.1×10^3
NO_2^-	-3.2×10^3	-1.79	1.9	0
NH_4^+	3.3×10^4	12.37	1.2	1.9×10^4
DIN	4.6×10^4	18.5	6.7	2.1×10^4
DON	5.2×10^4	28.76	75.84	-8.5×10^4
DRSi	3.8×10^4	21.45	2.5	3.4×10^4
P	1.4×10^2	0.1	0.02	1.0×10^2

Table 2.12: June 2015 net retention within Kinvara Bay was measured and used to calculate the projected concentration of the measured nutrients in the water column in the absence of assimilation by primary producers. The primary producer's transfer of nutrients was then estimated as the difference between the projected concentration and the actual measured concentration of the relevant nutrient within the bay as per calculations shown in Rocha et al., (2015).

	Net Retention (mol d^{-1})	Projected conc. (μmol L^{-1})	Measured Mean conc. (μmol L^{-1})	Transfer via PP (mol d^{-1})
NO_3^-	-1.7×10^4	-8.97	2.4	0
NO_2^-	-3.6×10^3	-2.01	0.4	0
NH_4^+	2.1×10^4	11.4	1.4	1.8×10^4
DIN	4.0×10^2	0.43	4.2	-6.8×10^3
DON	7.3×10^2	0.41	8.9	-1.5×10^4
DRSi	3.9×10^4	21.59	4.2	3.1×10^4
P	1.0×10^2	0.06	0.2	-2.6×10^2

Table 2.13: January 2016 net retention within Kinvara Bay was measured and used to calculate the projected concentration of the measured nutrients in the water column in the absence of assimilation by primary producers. The primary producer's transfer of nutrients was then estimated as the difference between the projected concentration and the actual measured concentration of the relevant nutrient within the bay as per calculations shown in Rocha et al., (2015).

	Net Retention (mol d^{-1})	Projected conc. (μmol L^{-1})	Measured Mean conc. (μmol L^{-1})	Transfer via PP (mol d^{-1})
NO_3^-	-1.4×10^4	-7.9	2.1	0
NO_2^-	-3.5×10^3	-1.9	1	0
NH_4^+	2.1×10^4	11.4	0.8	1.9×10^4
DIN	3.5×10^3	1.5	3.9	-4.3×10^3
DON	2.7×10^3	1.53	64.4	-1.1×10^5
DRSi	4.0×10^4	22.1	17.7	7.9×10^3
P	1.1×10^2	0.06	0.8	-1.4×10^3

2.6 Discussion

As SGD is temporally variable (Moore, 2010), studies only represent a snapshot in time; this study was conducted over two expected flow regimes twice to constrain this variability better. As SGD in karstic regions such as Kinvara Bay are highly dependent on meteoric recharge, it can be seen that SGD volumes may differ greatly during the expected high or low flow regimes. In particular, the January 2015 campaign had greater SGD volumes compared to the January 2016 campaign. Therefore, it is not appropriate to discuss seasonal variability based on these four campaigns alone and each campaign must be assessed independently.

2.6.1 SGD volumes

Due to the aquifer's karstic nature, groundwater in transit from land to the coast undergoes significant interaction with surface waters (Coxon and Drew, 2000). Consequently, runoff from land will be fed in part by groundwater. Hence, the freshwater input may be comprised of a mixture of surface and groundwater dependent on the volume and intensity of rainfall, and the aquifer's capacity to transport this (Rocha et al., 2015). This suggests that the amount of SGD is substantially dependent on meteoric recharge. Therefore, it is expected that SGD in Kinvara Bay would be higher during winter (average precipitation ≈ 472 mm) compared to summer (≈ 264 mm) during this study period (Figure 2.1).

During the summer campaigns SGD occurred in base-flow or low-flow conditions, with minimal surface runoff, as shown by elevated SGD/FW ratios, calculated in July 2013 (Rocha et al., 2015) and estimated in June 2015. The low flow values provided by this study of 2.43 – 4.1 x 10^4 m^3 d^{-1} were two orders of magnitude lower than estimates given by Cave and Henry, (2011). The latter study calculated freshwater discharge to the intertidal zone to be 1.2 – 2.7 x 10^6 m^3 d^{-1}, based on whole catchment water and salt budgets. However, SGD rates of this current study agree well with the lower range of estimates predicted by Rocha et al., (2015) for summer using radon tracers of 10.4 (± 6.3) x 10^4 m^3 d^{-1}, which included the July 2013 campaign of this study.

During the wettest campaign (January 2015), the peak SGD outflow rate of 4.9 m^3 s^{-1} was similar to the range of intertidal flows of 3.5 - 5.9 m^3 s^{-1} predicted by Cave and Henry, (2011). It was also in the lower range of estimates of 5 - 30 m^3 s^{-1} by Drew (2008) but was half the McCormack et al., (2014) hydrological modelling values of 9.75 - 10 m^3 s^{-1}. There was a marked difference between SGD volumes in the two winter campaigns (Table 2.2). Rainfall in the two-week period before sampling was approximately 64% lower in January 2016 (35.1 mm) compared to January 2015 (55 mm). The residence time within the aquifer is about seven days (McCormack et al., 2014), and thus rainfall has a short-term impact on flow rates. Cave and Henry, (2011) did an extensive review on the flow of groundwater through the Gort-Kinvara catchment and the impact rainfall could have on SGD rates. They concluded that during high rainfall, discharge volumes could quickly ramp up as a

number of additional pathways come into use. The pattern of rainfall can have a large impact on the flow of the system as, if the system had time to empty between precipitation events then the system may take time to refill and cause a lag with discharge. However, if the system has not been able to empty between rainfall events then an episode in one part of the catchment may cause overflow to normally inactive channels causing an increased SGD outflow at the springs. SGD flows return to background levels after a number of consecutive dry days. This may account for the difference between the two winter sampling campaigns as the lower precipitation was combined with warmer temperatures in January 2016 compared to January 2015. Additionally, there was a higher level of error associated with water/salt budgets compared to radon analysis (Gordon et al., 1996; Moore, 2010), which may have caused a higher SGD volume to be recorded in January 2015. An annual SGD rate of $10.9 \pm 9.6 \times 10^4$ m^3 d^{-1} was below estimates stated above but was consistent with that calculated by Rocha et al., (2015) for their summer budget of $10.4 \pm 6.3 \times 10^4$ m^3 d^{-1}. It would be expected that an annual SGD budget would have higher fluxes than a summer budget due to the inclusion of winter. However, July 2010 had an SGD outflow rate of $30.4 \pm 12.3 \times 10^4$ m^3 d^{-1} (Rocha et al., 2015), which was higher than any of the SGD flows calculated in this study and therefore was comparable with the annual budget.

2.6.2 Allochthonous nutrient transport

Groundwater throughout Kinvara was elevated in nutrients, particularly nitrogen, compared to surface waters (Kroeger and Charette, 2008; Ji et al., 2013; Erler et al., 2014; Null et al., 2014). Nitrate was the dominant nutrient in Kinvara Bay during all seasons. Nitrate is very soluble and is the most usable form of nitrogen for plants (Wakida and Lerner, 2005). Nitrate represents one of the most influential contaminants in karstic and porous groundwater systems worldwide (Johannes 1980; Spalding and Exner 1993; Einsiedl et al., 2010; Rocha et al., 2015). It is generally more enriched in fresh groundwater compared to brackish SGD (Johannes, 1980; Santos et al., 2008; Santos et al., 2009; Waska and Kim, 2011).

Nitrate concentrations were lowest in July 2013, while, the TDP concentration of 0.69 μmol L^{-1} was higher than the corresponding summer campaign in June 2015. As the salinity was brackish in the July 2013 campaign (Table 2.1) the presence of recirculated seawater may have accounted for the lower nitrate and higher P concentrations. Seawater is depleted in nitrogen during summer due to a high photosynthetic utilisation rate (Peng et al., 1987). Available P has been shown to increase in coastal marine ecosystems during summer as N declines and is not compensated by N_2 fixation (Conley et al., 2009). Thus, recirculated seawater may have lowered the nitrate concentration, which resulted in increased P concentration of SGD in July 2013. The EPA monitors the Kinvara Springs for nutrient species. The available EPA data from 2007 – 2010, showed that the average nitrate concentration was 112.9 μmol L^{-1} with a maximum of 258.1 μmol L^{-1}. NOx concentrations determined by Smith and Cave, (2010) ranged from 23.6 – 52.8 μmol L^{-1} in October 2009 while 33

μmol L^{-1} corresponded to a flood period (November 2009). The EPA data compares well with this study, which showed nitrate concentrations of 62.2 – 157.2 μmol L^{-1} (Table 2.3) while the values recorded by Smith and Cave, (2010) were lower. Ammonium concentrations measured by the EPA were low with an average of 1.7 μmol L^{-1} and a maximum of 3.3 μmol L^{-1}. These values were larger than values recorded in this study of 0.2 - 1.1 μmol L^{-1} (Table 2.3). The average molybdate reductive phosphate was 0.8 μmol L^{-1} with a maximum of 4.9 μmol L^{-1} measured by the EPA while TDP measured in this study was also low with values of 0.23 – 1.05 μmol L^{-1}, which is characteristic of SGD (Slomp Van Cappellen, 2004). Smith and Cave, 2012 also concluded that freshwater was not a source of P to the bay as salinity did not impact concentrations at Parkmore Pier over the tidal cycle. DRSi values were comparable over all campaigns (46.2 – 58.6 μmol L^{-1}) in this study but lower than the EPA average DRSi concentration of 114.3 μmol L^{-1}.

DO levels in SGD reached as high as 82.3% over the course of this study and accounted for the dominance of nitrate in this region. Well-oxygenated karstic aquifers prohibit anoxia-dependent removal processes and favour relatively conservative nitrate transport (Slomp and Van Cappellen, 2004). As groundwater flows toward the coastline, dissolved phosphate is removed via sorption to iron oxides or co-precipitation with dissolved aluminium, calcium or iron to mineral phases (Slomp and Van Cappellen, 2004). This phosphate removal occurs more efficiently in oxic aquifers. The different behaviours of nitrate and phosphate typically result in a steady increase in the N:P ratio along the groundwater flow path (Slomp and Van Cappellen, 2004). N:P ratios are a key factor in determining nutrient limitation for primary producers in coastal environments. Molar ratios are reflective of nutrient sources within the catchment and its biogeochemical history through the aquifer. N:P ratios greater than 16 indicate excess nitrogen, as phytoplankton typically assimilate nitrogen and phosphorus at an atomic ratio of near 16 (Redfield, 1958). Nutrient ratios differed significantly from that of the Redfield Ratio of 16 during all sampling campaigns. The critical N:P ratio for growth rates can be higher than the Redfield Ratio; estimates range from 20 to 45 mol N per mol P (Terry et al., 1985). The ratio of nutrients delivered to the aquatic environment is important in determining phytoplankton community and health. Shifts in this community structure have been documented in other studies and have been attributed to anthropogenic activities (e.g. Null et al., 2014). Due to the variable nature of SGD (Moore, 2010), there was no clear seasonal trend of the N:P ratio transported via SGD over these four campaigns (Table 2.6). However, the N:P ratios delivered via SGD were high during all campaigns. During the summer campaigns, when metabolism rates were expected to be highest, N:P ratios were 10 - 27 times greater than the Redfield Ratio and therefore supports the conclusion that SGD may drive the coastal zone toward P limitation of primary producers (Slomp and Van Cappellen, 2004).

Including DON in N:P molar ratios of all sampling campaigns increased them significantly in all cases suggesting SGD is an important vector for the transport of DON. Sewage accounted for over 72% of allochthonous P loading during this study. An average value of 286 m^3 d^{-1} This value was measured using literature sewage values and was higher than the sewage P flux estimated by Rocha et al., (2015) of 51% derived *in-situ* from the region of the bay where the sewage outflow pipe was located. Therefore, mitigation of this direct sewage source (Ciaran Cannon, 2010), which has now come into effect (as of spring 2017) may result in further primary production P limitation within the bay as the main allochthonous source has been removed. DRSi:N may also be important in structuring phytoplankton communities. DRSi:N ratios were in agreement with the literature value of 0.9 (Redfield et al., 1963) in the July 2013 campaign but below this value during all other campaigns. The oxidised forms of nitrogen present in high concentrations may alter the community structure and result in greater abundance of diatoms (Ghinaglia et al., 2004).

The macroalgae most dominant in Kinvara Bay in June 2015 exhibited N:P ratios greater than the Redfield ratio of 16. *Fucus vesiculosus* had an average N:P of 51 and *Enteromorpha intestinalis* had an average N:P of 72 (Manaswi Raghurama, 2015; Linh Trieu, 2015). These species are adapted for survival under low P conditions and may result in a shift in algal cover within Kinvara Bay, as species that can survive in low P high N conditions will dominate; this is discussed in more detail in Chapter 7. SGD has also been shown to contribute to P limitation in other karstic aquifers (Slomp and Van Cappellen, 2004; Pavlidou et al., 2014).

2.6.3 Autochthonous nutrient inputs

Sediment incubation studies were only performed during July 2013 and these values were used to derive the N budgets over all sampling campaigns. This may have introduced an error, as sediment activity would differ between summer and winter. The main differences between summer and winter are decreased light availability, lower temperatures and lower oxygen levels during winter. Light regulates the metabolic status of sediments and, in turn, exerts strong control on sediment nitrogen dynamics and the fate of inorganic nitrogen (Porubsky et al., 2009). While, increased temperatures have been shown to enhance DNRA and denitrification during summer, which increases sediment oxygen consumption (Giblin et al., 2013). In temperate estuaries, such as Kinvara Bay, where there is substantial nitrate loading over the course of the year, denitrification activity has been shown to correlate with ambient temperature (Herbert, 1999). Denitrification rates have been shown to be lower in winter than summer combined with lower oxygen consumption rates (Smith et al., 1985; Yoon and Benner 1992; Tuominen et al., 1998). Temperatures measured between 6.7 and 9.2 °C in the winter campaigns compared to 13.0 to 15.3 °C in the summer campaigns (Table 2.1). Thus, the rates associated with the summer sediment exchange in this study may decrease in winter and therefore may have overestimated benthic N removal during the winter

campaigns, which may explain the negative retention of nitrite in the January 2015 campaign and of nitrate and nitrite in the January 2016 campaign.

Sediment fluxes acted as a significant source of DIN to the water column during the June 2015 campaign (Manaswi Raghurama, 2015; Linh Trieu, 2015) but acted as a sink during the July 2013 campaign. $3.70 \pm 2.60 \times 10^3$ mol d^{-1} of DIN was lost through the seafloor during the July 2013 campaign (Rocha et al., 2015), which accounted for 100% of the DIN allochthonous flux calculated during July 2013 and June 2015 campaigns and accounted for 11% of the allochthonous nitrate flux in the January 2015 campaign and 71% in the January 2016 campaign. However, in the June 2015 campaign, there was a net gain of all DIN species into the water column from intertidal sediments. The benthic sediment added $2.6 \pm 1.1 \times 10^4$ mol N d^{-1} to the water column during this period, accounting for more than the average allochthonous inputs of $4.9 \pm 1.6 \times 10^3$ mol N d^{-1}. Thus, they acted as a significant source of DIN. The incubation period of five days may not have been sufficient to reach steady state (Manaswi Raghurama, 2015; Linh Trieu, 2015) and may have accounted for the difference between the July 2013 and June 2015 campaigns. Net removal of nitrate within the bay was stronger than nitrate addition; therefore, there was N fixation within the system during the summer campaigns. Nitrification is important in mediating N export from land by linking mineralisation and denitrification (Tobias et al., 2001). Similarly, DIN was cycled through sediments through coupled nitrification-denitrification due to exposure to light and oxygen in the intertidal zone during low tide (Rocha et al., 2015). The fact that sediment acted as a source of nitrate in the subtidal in July 2013 and the intertidal in June 2015 indicate that the benthic sediment served as a link in nitrogen mineralisation within Kinvara Bay.

Autochthonous production of P, measured in June 2015, was the largest input source to Kinvara Bay, accounting for 74.2% of the total P inputs (Manaswi Raghurama, 2015; Linh Trieu, 2015). The main allochthonous P source via sewage has been removed with the introduction of the wastewater treatment plant. Thereby, autochthonous production may mitigate against primary production P limitation associated with SGD.

2.6.4 Nutrient budgets

2.6.4.1 Exchange at Parkmore Pier

Summer campaigns showed a net import of DRSi and NO_3^- from the seaward side through the mouth of the bay while winter campaigns showed a net export (Table 2.9). NO_2^- was exported from the bay during all campaigns. June 2015 showed a net import of NH_4^+ and DON while all other sampling campaigns showed a net export of these nutrients. The net export of DON from Kinvara Bay was large in each sampling campaign except June 2015. The exchange at Parkmore Pier, however, accounted for less than 1% of the allochthonous load of DIN transported during all campaigns. There was a net export of DON of 1.5% during January 2015 and 24% during January

2016 increasing to 36% during July 2013. There was a net export of less than 1% TDP during January 2015 and an export of less than 1% during January 2016 rising to 59% during June 2015 from Galway Bay. Allochthonous loading of TDP and DON were substantially higher during winter due to the larger SGD flux. These results were consistent with those of Rocha et al., (2015) who found 100% retention of DIN during summer (2009 – 2013) in Kinvara Bay. The export of DIN at Parkmore Pier was minuscule compared to the allochthonous and autochthonous fluxes to the bay, and thus SGD fluxes have minimal influence on the outer Galway Bay. Nutrient retention within Kinvara Bay was almost 100% for DIN and DRSi annually.

2.6.4.2 DIN

Net retention within the bay was negative for nitrite across all seasons and for nitrate in July 2013, June 2015 and January 2016 (Tables 2.10 - 2.13) showing the removal of N species through the benthic substrate. This was reflected in the sediment incubation experiments conducted during July 2013 (Rocha et al., 2015). On a bay wide level the benthic sediment was a source of NH_4^+ but a sink for NO_3^- and NO_2^-. A positive retention for nitrate in January 2015 was due to the comparatively larger DIN flux associated with the high SGD volume. Sediment was thus very active in nutrient transformation in Kinvara Bay over all campaigns. Based on the magnitude of allochthonous fluxes, SGD-borne nitrate was reduced by the benthic sediment except in January 2015.

Transfer of DIN via primary production (PP) accounted for 9.7×10^3 (July 2013), 6.2×10^3 (June 2015), and 3.2×10^4 (January 2015) mol N d^{-1} suggesting a large flux associated with PP over the course of these campaigns. A denitrification flux of $3.7 \pm 0.84 \times 10^3$ mol N day^{-1} was estimated by Rocha et al., (2015) during summer. PP accounted for 68% of the autochthonous released from sediments in July 2013 and June 2015. This flux was less than the biological nitrogen fixation flux during summer campaigns (Tables 2.10 and 2.13) suggesting the bay was net autotrophic. Primary production is typically a seasonal process driven by light and temperature conditions and varies greatly through the year (Dürr et al., 2011). Metabolism rates are expected to be higher in summer due to higher temperatures and longer sunlight hours. During the January 2015 campaign the PP transfer was positive (Table 2.11) suggesting that net removal of DIN was greater than fixation and thus the bay was net heterotrophic. Turnover rates might be lower in winter campaigns than calculated here from summer sediment incubation experiments. As a result, the net retention and N turnover calculated for the two winter campaigns may be overestimated. Nutrient values measured at Parkmore Pier exhibited highest concentrations during January 2015 and lower concentrations of DIN during all other campaigns. The low levels of inorganic nitrogen observed in these time points can be attributed to greater biological consumption within the bay.

Net losses of DIN and DIP within the system may support net primary production. Other studies have shown that most of the DIN influxes are removed within the water column due to active biological uptake, such as Gamak Bay in the southern sea of Korea (Hwang et al., 2010). DO fluctuations throughout the bay may be attributable to sea temperature and biological activity (Pavlidou et al., 2014). DO levels were consistently higher in the summer campaigns compared to winter campaigns at Parkmore Pier (Appendix A).

2.6.4.3 DON

The internal loading of DON (Tables 2.10 and 2.12) exceeded the DIN flux channelled into primary production by about 60% during summer campaigns. Therefore, in order to balance the DIN flux, it can be assumed that approximately 1.09 ± 2.2 x 10^4 mol N d^{-1} of the DON load was recycled into bioavailable forms and contributed to primary productivity within the bay. Rocha et al., (2015) also found that 48% of DON (1.08 ± 0.87 x 10^4 mol N d^{-1}) was effectively contributed to primary production. Other studies have shown that there is a significant fraction of the DON pool that is labile and biologically available (Jackson and Williams, 1985; Thurman, 1985). Seitzinger and Sanders, (1997) showed that a portion of riverine DON was labile and contributed to estuarine productivity. In estuaries with a residence time of a week, there is a part of the DON that is utilised within the bay and more which is exported and used in the open ocean. The labile component of DON consists of low molecular weight compounds that can be assimilated by primary producers. The molecular characterisation of DOM that includes organic nutrients is described in detail in Chapter 8. Although this study concluded that DON in terrestrial groundwater was mainly refractory, there may be compounds in the 'typically recalcitrant' group of compounds that may be semi-labile and degraded (Seitzinger and Sanders, 1997).

The sediment-water exchange budget indicated that 100% of the allochthonous oxidised nitrogen was recycled through the benthos and released back into the water column as ammonium during all campaigns. The internal sink of DON (Tables 2.11 and 2.13) was substantially higher during winter campaigns as a result of higher DON fluxes observed due to lower recycling rates through PP, high precipitation and subsequent SGD flow rates. During summer campaigns, there was rapid exchange between primary production and DON, suggesting a low burial rate. Thus, DON was an active component in the N Cycle. During winter campaigns, primary productivity decreased and there may have been a higher burial rate within coastal sediments than was measured in the July 2013 incubation used for this study. The export of DON to Galway Bay was higher in the winter campaigns, which was consistent with lower recycling rates through primary productivity.

The primary production carbon yield derived from the net nitrogen fixation was calculated for summer, using the C:N molar ratio of 13.5 ± 2.09, to be approximately 1.1 x 10^4 mol C day^{-1}, 0.109 kg C m^{-2} yr^{-1}, classifying Kinvara Bay as mesotrophic (Nixon, 1995). Considering that 57% of

DON was channelled into PP and thus nearly half the DON was determined to be biologically available (Seitzinger and Sanders, 1997) within the residence time of 6.8 ± 1.7 days (Rocha et al., 2015) of SGD in Kinvara Bay, the carbon yield in Kinvara Bay was determined to be 0.172 kg C m^{-2} yr^{-1}. This was considered as mesotrophic for this dataset. Rocha et al., (2015) concluded that Kinvara Bay was eutrophic during summer, 0.313 kg C m^{-2} yr^{-1} for their dataset of four summers, which included July 2013. SGD-borne nitrate accounted for 1.93 ± 0.21 x 10^4 mol d^{-1} in their study and this was substantially larger than nitrate loading recorded in this study during summer campaigns. Therefore, Kinvara Bay was tightly bound by allochthonous loading of nutrients and may experience eutrophic conditions when SGD-borne DIN loads increase. DON, therefore, acted as a nutrient-loss pathway and as a source of N for productivity within Kinvara Bay, as seen in other studies (e.g. Neff et al., 2003).

2.6.4.4 DRSi

SGD transported a large amount of silicate into the bay due to the high concentration in the fresh groundwater endmember, which accounted for 100% of DRSi contributions compared to other DRSi input sources. This is in line with observations by Rocha et al., (2015) in Kinvara Bay. Enhanced DRSi has been recorded in other karstic systems such as the Caribbean coast of the Yucatan Peninsula (Null et al., 2014) and non-karst systems such as Laoye Lagoon, Hainan, China (Ji et al., 2013).

Silica dissolution in the photic zone is controlled by temperature, zooplankton grazing, diatom aggregation and bacterial colonisation (Nelson et al., 1995). Bacteria-mediated silicon regeneration may critically control diatom productivity (Bidle and Azam, 1999). DRSi was added to the system via SGD and a high benthic efflux and regeneration over all campaigns (Tables 2.10 - 2.13). DRSi may be added to the system through remineralisation from the benthic community and the mussels being farmed within the bay. Diatoms have an absolute requirement for silicon (Bidle and Azam, 1999) and are relatively high in food quality (Turner et al., 1998). SGD may thus support a stable community of diatoms while other types of algae may be highly dynamic depending on the bioavailable N:P ratios, which were highly variable. Phytoplankton in summer contained a mix of diatoms and dinoflagellates with 94 species recorded in 2012, but the most frequent genus was the diatom Pseudo-nitzschia (MI, 2015). Diatom and dinoflagellate blooms were common during summer. The number of diatoms decreased in winter due to light availability while there have been occasional blooms of microflagellates detected in Kinvara (MI, 2015). The removal of DRSi has also been associated with benthic eutrophication in coastal embayments of Hwasun Bay and Bangdu Bay, Korea (Kim et al., 2011).

2.6.4.5 TDP

Regeneration production of P may occur within the water column (Hwang et al., 2010). In fact, autochthonous production of P accounted for 600 mol d^{-1} (Manaswi Raghurama, 2015; Linh Trieu,

2015) while there was a net removal of 100 - 260 mol d^{-1} over all campaigns. Combining this with the N:P ratios provided by SGD supports the assertion that primary production P-limitation occurred within Kinvara Bay during these sampling campaigns.

2.7 Synopsis

Of the allochthonous sources to Kinvara Bay at the time of the study; sewage, wet deposition, runoff and SGD, SGD accounted for more than 65% of freshwater inputs across all campaigns. During summer campaigns, SGD occurred in base-flow conditions and accounted for 100% of freshwater inputs. SGD rates in Kinvara Bay were highly linked to meteoric recharge and were thus significantly higher in winter campaigns compared to summer.

Nutrient molar ratios (N:P) associated with SGD far exceeded that of the Redfield ratio of 16. Altered N:P ratios apply in particular in karst aquifers due to the well-oxygenated conditions that prevent anoxia-driven removal processes of N while P has an affinity for removal along the karstic flow path. N:P ratios were highly variable during this study. SGD accounted for almost 98% of nitrate loading and 76% of total DIN loads over the course of this study. Sewage delivered 82% of the ammonium and 72% of the TDP loads to Kinvara Bay during these campaigns. Therefore, treatment of sewage discharging directly into the bay to drinking water standards recently introduced will unlikely mitigate the high DIN loads associated with SGD. Removal of the TDP source from sewage may further drive Kinvara Bay to P-limited primary production. This could have significant implications for the algal cover and community structure living in this zone. Although there was an autochthonous release of P from sediments within the bay, there was net removal within the water column due to productivity.

Sediment incubation experiments showed that Kinvara Bay acted as a sink for nitrate and nitrite but a source of ammonia (Rocha et al., 2015). A portion of the DON transported via SGD was labile and was recycled into biologically available forms. A biologically available nutrient budget must include both the inorganic and organic portions of N (Seitzinger and Sanders, 1997). This study showed that almost 100% of DIN was retained within the bay. The bay switched from net autotrophic in the July 2013, June 2015 and January 2016 campaigns to net heterotrophic in the January 2015 campaign. Only a small proportion (1%) of the exogenous TDN load was exported to the wider Galway Bay due to tight benthic-pelagic coupling across all campaigns.

3. Investigation of Submarine Groundwater Discharge-borne Carbon (DIC, DOC and TAlk) and their Circulation in Kinvara Bay, Co. Galway

3.1 Introduction

The link between terrestrial and marine carbon cycles is not fully understood and has remained a poorly constrained component of the global carbon cycle (Maher et al., 2013). Submarine groundwater discharge (SGD) is now known to be a major pathway for terrestrial nutrients, metals and carbon to the coastal zone on a global scale (Moore, 2010) and may better elucidate the link between the terrestrial and marine cycles. Still, groundwater influxes are often the least studied components of coastal nutrient and carbon budgets (Porubsky et al., 2014). SGD has not been included in the global carbon cycle to date (Szymczycha et al., 2014) despite potential fluxes to the Atlantic Ocean equaling that of riverine inputs (Moore et al., 2008).

Most estuarine systems worldwide are net heterotrophic (respiration exceeds gross primary production) resulting in an overall increase in pCO_2 within the water column and a CO_2 source to the atmosphere (Gattuso et al., 1998; Abril et al., 2000; Cai et al., 2003; Zhai et al., 2005). Carbon budgets usually ignore groundwater as a potential driver of CO_2 build up in surface waters even though dissolved CO_2 may be highly enriched in groundwater (Macpherson, 2009; Dorsett et al., 2011). The major processes contributing to CO_2 enrichment within coastal aquatic systems are *in-situ* respiration driven by natural and anthropogenic organic matter inputs (Cole and Caraco, 2001; Richey et al., 1988), groundwater discharge (Jiang et al., 2008; Maher et al., 2013), terrestrial surface water runoff (Raymond et al., 2000) and precipitation of carbonate or silicate minerals (Hagedorn and Cartwright, 2010).

Rising anthropogenic CO_2 levels in the atmosphere have decreased the pH of the surface ocean by 0.1 pH units in the last 250 years (Cao and Caldeira, 2008). Acidification impacts fundamental processes that influence the overall structure and functioning of marine ecosystems (Duarte et al., 2013). Significant changes associated with acidification could have far-reaching consequences both for the marine environment and ecosystems, but also for the millions of people depending on these ecosystems and resources. The Kinvara Bay surface water systems are designated as Shellfish Waters, and acidification could have detrimental effects for the economy of the region.

Due to high concentrations of CO_2 and DIC, groundwater has naturally lower pH (6.70–7.30) and lower saturation states ($\Omega \sim 0.5$) than corresponding surface waters (Crook et al., 2012). SGD may therefore accelerate ocean acidification in coastal zones due to the delivery of low pH, high DIC waters. For example, de Weys et al., (2011) linked groundwater discharge to severe estuarine acidification in Tuckean Swamp, Australia. On the other hand, SGD has also been shown to transport large fluxes of total alkalinity (TAlk) to coastal zones, which then might buffer against acidification. Therefore, the relationship between TAlk and DIC within SGD is important for determining the impact of SGD on ocean acidification (OA). However, little is known about whether biogeochemical processes may provide feedbacks to ocean acidification (Santos et al., 2011) and what the role of SGD might be.

3.2 Sampling plan

To close carbon budgets and to further evaluate the role of SGD in ocean acidification dynamics in Kinvara Bay, a sampling plan was devised along the flow path from an inland borehole to the SGD springs in the intertidal zone and then the mouth of Kinvara Bay (Parkmore Pier). Four sampling campaigns were conducted, two during winter (January 2015 and 2016) and two during summer (July 2013 and June 2015). Time-series sampling was performed during low tide at the SGD springs (every 15 minutes); at the sewage outflow location in the bay during high tide (every 15 minutes) and over the full tidal cycle at Parkmore Pier (every 30 minutes). Sediment cores were collected (June 2015), and incubation experiments were conducted to determine autochthonous sources of carbon species and their role in the biogeochemistry of the bay.

3.3 Aims and hypotheses

Because carbonate aquifer systems, such as those connected to Kinvara, have a high propensity to transport large DIC and TAlk concentrations; this study seeks to gain a better understanding of the influence of SGD on the coastal carbon cycle. Particular attention will focus on determining DOC, DIC and TAlk loading and evaluating CO_2 fluxes within the bay, in order to assess the impact of SGD on ocean acidification (OA) in karstic regions. These studies are particularly important for understanding whether predicted ocean acidification in the future will be buffered by watershed inputs via SGD and shellfish culture can be sustained, or, alternatively, if SGD might accelerate acidification, in which case there will be drastic effects on the ecosystem and economy of Kinvara. Explicit null hypotheses are outlined below.

The Null hypothesis 1, Ho, states that Kinvara Bay acts as a net source of CO_2 to the atmosphere
The alternate hypothesis states that Kinvara Bay acts as a net sink of CO_2 from the atmosphere
The Null hypothesis 2, Ho, states that SGD-borne influxes can buffer the coastal ocean against acidification
The alternate hypothesis states that SGD-borne influxes will be a positive feedback on coastal acidification over the short term

3.4 Methods

Samples were syringe filtered through pre-combusted GF filters and collected in pre-cleaned, acid-washed 10 mL borosilicate amber glass bottles (DOC/DIC). Water was pulled into the syringe *in-situ* and then passed through a GF filter into the glass bottles. All filters and containers were rinsed several times with the sample before filling and samples were overfilled to ensure no headspace in the bottle. TAlk samples were collected unfiltered in tall narrow-necked borosilicate amber borosilicate glass bottles (Howland et al., 2000). Care was taken not to expose the samples to the atmosphere, as CO_2 exchange can occur quite rapidly. The bottles were overfilled by twice their volume to minimise contact with air and filled to the brim. The lids were closed tightly to remove any headspace or escape of gases to the atmosphere and then sealed. The analyses were carried out

as soon as possible. As a precautionary measure, collected samples were stored on ice in the dark and transported to the laboratory within three days for analysis.

In the field, at the same time water samples were collected, *in-situ* measurements of salinity, conductivity, temperature and pH were obtained using an Aquaread 1000 AP, calibrated prior to use with a freshwater conductivity (Varian 12,800 µS cm^{-1}), pH (Varian pH 4.00, 7.00 and 10.00) and ORP standards.

3.4.1 DOC/DIC measurements

Samples were analysed by high-temperature catalytic oxidation (HTCO) using an Elementar Vario TOC cube. Total dissolved carbon (TDC) was measured by injecting the water sample into the cube; it was then aspirated via a dosage syringe and directly injected into the combustion tube where catalytic oxidation takes place. High-temperature digestion at 850°C (freshwater) or 680°C (brackish/seawater samples) in an air/O_2 stream takes place converting total bound C to CO_2. Water vapour was removed from the sample by a drying process. CO_2 is then quantitatively determined by non-dispersive infrared (NDIR) giving the TDC concentration based on the calibration curve. DIC was determined automatically after acidification and purging in the sparger by treatment with phosphoric acid. This method is automated and very sensitive (Elementar, 2014). Non-purgable DOC was determined directly after external DIC had been removed. Care was taken to minimise exposure to avoid loss of CO_2 by covering the samples with a tin sheet.

Standards (Reagecon TOC and TIC standards 1,000 ppm as C) were tested with each run to determine the calibration curve and set the concentrations for the system; this allows a concentration value (mg/L) to be calculated for each sample. Quality control (QC's) samples were also run with every batch to ensure the accuracy of results. For DOC analysis, the limit of detection (LOD) was found to be 0.5 mg L^{-1} and limit of quantification (LOQ) was 0.6 mg L^{-1} (41.63 µmol L^{-1}). For DIC, the LOQ and LOD were 0.1 mg L^{-1} (8.3 µmol L^{-1}).

3.4.2. Sediment

Three undisturbed sediment cores were collected in June 2015 within the bay using an HTH Renberg Corer (Chapter 2). Whole core incubation studies by following the time-dependent gain or loss of DOC and DIC in the overlying water column at a constant temperature of 13°C (Allert and Mackin, 1989) and an overlying water height of 33 cm.

3.4.3 Total alkalinity (TAlk)

The samples were analysed by acidimetric titration (Gran procedure) (Wong, 1988; Howland et al., 2000; Abril and Frankignoulle, 2001). The pH meter and electrode were calibrated using standards (Varian pH 4, 7 and 10). The electrode was rinsed with milliQ water and allowed to equilibrate in a

sample for several minutes following calibration. The sample was titrated to pH 4.5 in less than 2 minutes using 0.01M sulphuric acid.

The plot of TAlk versus DIC allows for separation of the effects of biological (metabolism) and geochemical processes ($CaCO_3$ precipitation and dissolution) on the carbonate system (Andersson and Gledhill, 2013).

3.4.4. pCO_2 calculations

TAlk and pH measurements from the SGD springs, sewage location and Parkmore Pier were used to calculate pCO_2 values in the CO2SYS program (Lewis et al.,1998) using the set of constants (K1 and K2) from Mehrbach, (1973) refit by Dickson and Millero, (1987). Although this is considered a robust method for pCO_2 determination, associated errors do exist. The largest error source in this calculation is the accuracy of the pH measurements. pH for this study was determined *in-situ* and allowed to reach a steady reading before recording. The alkalinity titrations were conducted as quickly as possible post sample collection. This reduces the amount of precipitation of carbonate salts due to degassing (Macpherson, 2009). This procedure results in reported uncertainties of ~11% for the final CO_2 concentration in groundwater according to Atkins et al., (2013).

The flux of CO_2 across the air-sea boundary depends on the two parameters, firstly, the concentration gradient between the surface water and the air and, secondly, the physical transfer at this interface (MacIntyre et al.,1995). pCO_2 fluxes were calculated as:

$$F = - k \alpha (pCO_{2\,(W)} - pCO_{2\,(A)}) \quad (1)$$

Where, k is the wind speed-dependent CO_2 gas transfer velocity coefficient (Wanninkhof, 1992, 2014), α is the solubility coefficient for CO_2 in water (Weiss, 1974), ($pCO_{2\,(W)} - pCO_{2\,(a)}$) is the difference in partial pressure of CO_2 between the water and air. Atmospheric pCO_2 (380 ppmV) was assumed constant over all campaigns, although studies at Mace Head, Ireland, have shown that there may be a seasonal variation of 15.1 ± 1.1 ppmV (Bousquet et al., 1996).

pCO_2 fluxes have been computed using pCO_2 of water calculated by CO2SYS and k was derived using wind speed data collected by Met Eireann from the closest weather stations, Athenry, 26.2 Km north of Kinvara town, and Oranmore, 14.4 Km north of Kinvara town (http://www.met.ie/climate/daily-data.asp). Positive CO_2 fluxes represent fluxes from the bay into the atmosphere, while negative fluxes represent fluxes into the bay water from the atmosphere.

3.5 Results

3.5.1 SGD-derived inputs

Table 3.1: Summary of measured water parameters and carbon concentrations in the SGD endmember, measured at Castle Springs over the four sampling campaigns. Data are the result of the mean of several replicates (11 < n < 15) plus or minus the standard error of the mean (± SE). Meteorological information during the survey periods was obtained from the averages of Met Éireann weather stations Athenry, 26.2 Km north of Kinvara town, and Oranmore, 14.4 Km north of Kinvara town (http://www.met.ie/climate/daily-data.asp). N/A represents samples not analysed for this parameter. See Appendix D for *in-situ* measurements.

Parameter	July 2013	January 2015	June 2015	January 2016
Water Temperature (°C)	13.8 – 15.3	6.7 – 8.6	13.0 – 14.1	8.5 – 9.2
Salinity (ppt)	1.84 – 3.67	0.52 – 0.60	0.50 – 0.56	0.51 – 0.56
Dissolved Oxygen (%)	34.4 – 44.7	67.6 – 83.5	63.5 – 82.9	62.6 – 72.6
pH	6.92 – 7.57	7.12 – 7.85	6.96 – 7.93	6.99 – 7.15
14-day cumulative precipitation (mm)	16.8	53.2	20.1	35.1
DOC ($\mu mol\ L^{-1}$)	381.0 – 623.6	291.6 – 330.2	355.3 – 385.8	240.2 – 270.6
DIC ($\mu mol\ L^{-1}$)	N/A	4340.6 – 4693.6	3789.4 – 4148.7	4431.1 – 4940.6
TAlk ($\mu mol\ L^{-1}$)	4709.6 - 4716.8	4688.0 – 4813.6	4509.6 – 4648.0	5099.2 – 5192.7

Table 3.1 highlights the water chemistry records detailed in Chapter 2 and the C species concentrations taken over four campaigns during winter (January 2015, 2016) and summer (July 2013 and June 2015). DOC concentrations were higher in both summer campaigns compared to winter. Although there was only one set of DIC samples taken during summer, the concentration of DIC in SGD during June 2015 was lower than both winter campaigns. The mean of TAlk was higher in winter compared to summer but considering the variability did not exhibit a clear pattern of seasonality. January 2016 had the highest TAlk of all campaigns.

DOC, DIC and TAlk fluxes associated with January 2015 (Table 3.2) were the highest due to the high volume of SGD during that campaign (Chapter 2).

Table 3.2: Summary of SGD DOC, DIC and TAlk loads measured at the Castle Springs over the four sampling campaigns calculated by multiplication of the carbon specie concentration in SGD by the fresh SGD volume. Data are the result of the mean of several replicates (11 < n < 15) plus or minus the standard error of the mean (± SE). N/A represents samples not analysed for this parameter.

Parameter	July 2013 (x 10^4 mol d^{-1})	January 2015 (x 10^4 mol d^{-1})	June 2015 (x 10^4 mol d^{-1})	January 2016 (x 10^4 mol d^{-1})
DOC	1.0 ± 0.21	6.5 ± 0.14	1.5 ± 0.36	1.4 ± 0.06
DIC	N/A	97.6 ± 0.67	16.6 ± 0.41	25.6 ± 0.01
TAlk	11.5 ± 0.03	101.9 ± 0.87	18.7 ± 0.02	27.4 ± 0.24

Table 3.3: Estimates of SGD-borne carbon (DIC and DOC) and alkalinity in mass terms annually and for winter (January 2015 and 2016) and summer (July 2013 and June 2015), measured at Kinvara Springs. . --- data not measured

Parameter	July 2013 (kg d^{-1})	January 2015 (kg d^{-1})	June 2015 (kg d^{-1})	January 2016 (kg d^{-1})
DOC	125	780	185	168
DIC	---	1.2×10^4	2.0×10^3	3.1×10^3
TAlk	1.0×10^4	1.0×10^5	2.7×10^4	2.5×10^4

Mass loadings for DOC, DIC and TAlk were higher in January 2015 compared to the other three sampling campaigns (Table 3.3), due to larger SGD volumes. The DIC and DOC fluxes via SGD to Kinvara Bay were estimated to be 2.0 ± 1.4 kt C yr^{-1} and 0.1 ± 0.08 kt C yr^{-1}, respectively. Thus the DIC fluxes were approximately 20 times larger than the DOC fluxes. The total carbon flux via SGD, therefore, amounted to 2.1 kt C yr^{-1}.

Table 3.4: SGD molar ratios of TDC:TDP, DOC:TDN, DIC:TDN and TDC:TDN using measured parameters (DIN, DOC and DIC) from SGD at Kinvara Springs for winter (January 2015 and 2016) and summer (July 2013 and June 2015). --- Sample not measured. *TDC:TDP ratio calculated using DOC only as DIC was not measured at the SGD springs during July 2013.

	July 2013	January 2015	June 2015	January 2016
TDC:TDP	1,158.1*	10,430.9	23,426.7	4,812.9
DOC: TDN	6.8	1.9	4.5	2.6
DIC: TDN	---	28.2	48.7	48.3
TDC:TDN	---	30.1	53.2	50.9

The C:N ratios in SGD in this study were highly variable. During the winter campaigns, the C:N ratio of 1.9 - 2.6 was significantly lower than the summer campaigns C:N ratios. This was in line with higher DOC concentrations in the summer campaigns. The DIC:TDN and TDC:TDN ratios for January 2015 were lower than the June 2015 and January 2016 campaigns (Table 3.4).

3.5.2 Sewage inputs

Untreated effluent is discharged from the sewage outfall pipe into the bay at the ebb of high tide. Therefore, sewage had mixed with bay water, as shown by the variable salinity data (Table 3.5).

Solute concentrations were corrected by dilution back to the salinity of an inland borehole, Loughcurragh South (0.51 ppt).

Table 3.5: Summary of relevant water parameters and solute (DOC, DIC and TAlk) concentrations associated with sewage inputs. Data are the result of the mean of several replicates (11 < n < 15) plus or minus the standard error of the mean (± SE), adjusted for dilution with seawater back to the salinity of an inland borehole of 0.3 ppt. --- represents samples not analysed for this parameter. See Appendix D for *in-situ* values

Parameter	July 2013	January 2015	June 2015	January 2016
Salinity (ppt)	20.6 – 23.4	0.6 – 1.5	6.3 – 12.4	0.1 – 2.4
pH	7.6 – 8.3	7.4 – 7.8	8.2 – 8.7	7.3 – 8.2
DOC (μmol L^{-1})	124.4 – 305.6	619.6 – 685.9	446.8 – 532.5	477.5 - 588.0
DIC (μmol L^{-1})	2,020.4 – 2,199.9	1,720.7 – 2,001.3	2,603.7 – 3,096.7	2,620.7 – 2,745.5
TAlk (μmol L^{-1})	---	2,427.2 – 2,717.6	2,887.2 – 2,967,2	2,809.6 – 2,878.4

Measured fluxes of TAlk and DIC were relatively uniform over the four sampling campaigns. However, there was a high variability in the DOC fluxes, from a minimum of 124.4 μmol L^{-1} to a maximum of 685.9 μmol L^{-1}. These values were lower than literature values of 5,828.5 μmol, provided by Katsoyiannis and Samara, (2007). To be conservative, this literature DOC flux value (1.67 x 10^3 mol d^{-1}) was incorporated into budgetary analyses.

3.5.3 Wet deposition

Iavorivska et al., (2016) studied 22 coastal/island locations and determined the mean flux of organic carbon in rainwater to be 2.48 ± 2.1 mg C L^{-1}. 22 of these sites were located in Europe and had a mean DOC concentration of 2.60 ± 2.4 mg C L^{-1}, 216 ± 199.8 μmol L^{-1}. DIC inputs to Kinvara Bay via deposition were devised based on the values calculated by Worrall et al., (2003) for a British upland peat catchment, the North Pennines and are provided in Table 3.6. They estimated that 1.1 g C m^{-2} yr^{-1} of DIC is due to dry and wet deposition.

Table 3.6: Wet deposition values calculated for DOC and DIC in Kinvara Bay for each sampling time point. Fluxes were calculated for the surface area of the Bay using the concentration of DOC in precipitation determined by Iavorivska et al., (2016) for European coastal/island locations and the DIC calculated by Worrall et al., (2003) for a British upland peat catchment, the North Pennines. This was scaled using the seasonal rainfall that occurred during the 14-day period prior to sampling divided by 14 to determine the flux per day. See example in Appendix C.

	DOC (mol d^{-1})	DIC (mol d^{-1})
July 2013	1.1 x 10^3	1.4 x 10^4
January 2015	3.5 x 10^3	4.6 x 10^4
June 2015	1.3 x 10^3	1.7 x 10^4
January 2016	2.3 x 10^3	3.0 x 10^4

3.5.4 Allochthonous loads

Table 3.7: Percentage of allochthonous loading associated with each input: SGD, Sewage and Wet Deposition into Kinvara Bay over the course of the four campaigns. --- represents parameters not analysed in this study.

	SGD (%)	Sewage (%)	Wet Deposition (%)
DOC	89.5	5.7	4.8
DIC	99.4	0.3	0.3
TAlk	99.8	0.2	---

SGD accounted for over 99% of the allochthonous loading of DIC and TAlk (Table 3.7); this is not surprising considering the karstic nature of the aquifer. SGD accounted for 89.5% of DOC inputs, while sewage and wet deposition accounted for the remaining 10.5%. In most cases, the sewage inputs were within the error of the estimates and were non-significant. SGD was the primary source of carbon to the bay, in turn; any such exchange with the open ocean was also due to the presence of SGD within the coastal zone.

3.5.5 Sediment analyses

Other important C sources/sinks to consider within the coastal zone include diffusion from sediments (Null et al., 2014). According to sediment incubation experiments, sediment acted as a source of DIC and a sink of DOC during the June 2015 incubation experiments, shown in Table 3.8.

Table 3.8: Measured sediment DIC and DOC exchange fluxes by incubation core experiments measured in June 2015, close to Kinvara Springs.

Treatment	n	C Flux (mmol m^{-2} d^{-1})	Bay C Fluxes (mol d^{-1})
DIC	27	9.07 ±0.08	3.9 (±1.5) x 10^4
DOC	34	-0.81 ±0.27	-2.6 (±1.1) x 10^3

3.5.6 Fate of carbon species within the bay

Table 3.9: Mean DOC and DIC exchange at Parkmore Pier, the mouth of the bay over all sampling campaigns, negative values represent carbon flux out of the system, whereas, positive values equal carbon fluxes into the system. Time series analysis every 30 minutes except July 2013 (20 minutes) determined the DOC and DIC concentration at Parkmore Pier over two full tidal cycles. The difference between the flood and ebb fluxes represented the nutrient exchange at Parkmore Pier. See Appendix D for DOC and DIC concentrations measured *in-situ* and Appendix C for an example of the calculation of tidal exchange.

	July 2013 (mol d^{-1})	January 2015 (mol d^{-1})	June 2015 (mol d^{-1})	January 2016 (mol d^{-1})
DOC	-655.0	-2160.0	-37.9	-296.9
DIC	-971.5	240.0	-900.3	-1450.8

There was net export of DOC over all campaigns, while there was a net import of DIC during January 2015 (Table 3.9).

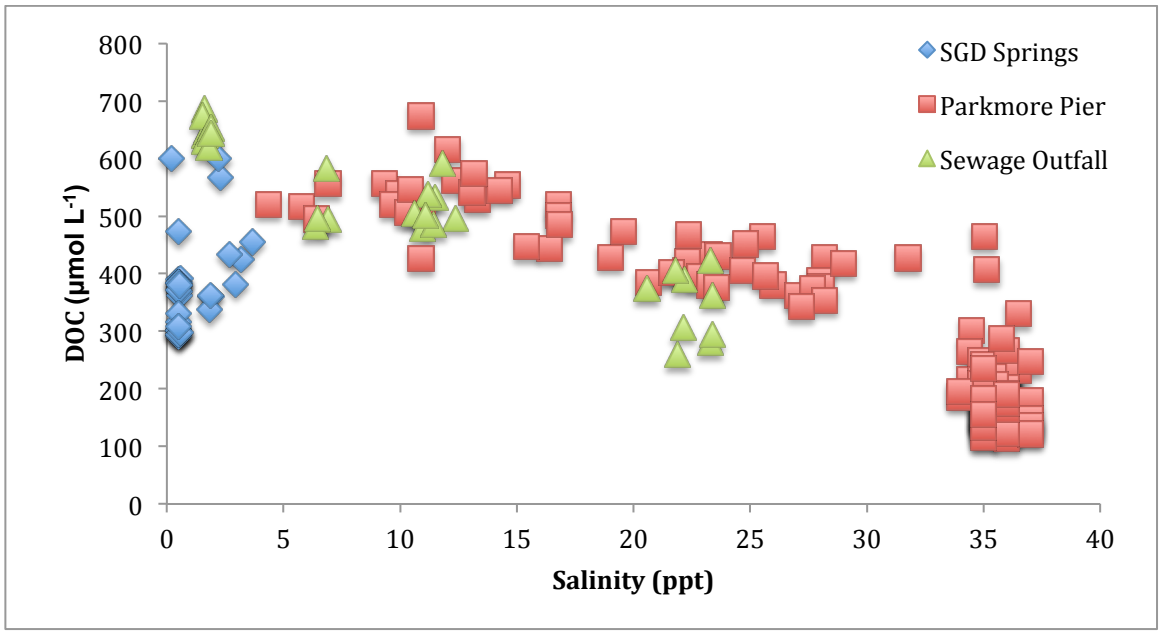

Figure 3.1: A plot of DOC versus salinity for samples taken at the SGD point, sewage point and within the bay over all sampling campaigns, n = 253, SGD (n = 42), sewage (n = 42), Parkmore Pier (n = 169)

As shown in Figure 3.1, DOC concentrations in SGD were variable between the three sampling locations. SGD-borne DOC was often lower than corresponding sewage and Parkmore Pier DOC concentrations.

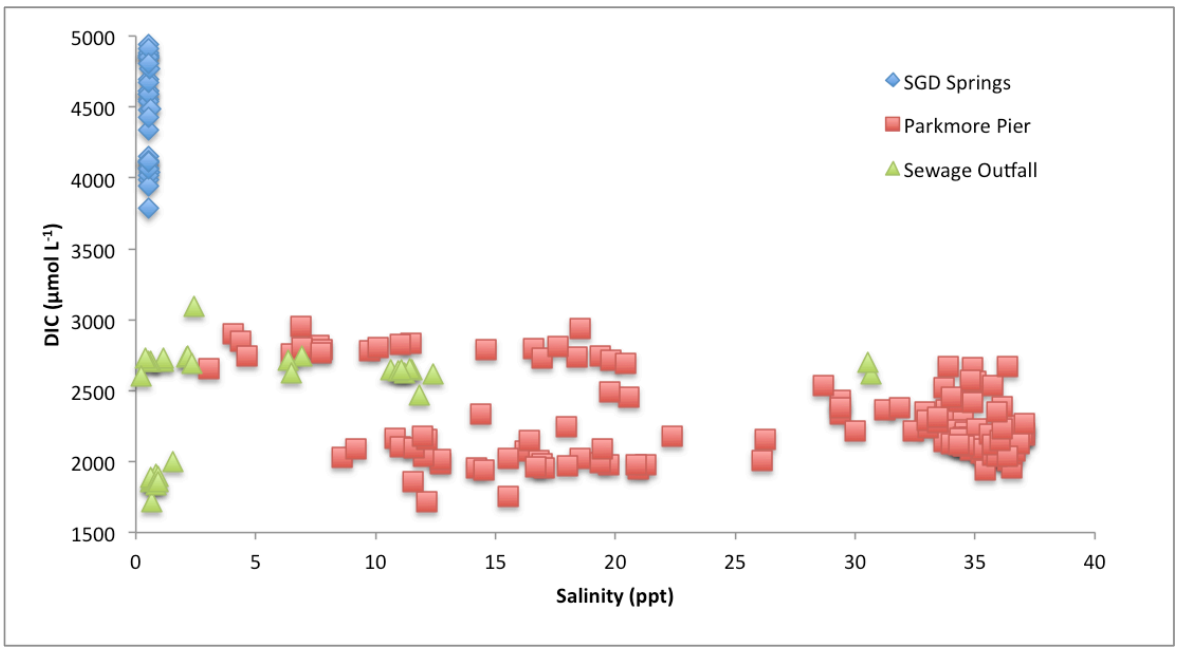

Figure 3.2: A plot of DIC versus salinity for samples taken from the SGD point, sewage outflow point and within the bay over all sampling campaigns, n = 206, castle (n = 34), sewage (n = 32), Parkmore Pier (n = 140)

As per Figure 3.2, the highest DIC concentrations were found close to shore, in SGD. The DIC values were relatively uniform at intermediate salinities, following a sharp decline from the SGD point.

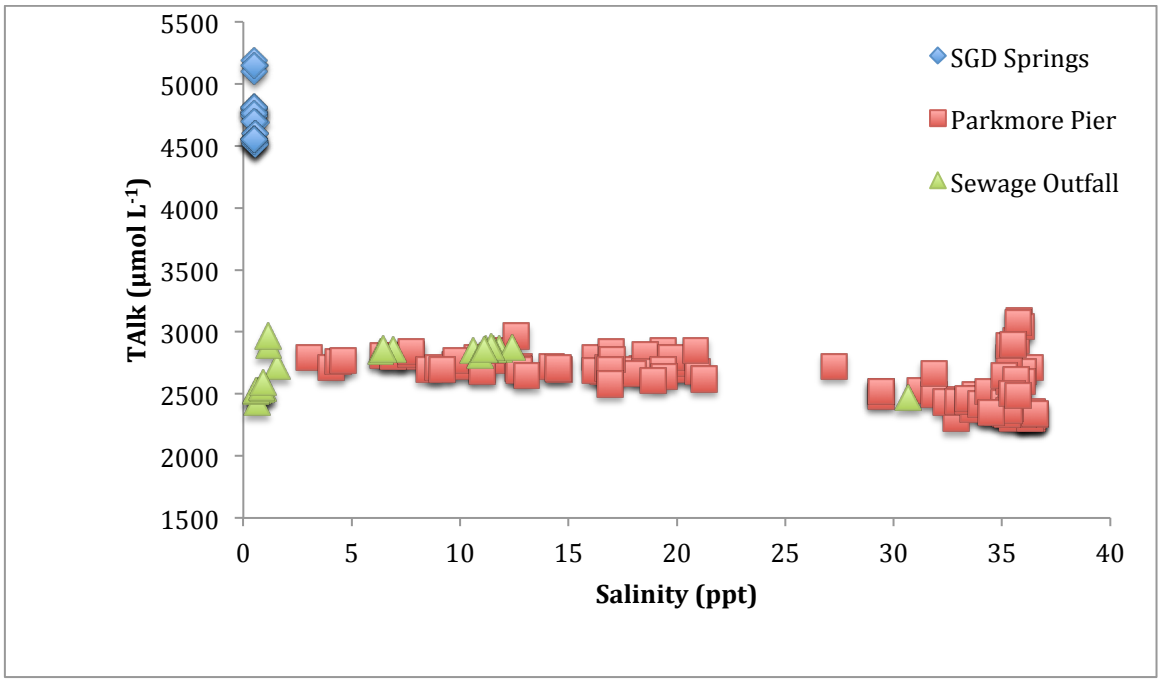

Figure 3.3: A plot of TAlk versus salinity for samples taken at the SGD point, sewage point and within the bay over all sampling campaigns, n = 167, SGD (n = 24), sewage (n = 23), Parkmore Pier (n = 119)

TAlk at the site of discharge was elevated compared to samples taken at intermediate to high salinities (Figure 3.3). These graphs support SGD as an important source of TAlk and DIC to the bay.

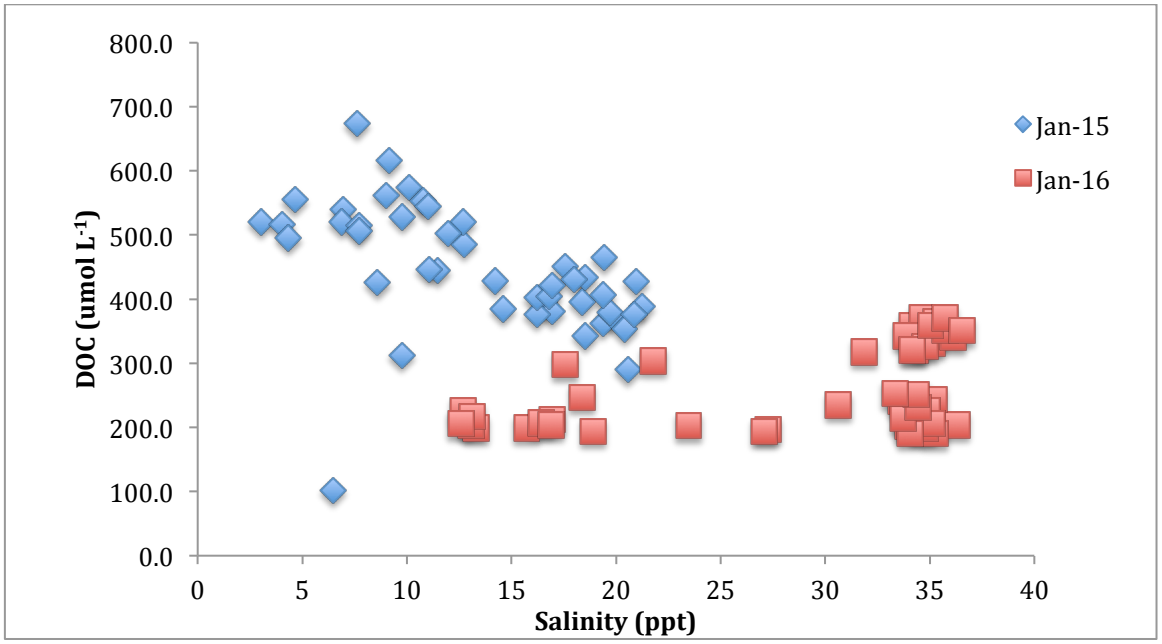

Figure 3.4: DOC concentration (µmol L^{-1}) versus salinity (ppt) measured at Parkmore Pier over two sequential tidal cycles every 30 minutes during January 2015 (n = 45) and January 2016 (n = 47).

DOC decreased with salinity during the January 2015 campaign but did not appear to have the same pattern in January 2016, as shown in Figure 3.4. Regression analysis for the decreasing trend in January 2015 had an R^2 value of 0.77.

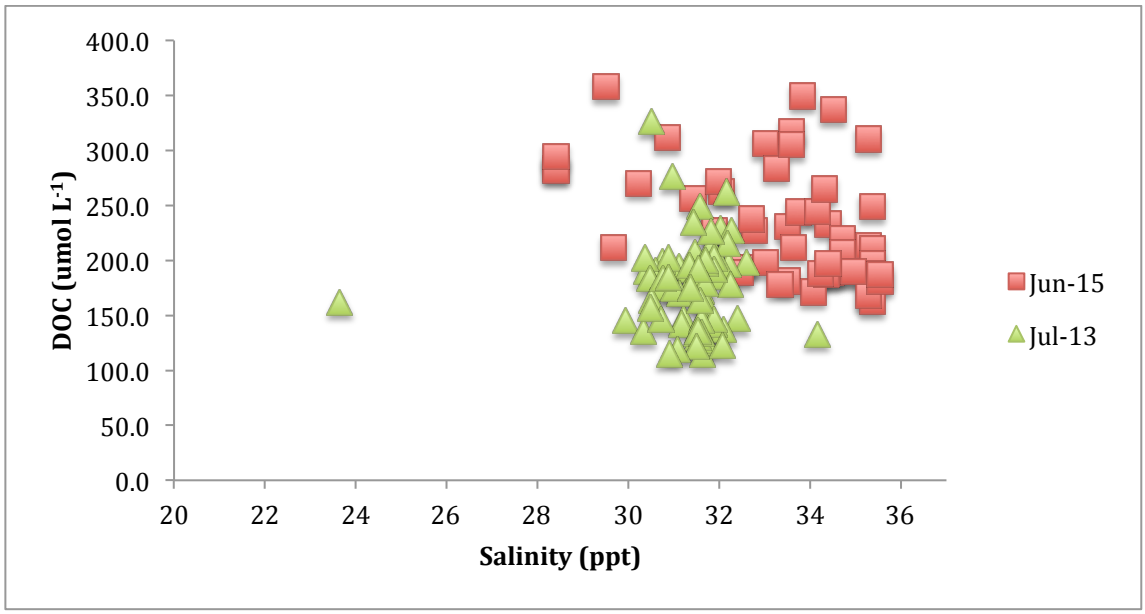

Figure 3.5: DOC concentration (µmol L^{-1}) versus salinity (ppt) measured at Parkmore Pier over two sequential tidal cycles during July 2013 (n = 73, samples every 20 minutes) and June 2015 (n = 49, samples every 30 minutes).

There was no clear pattern of mixing of DOC with salinity at Parkmore Pier during the summer campaigns (Figure 3.5). The salinity range during time series analysis in July 2013 was narrower due to the lower SGD volumes.

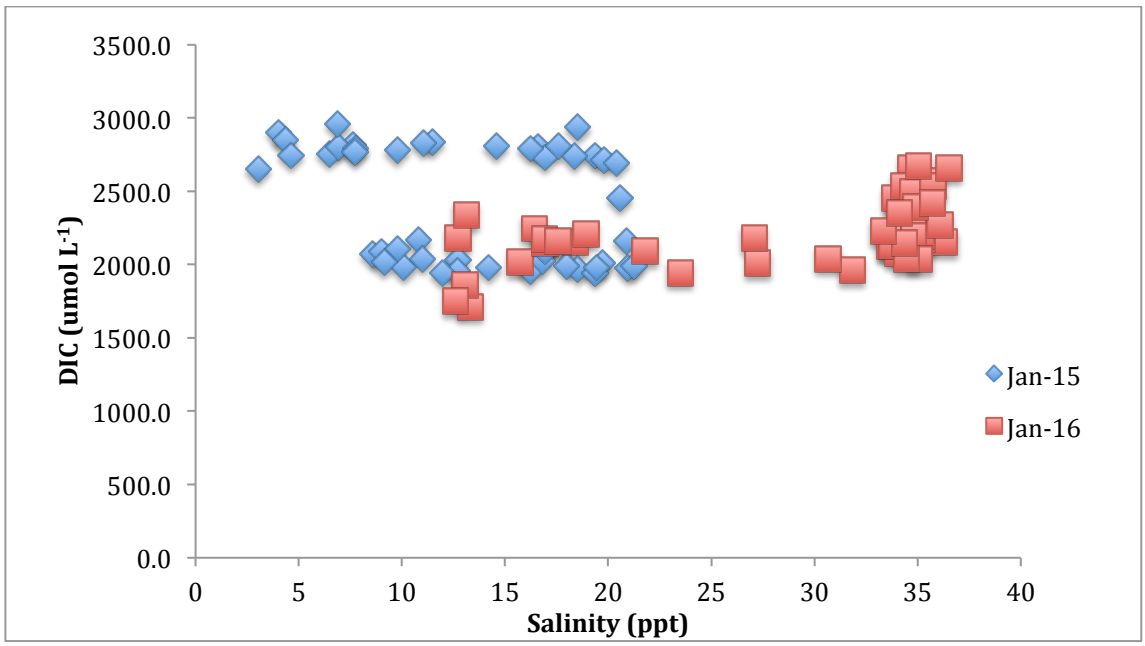

Figure 3.6: DIC concentration (µmol L^{-1}) versus salinity (ppt) measured at Parkmore Pier over two sequential tidal cycles every 30 minutes during January 2015 (n = 45) and January 2016 (n = 47).

Figure 3.6 shows that there were two water masses mixing at Parkmore Pier during January 2015. This period corresponds to the highest SGD inflows and shows that SGD may not be sufficiently mixed during high flows. DIC concentrations did not largely change over the course of the tidal cycle during the January 2016 campaign but higher salinity samples had higher DIC concentrations.

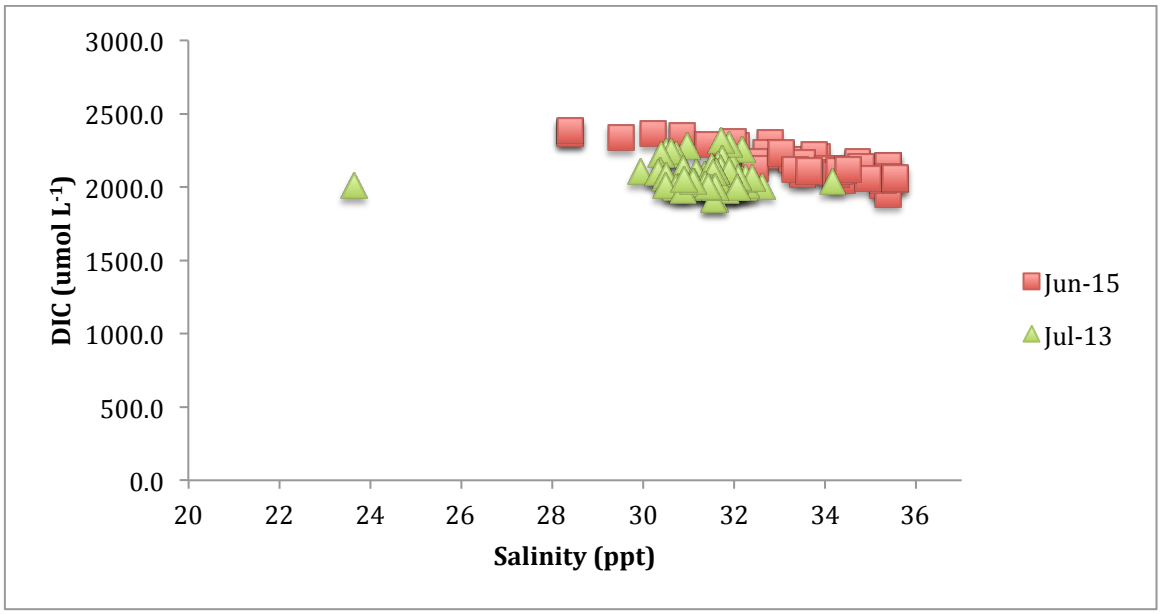

Figure 3.7: DIC concentration (µmol L^{-1}) versus salinity (ppt) measured at Parkmore Pier over two sequential tidal cycles during July 2013 (n = 73, samples every 20 minutes) and June 2015 (n = 49, samples every 30 minutes).

Figure 3.7 illustrates a negative trend of DIC with salinity at Parkmore Pier during the June 2015 campaign but no obvious trend for the July 2013 samples. Regression analysis had an R^2 value 0.77 for the June 2015 samples.

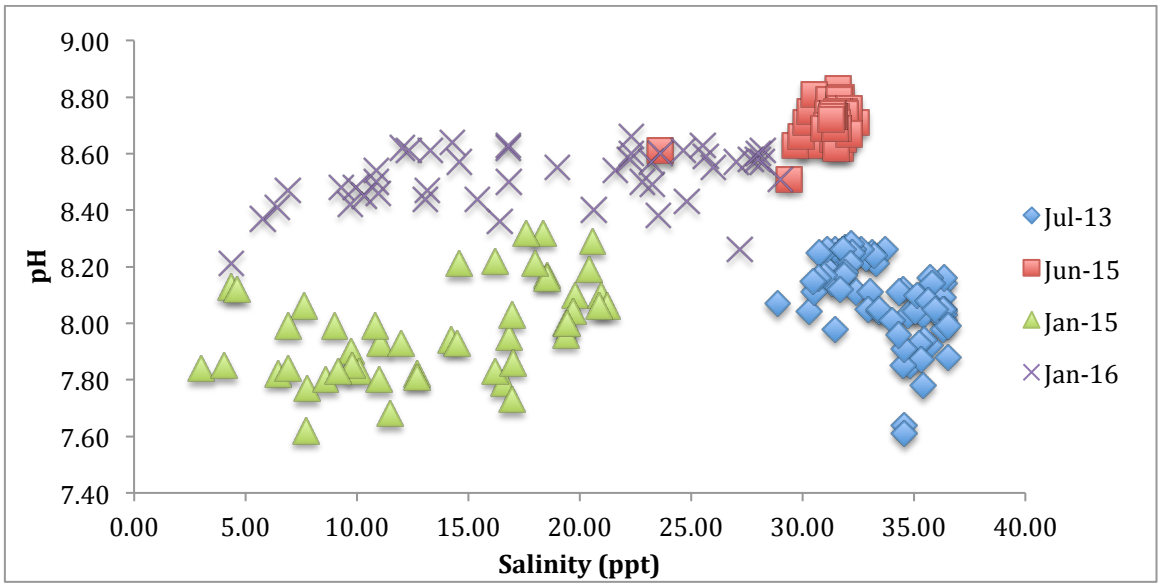

Figure 3.8: Mixing plots of pH versus salinity at Parkmore Pier during all sampling campaigns Samples were taken every 20 minutes in July 2013 (n = 72) and every 30 minutes during January 2015 (n = 51), June 2015 (n = 46) and January 2016 (n = 48).

Figure 3.8 illustrates the mixing curves of pH with salinity over each sampling time point. This graph shows that there was no clear trend of pH with salinity over all campaigns. The salinity range was narrower in summer (July 2013 and June 2015) compared to the winter campaigns (January 2015, 2016). Peaks correspond to high tide while troughs correspond to low tide.

3.5.7 pCO_2 calculations

Table 3.10: pCO_2values calculated using CO2SYS software for allochthonous sources using inputs of TAlk, pH and DIC; submarine groundwater discharge, sewage water and Parkmore Pier, collected across all sampling campaigns. --- Represents data not analysed.

Sample date	SGD (µatm)	Sewage (µatm)	Parkmore Pier (µatm)
July 2013	8370.5 – 15502.3	---	---
January 2015	6046.8 – 7122.2	1304.7-2483.7	500.3 – 1177.8
June 2015	777.8 – 16205.2	148.0 – 339.1	37.4 – 67.3
January 2016	17800.2 – 24494.8	49.3-243.5	49.3 – 243.5

pCO_2 levels at the SGD point far exceeded those at the sewage discharge point or Parkmore Pier. Dilution of SGD with seawater upon discharge may account for the decrease in pCO_2 levels within the bay in combination with SGD-driven pCO_2 degassing upon release and exposure to the atmosphere for each sampling time point, as shown in Table 3.10. CO_2 concentrations at the SGD discharge point in the intertidal zone were also calculated using CO2SYS (Table 3.11). CO_2 levels during winter were highly variable due to the large differences between January 2015 and January 2016 regarding SGD volumes and loading (Chapter 2) while summer concentrations were more uniform relative to each other.

Table 3.11: CO_2 concentrations (µmol L^{-1}) ranges calculated using the CO2SYS software for submarine groundwater discharge collected across each sampling campaign.

Sample date	CO_2 conc. (µmol L^{-1})
July 2013	295.8 – 621.2
January 2015	229.3 – 271.1
June 2015	303.6 – 627.8
January 2016	779.3 – 1074.1

A positive CO_2 flux was determined in January 2015 while there was a negative CO_2 flux from the water column to the atmosphere in June 2015 and January 2016 (Table 3.12).

Table 3.12: pCO_2 fluxes calculated using equation (1) and CO_2 fluxes determined by CO2SYS software for allochthonous sources; submarine groundwater discharge, sewage point and Parkmore Pier, collected across all sampling campaigns. --- Represents data not analysed.

Sample date	SGD (mmol m^{-2} d^{-1})	Sewage (mmol m^{-2} d^{-1})	Parkmore Pier (mmol m^{-2} d^{-1})
July 2013	-142.9	---	---
January 2015	-355.4	-85.8	-25.2
June 2015	-102.8	1.4	2.2
January 2016	-1278.9	-30.0	15.6

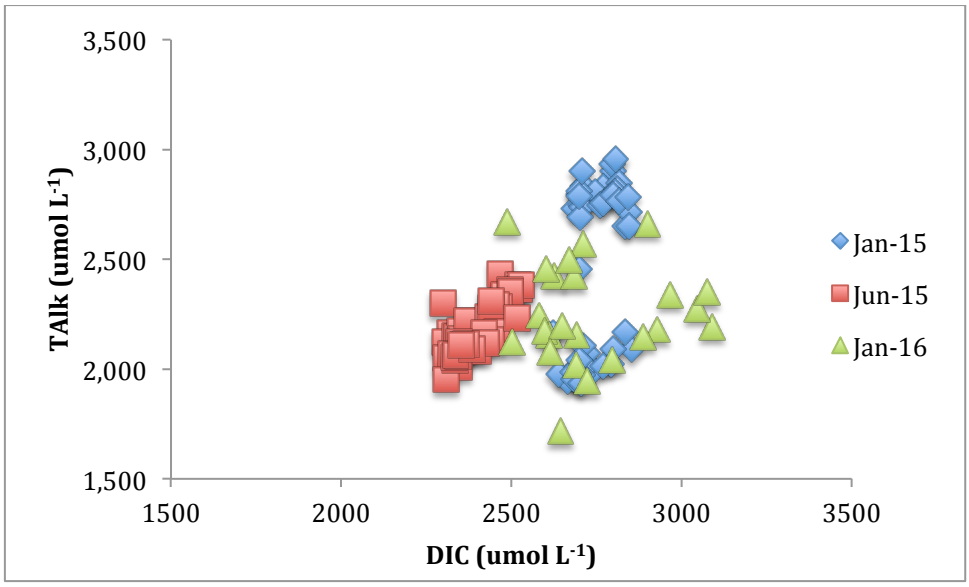

Figure 3.9: A graph of TAlk versus DIC for time-series sampling at Parkmore Pier over the course of two sequential cycles during January 2015 (n = 47), June 2015 (n = 48) and January 2016 (n = 23) sampling campaigns. TAlk data was not available for the July 2013 sampling campaign

During the January 2015 campaign there was two water masses mixing and no clear pattern for DIC versus TAlk. In the June 2015 campaign there was an increasing trend of DIC versus TAlk which had an equation of the line of y = 0.463x +1386.1, R^2 = 0.6,but the January 2016 campaign had no clear DIC versus TAlk relationship (Figure 3.9).

3.6 Discussion

3.6.1 Allochthonous carbon transport

Of the three allochthonous DIC and TAlk sources, SGD represented the highest concentrations and fluxes of DIC and TAlk. The higher DIC concentration in groundwater resulted in high loads that can be attributed to the geological structure of the Gort-Kinvara aquifer, as found in other studies (eg. Szymczycha et al., 2014). HCO_3^- in a karstic region may be due to weathering of carbonate minerals and atmospheric CO_2 (Cai et al., 2008). Absolute concentrations of DOC were higher in sewage and wet deposition compared to SGD in each campaign. However, sewage discharge and precipitation constituted a minor component of the hydrological budget, and therefore carbon fluxes associated with these inputs were small compared to SGD influxes. SGD accounted for

89.5% of the allochthonous loading of DOC and over 99% of DIC and TAlk inputs to the bay across all campaigns.

SGD has been shown to be the primary driver of DOC in many coastal aquatic ecosystems worldwide (e.g. Maher et al., 2013; Liu et al., 2014; Szymczycha et al., 2014; Stewart et al., 2015). The DOC concentrations of approximately 260 – 430 μmol L^{-1} in SGD measured here are consistent with those previously determined in Kinvara Bay by Smith and Cave, (2012) of 200 – 600 μmol L^{-1}. The latter study found that lower DOC values were associated with summer and coincided with lower discharge rates and therefore they concluded that SGD was not a significant source of DOC to the bay. This trend was found in other study locations (e.g. Maher et al., 2013). However, in this current study SGD had the highest DOC concentrations in the summer campaigns. During the winter campaigns, the DOC levels were lower and similar to oceanic values (Table 3.1; Figure 3.1). This pattern has also been reported previously: for example, groundwater was found to be a significant source of DOC and DIC to the Baltic Sea during summer and autumn (Szymczycha et al., 2014). Bacterial and chemical breakdown of organic matter within the aquifer or in surface streams may lead to a continuous production of DOC in summer due to higher temperatures (Cadée 1982). Significantly higher water fluxes coincided with the January 2015 sampling campaign (Chapter 2) and therefore corresponding DOC fluxes were higher during this period. During all other periods, SGD-borne DOC fluxes into the bay were similar. SGD was considered a significant source of DOC to the coastal region of Kinvara Bay at all sampling time points. DOC concentration at Parkmore Pier showed a negative trend with salinity during January 2015, which is consistent with the findings of Smith and Cave, (2012). At the other sampling time points, the DOC concentrations had high variability and DOC-salinity relationships could not be established. SGD-borne DIC was larger in both winter campaigns compared to samples taken in June 2015. The relatively low SGD DOC:N ratios of this study (2 – 5) were consistent with those found by Smith and Cave, (2012) previously. Smith and Cave, (2012) also showed that Kinvara Bay had lower C:N ratios observed during winter compared to summer in their study.

DIC analysis was not conducted for samples taken in July 2013 due to unforeseen circumstances. Nevertheless, this observation was consistent with that of Wang et al., (2015), who studied a subterranean estuary (STE) on the Jiulong River estuary, China. Tidal exchange samples taken at Parkmore Pier and DIC mass balance measurements indicate that a slight fraction of the allochthonous load of DIC (less than 1%) and DOC (less than 6%) into Kinvara Bay was exported to Galway Bay. The net export of DOC is consistent with Smith and Cave, (2012) who showed that Kinvara Bay exported DOC to Galway Bay during wet periods. Thus, SGD does not appear to have a significant impact on the carbon cycle of Galway Bay since nearly 100% of allochthonous and autochthonous carbon is retained within the bay across all campaigns.

The mixing plots showed that TAlk and DIC followed a similar trend with salinity. SGD, which has the lowest salinity, exhibited highest concentrations, and there were relatively uniform concentrations across intermediate to high salinities of sewage and Parkmore Pier. The opposite trend was observed for DOC (Figure 3.1), in which SGD had the lowest concentrations of DOC. Mixing plots at Parkmore Pier showed two distinct water masses during the January 2015 campaign due to higher SGD volumes. Vertical stratification has been shown at Parkmore Pier previously (Rocha et al., 2015). During June 2015, DIC mixed relatively conservatively at Parkmore Pier ($R^2 = 0.77$) with DIC decreasing with salinity. However, during all other sampling campaigns, there was no clear relationship between salinity and DIC. Therefore Null Hypothesis 2 cannot be accepted, as DIC did not mix conservatively within Kinvara Bay over the course of these four campaigns. In general, nonlinear concentration-salinity relationships reflect the existence of *in-situ* addition or removal of chemical species (Cai and Wang, 1998). The DIC and nutrient depletion found at intermediate salinities may be explained by CO_2 degassing and productivity (Guo et al., 2012).

3.6.2 Autochthonous carbon transport

Sediment incubation experiments were conducted during the June 2015 campaign based on the assumption that the benthic compartment reached steady state and therefore the fluxes measured across the sediment-water interface were considered representative of the bulk exchange (Capone et al., 2008). Organic carbon burial is a known sink of C in the ocean. The difference between delivery and burial is an estimate of net oceanic metabolism (Smith and Hollibaugh, 1993). The DOC sediment incubation experiments showed that the sediment within Kinvara Bay acted as a sink for DOC in the June 2015 campaign. The net loss of DOC ($2.6 \pm 1.1 \times 10^3$ mol C d^{-1}) through the seafloor accounted for up to 3.8% of the allochthonous DOC inputs during the January 2015 campaign and 14 – 20% of DOC inputs of the three other campaigns. It is important to note that sediment incubation experiments were only conducted in June 2015 and remineralisation rates of OM are highest during summer in other studies (Jahnke et al., 2005) and therefore burial may have increased during winter campaigns due to increased loading and lower productivity. The sediment sink and the increase in absolute concentrations suggest that the bay itself may be acting as a source of DOC through sloppy feeding or cell breakdown, as seen in Kinvara Bay previously using a N:P model (Rocha et al., 2015) and in other study sites (Møller et al., 2003; Møller 2007).). Mussels are filter feeders, Kinvara Bay has approximately 300 tonnes of commercially rope-grown and an unknown number of wild mussels at any time. These may be responsible for filtering 2 – 10% of the tidal prism volume (Smith and Cave, 2010). Mussels excrete particles as pseudofaeces, which may fuel benthic activity and increase the release of dissolved end products of OM mineralisation (Arnott and Vanni, 1996). DOC benthic flux has been shown to represent a significant source of DOC to the oceans. Global benthic flux has been shown to be comparable to

the riverine input of OC to the oceans (Burdige et al., 1992). These fluxes have been shown to play a significant role in marine biogeochemical cycles (Martens et al., 1992).

Benthic OM mineralisation, measured by incubation experiments, indicates that there was a net flux of 3.9 (±1.5) x 10^4 mol DIC d^{-1} to the water column across the entire bay. Hence, benthic release of DIC is the ultimate product from organic carbon mineralisation. This flux was on par with SGD fluxes and two factors greater than sewage influxes. The inputs associated with SGD accounted for 89.5% of allochthonous inputs and were 2.6 ± 0.7 x 10^4 mol d^{-1}, suggesting that release from sediments acted as an important part of the DIC budget particularly at intermediate salinities. Degradation of sedimentary organic matter produced by benthic microalgae may have accounted for the DIC effluxes, as seen in other studies during summer (e.g. Bertuzzi et al., 1997). The observed net loss of DIC from the sediments corresponded to 66.7% of the carbon taken up in the form of DOC, suggesting that carbon is efficiently recycled within surface sediments, which shows that sediments were important in the total metabolic carbon turnover in Kinvara Bay, as seen in other study locations (Jahnke et al., 2005).

3.6.3 pCO_2

The influence of the local karst geology plays a large factor in determining the carbonate chemistry of the groundwater and therefore the DIC and TAlk transported via SGD. Due to the high pCO_2 in fresh groundwater globally, SGD acted as a delivery mechanism of CO_2 to the water column in the bay as well as to the atmosphere. CO_2 fluxes in coastal zones are driven by biological productivity, hydrological factors (fresh-seawater mixing), and physical processes (wind-driven evasion) (Borges and Abril 2010; Maher et al., 2015). The CO_2 efflux is a likely sink of DIC that would balance some subterranean export (Wang et al., 2015).

The pCO_2 levels at the sewage point, located within the bay, were higher than the corresponding mouth of the bay during all measured campaigns (Table 3.12). The global average pCO_2 in upper estuaries is estimated to be 3,033 ± 1,078 µatm (Chen et al., 2012). pCO_2 fluxes associated with SGD far exceeded these global averages while levels at the sewage point within the bay were lower than these values. The corresponding atmospheric CO_2 flux associated with SGD during the winter campaigns was greater (355.4 – 1,278.9 mmol m^{-2} d^{-1}) than the global average of 188 ± 70 mmol m^{-2} d^{-1} (Chen et al., 2012). However, during the June 2015 campaign, this value significantly decreased to 102.8 – 142.9 mmol m^{-2} d^{-1}. SGD-borne DIC not released as CO_2 can be consumed by biological production stimulated by the high level of nutrients transported via groundwater (Liu et al., 2012). The bay acted as a source of CO_2 during January 2015 and a sink during June 2015 and January 2016 (Table 3.12) representing a drawdown of CO_2 into the water column. During the June 2015 campaign there was the greatest drawdown of pCO_2 found in this study. pCO_2 during this period fell below 250 µatm at the sewage point and below 60 µatm at Parkmore Pier. This period

corresponded to greater DO levels, in fact, DO was supersaturated, during both summer campaigns, and also corresponded to the highest pH levels. Heterotrophy in January 2015 was supported by large fluxes of organic carbon and CO_2 rich SGD. Thus, SGD-driven pCO_2 may have equilibrated with the atmosphere upon discharge in the January 2015 campaign but may have been channelled into primary production in the other campaigns. Hence, there was a respiration-production cycle on an annual scale. pCO_2 measurements support the findings of Chapter 3 that Kinvara Bay was net autotrophic in June 2015 and January 2016 but net heterotrophic in January 2015. January 2015 also corresponded to lower DO and pH levels. High primary production during spring and summer blooms has been shown in Bothnian Bay, which has reduced the annual net heterotrophy (Algesten et al., 2006). In oligotrophic North Atlantic waters, primary productivity was shown to be highly variable. In fact, Arstegui and Harrison, (2002) showed that PP controlled the transition of a system from net heterotrophy to net autotrophy.

There is a debate on the trophic status of coastal zones as a whole, as to whether these are net autotrophic or heterotrophic. Coastal seas, on the whole, have been categorised as net heterotrophic (Smith and Mackenzie, 1987; Smith and Hollibaugh, 1993) and net autotrophic (Mackenzie et al., 2000). Over the course of these three sampling campaigns, Kinvara Bay was shown to switch from net heterotrophic to net autotrophic depending on the conditions within the bay. During the wettest campaign, the bay was net heterotrophic and thus SGD had a great influence on the autotrophy of the system.

3.6.4 Ocean acidification

Ocean acidification is one of the leading anthropogenic problems of this century (Doney et al., 2009). Although pH is decreasing in the open ocean, this trend has not been observed in coastal ecosystems (Provoost et al., 2010). Coastal zones are more complex than the open ocean in terms of biogeochemical processes, anthropogenic inputs and impacts. pH dynamics in coastal zones cannot be adequately modelled to project changes in the future (Duarte et al., 2013). Therefore, predictions of pH trajectories remain uncertain. SGD delivered lower pH waters to the coastal zone in Kinvara Bay during all campaigns. The minimum pH associated with SGD was 6.9 in July 2013 and thus may accelerate OA based on these inputs alone. The buffering capacity of SGD is dependent on the DIC:TAlk ratio. Systems which have a DIC:TAlk ratio of near 1 and a pH of approximate 7.5 represent the minimum buffering capacity due to the carbonate system (Egleston et al., 2010). The DIC:TAlk in SGD was 0.9 over all campaigns, which is close to 1, while the pH of SGD was between 7.1 – 7.5. Therefore, TAlk delivered via SGD is at a minimum in terms of buffering capacity based on TAlk and DIC fluxes. During low tide at Parkmore Pier the pH was consistently lower than corresponding high tides over all campaigns (Appendix A) and may be attributed to the presence of SGD exiting the bay. Increasing pH trends toward the seawater end-

member due to the buffering of the marine carbonate system has been noted in previous studies of SGD in karst aquifers (e.g. Cai and Wang, 1998). Buffering capacity increases with increasing temperature due to shifts in acid-base dissociation constants (Egleston et al., 2010), which may account for seasonality effects. Other factors that may influence pH within the bay include variation in photosynthesis-respiration, diffusion of nutrients, CO_2 from bottom sediments, and $CaCO_3$ production-dissolution (Feely et al., 2009; Lee and Kim, 2015).

Metabolic activity has been shown to play a significant role in the pH control of coastal systems (Gattuso et al., 1998; Anthony et al., 2011). When in balance, primary production and respiration processes result in large diel variability but are essentially CO_2-neutral. Coastal phytoplankton blooms can modify pH significantly (Dai et al., 2008) while benthic microbial processes influence pH and alkalinity through sediment-water exchange in coastal zones (Cyronak et al., 2013). Algal beds have been shown to draw CO_2 down potentially offsetting the impacts of ocean acidification by increasing pH (Anthony et al., 2011). As CO_2 was metabolised within Kinvara Bay, there was a corresponding decline in DIC concentrations from source to sea. The plot of TAlk versus DIC allows for separation of the effects of biological (metabolism) and geochemical processes ($CaCO_3$ precipitation and dissolution) on the carbonate system (Andersson and Gledhill, 2013). As samples measured in June 2015 were the only samples to exhibit a linear pattern, analysis will be conducted for this campaign only. Geochemical processes affect TAlk and DIC concentrations in a ratio of DIC:TAlk of 2. Biological processes only affect DIC and thus the slope of the curve can provide information about the carbonate system of the bay (Cyronak et al., 2014). Equation of the line was determined as TAlk = 1.3009x – 936.47. The contribution of inorganic carbon metabolism on DIC was 65% as 1 mol of $CaCO_3$ is precipitated when TAlk decreases by two equivalents (Gattuso et al., 1996). Therefore, the biological to geochemical ratio of DIC flux was 2.03, as per calculations by Cyronak et al., (2013). This value was lower than those previously reported for water column measurements. As SGD is in close contact with the karstic aquifer, the non-organic carbonates may decrease this ratio (Gattuso et al., 1996; Cyronak et al., 2013a).

These results showed that production exceeded respiration during July 2013, June 2015 and January 2016, and there was enhanced CO_2 uptake from primary production associated with nutrient inputs delivered via SGD (Chapter 2). This was in direct correlation to higher pH and DO (supersaturated) measured during the summer campaigns. pH increase caused by enhanced biological production, resulting from SGD-driven nutrient inputs has been shown previously in Kinvara bay (Rocha et al., 2015) and other systems (e.g. Lee and Kim, 2015). SGD has been demonstrated to be a primary vector for solute transport to coastal zones and may contribute to buffering due to increased nutrients leading to higher productivity. Hence, mitigating activities to reduce the nutrient export from land may reduce the buffer within coastal zones and lead to

decreasing pH and ocean acidification. Naturally low saturation state ($\Omega < 0.6$) was measured in groundwater discharging to Kinvara Bay. The impact that the low saturation state combined with ocean acidification could have on calcifying organisms grown within Kinvara Bay are not yet known and is an important area for further research.

Null Hypothesis 3 cannot be rejected. SGD may buffer against ocean acidification due to higher TAlk levels in combination with increased metabolism associated with high DIN influxes.

3.7 Synopsis

While sewage and wet deposition had the greatest absolute concentrations of DOC, SGD delivered larger quantities of carbon, both DOC and DIC, which accounted for greater than 90% of allochthonous inputs due to sheer volume. C:N:P ratios far exceeded the Redfield Ratio confirming the limiting nutrient in Kinvara Bay to be P. Net retention of DOC and DIC within the bay was nearly 100% over all sampling campaigns. Sediments were an active link in the carbon cycle as they acted as a sink of DOC and a source of DIC in incubation studies performed for the June 2015 campaign. Net loss of DIC from the sediments corresponded to 66.7% of the carbon taken up in the form of DOC. The bay was net heterotrophic during January 2015 but net autotrophic in June 2015 and January 2016. Losses of DIC during the June 2015 campaign were primarily due to biological uptake, which in turn draws down pCO_2 and provides an associated enhancement of dissolved oxygen and pH at intermediate salinities (Dai et al., 2008). This study showed that SGD delivers low pH waters to the coastal zone in conjunction with high fluxes of DIC and TAlk, which have a critical role in the carbonate system of coastal zones. pH increased with distance from shore and can be attributed to seawater mixing and productivity within the bay associated with SGD-borne DIN loading.

4. Characterisation of Submarine Groundwater Discharge (SGD)-borne Dissolved Organic Matter (DOM) in a Karstic Aquifer, Ireland

4.1. Introduction

Dissolved organic matter (DOM) is an important part of the carbon cycle, and its biogeochemical fate in the ocean is critical to fully understand climate change (Jiao et al., 2010) as well as elemental cycling (Chen and Jaffé, 2014). The three leading roles played by DOM in coastal biogeochemistry are 1) acts as a vehicle for nutrient mobility and might control the balance and accumulation of N and P in coastal areas; 2) it acts as a binding agent for metals and thus increases metal toxicity and mobility, and 3) controls pH, which influences availability of toxic metals. Consequently, its presence and dynamics potentially affect the physical, chemical and biological properties of ecosystems worldwide. Autochthonous production has been shown to be the primary source of DOM (95%) to the world's oceans with terrestrial DOM representing only 2 - 3% (Opsahl and Benner, 1997; Stedmon and Markager, 2005a). However, terrestrial-derived DOM may be significant in coastal zones due to larger freshwater and associated material influxes. Fresh SGD has been estimated to account for 5 - 10% of the world's DOC influx into coastal oceans (Dai et al., 2012), yet few studies have been conducted to determine the biogeochemical properties of the DOM pool.

Due to its complex nature, DOM is classified into two broad groups, humic-like and protein-like components (Coble, 1996; Parlanti et al., 2000; Yamashita et al., 2008). Humic substances (HS) are among the most widely distributed organic materials on the planet (Murphy et al., 2008). HS are key components in soil. Subsurface microbial activity can release organic matter from soils (Longnecker and Kujawinski, 2011) that can be incorporated into groundwater as it percolates from land to the subsurface. There are many possible sources of dissolved HS in aquatic environments including partially degraded material from plants and algae such as lignin, tannins and flavonoids, microbial products and structural polymers of vascular plants known as lignocellulose (Moran and Hodson, 1990; Osburn and Morris, 2003). These vary in concentration and composition from environment to environment. HS are often thought of as refractory, and therefore, assumed to be largely resistant to bacterial degradation (MacCarthy, 2001; Moran and Hodson, 1990). However, it is possible that a fraction of this pool may be biologically available for consumption as a primary substrate for bacterial communities, making it also important in supporting bacterial secondary production in aquatic ecosystems (Moran and Hodson, 1990). Studies show that HS moderate bacterial activity through trace metal chelation, P cycling and enzymatic activity effects (Stewart et al., 1982; Visser, 1985). Numerous studies also show that sunlight-mediated reactions can convert refractory DOM into more labile material (De Haan, 1993; Moran and Zepp, 1997; Moran et al., 2000; Amado et al., 2006; Stubbins et al., 2012). Photodegradation of HS can increase the turnover rates of DOM by converting it to inorganic nutrients, which may act as bacterial substrate (Miller and Moran, 1997). Protein-like peaks are thought to be derived from microbial activity (Cammack et al., 2004; Yamashita and Tanoue, 2004) and constitute bioavailable, labile organic fractions

(Hudson et al., 2007). Due to the number of sunlight hours and temperature, photobleaching of CDOM may be seasonal, increasing during summer months. Additionally, CDOM plays a key role in light penetration in surface waters, which will modify the behaviour of autotrophs and subsequently heterotrophs in both positive and negative ways (Moran and Zepp, 2000).

EEMF-PARAFAC is the widely accepted method for DOM analysis (Fellman et al., 2010) and has been applied in many environments, including lakes (Cory and McKnight, 2005; Yao et al., 2011), estuaries (Bertilsson and Tranvik, 2000; Stedmon and Markager, 2005), rivers (Mostofa et al., 2010) and bays (Yamashita et al., 2008; Singh et al., 2010). CDOM, however, has only been used as a natural tracer of groundwater in a few studies (Baker and Genty, 1999; Baker and Spencer, 2004; Lapworth et al., 2007; Lapworth et al., 2008; Chen et al., 2010; Mudarra and Andreo, 2011), with little focus on the discharge of this water directly to the coastal ocean.

Kim et al., (2012) highlight that SGD-driven DOM plays a significant role in coastal carbon cycles and more studies need to be conducted in this field. Furthermore, SGD, both fresh and brackish, were characterised by relatively high CDOM and DOC in the subterranean estuary (STE) of a volcanic island, Jeju (Kim et al., 2013). Yang et al., (2015) compared DOC and DOM concentration, composition and bioavailability in two subterranean estuaries (STEs) of southwest Taiwan with contrasting pollution levels. They found that groundwater DOM was highly non-conservative and that DOM composition can be modified within the STE. They also found a direct correlation between CDOM and pollution, as the highly polluted STE had corresponding higher fluorescence intensities compared to the STE experiencing lower pollution. Thus, to better constrain the sources and importance of SGD-borne DOM in coastal oceans, various hydrogeological, oceanic and biogeochemical conditions must be studied.

4.2. Sampling site and strategy

4.2.1 Sampling site

Possible DOM sources to SGD in Kinvara include (1) groundwater recharge throughout the catchment, (2) groundwater flow from upstream, (3) desorption from soils as water percolates through and (4) possible seawater intrusion. Sources to surface water in the region may include (1) oxidation of soil organic matter, (2) autochthonous production by organisms, (3) precipitation, and (4) exchange with underlying groundwater. The interaction of surface and groundwater is critical in this aquifer, and therefore, surface DOM may also be transported through the subterranean pathway to the coastal zone, allowing for modification on land.

The null hypothesis (H_0) states that SGD transports bioavailable materials (protein-like peaks) to Kinvara Bay.

The alternate hypothesis (H_1) is that SGD-borne DOM is refractory, representing humic-like material, in Kinvara.

4.2.2 Sampling procedure

Groundwater from wells, boreholes and the submarine groundwater discharge springs (known as the Castle and the Arch) was collected over nine sampling campaigns from November 2012 to June 2014. Surface samples were collected from streams, rivers and turloughs throughout the catchment area. Sampling was conducted over two full tidal cycles during summer and winter at Parkmore Pier. Samples were filtered through pre-combusted GF filters and collected in pre-cleaned, acid-washed amber glass bottles. All filters and containers were rinsed several times with the sample before filling. A flow through cell was used, and wells purged, where appropriate. Collected samples were stored on ice in the dark and transported to the laboratory within three days for analysis.

At the same time water samples were collected, *in-situ* measurements of salinity, conductivity, temperature, pH and GPS coordinates were obtained using an Aquaread 1000 AP, calibrated prior to use with a freshwater conductivity (Varian 12,800 µS cm^{-1}), pH (Varian pH 4.00, 7.00 and 10.00) and ORP standards (+129 mV).

4.3. Methodological principles

There have been significant improvements in DOM characterisation techniques over the last 25 years due to advances in spectroscopic techniques such as absorbance and fluorescence. These methods provide a better alternative to traditional approaches which were labour intensive, specialised and required large quantities of sample (Coble et al., 1990; Coble, 1996; McKnight et al., 2001) Now, Chromophoric DOM (CDOM), the optically active fraction acts as a tracer for the wider DOM pool. Fluorescence characterisation allows for the elucidation of the biogeochemical fate of DOM in coastal zones by incorporating a routine, fast, reliable method for analysis.

4.3.1 Principles of fluorescence

Molecular absorbance occurs when a molecule exposed to light of a given wavelength (equal to the energy gap between the ground and excited states, termed energy levels) is promoted to an electronically excited state. The amount of light absorbed is proportional to the concentration of the absorbing molecule. The Beer-Lambert Law describes this proportionality between absorbance and concentration (Osburn and Morris, 2003):

$$A = \varepsilon Cl = \log_{10} (I_o/I) \qquad (1)$$

Where, A = absorbance, I_0 and I = the intensity of incoming and transmitted light, respectively, ε = molar absorptivity coefficient (L mol^{-1} cm^{-1}), C = concentration (mol L^{-1}) and l = path length (cm).

Absorbance describes the transition of the fluorophore from the ground state (S_0) to an electronically excited state, S* (Osburn and Morris, 2003). In most molecules, the electron undergoes radiationless deactivation and relaxes to the lowest energy level of S_1 (Lakowicz 2006). In fluorophores, fluorescence emission then occurs through relaxation from the lowest energy level of S_1 (Kasha's Rule) through emission of light. A Jablonski diagram is incorporated below (Figure 4.1) to illustrate the possible processes involving the absorption and emission of light.

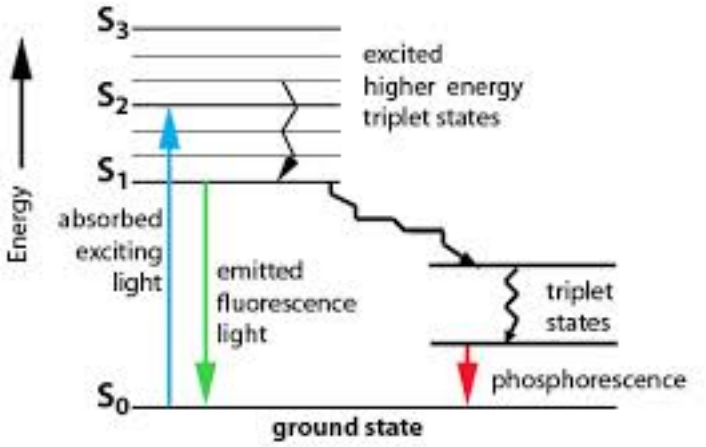

Figure 4.1: A simplistic Jablonski Diagram

The emission spectrum is independent of the excitation wavelength, and therefore, the emission spectra of a given fluorophore at different excitation wavelengths will vary in intensity but not shape. The opposite is also true; the excitation spectrum is independent of the emission wavelength. In Excitation-Emission Matrix (EEM) spectroscopy, the fluorescence spectrum is measured as a function of these two factors (excitation and emission wavelengths), which allows the spectra of specific chemical compounds to be assigned (Coble, 1996). EEMs are collected by measuring several emission spectra over a range of shifting excitation spectra (Coble et al., 1990; Kim et al., 1990; McKnight et al., 2001; Singh et al., 2010) to produce a matrix and increase selectivity and sensitivity. EEMs provide the wavelength-independent fluorescence maximum (Ex_{max}/Em_{max}) (Coble, 1996).

Fluorophores are typically compounds that readily absorb sunlight and contain functional groups, such as aromatic rings, conjugated double bonds or some rigid structure (C=C, C=O), which prevents relaxation through torsional energy. The aromatic amino acids, tyrosine, phenylalanine and tryptophan, the coenzymes NADH, NADPH and vitamins (A, B, D and E) are examples of fluorophores. Relevant to this study is the evaluation of humic and fulvic acids, containing multiple bonds from the aromatic, aldehyde and ketone functional groups (Osburn and Morris, 2003).

The local environment surrounding a fluorophore can affect the fluorescence signal. Factors such as pH, temperature, concentration and polarity can influence the emission of a given fluorophore.

Factors such as pH and temperature were measured *in-situ* for every sample and then subsequently controlled.

4.3.2 Methodology employed

Samples were analysed by high-temperature catalytic oxidation (HTCO) using an Elementar Vario TOC cube (detailed in Chapter 4).

4.3.2.1 Absorption spectroscopy

Absorbance was measured using a HACH spectrophotometer zeroed using MilliQ water at 350 nm to determine the presence of inner filter effects. The Beer-Lambert Law described above is not valid for samples at high concentrations due to quenching, known as inner filter effects. Part of the excitation and/or emitted light is reabsorbed by the sample, and the measured intensity of the fluorescence is thus quenched. At α_{350}, an absorbance reading of less than 0.8 is believed that inner filter effects are not interfering. Above 0.8, inner filter effects can be minimised by reducing the absorbance of the sample by appropriate dilution using MilliQ water (Guo et al., 2010).

Absorbance readings at 275 – 295 nm and 350 – 400 nm were read to determine the slope ratio (Helms et al., 2008). Spectral slopes, S, were calculated according to the linear regression of the log-transformed α spectra. Absorbance units were converted to absorption coefficients as follows:

$$\alpha = 2.303A/l \quad (2)$$

Where α = Napierian absorption coefficient (m^{-1}), A = absorbance, and l = path length (0.01 m).

This was then log transformed, and linear regression was carried out using the equation below (Twardowski et al., 2004):

$$\alpha(\lambda) = Ae^{-Se\lambda} \quad (3)$$

Where α = Napierian absorption coefficient (m^{-1}), λ = wavelength, A = amplitude, and Se = spectral slope parameter (nm^{-1}).

This ratio can be related to DOM molecular weight. It can be measured with high precision and allows for comparison between dissimilar water bodies, as it is largely independent of CDOM concentration.

Also, the average sample absorbance between 700 - 800 nm was measured to account for offsets due to drift, temperature, scattering and refractive indices differences (Green and Blough, 1994).

SUVA254 was determined by measuring the absorbance at 254 nm and converted using equation (3) to α254 (m^{-1}) values were then normalised using the DOC concentration (mg L^{-1}).

4.3.2.2 EEMF spectroscopy

Fluorescence was measured using a Varian Cary Eclipse Luminescence Spectrophotometer with a 150 W continuous output Xe arc lamp. EEMs were generated for each sample over excitation wavelengths between 220 - 500 nm in 5 nm intervals and emission wavelengths between 280-620 nm in 2 nm intervals, with 5 nm bandwidths on both excitation and emission modes.

The instrument was calibrated before use using sealed diffuser and pure water cells according to the manufacturer's guidelines. This calibration carried out six tests to ensure that the spectrofluorometer was operating accurately. These tests checked the wavelength accuracy emission monochromator (Xe arc lamp), the spectral bandwidth accuracy for both the excitation and emission slits, stray light and the Raman water sensitivity at excitation 350 nm and 500 nm. Daily Raman calibration was also conducted by collecting the water Raman peak of distilled water before each experiment to monitor instrument stability. No apparent variation was found in the water Raman intensity during this investigation.

The quartz sample allows for UV fluorescent measurements. Cuvettes were stored in 10% hydrochloric acid (HCl) under a fume hood and flushed extensively with MilliQ water before analyses to minimise the presence of interferants. The instrument was run at room temperature to prevent condensation on the cuvette walls. Samples were stored in the dark and remained sealed to prevent quenching by O_2 exposure and photodegradation. Prior to analysis samples were kept at a steady temperature of 20°C in a water bath to minimise temperature effects. All fluorescence signals were acquired in signal over reference ratio mode (S/R) to eliminate potential fluctuation of the Xe lamp. All samples from a given experiment were analysed on the same day, where possible, to avoid the small error associated with day-to-day variability.

4.3.2.3 PARAFAC modelling

The output from the EEMF was modelled using parallel factor analysis (PARAFAC), a statistical tool based on alternating least square algorithm to minimise the sum of squared residuals across the dataset and from this the underlying structure of the EEMs (Stedmon and Bro, 2008). PARAFAC can statistically decompose EEMs into groups of covarying analytes, known as components (Stedmon et al., 2003; Stedmon and Bro, 2008) for which a standard terminology is now widely accepted (Coble et al., 1993; Coble, 1996; Stedmon et al., 2003). Since PARAFAC was first used to characterise CDOM fluorescence, it has become a widely accepted and indeed the standard technique in the field (Stedmon and Bro, 2008; Fellman et al., 2010).

Before modelling, Rayleigh scatter was eliminated and Raman scatter was removed by subtracting a daily MilliQ blank from each EEM. Additionally, a calibration of the fluorescence intensity using the integrated area of a water Raman peak was performed. This calibration allows for inter-

laboratory comparison as instrumental differences have been removed using the A_{rp} method (Lawaetz and Stedmon, 2009). A PARAFAC model was then created and validated in MATLAB 2012 (Mathworks) using the DOMFluor toolbox (Stedmon and Bro, 2008) using a large number of samples (n = 305) with non-negativity constraints applied on all modes (Andersen and Bro, 2003). No obvious residues were found using split-half validation after fitting the component model. Furthermore, random initialisation (n = 10) was conducted to ensure the fit (sum of squared error) was not, in fact, a local minimum.

4.3.2.4 Indicator parameters

The below indicator parameters have been used in many studies to extract more information from these spectra and are incorporated into this investigation. These ratios are largely independent of CDOM concentration (Helms et al., 2008), which is important in SGD zones due to the spatial and temporal variation associated with these systems.

SUVA254 is a measure of the dissolved aromatic content (Weishaar et al., 2003).

The Fluorescence Index (F.I.) is a two-dimensional index of the ratio of fluorescence emitted at two wavelengths (450/500 nm at 370 nm excitation) and has been used as a precursor for organic matter source identification (McKnight et al., 2001). Essentially, this is the relative contribution of aromatic DOM vs. non-aromatic DOM. Microbially derived sources exhibit a greater ratio (≈1.9) than that of terrestrially derived sources (≈1.4).

The Humification Index (HIX) is used to determine the degree of humification within a natural system. Ohno, (2002) found it statistically advantageous to define the HIX as the fluorescence intensity in the 300-345nm region divided by the sum of the fluorescence intensity in the 300-345 and 435-480nm regions. This statistic is based on the idea that the emission spectra of fluorescence will shift towards longer wavelength as humification of DOM proceeds due to lower H:C ratios (Zsolnay et al., 1999). Less humified material is expected to be more labile, as these materials have lower aromaticities (higher H:C ratios) making them more susceptible to microbial degradation. The use of the ratio allows for the primary inner filter effect to be ignored (Ohno, 2002).

Spectral Slope is determined by calculating the ratio of the slope at the shorter wavelength region (275-295 nm) to that of the longer wavelength region (350-400 nm) and is related to DOM molecular weight (Helms et al., 2008).

4.4. Results and discussion

4.4.1 Hydrochemical parameters

Surface and groundwater sampled inland throughout the catchment were fresh as indicated by low salinity values (<0.3 ppt). While SGD primarily exhibited fresh characteristics, there were two sampling campaigns, whereupon it was brackish, September 2014 (7.65 ppt) and July 2013 (2.49 ppt). Therefore, there was low variation in the salinity data, ranging from 0.21 – 7.65 ppt over the sampling period. The higher salinity may be due to seawater intrusion into the aquifer attributed to reduced precipitation during these times. At all other times, SGD represented meteoric recharge, as indicated by its fresh characteristic.

Parkmore Pier had salinity lower than 35 ppt at low tide for all sampling campaigns, highlighting the presence of freshwater exiting the bay. Salinity showed a clear seasonal pattern. During high flow campaigns, the presence of freshwater at the mouth of the bay was more pronounced and salinity fluctuations were connected to the tidal cycle, ranging from 5 – 28 ppt, compared to low flow conditions where salinities were more uniform, 33 – 36 ppt (Appendix E). The salinity of samples collected at the sewage outflow point was fresh to brackish (0.26 – 8.13 ppt) with a clear seasonal trend. Fresh salinity was recorded during high SGD flow, while brackish salinity was measured during base flow. The brackish salinity suggests rapid dilution with bay water, as expected, because sewage is discharged during the ebb of high tide. During winter, there was lower salinity in the bay as a whole. As shown in the Table 4.1, SGD had a relatively stable temperature profile (taken over all seasons) compared to sewage or seawater due to the thermo-insulating effect of the aquifer.

Table 4.1: Ranges of *in-situ* monitoring parameters at input locations (SGD and Sewage) and the mouth of Kinvara Bay (Parkmore Pier), over all sampling campaigns, includes seasonal variability during high and low flow conditions

Parameter	SGD	Sewage	Parkmore Pier
Temperature (°C)	8.6 – 15	7.5 – 18.0	7.7 – 18.6
pH	6.3 – 7.8	7.7 – 8.5	8.0 – 8.5
DO (%)	34.4 – 79.8	88.3 – 102.8	88.8 – 111.4

4.4.2 SGD-borne DOC

Table 4.2: Summary of measured DOC concentration in SGD endmember, measured at Castle Springs over the nine sampling campaigns. Data are the result of the mean of several replicates (11 < n < 15) plus or minus the standard error of the mean (± SE).

Sampling Campaign	DOC ($\mu mol\ L^{-1}$)
March 2013	725.7 ± 32.8
July 2013	429.2 ± 11.3
May 2014	721.5 ± 36.0
August 2014	304.9 ± 2.6
September 2014	475.2 ± 11.0
January 2015	303.7± 6.4
March 2015	386.1 ± 8.4
June 2015	379.9 ± 12.2
January 2016	261.1 ± 2.8

DOC concentrations were not available for the October 2012 dataset (Table 4.2), but these samples have been included in the overall CDOM analysis. DOC concentrations taken from inland boreholes were larger (Appendix E) and therefore, indicate possible removal or dilution processes occurred within the aquifer. Such processes include absorption by aquifer materials, biodegradation processes or dilution by lower DOC water due to surface-groundwater interactions in the aquifer, which may result in dilution due to rainfall and mixing of rivers and groundwater.

4.4.3 SGD-borne DOC seasonal variation

Both SGD and its solute content are known to be highly variable both spatially and temporally (Moore, 2010). DOC was normally distributed as evidenced by the Shapiro-Wilk normality test *p*-value of 0.136, df = 7, chi-squared = 7.

The DOC concentration was variable over the sampling period, with no clear pattern emerging. ANOVA analyses (Table 4.3) showed that March 2013 and May 2014 had the highest DOC concentrations and were statistically greater than all other sampling campaigns but not from each other as indicated by their respective *p* values (Table 4.4; Appendix E). For all other sampling campaigns, *p* values were greater than 0.05 and therefore cannot be statistically separated from one another. During very low SGD flow, as indicated by brackish salinities, DOC concentrations cannot be statistically separated from high flow conditions, when salinity was near-zero, excluding times when fertilisation runoff occurs.

Table 4.3: ANOVA results after testing the null hypothesis that H0: Mean DOC concentration, measured at Castle Springs, over eight sampling campaigns is the same for all seasons.

	Df	Sum Sq	Mean Sq	F Value	Pr(>F)
Seasons	7	562219	80317	17.69	$3.42e^{-06}$
Residuals	15	68094	4540		

Table 4.4: Summary p values based on Tukey's Honest Significance Difference (HSD), following ANOVA analysis, for DOC concentrations in the SGD endmember, measured at Castle Springs over the eight sampling campaigns. Highlighted results are significant as $p<0.05$ at significance level, $\alpha = 0.05$.

	Jan-15	Jan-16	Jul-13	Jun-15	Mar-13	Mar-15	May-14
Jan-16	0.99						
Jul-13	0.48	0.18					
Jun-15	0.94	0.63	0.97				
Mar-13	0.00	0.00	0.01	0.00			
Mar-15	0.87	0.50	0.99	0.99	0.00		
May-14	0.00	0.00	0.00	0.00	0.99	0.00	
Sep-14	0.46	0.17	1.00	0.97	0.01	0.99	0.00

4.4.4 EEMF-PARAFAC

EEM data were fitted to a 3-component model (Figure 4.2; Appendix F). No obvious residues were obtained from this model for this dataset after it was validated by split-half analysis and random initialisation (n = 10). The fluorescence signal remaining in the residuals was non-systematic and represented instrument noise (Stedmon et al., 2003; Stedmon and Bro, 2008). When more than three components were modelled, the result from the two split data arrays was not validated as the model was attempting to model instrument noise.

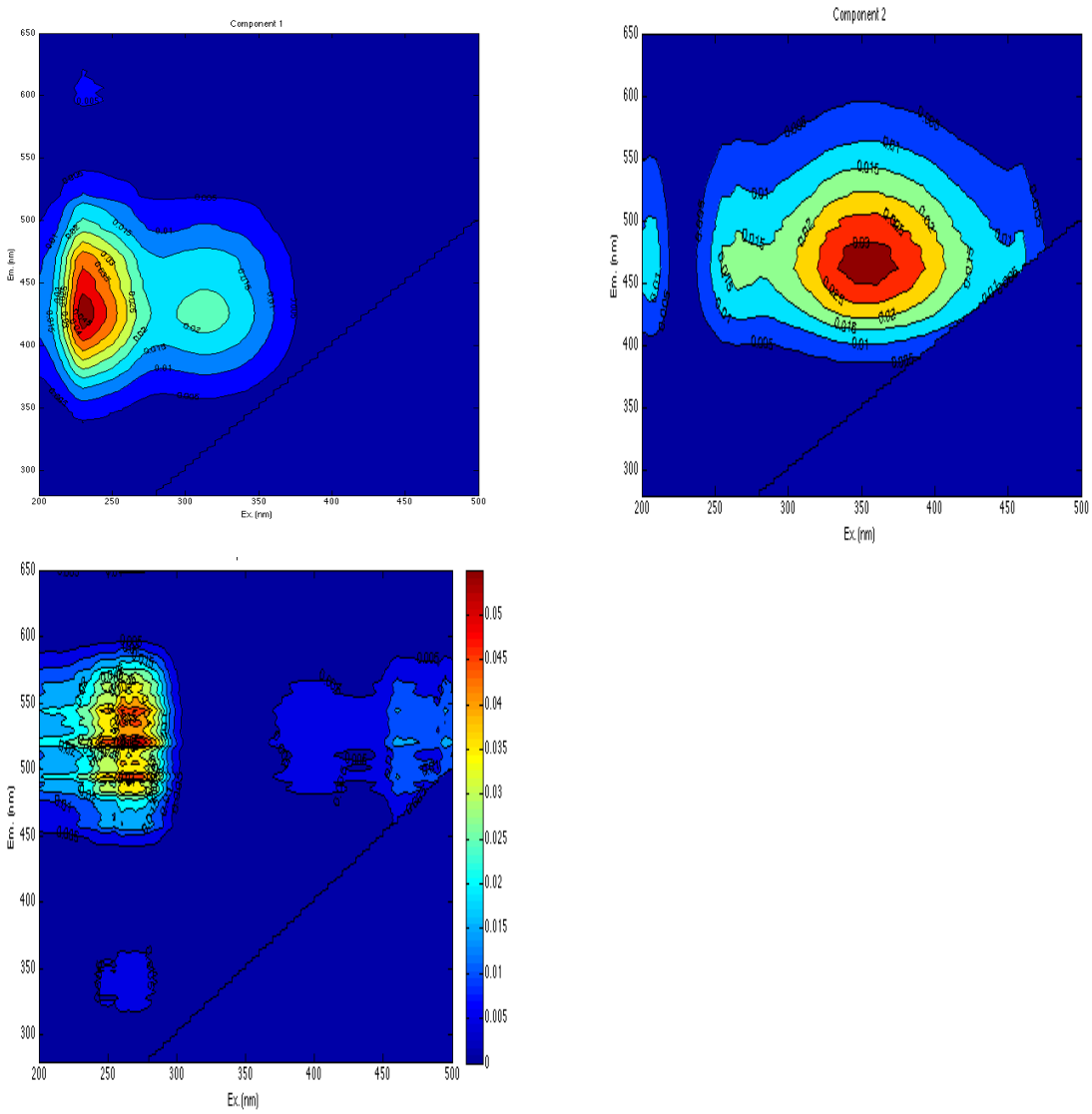

Figure 4.2: EEM Components from the validated annual three-component EEMF. Component 1, 2 and 3, n = 305, measured over ten sampling campaigns. Samples were collected based on a continuum of water flow which includes inland, the SGD springs, sewage outflow location within the bay, Parkmore Pier and Galway Bay.

The three components identified represent the majority of samples. Hence, each component may not be found in every sample, and some samples may have peaks not designated as a part of the overall model (Stedmon and Bro, 2008). Due to the complex nature of DOM, it is likely that each component represents a group of fluorophores with similar fluorescence properties and variability as opposed to an individual fluorophore (Stedmon and Markager, 2005b).

Visual analysis of the identified components (Figure 4.2) highlights fluorescence maxima characteristic of organic fluorophores with multiple excitation and emission maxima. The spectral features and contours of the modelled PARAFAC components fit well with components identified previously by other authors (Table 4.5). Each component in this model represents a mixture of fluorophores that the model was unable to separate out because they co-vary within the dataset, resulting in secondary peaks (Stedmon and Markager, 2005).

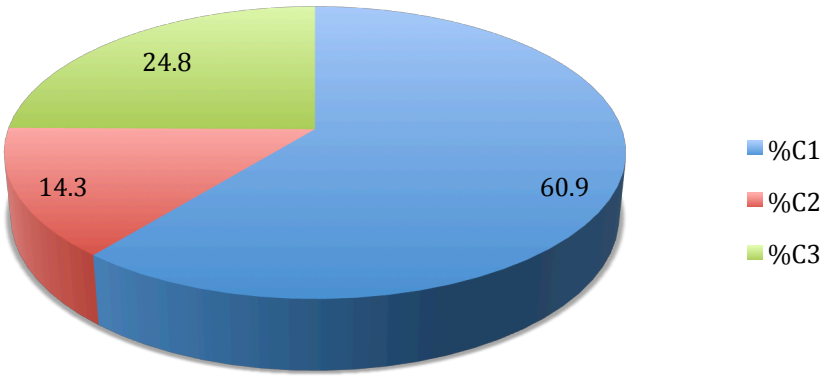

Figure 4.3: Pie chart of the percentage of each component (C1, C2 and C3) in the overall validated annual three-component EEMF model, measured over ten sampling campaigns, n = 305. Samples were collected based on a continuum of water flow which includes inland, the SGD springs, sewage outflow location within the bay, Parkmore Pier and Galway Bay.

C1 represents 60.9%, C2 represents 14.2%, and C3 represents 24.8% of the score intensities of the combined model. Therefore, C1 is the dominant component of the system, representing close to two-thirds of the overall intensities (Figure 4.3). C3 is the second most intense followed by C2.

The number of components identified in the literature using EEMF-PARAFAC from different aquatic environments has ranged between 3 to 13 to date (Coble, 1996; Yamashita and Tanoue, 2004; Cory and McKnight, 2005; Stedmon and Markager, 2005; Yamashita et al., 2008; Murphy et al., 2008). Identification by peak position and shape may vary from study to study depending on the number of samples analysed, sources and types of CDOM, processes that control CDOM variability and mixing in the environment from which the study was conducted (Coble, 1996; Stedmon and Markager, 2005; Singh et al., 2010). Bearing this in mind, comparison of spectral characteristics of each component with those reported in previous studies was conducted. Components 1, 2 and 3 are predominantly similar to ubiquitous humic-like peaks previously reported (Coble, 1996). Broad excitation spectra are characteristic of higher plant origin and may be due to overlapping chromophores (Coble, 1996). However, secondary peaks within the components yield more information and may indicate more diverse sources.

C1 has been shown to be a photoproduct of soil-derived DOM, which results in a photorefractory component (Chen et al., 2010). C1 has a secondary peak resulting from Peak C, visible humic-like material. C2 is also representative of Peak C, a humic-like material with a secondary peak of unknown source. C3 has the longest emission wavelength maximum among the components identified, which has been linked to soil fulvic acid and suggests it may have the highest degree of aromaticity. Component 3 is, therefore, a mixture of Peak A/C and soil fulvic acid. This may be

derived from agricultural catchments as described in Stedmon and Markager, (2005) and is known to be rapidly produced and removed making its identification difficult (Singh et al., 2010).

However, a minor secondary peak indicative of tryptophan-like components indicates a more biologically available component within SGD, which has been associated with amino acids free or bound in proteins. This peak represents a source of autochthonous DOM and has been linked to recent biological production and has previously been identified in fresh and marine environments (Chen et al., 2010; Fellman et al., 2010). The secondary peak of 200/600 has very low intensity (0.005 R.U.). As this peak has emission greater than 550 nm, it was removed from data analysis as it is most likely associated with instrument artefacts and insufficient elimination of secondary Raman and Rayleigh scatter in the EEMs during the post-processing stage (Murphy et al., 2008; Kowalczuk et al., 2009).

In some studies, the DOC concentration has been shown to be strongly correlated with DOM intensity, as there are only humic and fulvic acids present (Wu et al., 2007). For this study, it could be assumed that DOM is made up of primarily humic substances for July 2013, August 2014, September 2014, January, March, and June 2015. This is not the case for March 2013 and May 2014, which had peak intensities indicative of protein-like materials. Anthropogenic influence may have increased during these periods as they correspond to fertilisation seasons and agricultural wastes may percolate into groundwater. These two sampling campaigns also corresponded to maximum concentrations of DOC, 725.7 ± 32.8 μmol L^{-1} (March 2013) and 721.5 ± 36.1 μmol L^{-1} (May 2014).

Table 4.5: Fluorescence characteristics of validated annual three-component EEMF model: excitation and emission maxima, compared with previously identified components. Bold Q components indicative of Quinone-like moieties (Cory and McKnight, 2005), n = 305 over ten sampling campaigns. Samples were collected based on a continuum of water flow which includes inland, the SGD springs, sewage outflow location within the bay, Parkmore Pier and Galway Bay.

Kinvara Model Ex/Em (nm)	Previous Model (literature)	Description	References
C1: 240/425	250 – 450	Humic-like/ Photorefractory product **Q1**	Chen et al., 2010
C1: 320/425	320/415	Microbial degradation product	Chen et al., 2010
C1: 230/600 (minor)	Unidentified in the literature		
C2: 350/ 460	350/420 – 480	Peak C – Humic-like material **SQ1**	Coble, 1996
C2: 210/460	Unidentified in the literature		
C3: 260/500	260-380/ 490	Peaks A/C – Terrestrial humic-like	Murphy et al., 2008
C3: 260/520, 550	<250/520	Soil Fulvic acid **Q3**	Coble, 1996; Stedmon et al., 2003
C3: 260/340 (minor)	275/340	Tryptophan-like	Coble, 1996; Yamashita et al., 2008
C3: 460, 500/525 (minor)	455/521	Soil Fulvic like	Stedmon and Markager, 2005b

Quinone moieties were detected within the HS outlined in Table 4.5. Quinones are biomolecules found in living cells, extracellular material and detrital organic material. Quinone moieties are known to affect the electron shuttling ability of humic and fulvic acids (Fimmen et al., 2007). Quinones have been shown to contribute to the optical properties of humic DOM, and research shows that more than 50% of CDOM fluorescence is potentially as a result of these structures (Cory and McKnight, 2005). Thus, quinone-like moieties within the humic substances are ubiquitous to the EEM of every sample as they are present in each of the components to some

degree. Quinone-like components are involved in redox reactions (Leenheer and Croué, 2003). SQ1 is associated with humic substances from higher plant material and may be as a result of lignin breakdown, which causes enrichment of higher aromatic carbon fractions (Cory and McKnight, 2005). Q1 and Q3 represent oxidised components. Q3 has been linked to microbial precursor material and may be associated with the T peak.

4.4.5 CDOM absorbance in Kinvara Bay

CDOM absorbance values exhibited non-conservative mixing with salinity measured at each sampling location during the course of this study (Figure 4.4). There was no clear relationship of CDOM absorbance with salinity in Kinvara Bay over the course of this study. However, SGD absorbance was higher in summer compared to winter (Appendix E), which is comparable to the EEMF-PARAFAC model (Figure 4.2). In general, higher salinity samples during summer at Parkmore Pier and seawater samples had lower absorbance than lower salinity samples. Hence, the larger proportion of SGD mixed with bay water at Parkmore Pier increased the absorbance readings. However, there were an insufficient number of samples to create a clear relationship between CDOM absorbance and salinity in this study.

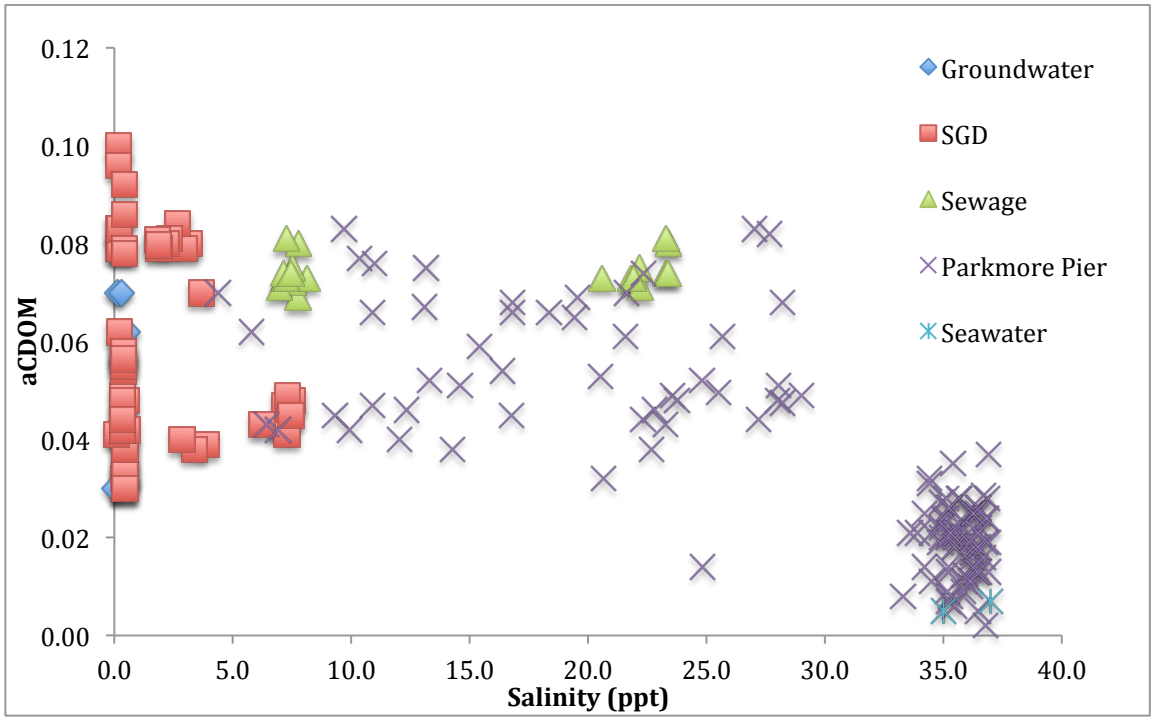

Figure 4.4: An annual mixing curve of CDOM absorbance values (aCDOM) vs. salinity (ppt) measured at all locations, inland, SGD springs, sewage outflow location within the bay, Parkmore Pier and Galway Bay over the course of the sampling campaigns, n = 216

4.4.6 Modelled CDOM scores in Kinvara Bay

Kinvara Bay is fed by sinking rivers, streams, and turloughs through SGD, and the acquired EEMs reflect their influence as mainly terrestrial humic and fulvic acids are transported to the coastal ocean via SGD. The catchment land use is dominated by agriculture, while fisheries are important within the coastal zone (Einsiedl 2005; Schubert et al., 2015). The three endmembers considered in Kinvara Bay are SGD and sewage from the landward side and import of seawater from the ocean.

Considering the CDOM score, the input factors from SGD (0.58 ± 0.2, n = 92) and sewage (0.60 ± 0.3, n = 20) were higher that Parkmore Pier (0.27 ± 0.1, n = 31). The high variation was due to mixing of SGD within the bay, and therefore Parkmore Pier will include a portion of terrestrial-derived CDOM. Before discharge, as the groundwater flows through the catchment, there was slightly higher humic-like material intensity and some labile peaks. Therefore, there may be removal processes occurring within the subterranean pathway. This applies in particular to samples taken near the peaty areas as these contain protein-like components. Turloughs, including Coole and Ballinduff, also had protein-like components, which may be due to the filling/drainage system within these zones and the fact that these have the greatest interaction with humans and agriculture, and therefore, experience higher anthropogenic pressures. In fact, during low flow when the turloughs were empty, these were used as grazing land. These protein-like peaks are considerably removed due to conservative mixing before discharge except during March 2013 and May 2014.

Humic substances are thought to account for 60 - 70% of the total organic carbon in soils and 40 - 60% of DOC in natural waters (Mobed et al., 1996). HS may have been introduced into percolating groundwater as a result of soil lixiviation within the watershed and from microbial action on the sedimentary organic matter (Artinger et al., 2000). Soils are by far the primary source of organic carbon to groundwater. However, there appear to be minor peaks indicative of photodegradation (C1) and more labile materials (C3). The components show that both bio- and photo- degradation pathways exist to some degree within the coastal zone.

Soil-derived DOM and photo-induced transformations of biomass have been shown to be critical degradation pathways in previous studies (Maie et al., 2007; Chen et al., 2010). Degradation pathways may exist within Kinvara Bay due to a residence time of approximately seven days (Rocha et al., 2015), and within the flow path as groundwater travels above the surface for extended periods *en route* to the SGD springs, which allows for photo-degradation (Chen et al., 2010). The presence of protein-like substances implies autochthonous production and active microbial processing of DOM. This was a weak secondary peak (fluorescence intensity = 0.005) in groundwater of this region, suggesting that the combination of the high humification index, high aromaticity and the rapid transport of water allows for little microbial modification within the aquifer for most of the year. The T peak has been linked to increasing anthropogenic inputs and urbanisation (Hudson et al., 2007; Guo et al., 2010) such as wastewater effluents and fertiliser runoff (Ibánhez and Rocha 2014), which are both present in this catchment. Peak T was visually identified as a secondary component in SGD samples in March 2013 and May 2014, and also, in some inland samples outlined above. In the overall model, the intensities were subtle (0.005 R.U.) due to the absence of this component in the majority of samples and therefore, were not validated as a 4-component model. Thus, the presence of the T peak in this model was assumed to be as a

result of fertiliser runoff due to the time of year it was present and the fact that it was not detected in the samples taken near the sewage outflow pipe during high or low SGD flow conditions.

The seasonal mean SGD CDOM score was higher in spring/summer (0.71 ± 0.1, n = 22) than in autumn/winter (0.28 ± 0.0, n = 20). Significant seasonal trends were experienced for CDOM at the discharge point for all components. Highest intensities of all components were associated with low flow discharge rates. This may be due to the greater residence time within the aquifer, allowing for interaction between SGD and aquifer solids, which, in turn, may mobilise DOM within the soil enabling it to be delivered to the coastal zone via SGD. This explains the increase in humic and soil fulvic-like components during this time. Therefore, the production of protein-like CDOM in Kinvara Bay reflects the seasonal production of both autochthonous and allochthonous DOM. Peak T has been shown to be more intense in summer due to reduced base flows and lower dilution in a river in N.E. England (Baker 2002; Baker et al., 2003).

Sewage is composed of a heterogeneous mixture of organic compounds including fulvic acids, proteins, carbohydrates, lipids surfactants (Ahmad and Reynolds, 1999). Generally, wastewater CDOM is composed of humic-like materials and highly labile components consisting of protein-like fractions (Guo et al., 2010). The composition will vary depending on the age and type of sewage system as well as how and when it discharges into the coastal zone. In Kinvara Bay, sewage comprised a combination of domestic waste, industrial wastes, surface runoff and storm flow. Sewage inputs exhibited very low-intensity tyrosine-like (B) peaks. The B peak was not included in the overall model of the bay suggesting that sewage inputs were not a primary source of CDOM to the coastal zone in this study. This may be due to the small volumes discharged daily (286 m^3 d^{-1}) resulting in rapid dilution with bay water and/or rapid turnover of the relatively low fluxes. Tyrosine fluorescence has been shown to be inhibited through energy transfer to tryptophan and quenching by neighbouring groups (Lakowicz, 1983). Chapter 2 of this study demonstrated that Kinvara Bay was autotrophic during the summer campaigns and December 2016. Rocha et al., (2015) in their recent publication also showed tight benthic-pelagic coupling and eutrophic conditions during summer. This may have caused rapid turnover of any labile materials present in sewage and, therefore, only humic-like materials remained for identification. Additionally, this peak has also been shown to be masked by the first order Raman scatter band (Mayer et al., 1999), and therefore, identification is difficult.

On the contrary, higher CDOM intensities were observed at Parkmore Pier during winter compared to summer. This observation is in line with studies carried out previously linking high intensities to high precipitation rates (Stedmon and Markager, 2005; Kowalczuk et al., 2009). Differences between Parkmore Pier (0.219 R.U.) and the SGD site (0.695 R.U.) were larger during the summer campaigns and may be due to higher temperatures and longer sunlight hours resulting in increased

productivity and removal of CDOM within the transit path. Kinvara Bay has been shown to switch from autotrophic to heterotrophic (Chapter 2 and 3) depending on SGD conditions. Thus, some of this refractory DOM may in fact support primary and secondary production. Fluorophores can also be removed at intermediate salinities, through the mixing path of the bay, due to photobleaching, adsorption to particles and/or flocculation (Benner, 2002).

CDOM was more persistent during winter as the differences between SGD (0.381 R.U.), and Parkmore Pier (0.304 R.U.) were smaller. This is in direct correlation with DOC concentrations, which were also reduced between the SGD site and Parkmore Pier during these campaigns (Chapter 3). Importantly, the M peak, known to be from a marine source (Coble, 1996), was not present in the 3-component model and also was not a major peak at Parkmore Pier. Therefore, terrestrial CDOM dominated the coastal zone of Kinvara Bay. Therefore, it can be concluded that CDOM contributed to coastal and oceanic carbon storage and was not utilised within the bay. Photodegradation of CDOM is expected to be higher in summer due to longer sunlight hours and increased temperatures compared to winter. This may act as an important removal pathway during summer contributing to the larger difference between SGD and Parkmore Pier during summer.

4.4.7 Relationship of CDOM optical properties and salinity

The CDOM scores exhibited non-conservative mixing behaviour with salinity (Figure 4.5). Since *p* was less than the alpha value of 0.05, data was not normally distributed for CDOM vs. Salinity. This may be due to the high seasonal variability of CDOM in SGD and indeed the high variability of SGD (Chapter 2) on an annual scale. Brackish SGD had intensities lower than those of fresh SGD. Variability in CDOM scores decreased as salinity increased. Negative correlation with salinity indicates that terrestrial discharge is the primary source of CDOM within the bay (e.g., Kowalczuk et al., 2009).

However, at times of peak CDOM intensity (summer 0.71 ± 0.1 R.U.), there was removal within Kinvara Bay as CDOM scores at intermediate to high salinities were relatively uniform throughout the year. Groundwater gains autochthonous CDOM from being in direct contact with soil and sediments *en route* to the coastal zone. During winter, the CDOM score was low (0.28 ± 0.0 R.U.) resulting in humic-like, non-bioavailable CDOM. However, SGD may have contributed to productivity during the summer when protein-like peaks were observed. During summer there is an increase in the fertilisation of agricultural land as well as an increase in population due to tourism. Anthropogenic pressures have been shown to have a direct link with protein-like peaks (Yang et al., 2015). While, in addition, sunlight hours are longer, and metabolism rates are expected to be highest during summer. Photodegradation of CDOM releases a source of nutrients to the water

column (Stedmon et al., 2007). This was coupled with high levels of DIN (Chapter 2, Rocha et al., 2015). Therefore, any bioavailable material can be quickly utilised (Rocha et al., 2015).

By comparison, SGD-borne CDOM scores were relatively uniform with intermediate to higher salinities during winter, and therefore CDOM material transported through Kinvara Bay and contributed to oceanic carbon storage. Humic-like DOM in this analysis was highly resistant to degradation, and important processes may include accumulation in the sediment and/or export to deeper waters. The export of DOM to deeper waters as a result of mixing and downwelling of water parcels is an essential part of the DOM cycle (Jiao et al., 2010).

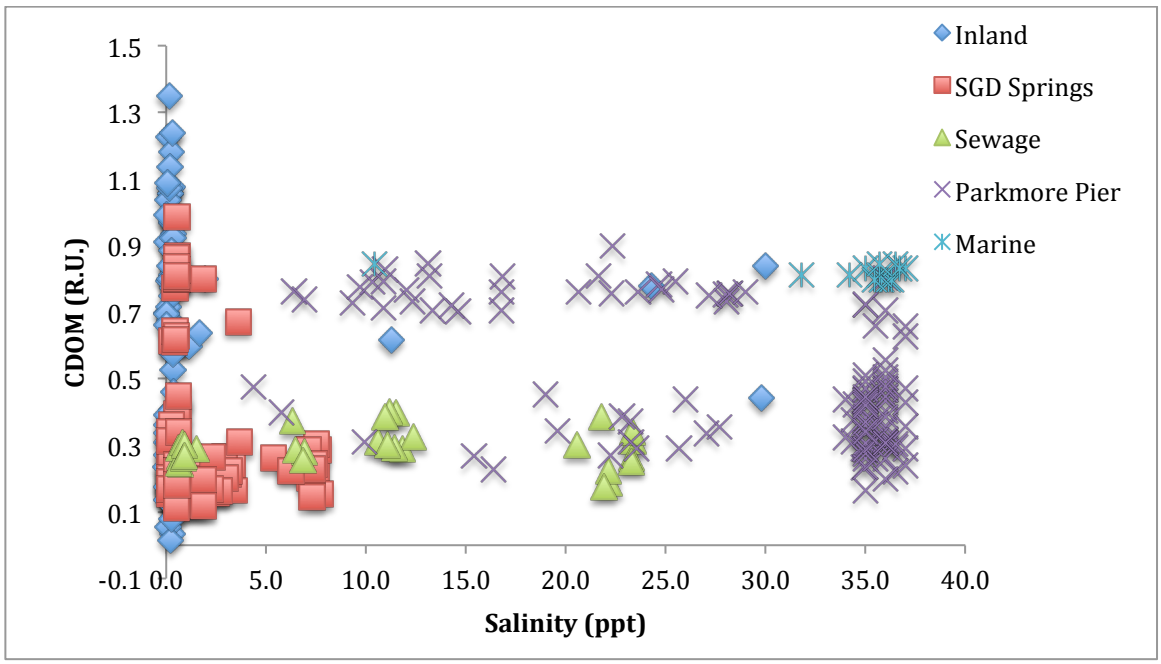

Figure 4.5: An annual mixing curve of CDOM Scores (R.U.) vs. salinity (ppt) measured at all input locations and through Kinvara Bay over the course of the nine sampling campaigns, n = 335. Samples were collected based on a continuum of water flow which includes inland, the SGD springs, sewage outflow location within the bay, Parkmore Pier and Galway Bay.

4.4.8 Spectral indices

There are a variety of diagnostic indices used in conjunction with EEM analysis to better quantify fluorescence sources and properties. Average values were calculated annually at the discharge point, the sewage point and Parkmore Pier (Table 4.6). The fluorescence index (F.I. ≈ 1.4) and spectral slope ($S_{275-295} < S_{350-400}$) at both the discharge site and Parkmore Pier indicate that DOM transported through Kinvara Bay is terrestrial in origin.

Table 4.6: Summary of measured indicator parameters in SGD and sewage endmembers, measured at the sewage outfall pipe located within the bay and Kinvara Springs compared to the mouth of the bay, Parkmore pier over the course of the ten sampling campaigns. Data is provided as a range of the lowest to highest measured data as the result of several replicates (20 < n < 100).

Parameter	SGD	Sewage Point	Interpretation	Parkmore Pier	Interpretation
Fluorescence Index (F.I.)	1.1 – 1.8	0.9 – 1.6	Terrestrial/ Aquatic signature	0.95 – 1.99	Terrestrial/ Aquatic signature
Humification Index (HIX)	0.90 – 0.96	0.83 – 0.95	Humified, dependent on high and low flows	0.75 – 0.92	Humified
Spectra Slope, S, at 275-295 nm	0.012	0.012		0.013	
Spectra Slope, S, at 350-400 nm	0.016	0.017	$S_{275-295} < S_{350-400}$ indicative of terrestrial material	0.015	$S_{275-295} < S_{350-400}$ indicative of terrestrial material
Spectral Slope Ratio (Sr)	0.68 – 0.74	0.70	Terrestrial signature	0.75 – 0.91	Increased
SUVA 254 ($L\ mg^{-1}\ cm^{-1}$)	7.1 – 22.4	8.25 – 9.42	High aromaticity	3.3 – 14.6	Lower aromaticity

For this study, the annual average F.I. values for all groups were approximately 1.4 for each season, indicating a terrestrial origin of CDOM (McKnight et al., 2001). Some samples over the course of the study experienced F.I. higher than 1.4, this could be due to temporary microbial activity at these sites (Singh et al., 2010). Parkmore Pier also had an F.I. of approximately 1.4, showing that this was mainly dependent on terrestrial sources of DOM, as a result of the high SGD fluxes. There was variability in the low salinity samples due to periodic microbial activity within the aquifer (Singh et al., 2010). At higher salinities, there may be variability with tidal fluctuations as seawater may dominate at high tide and cause the F.I. to increase during these times (Figure 4.6).

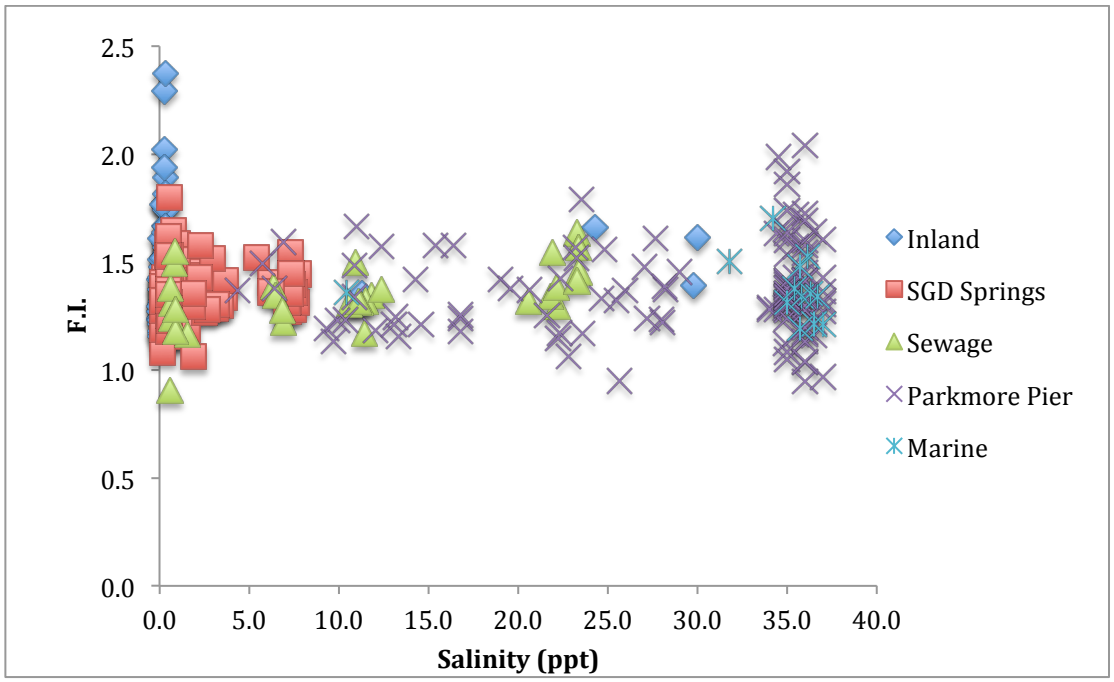

Figure 4.6: Measured Fluorescence Index (F.I.) variability with salinity fluctuations measured in the SGD, sewage and marine endmembers and throughout the bay, over the course of the sampling campaigns (n = 333). An F.I. of 1.4 represents terrestrially borne CDOM and of 1.9 represents microbially derived CDOM.

The average annual HIX was found to be 0.90 – 0.96 for all groundwater and SGD samples; this is highly humified material and therefore has low biological availability (Ohno, 2002). High HIX values were also recorded at the sewage outflow site, which had an HIX of 0.83 – 0.95. The HIX was large due to the influence of SGD within the bay and the area in which sewage discharge occurred. However, the HIX at Parkmore Pier was reduced to 0.75 – 0.92, suggesting possible degradation leading to higher biologically available material and/or dilution of terrestrial CDOM with marine CDOM (Figure 4.7). HIX was largely dependent on tides and SGD flow conditions. During low tide and at high SGD flow, the HIX was at the upper range representing samples similar to groundwater samples, whereas, the lower value was found during low flow and high tide conditions. Therefore, this suggests the greatest removal of the highly humified CDOM was due to seawater mixing. Thus, the vast majority of this material was not mineralised within the coastal zone and was transported to the Atlantic Ocean, where, it may have contributed to global C storage. As HIX has been shown to exhibit conservative behaviour, its identification within seawater environments may be used as a tracer for terrestrial DOM.

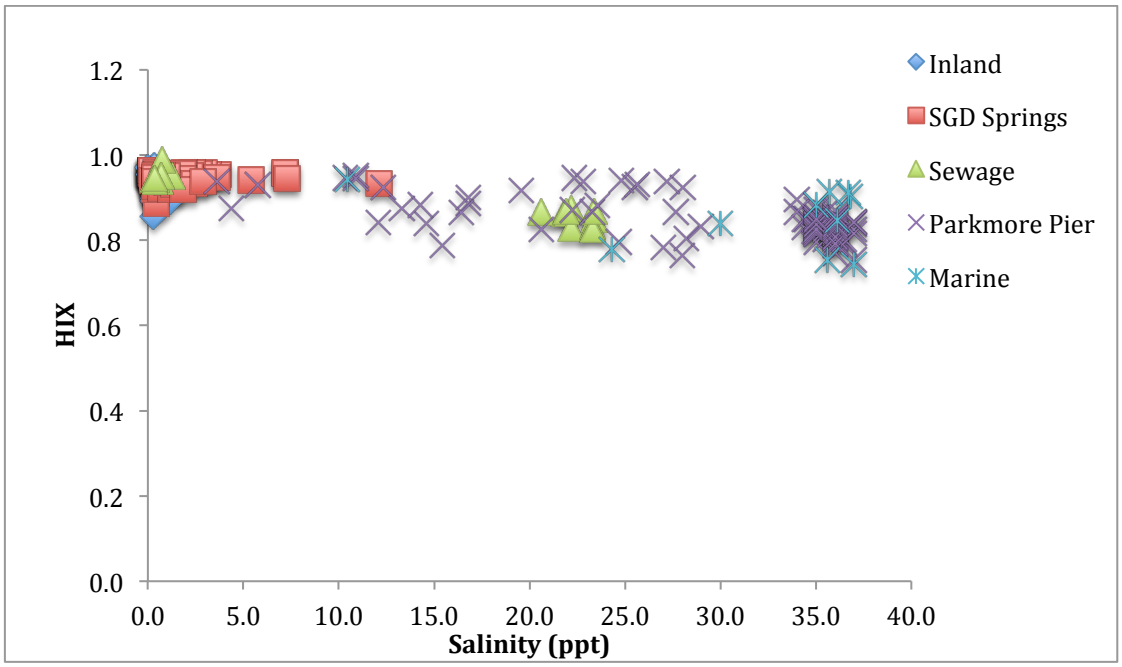

Figure 4.7: Mixing curve of Humification Index (HIX) and Salinity (ppt). Samples were collected based on a continuum of water flow which includes inland samples, the SGD springs, sewage outflow location within the bay, Parkmore Pier and Galway Bay, n = 201.

The SUVA254 data, although only conducted using a subset of samples, confirmed that the groundwater was characterised by high aromaticity in accordance with its terrestrial/aquatic origin (Weishaar et al., 2003), although there is a large range associated with the variability of SGD. The decrease in this value at Parkmore Pier indicates possible dilution with seawater as the somewhat lower aromatic material was periodically detected at the SGD point and at Parkmore Pier. The high variability associated with the SUVA values at Parkmore Pier may be due to tidal fluctuations within the bay, whereupon higher SUVA is associated with the low tide freshwater influences and the lower values associated with the high tide seawater dominance.

The spectral slope information further supports the terrestrial origin of CDOM within the bay (Helms et al., 2008; Helms et al., 2013). The Sr for SGD was 0.68 – 0.74. In Parkmore Pier, this was again significantly dependent on the flow regime with the greatest similarity recorded during high SGD flow conditions when the salinity within the bay was substantially reduced due to the high volumes associated with SGD. During low flow conditions, the Sr was increased, however still representing a terrestrial signature. Higher S values may be due to preferential sorption of the high molecular weight hydrophobic DOM components to soil *en route* or photodegradation of the high molecular weight fraction upon discharge during summer (Osburn et al., 2009). Due to the limited photo-exposure between discharge and sampling, the more likely scenario is that there was sorption of the CDOM components due to longer residence times within the aquifer.

4.4.9 Anthropogenic pressures and CDOM components in Kinvara Bay

Anthropogenic CDOM including sewage inputs was not a significant CDOM source to the bay. Protein-like components have been shown to be an effective environmental quality indicator of

anthropogenic pressures (Ibánhez et al., 2017). In this study anthropogenic influences appeared to be minimal due to the low intensity of the T peak (R.U. = 0.005), which was only seasonally derived. CDOM was intrinsically linked to critical biogeochemical processes including primary production and organic matter mineralisation.

Continual analysis of Kinvara Bay is imperative as population growth, increased demand for food and global warming are significant problems for the future on a global scale. Increased temperatures cause a lowering of the water table, which in turn, permits the bacterial breakdown of peat (Baker and Spencer, 2004). Therefore, global warming has been shown to increase DOC released from land, linked with increased agriculture and subsequently increased fertiliser; this could potentially lead to increased anthropogenic pressures causing higher proportions of protein-like components to enter the coastal zone and cause an increase in productivity, which may result in eutrophication and algal blooms. Humic-like materials, therefore, may be taken as a baseline for the evaluation of anthropogenic pressures. Presently, Kinvara Bay can be deemed to be relatively pristine regarding CDOM inputs. Hudson et al., (2007) stated that the study of OM in freshwaters was not yet as widespread as that in marine sciences and that continual analysis needs to be implemented.

4.4.10 Further statistical analysis

CDOM represents a sub-fraction and therefore only describes a portion of the dynamics of the total DOM pool. It is not currently possible to determine how much of the total DOM pool is represented by CDOM. Therefore, this technique (EEMF-PARAFAC) is a useful tool for tracing the dynamics of DOM in natural ecosystems, but the exact, chemical make-up of the DOM is not determined (Stedmon et al., 2003; Stedmon and Markager, 2005; Stedmon and Bro, 2008). In addition to EEMF-PARAFAC, FT-ICR-MS analysis was conducted on a subset of samples and a further incubation study to determine the elemental makeup of compounds entering the coastal zone as a result of SGD (Chapter 6).

4.5 Synopsis

SGD transported terrestrial humic-like compounds to the coastal ocean of Kinvara Bay, supported by the validation of a 3-component model that showed HS including visible humic acids and soil fulvic acids dominated. This material was highly humified and was transported through Parkmore Pier to Galway Bay, and subsequently, the Atlantic Ocean where it may have contributed to global carbon storage during winter and any protein-like components observed during summer were quickly removed from the coastal ecosystem.

Transformations and/or dilution may have occurred during transport as spectral indices showed a reduction in humification (SGD, 0.94 ± 0.02 and Parkmore Pier, 0.83 ± 0.05) and aromaticity. Seasonal effects show that DOM was largely depleted during summer months at Parkmore Pier, highlighting possible removal processes within the bay such as photodegradation due to longer

sunlight hours and higher temperatures and due to biodegradation resulting from greater productivity.

The null hypothesis that SGD transported biologically available CDOM to Kinvara Bay cannot be rejected as there was a low intensity Protein peak observed in the 3-component model. The rapid transport capacity of the karstic aquifer has the potential to provide a direct channel for low humified, labile material as shown due to the presence of such peaks seasonally.

5. The Potential Effects of Increased Anthropogenic Pressures on the Inferred Dissolved Organic Matter (DOM) Concentrations in Kinvara Bay

5.1 Introduction

Multiple stressors can affect natural coastal ecosystems. Anthropogenic pressures are becoming increasingly critical due to population growth. Shallow coastal bays and estuaries are, in particular, vulnerable to such pressures (McGlathery et al., 2007). Studies have been conducted to determine particular stressors on coastal zones globally, but studies of cumulative effects of multiple stressors are less frequent (Crain et al., 2008). Cumulative interaction effects may be additive, synergistic or antagonistic.

Anthropogenic pressures have led to significant consequences threatening the marine environment such as increased productivity and eutrophication (McQuatters-Gollop et al., 2009). Understanding eutrophication, what causes it, its effects on the coastal zone and its interaction with the open ocean on a long-term scale are key topics in addressing these issues (Jessen et al., 2015). The focus of eutrophication studies has largely been on examining nutrient inputs (Moore, 2010; Lee et al., 2012; Ibánhez et al., 2013; Ibánhez and Rocha 2014; Rocha et al., 2015), as the definition typically used in these studies is the enrichment of an aquatic environment by nutrients. However, another definition based on organic loads has been proposed, which defines eutrophication as the increase of organic matter supplied to an ecosystem (Nixon 1995). DOM drives productivity and biogeochemical cycles in the coastal zone by acting as a substrate for the detritus-based food webs, characteristic in many of these coastal regions (Goñi et al., 2003). In addition, DOM is consumed by microbial activities (Ibánhez and Rocha 2014; Jiao et al., 2010). It, also, plays a vital role in the mobilisation and availability of nutrients, metals and pollutants, which mediates biogeochemical cycles on a global scale (Kujawinski, 2011; Baker and Spencer, 2004; Benner, 2002). Therefore, in addition to the well-documented water quality parameters (nutrient concentrations, oxygen, biological oxygen demand and chlorophyll), and organic matter loads should also be studied in strategic plans for coastal zone monitoring.

The quality of SGD entering the coastal zone is an important issue regarding the trophic status of coastal regions (Moore, 2010). It is critical to gain an understanding of carbon and nutrient biogeochemistry to sustain coastal water resources for the future. Notably, shellfish and aquaculture industries have increased in recent years throughout the world (Gyllenhammar and Håkanson, 2005; Dalsgaard and Krause-Jensen, 2006; Hwang et al., 2010), including in Kinvara Bay. This sector of the economy needs high-quality water to be sustainable in the long-term. The growth of marine organisms is largely dependent on inorganic nutrients, but often overlooked is the importance of DOM on community structures and ecosystem functioning (Nixon, 1995). A good cultivation region is maintained by a balance of nutrients, as too low will not provide sufficient growth, but high concentrations may result in eutrophication and hypoxia, which in turn, destroys shellfish growth and, hence, this industry. This study focused on the impact of two prominent

anthropogenic pressures, land use and plastic pollution, on CDOM and DOC concentrations and predicts two future scenarios where these forms of pollution have increased and accumulated due to population growth.

5.1.1 Future scenario 1: land use alteration

SGD has been shown to deviate from the Redfield Ratio as SGD often has higher N:P ratios due to land use within catchments (Chapter 2; Slomp and Van Cappellen, 2004). The addition of inorganic fertilisers in agricultural regions increases the concentration of nitrogen in the coastal zone (Pavlidou et al., 2014; Spalding and Exner 1993). The C:N:P ratio of biomass in the coastal areas is significant in many ecological processes. Higher N:P ratios could result in a shift of algal species and cover. SGD has been shown to contribute to algal dominance as nitrification of the coastal body proceeds via this pathway (Semple 1997; Costa Jr. et al., 2008).

Currently, Kinvara Bay is periodically eutrophic during summer, and SGD-borne N loading is the primary driver in the Bay (Rocha et al., 2015). This study combines this with a potential future scenario, in which there is a shift in land use toward intensive agriculture. Increased demand for food may lead to intense agricultural activities, which will cause further contamination of SGD and a further change in the N:P loading. Increased fertiliser application results in higher productivity and a subsequent increase in suspended particulate matter (SPM) (Slomp and Van Cappellen, 2004; Rocha et al., 2009; Lee et al., 2012; Ji et al., 2013; Rocha et al., 2015). A shift in SPM within the coastal zone may result in a change in primary production affecting DOM dynamics. Therefore, studies are critical to determining the current and possible future forecasts of the effects of SGD-borne DOM on coastal environments regarding ecological status.

5.1.2 Future scenario 2: biodegradable microplastic pollution

In addition to the anthropogenic stressors outlined above, which may cause an increase in nutrients and DOC exported from land, another marine pressure that has been receiving attention in recent years is plastic litter. The accumulation and fragmentation of plastics represent a long-term change that is ubiquitous globally (Barnes et al., 2009; Imhof et al., 2012). Plastics are lightweight, versatile, durable, strong and cheap. These characteristics make them very suitable for a broad range of industries (Andrady, 2003; Andrady, 2011). Plastic production has reached volumes of thirty million tonnes in the US alone and is continuing to grow due to its significant contribution to output and economy on a global scale (Derraik, 2002). Ivar do Sul and Costa, (2014) reviewed 101 works on microplastic pollution and concluded that microplastics were widespread in oceans and sediments as over several million tonnes of plastics have been produced since the middle of the last century (Barnes et al., 2009). Green et al., (2015) estimated that 5% of all plastic produced enters the marine environment. The growth of this industry and its subsequent pollution can have detrimental effects on the coastal zone as plastics are highly persistent (Gall and Thompson, 2015). Marine litter comprises 60 - 80% plastic and in some cases may even be as high as 90 - 95%

(Moore, 2008). Marine plastic is known to have major effects on marine biota, including ingestion of plastics and entanglement in larger fishing nets and tangled ropes (Derraik, 2002; Gregory, 2009; Gall and Thompson, 2015).

This section of the study focused on the increased loading of biodegradable microplastics in the coastal zone and the effects it may have on DOM released to the water column. Microplastics are small pieces of plastic debris, less than 5 mm, and have been accumulating in coastal zones all over the world for many years (Moore, 2008). Microplastics consist of two types of particles, (1) larger portions broken into fragments and (2) resin pellets and powders. Due to their small size they can be easily ingested by marine organisms, which may cause physical harm. Ingestion of such materials is not unique to the marine environment as many birds, and land-based mammals are also threatened (Gregory, 2009). Ingestion may also cause toxicity problems due to the manufacturing process and chemical properties of such materials. Chiefly, Persistent Organic Pollutants (POPs) are of great concern. These can be found universally in low concentrations in seawater and as their name suggests they are highly persistent (Andrady, 2011). These are hydrophobic pollutants and can concentrate up in microplastics to several orders of magnitude higher than the surrounding seawater. Therefore, ingested materials pose severe consequences as POPs enter the food web.

Oil-based polymers are virtually non-degradable, difficult to reuse and lead to serious environmental concerns (Song et al., 2009). Biodegradable plastics are now in everyday use and compose of polymeric materials that decompose through chemical processes carried out by microorganisms into carbon dioxide, water, methane, inorganic compounds and biomass in the environment. Photo-oxidative degradation is the primary breakdown process for many polymers, including HDPE and nylon in the marine environment. Significant uncertainties exist around degradability of such materials in marine environments. Most studies have focused on the ecological consequences of such debris (Derraik, 2002; Andrady, 2011; Gall and Thompson, 2015; Green et al., 2015). For example, Green et al., (2015) showed that the presence of a biodegradable plastic bag, in widespread use today, in a benthic ecosystem created anoxic conditions in sediment, which altered marine assemblages and reduced primary productivity. However, Guzman et al.'s (2010) research showed that increased polymer blend could lead to increased productivity and subsequent algal blooms. The coastal zone may encounter substantial levels of plastic pollution as waves and tides tend to wash up plastic waste to the shoreline (Tosin et al., 2012) while rivers and SGD may transport land-derived pollution (Moore, 2010). As biodegradable plastics break down due to processes in the marine environment, higher concentrations of CDOM are expected to be present due to the organic nature of such materials.

5.2 Specific hypotheses of this experiment

The overarching hypothesis of this research was to determine whether future scenarios of both land-use changes (leading to higher N:P ratios) and plastic pollution could have an effect on the relatively pristine CDOM components present in Kinvara Bay (Chapter 4). To determine this, six specific hypotheses are described below:

Null Hypothesis 1, H_0: Biodegradable plastic marine pollution does not alter the types of CDOM components effluxed from the sediment cores compared to the control
Alternative Hypothesis 1, H_1: Biodegradable plastic marine pollution alters the CDOM components effluxed producing highly refractory materials compared to the control

Null Hypothesis 2, H_0: The DOC/CDOM fluxes from the sediment to the water column increase with an increase in plastic pollution
Alternative Hypothesis 2, H_1: The DOC/CDOM fluxes remain unchanged with an increase in plastic pollution

Null Hypothesis 3, H_0: The sediment-water DOM fluxes will shift to a more labile fraction with an increase in Kinvara Bays SPM
Alternative Hypothesis 3, H_1: The sediment-water DOM flux will remain unchanged despite an increase of SPM

Null Hypothesis 4, H_0: The DOC/CDOM fluxes increase with an increase in Kinvara Bays SPM
Alternative Hypothesis 4, H_1: The DOC/CDOM fluxes remain unchanged with an increase of the SPM

Null Hypothesis 5, H_0: Biodegradable plastic marine pollution in combination with increasing SPM has a synergistic effect on the CDOM present.
Alternative Hypothesis 5, H_1: Biodegradable plastic marine pollution has no CDOM combination effect with SPM

5.3 Sampling procedure

16 undisturbed sediment cores (methodology described in Chapter 2) were collected from the intertidal zone near the SGD discharge point and from Parkmore Pier in June 2015. At the same time, SGD and seawater were sampled. Water samples were filtered through pre-combusted GF filters and collected in pre-cleaned, acid-washed 10 mL amber glass bottles. All filters and containers were rinsed several times with the sample before filling. Samples were stored on ice in the dark and transported to the laboratory within three days for analysis.

In the field, at the same time water samples were collected at the SGD springs, *in-situ* measurements of salinity, conductivity, temperature and pH were recorded using an Aquaread 1000 AP, calibrated prior to use with a freshwater conductivity (Varian 12,800 μScm^{-1}), pH (Varian pH 4.00, 7.00 and 10.00) and ORP (+229 mV) standards. Higher salinity measurements were taken manually using a refractometer and confirmed using conductivity readings.

5.4 Methodology

5.4.1 Sediment flux analysis

The following sampling strategy was devised to determine the impact of SPM and biodegradable microplastic and their combined effect (Table 5.1). Sediment corers had an inner diameter of 6.4 cm. Approximately 10 cm of sediment was collected in each core, resulting in a sediment core volume of 100.5 cm^3. The sediment cores were covered with bay water for transport. Cores were allowed to aerate for two days to allow full equilibration of the sediment-water fluxes and settling of sediment before water was removed. A future scenario in which nitrogen enrichment has caused a shift and an increase in macroalgae growth, and hence, SPM in the bay was predicted. To achieve this SPM, 1 g of dried and ground *Fucus* (n = 3) and *Enteromorpha* (n = 3) was added to the cores. 1 g equates to inputs of 4.8 g N m^{-2} *Fucus* and 10.9 g N m^{-2} *Enteromorpha*, which is equivalent approximately to 25 - 50% of the summer N loadings of 25.9 g N m^{-2} yr^{-1} (Rocha et al., 2015). In terms of current biomass (Manaswi Raghurama, 2015), this equates to a 42% increase in *Fucus*. During the time of this study, *Enteromorpha* growth was at a seasonal high and therefore the current biomass was used in the experiment. Microplastics were then added to determine the combined effect of both scenarios and also added to another set of core*s* (n = 3). Microscopic (< 150 μm) poly(lactic) acid (PLA), a biodegradable aliphatic polyester (Shah et al., 2008) was added to the cores at a dose of 59 g m^{-3}. The dosage level chosen was on the basis that sediment anoxia is problematic above this dose. Filtered aged seawater (300 cm^3) was added to create a concentration gradient between the sediment and water to allow DOC and CDOM fluxes to be calculated. Control cores (n = 3) were utilised to determine the present sediment-water carbon fluxes, in which, no OM or biodegradable microplastics were added. Cores were aerated for five days with a pump and air stone and a plastic funnel were placed on the top opening to prevent evaporation. Day and night conditions were simulated naturally by placing the cores on a windowsill. Therefore, the cores were exposed to natural daylight in June 2015 (sunshine duration is between 5 and 6.5 hours; www.met.ie/climate/sunshine.).

Table 5.1: Experimental Design of core incubation experiment conducted in June 2015 from cores collected in the intertidal zone at Kinvara Springs.

Identification	Treatment added	Replicates
C (Control)	None	3
CMP (Microplastics)	Microplastics	3
MA (Macroalgae A)	*Fucus vesiculosus*	3
MB (Macroalgae B)	*Enteromorpha intestinalis*	3
MAMP	*Fucus vesiculosus* + Microplastics	3
MBMP	*Enteromorpha intestinalis* + Microplastics	3

5.4.2 Water analysis

Time series (104 hours) of CDOM (n = 338) and DOC concentrations (n = 145) were determined by EEMF-PARAFAC analysis (Chapter 4) and High-Temperature Catalytic Oxidation (HTCO) analysis (Chapter 3), respectively. At each time point, 20 mL of water was collected from each core and filtered immediately through Whatman GF filters and stored in Vaccutainer™ vials. The collected water samples were stored frozen until analysis.

5.4.3 Flux estimation

DOC flux was determined according to Forja and Gómez-Parra, (1998), using the below equation derived from a flux equation based on Fick's first law of diffusion:

$$C = \alpha - b*\exp(-kt) \quad (1)$$

Where C is the concentration at time t, α is the concentration at steady state, and b is the concentration at steady state minus concentration at time zero. K is a parameter related to benthic activity, the coefficient of the species under study, porosity and thickness of the sediment-water interface and the ratio between volume and surface area of the overlying water. K was estimated using the Solver tool in Microsoft Excel. This tool minimises the total sum of squares between experimental concentration data and theoretical concentration based on equation 1.

Flux was then calculated by:

$$J = R*b*k \quad (2)$$

Where J is the flux, R is the ratio of the volume of overlying water to sediment surface area, and k is the coefficient estimated as above.

5.4.4. Statistical analyses

Statistical analyses was conducted using the R software package (R Development Core Team 2008) and MathWorks software package, Matlab. In determining the significance of the treatments from the control boxplots and two-way analysis of variance (ANOVA) was employed using R. The assumptions of ANOVA are 1) normally distributed data, 2) independent samples, 3) common

variance between samples and 4) randomly and independently selected samples within the group. The assumptions that the samples are independent of one another and taken randomly within the group are satisfied due to the design of the experiment. Normality was assessed within R using Q-Q plots and the Shapiro-Wilk normality test. The Sharpio-Wilk tests the Null hypothesis that the samples came from a normal distribution. Therefore, for p values < 0.05, the null hypothesis is rejected, and samples are not normally distributed. For treatments that displayed significant effects, Tukey's Honest Significance Difference (HSD) test was conducted for further evaluation of the differences between treatments. CDOM analyses were carried out using the CDOM toolbox in Matlab, and validation was ensured using random initialization and split-half validation (Stedmon and Bro, 2008).

5.5 Results

5.5.1 Current status of Kinvara Bay

Linh Trieu, (2015) identified and quantified microplastic concentration in bay water and sediment samples. About seven particles per litre were present in SGD and Parkmore Pier waters, while the sewage outfall site had significantly less. The higher concentrations of microplastics at these locations were attributed to anthropogenic activity. The SGD site is located beside Dunguaire Castle, which is a popular tourist attraction and Parkmore Pier supports water activities such as fishing and sailing. The majority of particles identified were plastic fragments and then plastic fibres at all locations. The percentage of plastic beads was 10% at Parkmore Pier and 0% at the SGD and sewage sites. Microplastics in the sediment collected at the SGD site was determined to be 674 ± 83 particles/kg.

Fucus vesiculosus was the most dominant macroalgae species at the SGD springs, followed by *Enteromorpha intestinalis*. Near the sewage point, *Ascophyllum nodosum* was the dominant species. *Ascophyllum nodosum* and *Fucus vesiculosus* were found to be dominant at Parkmore Pier. At the time of the study, untreated sewage was discharged into the bay at high tide, however plans were in place to treat sewage to drinking water standard (Ciaran Cannon, 2010), and therefore, future scenarios did not consider this a critical element and were conducted using SGD inputs alone.

5.5.2 DOC

Due to unforeseen circumstances, DOC concentrations were not determined for every sample taken. 152 representative samples were analysed for DOC flux concentration and were conducted across all treatment types. Results outlined in Table 5.2 provide the number of samples analysed (n) for each treatment. The treatment containing the *Fucus* species released the highest DOC concentration, the control, as expected, had the lowest DOC concentration.

Table 5.2: Summary of measured DOC concentration flux (µmol cm^{-1} hr^{-1}) from the incubation sediment cores from each treatment type. See Appendix H for raw data.

Treatment	n	DOC (µmol cm^{-1} hr^{-1})
Control	34	0.302
Microplastics	35	0.402
Fucus	17	3.013
Microplastics + *Fucus*	19	1.662
Enteromorpha	15	1.132
Microplastics + *Enteromorpha*	32	0.914

The assumptions of ANOVA were satisfied. The data was normally distributed as the Shapiro-Wilk test had a *p*-value of 0.327 and the Q-Q plot did not exhibit significant deviations from the line. Many of the treatments were statistically significant compared to one another (Tables 5.3 and 5.4).

Table 5.3: ANOVA results after testing the null hypothesis that H0: Mean DOC concentration measured at Castle Springs over eight sampling campaigns is the same for all seasons.

	Df	Sum Sq	Mean Sq	F Value	Pr(>F)
Seasons	5	128.52	25.704	98.59	$2e^{-16}$
Residuals	139	36.24	0.261		

Table 5.4: *p* values based on Tukey's Honest Significance Difference (HSD), following ANOVA analysis, evaluating differences between each treatment type values in bold indicate a significant difference between two values ($p < 0.05$) at significance level, $\alpha = 0.05$.

Control	Microplastics	*Fucus*	Microplastic+ *Fucus*	*Enteromorpha*	Microplastics+ *Enteromorpha*
Control	0.999	**0.000**	**0.000**	**0.007**	**0.000**
Microplastics		**0.000**	**0.000**	**0.008**	**0.000**
Fucus			**0.041**	**0.000**	**0.000**
Microplastics+ *Fucus*				**0.000**	**0.000**
Enteromorpha					0.964

5.5.3 CDOM

CDOM data were fitted to a 5-component model. Split-half validation and random initialisation were performed, and no obvious residues were obtained for this dataset. Visual identification of the five components identified showed fluorescence maxima characteristic of organic fluorophores with multiple excitation maxima and a single emission maximum for each component. As such, each peak represents a mixture of covarying fluorophores due to the complexity of natural DOM. Comparison of spectral characteristics observed in this study with those components previously identified by other authors fit well and are outlined below (Table 5.5). These five components were

classified into two groups, three are humic-like materials characteristic of terrestrial inputs, and two are protein-like components, indicative of anthropogenic stresses.

Table 5.5: Fluorescence characteristics of validated 5-component EEMF model: excitation and emission maxima, compared with previously identified components. n = 338 for all treatment groups. See Appendix G for model output.

This model Ex/Em	Previous Model (Literature)	Source and description	Reference
C1: 225/315 275/315	 275/310	Peak B – tyrosine-like	Coble 1996
C2: 230/425 350/425	260/380-460 350/420-480	UV humic-like Peak C – humic-like	Stedmon et al., 2003; Coble 1996
C3: 245/460 350/460	260/380–460 350/420-480	Peak A – humic-like Peak C – humic-like	Coble 1996
C4: 220/360 275/360	 275/340	Peak T – tryptophan-like Derived from algal exudation	Coble 1996; Stedmon and Markager 2005
C5: 275/490 350/490 460/490	260-380/490 260-380/490	Peak A/C – terrestrial humic-like	Murphy et al., 2008

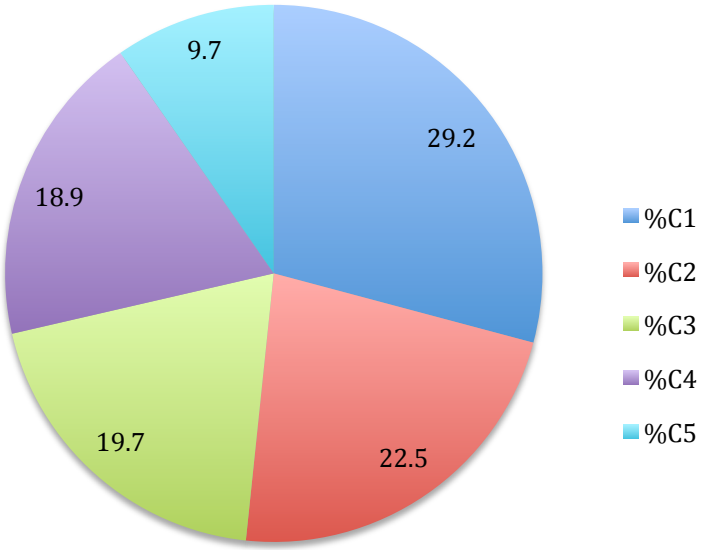

Figure 5.1: Pie chart of the percentage of each component (C1-C5) in the validated annual 5-component EEMF model, measured over all treatment groups, n = 338.

As shown in Figure 5.1, C1 accounted for 29.1%, C2 for 22.5%, C3 for 19.7%, C4 for 18.9% and C5 for 9.7% of the overall model. Therefore, humic-like materials accounted for 51.9%, whereas, protein-like components accounted for 41.4%. In particular, the tyrosine-like component accounted for the highest individual intensity, 29.1%. Therefore, protein-like components consisted of a significant portion of the CDOM fluxes.

Table 5.6: Summary of measured CDOM score in each treatment group, measured from each core flux over the course of the incubation study.

Treatment	C1	C2	C3	C4	C5
Control	0.055	0.087	0.074	0.051	0.037
Microplastics	0.062	0.107	0.091	0.058	0.046
Fucus	0.239	0.195	0.184	0.214	0.093
Microplastics + *Fucus*	0.266	0.215	0.199	0.225	0.104
Enteromorpha	0.632	0.424	0.365	0.371	0.172
Microplastics +*Enteromorpha*	0.604	0.413	0.350	0.282	0.167

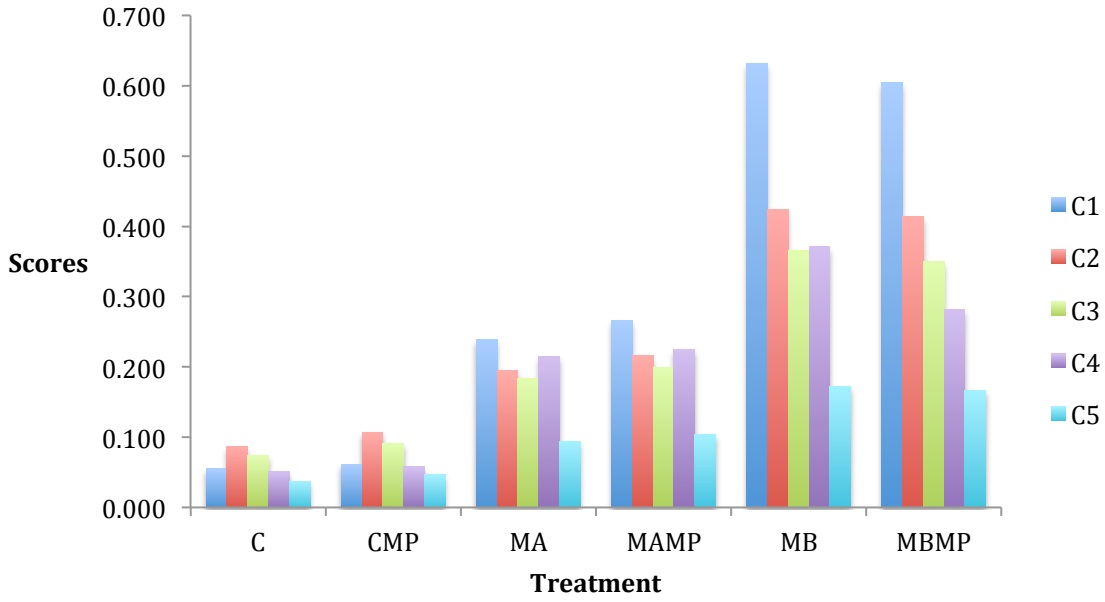

Figure 5.2: Bar chart of the EEMF-PARAFAC model output component 1-5 scores for each treatment group. C = control, CMP = Microplastics only, MA = *Fucus* treatment, MAMB = *Fucus* plus microplastics, MB = *Enteromorpha* treatment, MBMP = *Enteromorpha* plus microplastics

Table 5.6 and Figure 5.2 illustrate the scores for each component (C1 – C5) for each treatment. For each component, there is an increasing trend from the control to the SPM added samples. The treatments containing the microplastic do not appear to differ substantially from their respective non-added sample. Significance was performed using analysis of variance (ANOVA) in R, after verification of the assumptions of Normality and sample independence. The Shapiro-Wilk test was conducted for each of the components (C1 – C5) identified, and *p* was greater than 0.05 in all cases. Therefore, the Null hypothesis that the data is normally distributed cannot be rejected. The F value of 9.67 exceeds the critical F value (5, 24) of 2.5207 at significance level $\alpha = 0.05$ (Table 5.7). Therefore, this indicates a significant difference between these groups of variables. The *p*-value was used to determine which variables are significantly different from the control and each other (Table 5.8).

Table 5.7: ANOVA results after testing the null hypothesis that H0: Treatment groups for each component of the validated 5-component model are identical.

	Df	Sum Sq	Mean Sq	F Value	Pr(>F)
Seasons	5	0.4931	0.09862	9.67	$3.72e^{-05}$
Residuals	24	0.2448	0.01020		

Table 5.8: *p* values based on Tukey's Honest Significance Difference (HSD), following ANOVA analysis, of treatment groups for each component of the validated 5-component model (C1 – C5). Values in bold indicate a significant difference between two values ($p < 0.05$). MP = microplastics

C1	MP	*Fucus*	MP + *Fucus*	*Enteromorpha*	MP + *Enteromorpha*
Control	0.999	**0.027**	**0.006**	**0.000**	**0.000**
MP		0.360	**0.008**	**0.000**	**0.000**
Fucus			0.997	**0.000**	**0.000**
MP + *Fucus*				**0.000**	**0.000**
Enteromorpha					0.997
C2	MP	*Fucus*	MP + *Fucus*	*Enteromorpha*	MP + *Enteromorpha*
Control	0.888	**0.000**	**0.000**	**0.000**	**0.000**
MP		**0.000**	**0.000**	**0.000**	**0.000**
Fucus			0.818	**0.000**	**0.000**
MP + *Fucus*				**0.000**	**0.000**
Enteromorpha					0.985
C3	MP	*Fucus*	MP + *Fucus*	*Enteromorpha*	MP + *Enteromorpha*
Control	0.878	**0.000**	**0.000**	**0.000**	**0.000**
MP		**0.000**	**0.000**	**0.000**	**0.000**
Fucus			0.882	**0.000**	**0.000**
MP + *Fucus*				**0.000**	**0.000**
Enteromorpha					0.912
C4	MP	*Fucus*	MP + *Fucus*	*Enteromorpha*	MP + *Enteromorpha*
Control	0.999	**0.000**	**0.000**	**0.000**	**0.000**
MP		**0.000**	**0.000**	**0.000**	**0.000**
Fucus			0.980	**0.000**	**0.000**
MP + *Fucus*				**0.000**	**0.002**
Enteromorpha					**0.000**
C5	MP	*Fucus*	MP + *Fucus*	*Enteromorpha*	MP + *Enteromorpha*
Control	0.848	**0.000**	**0.000**	**0.000**	**0.000**
MP		**0.000**	**0.000**	**0.000**	**0.000**
Fucus			0.683	**0.000**	**0.000**
MP + *Fucus*				**0.000**	**0.000**
Enteromorpha					0.977

There was a significant difference for components 2 – 5 for Control<*Fucus*<*Enteromorpha*, this is not true for C1, where there was no significant difference between the Control and *Fucus*, but there was between the Control and Microplastics+*Fucus*. For all components, there was no significance between the plastic treatments component scores and the respective control.

5.6 Discussion

5.6.1 Justification of future scenario predictions

Hejzlar et al., (2003) studied DOM concentrations from 1969-2000 and found that DOM increased by 7% related to future climate change scenarios on a global level. Therefore, the future scenario where *Fucus* and *Enteromorpha* dominate and accumulate is a reasonable assumption as SGD inputs increase N concentrations, and these levels are expected to increase with increasing anthropogenic pressures and climate change due to land use change, population growth and greater release from sediments (Moore, 2010).

Due to the low residence time and relatively well-oxygenated conditions in the subterranean estuary (STE), denitrification within the STE is not a dominant process (Slomp and Van Cappellen, 2004) and NO_3^- concentrations remain high at the discharge point. On the other hand, dissolved PO_4^{3-} can be rapidly removed due to interaction with aquifer solids, in particular, sorption to Fe-oxides and/or co-precipitation with dissolved Fe or Ca into mineral phases, or carbonate uptake. Hence, SGD has a high C:N:P ratio, which deviates from the Redfield ratio of 106:16:1 (Redfield, 1958; Slomp and Van Cappellen, 2004). Deviations from the Redfield ratio are expected as this Ratio is based on marine phytoplankton and was calculated based on measurements from deep oceanic waters (Sardans et al., 2012). Deviations are used to determine the limiting nutrient in the growth of the plant. Therefore, areas dominated by SGD inputs have the potential to shift coastal ecosystems from N-limited to P-limited (Slomp and Van Cappellen, 2004). High N:P ratios are particularly true in regions, such as Kinvara Bay, where SGD is the primary freshwater source to the coastal zone with inputs as high as 21.4 (± 5.7) x 10^4 m^3 d^{-1} during high flow (Chapter 2). Sewage accounted for more than 50% of the TDP delivered to the bay, at the time of this study. Sewage is not treated to drinking water standards, which will cause a reduction in the TDP concentrations causing further P limitation (Rocha et al., 2015). Thus, in the future scenario, there will be no mitigating factor for the high DIN loads associated with SGD.

The critical C:N ratio of *Enteromorpha* spp., i.e. that's required for balanced growth, is ~9.6 (Viaroli et al., 2005). *Enteromorpha intestinalis* had an average C:N:P of 736:72:1. While *Fucus* had a higher C:N:P ratio of 1291:51:1 and was the species most adapted for survival under SGD conditions (Linh Trieu, 2015; Manaswi Raghurama, 2015). The *Ascophyllum*, *Fucus* and *Enteromorpha* in Kinvara Bay appeared to be N-enriched and P-limited compared to ratios published by Atkinson and Smith, (1983) suggesting that they have adapted to survival in a high

SGD influenced area (altered N:P ratios). Atkinson and Smith, (1983) showed *Enteromorpha* spp., had an N:P ratio of 35:1 in Rhode Island. While *Fucus* and *Ascophyllum* were not studied by Atkinson and Smith, (1983) the mean N:P ratio was 35 and the median was 30 for all studied benthic species. These macroalgae have a higher tolerance for lack of P as they have a greater capacity for storing P. Therefore, these species were most tolerant to SGD conditions in which P is limited. The trend provided in this study was *Fucus vesiculosus* > *Enteromorpha intestinalis* > *Ascophyllum nodosum*. This trend was consistent with the dominant species in the bay. Where SGD was highest, *Fucus* and then *Enteromorpha* dominate and at the sewage outflow pipe (where N:P ratios were lower) *Ascophyllum* was dominant. At Parkmore Pier, both of these factors must have been influential, as *Fucus* and *Ascophyllum* were both present.

Future scenario 2 was also realistic as increased dependency on industry to accommodate current lifestyle, increased population and increased industrial activities will lead to accumulation of plastics in the coastal zones due to waste and litter. In fact, 5% of plastics produced will eventually enter the marine environment (Green et al., 2015). Jambeck et al., (2015) predicted that plastic pollution is expected to increase by an order of magnitude unless improvements to waste management are implemented. The SGD and Parkmore Pier sites had larger concentrations of microplastics compared to the sewage outfall zone. The level of microplastics at the SGD site (674 ± 83 particles kg^{-1}) (Linh Trieu, 2015) was considerably greater than maximum levels (390 particles kg^{-1}) reported by Claessens et al., (2011) along the Belgian coast. The SGD springs are close to Dunguaire Castle, which hosts a large number of tourists every year. Also, the sinking rivers and streams inland are a direct link for microplastic contamination on land to be discharged to the coastal zone via SGD. Hence; microplastics may accumulate in groundwater due to the large catchment area (483.41 km^2). Parkmore Pier supports water activities such as shellfish farming and fishing. These activities are higher during summer months, the time at which this study was conducted and result in increased litter. The status of Kinvara Bay has been worsening over recent years and was recently classified as 'Bad' according to the latest EPA water quality report (EPA 2015). Therefore, prediction of future scenarios such as these is important to mitigate and understand the deterioration and detrimental effects this might have, to try to prevent further deterioration.

5.6.2 Macroalgae cover

Regions with increased nutrient supply show elevated nutrient uptake rates (Valiela et al., 1997). Many studies have shown that increased nutrient concentrations, in particular, nitrogen, strengthen macroalgae growth (Smith, 1981; Twilley et al., 1985; Taylor et al., 1995; Valiela et al., 1997). Therefore, different nutrient regimes may change the morphology of the macroalgae community. SGD regions, which have higher N:P ratios, will, therefore, have a direct impact on the macroalgae community in the relevant coastal zones. Studies of, and further predictions of, eutrophication in

shallow coastal bays support a shift from seagrass dominance to ephemeral, bloom-forming algae, and ultimately, to phytoplankton dominance in highly eutrophic systems (Duarte, 1995; McGlathery et al., 2007). Seagrasses are slow growing and dominate in systems with limited nutrients as they have low nutrient requirements. Macroalgae and phytoplankton are fast growing and have a higher nutrient requirement. SGD transports large fluxes of nutrients to the coastal zone, particularly DIN (Kroeger and Charette, 2008; Santos et al., 2008; Santos et al., 2009; Moore, 2010). Additionally, in eutrophic coastal zones, light also becomes a limiting factor. These species are excellent competitors under low light conditions as they are positioned closer to the surface and can exploit light (Duarte, 1995).

Although classically thought of as an estuarine species *Fucus vesiculosus* showed definite growth when transplanted to a marine environment (Lein, 1984). *Enteromorpha intestinalis* is tolerant of low salinities and is often found in areas where there is freshwater drainage (Fish and Fish, 2011). *Enteromorpha intestinalis* has the highest growth rates at salinities 15 – 20 psu. *Enteromorpha* have a broad temperature range of 10 – 20 °C for optimum growth conditions (Fortes and Lüning, 1980). *Fucus* also exhibits a broad range for growth, 10 – 24 °C, can survive from 5 – 26 °C (Graiff et al., 2015). This supports the findings of this species at both the SGD springs and the mouth of the bay. SGD is pulsed into Kinvara Bay due to the location of the springs in the intertidal zone. Therefore, *Fucus vesiculosus* can tolerate and proliferate in tidal-dominated SGD areas, which experience salinity fluctuations. *Enteromorpha* spp. is a thin blade macroalga and has been shown to dominate in a lagoon in Venice that is highly N-enriched (Sfriso et al., 1992). Valiela et al., (1990) also showed a dominance of *Enteromorpha* at Waquoit Bay, Cape Cod, a coastal zone influenced by SGD seepage with increased DIN inputs. SGD may have a heightened impact in shallow coastal zones due to their limited volume and restructured water exchange with the open ocean. Therefore, residence time may increase allowing modification of SGD-derived nutrients within the coastal zone.

Enteromorpha spp. have been demonstrated to have high nitrogen requirements and a reduced ability to store nutrients (Lavery and McComb, 2009), such that when pulses of nutrients are of high concentration, *E. intestinalis* can delay growth in favour of saving energy to maximize nutrient uptake and storage (Fong et al., 2004). It can be used as an indicator of eutrophication and there is enhanced growth in areas of abundant nutrient supply (Fish and Fish, 2011). Low growth rates were observed for salinities of < 5 and > 25 psu (Martins et al., 1999). *Enteromorpha* spp. can be considered as an indicator of freshwater SGD input, thus, it is reasonable to expect increased growth of these species in areas of freshwater SGD input, due to their desired salinity range. Thus, it is competitively superior relative to less freshwater tolerant species in areas influenced by freshwater, particularly combined with high nitrate concentrations (Choi et al., 2010). Welsh,

(1980) showed that nutrient removal over a marsh-mudflat was due to uptake by the geochemical or biological activity of the sediments and the macrophyte, *Enteromorpha lactuca*.

Sfriso et al., (1992) demonstrated the macroalgal community structure changed in The Lagoon of Venice as a result of increased pollution from land. The dominant macroalgae in the lagoon were *Enteromorpha rigida,* and they showed that the levels of plant nutrients and pollutants were influenced by the seasonal cycles of the macroalgae community. Seasonal cycles of *Enteromorpha* have been documented to have maximum biomass in spring and a die off period from late summer due to changes in temperature and nutrient concentration in the water column (Chávez-Sánchez et al., 2018).

Nutrient assimilation capacities of the species present will determine the impact of nutrients in the coastal zone. R-selected species, such as *Enteromorpha*, have high absorption capabilities and therefore have rapid growth rates when nutrient concentrations are high. Sommer, (1984) proposed three nutrient assimilation strategies for phytoplankton: high maximum nutrient uptake rates coupled with high growth rates, species that have high uptake rates but lower growth rates, and therefore, have storage capacity and species adapted to limited nutrient scenarios (Litchman and Klausmeier, 2008). Fast growing macroalgae, such as *Enteromorpha*, have increased decomposition rates compared to perennial macroalgae, such as fucoids, and therefore, may release more OM to the system (Bergström, 2005). In this study, this is in agreement with this study, which showed cores treated with *Enteromorpha* released the largest proportion of CDOM. As macroalgae dominate the nutrient biogeochemical cycles of these ecosystems, they function as high-quality food for organism lower on the food chain, such as the microbial communities (Martins et al., 1999). The OM produced from macroalgae can also move quicker through microbial and consumer food webs (Valiela et al., 1997). This is in direct correlation to the findings of this study, which shows an increased flux of labile materials increasing the productivity within Kinvara bay when *Enteromorpha* dominates.

5.6.3 DOC

Changes in carbon concentrations were due to the metabolism of the microbial community within the sediments. All cores acted as a source of DOC to the water column. There was a significant increase in DOC fluxes from the sediment under both future scenarios compared to the control experiments. The presence of microplastics alone did not alter these fluxes significantly compared to the control. In fact, the DOC fluxes were lower in the presence of both SPM and microplastics compared to the added SPM alone. This supports the conclusion that microplastics may not be a significant source of C to the coastal zone, either as refractory or labile materials. This may be due to the timeframe of the experiment, not allowing sufficient degradation of plastic fragments (Imhof et al., 2012). In the cases of added SPM, it can be seen that both *Enteromorpha* and *Fucus* released

DOC to the water column as they had C:N ratio of 10 and 25, respectively. *Fucus* released a higher concentration of DOC compared to the *Enteromorpha* treatment, possibly due to the higher C;N ratio of 25.

5.6.4 CDOM

Under control conditions, CDOM fluxes consisted of humic and protein-like components. Humic-like components accounted for 65% of the overall control flux, while tyrosine-like peaks accounted for only 18%, compared to 29% when all the treatments were considered. Protein-like peaks were not identified in the water column (Chapter 4), suggesting that these peaks were quickly utilised and/or rapidly diluted with seawater under natural conditions. Studies have shown that there is tight benthic-pelagic coupling due to high DIN concentrations associated with SGD (Rocha et al., 2015). Future scenarios predict higher levels of these materials being transported and therefore would lead to greater productivity, which may have deleterious effects in the coastal zone, such as eutrophication and harmful algal blooms. Currently, humic-like materials transported to the open ocean contribute to carbon storage. Protein-like peaks were detected when DOC concentrations were highest due to increased anthropogenic activity on land (Chapter 4, March 2013 and June 2015). If protein-like compounds become dominant in the coastal zone, the biological filter would lead to eutrophication within coastal waters, which would eventually lead to transport of labile materials to the outer Galway Bay.

Increased nutrient and DOC concentrations have been shown to cause a change in phytoplankton community composition (Klug and Cottingham, 2001). Rochelle-Newall and Fisher, (2002) showed that phytoplankton was not a direct source of CDOM fluorescence in marine and estuarine environments. In fact, they showed that CDOM fluorescence is observed due to bacterial production using the phytoplankton's non-fluorescent organic matter. Bacteria dominate OM degradation (Lancelot et al., 1993; Jiao et al., 2010), and, they, themselves, are an important active pool of organic carbon in sediments. DOM released during bacterial degradation results in the release of OM specific to bacteria, such as D-alanine, which has been shown to be more refractory than plant-derived OM (Veuger et al., 2006). This recalcitrant DOM is an important biotic feedback as it allows for the retention of nutrients and OM during eutrophication (McGlathery et al., 2007). Nielsen et al., (2004) reviewed over 100 published studies and determined that all types of detritus contain some refractory pools that could contribute to long-term nutrient retention. In this study, it can be concluded that the presence of macroalgae caused an increase in each component, even if it was not a direct source of CDOM.

There were no significant differences between the control and microplastic treatment suggesting that microplastic pollution is not as great a concern as a change in SPM resulting from land use change in terms of labile CDOM entering the water column. This may be due to the nature of

plastics, highly saturated polymeric materials, which are difficult to utilise as an energy source within an aquatic ecosystem. However, microplastics did not increase the intensity of refractory components either. Thus, the five-day evaluation period may not have provided a representative timeframe for such changes. Therefore, null hypothesis 1 cannot be rejected; there was no significant shift in the types of components entering the water column due to increased plastic pollution. However, plastic litter remains a serious issue as many species ingest these materials leading to increased incidences of fish kills. Plastic pollution represents a long-term environmental concern as the highly refractory material is slow to decompose (Imhof et al., 2012).

The *Fucus* and *Enteromorpha* treatments were significantly different from the control and from each other. C4 has previously been identified in the literature as tryptophan-like derived from algae exudation (Coble 1996; Stedmon and Markager 2005). This component has also been documented in bacterial extracellular polymeric substances (Zhang et al., 2012), marine phytoplankton cultures (Romera-Castillo et al., 2011) and algal media (McIntyre and Guéguen, 2013). *Enteromorpha* produced scores for each component at a significantly higher level than *Fucus* treatments, although *Fucus* released more DOC to the water column. *Fucus*, therefore, released a larger proportion of non-fluorescing DOC that was not detected in EEMF-PARAFAC analysis. Hence, the null hypothesis 3 was accepted as a change in Kinvara's SPM; in particular, an increase in *Enteromorpha* will cause an increase in bioavailable CDOM entering the bay. These macroalgae thrive in N-enriched waters and can survive under the P-limiting capacity of SGD (Björnsäter and Wheeler, 1990). Climate change projections show significant global warming and alterations in the amount of precipitation, which will impact the hydrological cycle (Green et al., 2011). Hence, as SGD levels are expected to increase with climate change due to wetter weather, the macroalgae blooms may worsen. This will cause a large efflux of labile material to the water column; of particular interest are labile materials that add an energy source to the coastal zone, which in turn will fuel productivity.

Therefore, coastal management strategies need to monitor the dominance of macroalgae in the region as both *Fucus* and *Enteromorpha* have been shown to increase the lability of CDOM, with an emphasis on *Enteromorpha* dominance due to their feeding strategies. Although, as blooms are prevalent due to *Enteromorpha* growth largely in summer and then subsequent die off in autumn, these two seasons will be affected the most. Therefore, the presence of either of these species of macroalgae can be used as a precursor of bioavailable CDOM. Anthropogenic activities and sewage impacted waters exhibit high protein-like fluorescence intensities (Baker 2002; Baghoth et al., 2008; Lapworth et al., 2008; Chen et al., 2010; Guo et al., 2010). An increase in protein-like components is not surprising as the algal material is mainly composed of proteins. With respect to protein-like components, tryptophan-like components have been documented to be more biodegradable than tyrosine-like components, which are more refractory in natural aquatic

environments (Yamashita and Tanoue, 2004; Maie et al., 2006) due to the more degraded peptide nature of tyrosine-like compounds (Fellman et al., 2010).

In addition to the increase shown in this study attributable mainly to increases in N, resulting from anthropogenic pressures on land as well as global change. Climate change is also expected to increase temperature and in turn UV-B radiation. Concentration may increase, and chemical composition of DOM may be altered by future scenarios, as shown in this study, which subsequently influences the depth of penetration of radiation in natural waters (Häder et al., 2007). Null hypothesis 5 can be rejected as the combination of increased plastic pollution and a change in SPM does not have a multiplying effect. From ANOVA studies, it can be seen that plastic pollution is not significant, and therefore, null hypothesis 6 that a change in SPM is the primary driver for CDOM lability in the future is accepted.

5.7 Conclusion

The future scenarios highlighted here may become apparent if anthropogenic pressures increase, such as a change in land-use, population growth and global warming. These scenarios showed an increase in both refractory and biologically available materials, in the form of protein-like peaks, entering the bay through sediment-water fluxes. Changes on land will also cause pollution in the groundwaters transported below, particularly, in karst regions, as surface-groundwater interactions are prevalent. Given the enormous concentrations of nutrients entering the bay as a result of SGD, it is paramount that DOC and CDOM components be monitored to avoid extreme eutrophication and deterioration of this coastal zone, on which many people rely for their livelihoods.

6. Identification of Dissolved Organic Carbon (DOC) Complexes in an Incubation Study of Submarine Groundwater Discharge (SGD) using Solid-Phase Extraction (SPE) and Fourier-Transform Ion Cyclotron Resonance Mass Spectrometry (FT-ICR-MS)

6.1 Introduction

Little is known about the sources, types and concentration of organic matter delivered to the coastal ocean as a result of SGD (Lapworth et al., 2008; Chen et al., 2010). Molecular characterisation of dissolved organic matter (DOM) is essential to bridge these gaps in our current knowledge and to understand the sources and fluxes of this organic carbon pool to the coastal zone. The complex nature of this pool has been the biggest obstacle associated with its characterisation (Stedmon et al., 2003). Oceanic DOM contains humified products of plant decay dissolved in freshwater, as well as protein and polysaccharide components due to phytoplankton metabolism (Nebbioso and Piccolo, 2012). Therefore, biogeochemical processes within the coastal zone influence oceanic DOM. There are four primary processes that remove DOM from the water column in coastal zones: (1) photochemical reactions (Moran and Zepp, 1997; Lange et al., 2003; Osburn et al., 2009); (2) aggregation of DOM due to changes in ionic strength when seawater and freshwater mix (Søndergaard et al., 2003; Stephens and Minor, 2010); (3) sorption to particles (Tremblay et al., 2005); and (4) biodegradation (Guillemette et al., 2013). The reactions and subsequent breakdown of organic matter in the coastal zone are largely dependent on the lability of DOM.

6.1.1 DOM lability

DOM lability can be characterised as labile DOM (LDOM), semi-labile DOM (SLDOM) or recalcitrant DOM (RDOM) although, in reality, a continuum of biological activity exists along these categories (Carlson and Ducklow, 1996). The labile portion accounts for less than 20% of total DOC in the ocean but is bioavailable and turns over rapidly (Moran and Hodson, 1990; Gan et al., 2016), and therefore, contributes significantly to productivity. This pool plays a major role in the microbial loop and interacts with dissolved inorganic carbon (DIC) and DOC pools (Jiao and Azam, 2011; Gan et al., 2016). Labile materials are predominately in the form of lipids and proteins. Organic nutrients, including nitrogen and phosphorus, can be analysed directly using FT-ICR-MS. DON has been shown to be an essential nutrient in coastal biogeochemical cycles and is elevated in SGD (Chapter 2). DON can contain a complex mixture of compounds including lipids, lignin, polyphenols and proteins with variable chemical structures and biodegradability (Benner and Kaiser, 2011). SLDOM can persist for months to years and accounts for a significant proportion of DOM exported from the euphotic zone to greater depths. RDOM is the most persistent as it is highly resistant to biological degradation and may be stored for millennia and leads to a fixed carbon pool in the ocean (Jiao et al., 2010). Notable refractory compounds include black carbon (BC) and highly unsaturated organic compounds. Over the last few centuries, production of black carbon has increased dramatically due industry combined with increased deforestation, agriculture shift, population growth and energy supply (Schmidt and Noack, 2000). Therefore, studies of this material are crucial to determine its entry in coastal zones worldwide.

Of the four primary removal processes, photo- and bio- degradation were investigated in this study and are described in more detail in the following sections.

6.1.2 Photodegradation

Numerous studies show that sunlight-mediated reactions convert refractory DOM into more labile material (De Haan, 1993; Allard et al., 1994; Salonen and Vähätalo, 1994; Moran and Zepp, 1997; Moran et al., 2000; Amado et al., 2006; Stubbins et al., 2012). Increased secondary production in microbial communities following photo-exposure of natural DOM has been documented (Miller and Moran 1997). Biologically available photo-products of DOM include a number of low molecular weight compounds, such as formic acid, citric acid, pyruvic acid, and acetic acid, and N-rich compounds which can be more readily assimilated by the bacterial population (Bushaw-Newton and Moran, 1999; Brinkmann et al., 2003; Bushaw-Newton et al., 2008).

Photochemical degradation can, however, also produce substrates that resist further biodegradation (Anesio et al., 2005; Mopper et al., 2015). The mechanisms that lead to a photochemical decrease of bacterial DOC degradation are not yet clear. However, irradiation has been shown to result in photo-mineralisation, photo-ammonification, photo-bleaching, photo-humification and photo-production of new DOM (Helms et al., 2013), as well as direct formation of DIC, CO and carbonyl-containing compounds (Valentine and Zepp, 1993; Zepp, 2003) and production of toxic compounds, such as H_2O_2 (Moran and Covert, 2003).

DOC concentration and quality and the amount of sunlight energy are major factors that regulate DOC photo-degradation (Farjalla et al., 2009). Photochemical degradation of DOM is likely to have important effects on the biological productivity of many aquatic ecosystems in SGD-influenced zones as the semi-labile and/or recalcitrant DOM transported through these aquifers may become biologically available upon discharge due to light exposure. Further to this, the loss of colour due to photobleaching of CDOM will have a strong effect on the optical properties of the coastal ocean (Moran et al., 2000) as it may allow penetration of UV and photosynthetically active wavelengths, and thus, promote productivity.

6.1.3 Biodegradation

In contrast, fewer studies have focused on biodegradation (Kujawinski et al., 2009), although, it has been shown to be a significant removal process within coastal systems worldwide (Moran and Hodson, 1990; Grøn et al., 1992; Yamashita and Tanoue, 2004; Guillemette et al., 2013). Guillemette et al., (2013) in their study of lakes evidenced a highly reactive terrestrial DOC pool that is processed due to interactions with nutrients. DOC turnover may almost exclusively be the result of degradation by microbes due to their large population and their efficiency at low substrate concentrations in groundwater systems (Moran and Hodson, 1990).

The labile component of CDOM can be consumed by microorganisms and subsequently converted into DIC or transformed into refractory DOM (Yamashita and Tanoue, 2004; Lønborg et al., 2010).

Biodegradation may be primarily responsible for the overall remineralisation of DOC and losses of the amino acid component of DOM (Benner and Kaiser, 2011). Overall, biodegradation tends to be chemically selective during early stages of OM decomposition resulting in the gradual enrichment of resistant molecules in the remaining organic detritus (Hedges and Prahl, 1993). Nutrient concentrations, temperature, and the quality of the DOC pool are major factors that limit bacterial DOC removal in aquatic ecosystems (Farjalla et al., 2009). Terrestrial DOM, as such, likely supports high levels of bacterial metabolism and CO_2 production globally but the bioavailability of DOM varies significantly, from <1% to >75%, depending on the molecular weight of fractions present (Sun et al., 1997). Therefore, bacterial respiration and DOC photochemical mineralisation play significant roles in the net heterotrophy pattern found in most aquatic ecosystems worldwide (Farjalla et al., 2009). Autochthonous DOC is considered more bioavailable than allochthonous DOC (Cauwet, 2002) while humic DOC is considered more susceptible to photodegradation due to its light absorbing characteristics (Bertilsson and Tranvik, 2000; Amado et al., 2006).

6.2 Research aims

To date, the molecular-level composition of SGD-derived DOM within coastal zones has eluded detailed description of mechanisms that add or remove compounds from the pool (Longnecker and Kujawinski, 2011). Understanding the degradation processes within the bay will allow for a greater understanding of the impacts of SGD-borne DOM on the carbon cycle. Labile degradation products may fuel productivity within the bay resulting in CO_2 release, especially since SGD is accompanied by high concentrations of inorganic nutrients (Chapter 2) whereas recalcitrant products resist breakdown and contribute to C storage. As groundwater travels through the subterranean path, DOM accumulates; hence, over time SGD may relocate recalcitrant C stocks on land to the ocean. The study was conducted in September 2014, as DOC concentrations and metabolism rates are highest during summer (Rocha et al., 2015) and therefore influences within the bay are expected to be more pronounced. This study aims to determine the impact of SGD-derived DOM on the carbon cycle of Kinvara Bay by obtaining a chemical fingerprint of DOM using EEMF-PARAFAC combined with FT-ICR-MS analysis. This technique not only allows the types of components (terrestrial versus marine, labile versus refractory) to be inferred by EEMF-PARAFAC but also gives molecular information that can be used to determine degradation processes by analysis of indicator molecules and therefore their subsequent impact on the C cycle.

EEMF-PARAFAC utilises chromophoric (CDOM) as a precursor for the wider DOM pool (Coble, 1996). This method is useful for broad characterisation of sources and types of CDOM present (Green and Blough, 1994). FT-ICR-MS further advances knowledge on molecular-level details of DOM and allows for the elucidation of indicators, such as amino acids and lignin, on a molecular scale (Koch et al., 2005). FT-ICR-MS studies utilise molar ratios, namely H/C, O/C and aromaticity to evaluate DOM regarding its biogeochemical availability further. Increased mass

resolving power allows for identification of indicator molecules that may not be translated in EEMF-PARAFAC. Identification of low levels of labile materials using EEMF-PARAFAC may not be possible when refractory compounds dominate due to the least squares algorithm employed.

The null hypothesis (H_0) states that SGD-borne DOM degradation pathways produce labile materials

The alternative hypothesis (H_1) rejects this hypothesis and states that SGD-borne DOM degradation pathways result in further recalcitrance.

Hypothesis 2: SGD-borne DOM in autumn contains a higher proportion of refractory compounds compared to winter SGD-borne CDOM

6.3 Sampling protocol

A continuum of SGD delivery was collected from an inland borehole (Loughcurragh South), the two largest springs (known as the Castle and the Arch), the mouth of the bay (Parkmore Pier) and seawater (at both high and low tide) in September 2014. An incubation study was conducted to determine the processes that SGD-borne DOM may undergo *en route* to the open ocean without the interference of autochthonous production.

Winter SGD samples were taken in January 2015 to compare high and low flow SGD composition. Due to the slower flow of SGD during autumn, it is hypothesized that degradation may occur within the subterranean pathway and lead to higher recalcitrance.

6.3.1 *In-situ* samples

SGD samples (n = 12) were collected *in-situ* in pre-combusted 1L glass bottles. Samples were filtered through pre-combusted GF filters using an acid-rinsed vacuum pump into pre-cleaned, acid-washed (10% HCl followed by MilliQ water), pre-combusted (at 450°C for 4 hours) amber glass bottles (250 mL) in duplicate, rinsed with the sample several times before filling.

In the field, at the same time, *in-situ* measurements of salinity, conductivity, temperature, total dissolved solids (TDS), dissolved oxygen (DO) and pH were obtained using an Aquaread 1000 AP, calibrated prior to use with freshwater conductivity (Varian 12,800 µS cm^{-1}), pH (Varian pH 4.00, 7.00 and 10.00), turbidity (0 NTU), DO (100% saturation) and ORP (+229 mV) standards.

6.3.2 Incubation experiments

In-situ SGD water samples (n = 16) were collected at time zero (T0) of the incubation study from the SGD springs. To study photo- and bio- degradation processes, a specific sampling strategy was devised (Figure 6.1).

A portion of samples (n = 8) were filtered (as above), and a portion remained unfiltered (n = 8) into pre-cleaned, acid-washed (10% HCl followed by MilliQ water), pre-combusted (at 450°C for 4 hours) amber glass bottles (dark) and clear glass bottles (light) in duplicate, rinsed with the sample several times before filling.

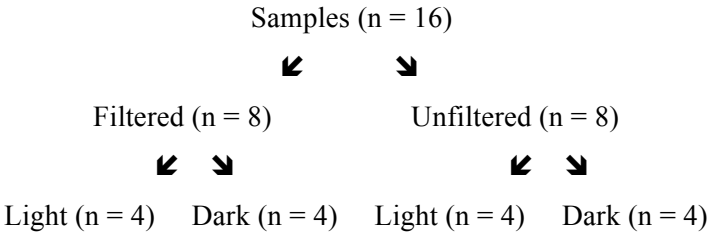

Figure 6.1: Incubation study sampling strategy for SGD collected from the Kinvara Springs in September 2014

An incubation time of nine days was assigned to the experiment as the residence time of groundwater in Kinvara Bay is known to be 6.8 ± 1.7 days determined using naturally occurring radium isotopes, ^{224}Ra and ^{223}Ra (Rocha et al., 2015). Samples were submerged in a recirculating water bath maintaining a constant temperature of 16.5 °C (to maintain *in-situ* conditions). Samples were pumped with a peristaltic pump through circulating tubes (1.6 cc min^{-1}) resulting in a sample turnover period of 2.5 hours inside the bottle, which was considerably lower than the residence time of the bay, and therefore, sufficient mixing was achieved. Samples were sealed with paraffin wax to remove any exposure interference; care was taken to place wax on the top layer of the water as to not contaminate the water sample below. A three-way valve was inserted for sample collection prior to sealing; by this means, individual samples were collected without opening or interfering with the remaining sample ensuring that the *in-situ* conditions were maintained.

Sampling for DOM and DOC was conducted before (T0), on day five (T1) and upon completion, day nine (T2), of the incubation. Samples were filtered through pre-combusted (at 450°C for four hours) Whatman 0.45 μm GF filters and collected in 10 mL amber glass bottles. As the samples were not poisoned, it is noted that this filtration method does not remove the entire microbial community.

6.3.2.1 Photobleaching protocol

Samples were irradiated using natural light and an iodine super sunlight lamp (Photo Accessories LPL). Control samples were filtered through GFF filters to remove the bacterial community to ensure that any DOM degradation was due to photodegradation. Dark control samples were stored in amber glass bottles wrapped in tin foil to avoid any light exposure.

6.3.2.2. Biodegradation protocol

Samples were wrapped in tin foil to prevent irradiation of the samples. Control samples were filtered and stored at 4°C in the dark.

6.4 Methodology

6.4.1 DOC analysis

Samples were analysed for DOC concentration by high-temperature catalytic oxidation (HTCO) using an Elementar Vario TOC cube (Chapter 3). The DOC concentration determines the loading of the sample onto the PPL cartridges in FT-ICR-MS (Section 6.3.3) and was used to determine the percentage recovery to allow for further analysis.

6.4.2 EEMF-PARAFAC analysis

CDOM analysis was conducted using absorbance and EEMF-PARAFAC analyses. EEMs were generated for each sample over excitation wavelengths between 220 - 500 nm in 5 nm intervals and emission wavelengths between 280 - 620 nm in 2 nm intervals, with 5 nm bandwidths on both excitation and emission modes.

6.4.3 FT-ICR-MS

The application of soft ionisation techniques, such as electrospray ionisation (ESI), has further advanced the applicability of FT-ICR-MS for natural organic matter characterisation (Kujawinski et al., 2002) as humic substances can be ionised (Stenson et al., 2002).

6.4.3.1 Extraction of DOM

Before extraction, samples were filtered and acidified to pH 2 (HCl, MS grade). For electrospray ionisation, mass spectrometry concentrated salt-free samples are required for accurate analysis (Koch et al., 2005). In this study, DOM compounds were extracted and concentrated using reversed-phase SPE using commercially available PPL cartridges that have been shown to be the most efficient with an average 62% DOC (Dittmar et al., 2008). The extract does not include salt and other constituents, thereby allowing for a further range of analytical techniques (Dittmar et al., 2008), including FT-ICR-MS. Subsamples were taken to account for functional groups, such as carboxyl, hydroxyl, amine and amide, which have acidic or basic characteristics, which increase their solubility in the aquatic environment due to the amphiprotic nature of water. However, the DOC concentrations in the subsamples for this experiment were too low to allow for direct injection into the FT-ICR-MS and, therefore, these functional groups could not be analysed directly.

PPL cartridges (Varian 1G), were activated a day before extraction using methanol and acidified milliQ water (with HCl to pH 2) then left to soak in methanol overnight. The next day, cartridges were rinsed with MilliQ water, and the samples were passed through the cartridges using gravity at a flow rate of < 10 mL min^{-1} and then eluted with pure methanol (6 mL per 1g of PPL adsorber) and collected in pre-combusted 10 mL amber glass bottles. These were stored frozen in the dark until further analysis. The volume of each sample loaded onto the cartridge was adjusted according

to 1 mg of DOC per sample to avoid overloading the SPE cartridge. The samples had a range of DOC concentrations (Table 6.1). Samples and process controls were carried out in duplicate.

For determination of extraction efficiencies, 100 µL subsamples of the extracts were transferred using a clean Hamilton glass syringe to pre-combusted 10 mL amber glass vials, covered loosely with pre-combusted aluminium foil, evaporated at 50°C overnight, and picked up in 10 mL of MilliQ water and acidified for DOC analysis. SPE-DOC was determined in the laboratory of the Research Group for Marine Geochemistry at the University of Oldenburg by high-temperature catalytic oxidation (HTCO) on a Shimadzu TOC-VCPH instrument equipped with a TDN unit.

Extraction efficiencies were calculated by comparison of DOC concentration in the original sample to that in the SPE-DOM extract and were found to be between 50 – 80 % of all samples (n = 20, including replicates and seawater samples). The extracts were stored in the dark in the freezer until analyses. The DOC extraction efficiencies were carried out in duplicate for each sample and found to be highly reproducible with a coefficient of variance of <5% between duplicates. The DOC control value of 11.33 µmol L^{-1} (average, n = 2) was subtracted from each sample for final analysis.

6.4.3.2 FT-ICR-MS protocol

An ultra-high resolution Bruker solar8 15 Tesla FT-ICR-MS in the laboratory of the Research Group for Marine Geochemistry at the University of Oldenburg was employed for DOM characterisation. The instrument was calibrated with an internal standard comprising over 100 known $C_xH_yO_z$ molecular formulae over the mass range of the samples. For each mass spectrum, 500 scans were accumulated. Mass errors of <1 ppm for all spectra were achieved using this method. SPE-DOM methanol extracts were diluted with milliQ water and methanol (99.9% MS grade) to yield a methanol to water ratio of 1:1 v/v and a DOC concentration of 20 mg C L^{-1}. Negative electrospray was used as the ionisation source. Ions were produced at atmospheric pressure by an external ESI ion source and entered the evacuated skimmer region of the spectrometer through a standard interface consisting of a heated metal capillary. This is selective for species that exist as ions in solution or those with acidic or basic functionality capable of donating or stabilising excess electrodes. The negative-ion ESI exhibited singly charged deprotonated species. A syringe pump at 0.5 µL min^{-1} maintained sample flow rate through the fused silica capillary.

6.4.3.3 Data analysis

The process control samples showed several peaks. The multitude of the molecular formulas in the samples was corrected for by the formulas found in the control. As such, any molecular formula present in either of the process control samples (S/N > 4) was deleted in each sample on a presence/absence basis. Therefore, sample handling and error have not contributed to the identification of DOM components.

The information contained in an ultra-high resolution FT-ICR-MS spectrum of natural OM is expansive and typically includes more than 10,000 signals, each having an m/z (mass-to-charge ratio) value and a corresponding measure of abundance. Ions generated fell within the range 250 < m/z < 800. The accurate m/z values were determined to 6 decimal places. Calibration of the mass spectra was carried out in the associated Bruker Software (DataAnalysis 4.0, SP 4) using an in-house mass list of known compounds. The measurements were performed in duplicate for each sample to test the reproducibility of peak detection and molecular assignment methods. These were averaged before data analysis. The peak intensity of each identified molecular formula was then normalised to the sum of all peak intensities detected in that sample. Only compounds with a signal-to-noise ratio of 4 or higher were accepted and further analysed (Seidel et al., 2014). Although high and low molecular weight compounds have been found in DOM (Tremblay et al., 2007), the number of elements present is very small. C, H and O are by far the most common elements and N, P and S may be present, but to a lesser degree (Koch and Dittmar, 2006). Consequently, formula assignment was conducted using only six elements; $^{12}C_{1\text{-}50}$ $^{1}H_{1\text{-}150}$ $^{16}O_{1\text{-}70}$ $^{14}N_{0\text{-}4}$ $^{31}P_{0\text{-}1}$ $^{32}S_{0\text{-}2}$, as other elements tend to be very rare.

Samples were measured in negative ionisation mode, which preferably ionises acidic moieties (for example, carboxylate functional groups) predominantly found in solid-phase extracted DOM. Of the detected compounds, only those with unambiguously assigned monoisotopic molecular formulae were used for further investigation and analyses. The number of heteroatoms (C, H, N, O, P, S) assigned to each intensity-weighted, normalised, averaged molecular formula was used to calculate molar ratios, H/C and O/C, AI_{mod}, double bond equivalence (DBE) and compound groups. Compounds and compound groups in this study refer to a mixture of isomers. A molecular formula assigned from FT-ICR-MS may represent millions of constitutional isomers and therefore, does not necessarily describe a particular structural entity or functional group in the sample. Nevertheless, the elemental composition can be used to derive structural information, such as the degree of saturation and resemblance to known molecular building blocks like sugars and amino acids (Koch and Dittmar, 2006). As a result, the compounds identified and all subsequent interpretations are ‘compound-like', which may be represented by a particular molecular formula and are useful for inferring structures and the processes occurring. Therefore, these are not unambiguous characterisations, and it should be kept in mind that alternative molecular structures may be possible. Molecular formulae may be assigned to more than one classification group and, thereby, the sum of all the relative abundances of all groups may be greater than 100%. This was not the case in this study, only one molecular group was assigned for each molecular formula, and the sum of all relative abundances equalled 100%.

DBE is a well-established tool in mass spectrometry and describes the total number of double bonds plus aliphatic rings in a molecule. DBE is an indication of carbon saturation in any given

molecule, which in turn may describe the types of compounds present. A decreasing number of H atoms in a molecule represents increased unsaturation and results in higher DBE values.

Double Bond Equivalence (DBE) is given by:

$C - H/2 + N/2 + 1$ (1)

Where, C, H and N represent the number of their respective atoms in the molecule.

The aromaticity of a compound was calculated and then expressed as the modified aromaticity index, AI_{mod}. It utilises an alternative double bond equivalence ratio, known as DBE_{AI}/C_{AI}, in which C is reduced by the total number of heteroatoms present. This alternative DBE is on the basis that DOM may contain heteroatoms that contribute to the number of double bonds but have no bearing on the aromaticity, condensation or the formation of rings within the molecules. This is the most conservative approach as it accounts for all heteroatoms present and therefore, aromaticity may, in fact, be higher than shown. Values with $AI_{mod} > 0.5$ indicate aromatic compounds and samples $AI_{mod} \geq 0.67$ are clear indicators for condensed aromatic compounds.

Van-Krevelen plots have been used extensively in the literature to assign distinct compound groups and allow comparison of samples both within and between experiments (Tremblay et al., 2007). These plots are essentially element-ratio plots, in which each dot represents a molar ratio of H/C on the y-axis as a function of the molar ratio of O/C on the x-axis. The position of the cluster of points may be used to determine patterns that are used to infer source material, degradation and changes in bulk material, as certain molecules occupy a unique space within the plot. Molecular classification can be conducted into broad compound groups based on their O/C, H/C and Al_{mod} relationships. Groups analysed in this study include (1) black carbon ($Al_{mod} < 0.67$), (2) polyphenols ($0.5 > Al_{mod} > 0.67$), (3) highly unsaturated organic compounds ($Al_{mod} \geq 0.5$, $H/C \geq 1.5$, $O/C \geq 0.9$), (4) unsaturated aliphatics ($2 > H/C \geq 1.5$, $O/C \geq 0.9$, $N > 0$), (5) saturated fatty acids ($H/C \geq 2$, $O/C \geq 0.9$), (6) sugars ($O/C < 0.9$), and (7) peptides ($2 > H/C \geq 1.5$, $O/C \geq 0.9$, $N = 0$).

All statistical calculations were performed using the R statistical platform version 3.2.1 (R Development Team 2008) and Matlab. To determine the statistical significance between treatments two-way analysis of variance (ANOVA) was conducted. For significant effects, Tukey's Honest Significance Difference (HSD) test was employed for further evaluation of the differences between treatments. CDOM analysis was conducted using the CDOM toolbox in Matlab to determine the CDOM components and validation was ensured using random initialization and split-half validation (Stedmon and Bro, 2008).

6.5 Results and discussion

6.5.1 Hydrological parameters

Table 6.1: Summary of measured water parameters and DOC concentrations in each sample group, measured *in-situ* throughout Kinvara Bay in September 2014 and at the Castle Springs in January 2015

Sample	Conductivity (mS cm^{-1})	Salinity (ppt)	pH	DO (%)	DOC (μmol L^{-1})
Seawater high tide	51.70	35.5	8.42	103.6	248.61 – 256.32
Parkmore Pier (PP)	48.44	33.1	8.51	104.3	269.87 – 274.32
Seawater low tide	48.14	32.9	8.32	103.0	224.77 – 227.49
Arch (SGD)	12.09	7.8	7.78	74.8	522.21 – 528.60
Castle (SGD)	10.33	6.6	7.55	58.6	307.01 – 461.04
Winter SGD (Castle)	0.49	0.4	7.47	77.7	291.57 – 330.19
Loughcurragh South (Groundwater)	0.36	0.2	7.24	41.2	637.53 – 642.37

Unsurprisingly, groundwater and SGD exhibit lower conductivity, salinity, DO and pH than seawater, but higher DOC concentrations (Table 6.1). DOC concentrations at the Arch discharge point are due to a mixture of seawater and SGD; this is shown by the higher salinity and DOC values compared to the Castle. Cave and Henry (2011) showed that the Arch SGD flow may dry up during dry spells. They concluded that the Castle flow draws from a deeper source than the Arch. During September 2014, the Castle flow is approximately 20% seawater due to the brackish nature of SGD during this season. However, the Arch has a higher proportion of seawater mixing, shown by the higher salinity.

6.5.1.1 SGD seasonal impacts

Table 6.2: Summary of measured water parameters in the SGD endmember, measured at Castle Springs during autumn (September 2014) and winter (January 2015), taken as T0 of the incubation study.

	September 2014	January 2015
Conductivity	10.33 – 13.43 (mS cm^{-1})	570 (μS cm^{-1})
Salinity (ppt)	5.8 – 7.2	0.3 – 0.4
pH	6.91 – 7.49	7.12 – 7.85
DO (%)	41.2 – 67.4	67.6 – 83.8
Temperature (°C)	14.6 – 15.5	6.7 – 8.6
ORP (+mV)	139.6 – 180.5	196.1 – 227.4
TDS (mg L^{-1})	8.014 – 8,729	23 - 315

The autumn samples experienced longer sunlight hours and higher temperatures, but lower DO levels compared to winter samples (Table 6.2). Availability of light affects the degree of photodegradation that may occur in the coastal zone. In addition, higher temperatures in autumn

combined with longer sunlight hours allow for higher production rates within the coastal zone. DO is an essential molecule for productivity, and the lower DO value may inhibit biodegradation during autumn conditions within the incubation study. The autumn samples have brackish salinities of 5.8 – 7.2 ppt. In comparison, the salinity of the winter samples indicates fresh SGD is entering the bay.

6.5.2 DOC

DOC concentrations in the landward samples were two-fold higher than seawater samples. The inland borehole had the highest concentration of DOC at 641.9 ± 3.46 μmol L^{-1}. The arch and castle represent the SGD springs, (386.4 ± 42.1 μmol L^{-1} Castle, 527.9 ± 7.4 μmol L^{-1} Arch). The DOC concentrations were reduced here due to mixing with seawater as the SGD was brackish during this sampling campaign. DOC at higher salinities (Parkmore Pier) was lower than DOC at the discharge point suggesting removal of land-borne DOC within the bay and/or mixing with seawater. During all seasons at intermediate salinities, there was a net increase in DOC; this is also reflected in the release of CDOM from sediments. The high variability associated with the lower salinities was due to the seasonal effects of SGD whereupon winter DOC concentrations in SGD were lower than those in summer (Chapter 3).

A filtered control was analysed for DOC to determine the impact of experimental design, background contamination level and associated measurement error; this was found to be 35.39 ± 4.66 μmol L^{-1} (within the error limit for many samples) and was subtracted from each sample.

Table 6.3: Incubation DOC concentrations taken at T0 and the end of the SGD incubation experiment for all treatment groups in September 2014. Units are μmol L^{-1}

Sample	DOC (μmol L^{-1})	n	Standard Error (μmol L^{-1})
T0	245.9	4	42.12
Filtered Light	266.4	4	81.93
Filtered Dark	271.2	4	49.63
Unfiltered Light	270.1	4	46.54
Unfiltered Dark	261.5	4	37.22

Accounting for the relatively large error associated with DOC measurement, there was no significant difference between T0 and the treatments (Table 6.3; Figure 6.2). This suggests that DOC is highly refractory and not susceptible to degradation within the timeframe of this incubation.

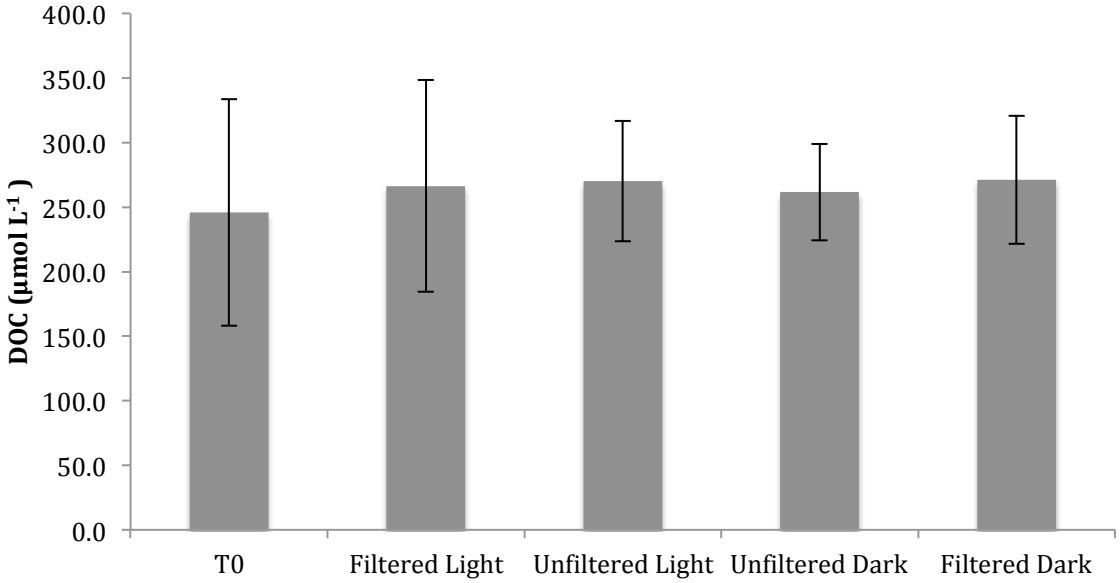

Figure 6.2: Bar chart of DOC concentrations taken at T0 (n =4) and the end (n = 4) of the incubation experiment for all treatment groups including error bars (Standard Error). Units are µmol L^{-1}.

6.5.3 EEMF-PARAFAC

In total, 113 EEMs were combined and fitted to a 2-component model. No obvious residues were obtained after the model was validated by split-half analysis and random initialisation (Stedmon and Bro, 2008). The residual analysis confirmed that the 2-component model was adequate. The fluorescence signal remaining in the residuals was non-systematic and represented instrument noise. It was not possible to validate the two split data arrays with a higher number of components as the model was attempting to model instrument noise.

Peak identification confirmed spectral characteristics of organic fluorophores with multiple excitation and emission maxima. Components are predominately of humic-like origin, due to the emission maxima > 400 nm in all cases (Table 6.4), which fit well with components identified previously by other studies (Coble, 1996; Stedmon et al., 2003). Both peaks A and C are present, representing humic-like fractions of CDOM present in fresh water and deep seawater, indicating terrestrial organic matter sources (Coble, 1996). However, components (Figure 6.3) have shifted from the original model (Chapter 4), which suggests biogeochemical processing.

Table 6.4: Fluorescence characteristics of validated annual two-component EEMF model: excitation and emission maxima, compared with previously identified components. Bold Q components indicative of Quinone-like moieties (Cory and McKnight, 2005), n = 113 over the incubation period.

Kinvara Model Ex/Em (nm)	Previous Model (literature)	Description and source	References
C1: 235/425	250/450	Humic-like/ Photorefractory product **Q1**	(Chen et al., 2010)
C1: 235/475			
C1: 275/425	260/380 - 460	Peak A - Visible Humic-like	(Coble, 1996)
C1: 275/475			
C2: 250/ 460	260/380 - 460	Peak A - Visible Humic-like	(Coble, 1996)
C2: 325/460	320 – 360/420 - 460	Visible humic-like	(Stedmon et al., 2003)

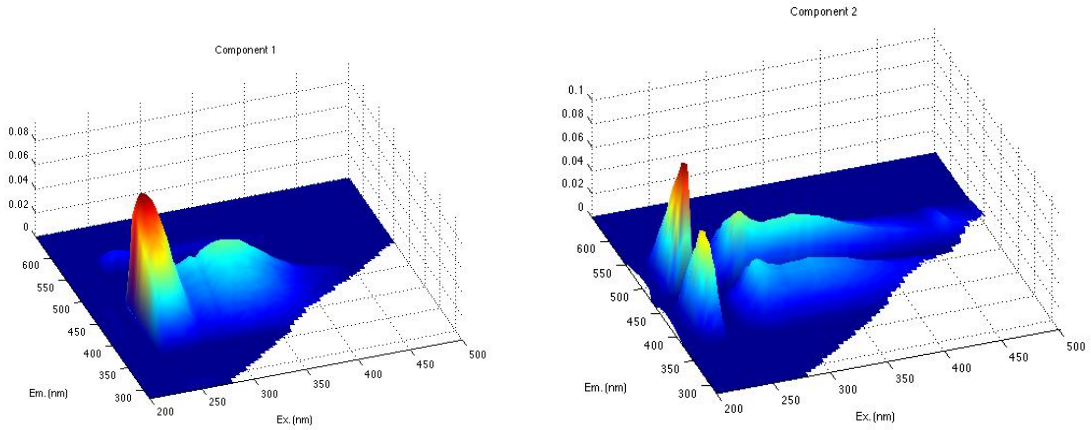

Figure 6.3: Component 1 and 2 EEM surface plots of the incubated SGD samples.

The original model (Chapter 4) consisted of 3 components. The components were predominately terrestrial humic-like material similar to the incubation results. It is important to note that Peak T was not present in T0 samples of the incubation. In the original model, Peak C and soil fulvic acid were the main components of SGD followed by Peak A, visible humic-like material. However, after the incubation, these peaks were no longer validated, and the samples consist of visible humic-like materials only. Previous studies have linked a large decrease in Peak C compared to a smaller decrease in Peak A with irradiation and subsequent photobleaching (Helms et al., 2013).

The Humification Index, HIX, of T0 samples was 0.95 ± 0.01 and agrees well with the HIX of 0.94 ± 0.02 from the original model (Chapter 4). This suggests highly humified material associated with SGD; this decreased to 0.84 ± 0.03 over the course of the incubation study, which was comparable to the HIX found at Parkmore Pier (0.83 ± 0.05), suggesting the incubation study was reflective of natural conditions. Although an HIX of 0.84 ± 0.03 was still indicative of humified material, it may indicate some level of degradation or change in materials through the coastal zone.

The incubation study EEMF-PARAFAC results showed that humic-like materials present in Kinvara Bay were highly resistant to degradation. There were no labile components (peak B or peak T) given in the EEMF-PARAFAC model. Therefore, bio- and/or photo- degradation do not produce bioavailable compounds, in the form of protein-like peaks, as shown in other studies (Mopper et al., 1991; Zepp, Callaghan and Erickson, 1995; Bertilsson and Tranvik, 2000; Rosenstock, Zwisler and Simon, 2005; Chen and Jaffé, 2014).

EEMF-PARAFAC utilises CDOM as a precursor for the wider DOM pool. In this study, there was a net removal of SGD-derived DOC over the representative residence time within the bay, which has been shown to be due to seawater mixing (Chapter 3). EEMF-PARAFAC utilises an algorithm for least squares across the whole dataset and therefore may not be sensitive enough to detect low levels of labile materials produced from the incubation in the presence of the highly humified material. FT-ICR-MS analysis provided a molecular fingerprint of all DOM molecules present and therefore more detail about any degradation products that may be present in smaller amounts.

6.5.4 FT-ICR-MS analysis

DOM is a complex mixture of heterogeneous organic compounds, which in this study consisted of 36,744 different compounds resolved with a mean mass ranging from 154.0510 to 1983.530145 Da; of these, 11,242 had assigned formulae (30.6%). The highest assigned molecular mass was 1036.3702 Da. The reliability of assigning formulae is higher at lower nominal masses and decreases with increasing nominal mass due to the larger number of possible elemental combinations for one detected peak (Koch et al., 2007). Therefore, higher masses (>1036.3702 Da) were not included for analyses to avoid false elemental conclusions. It should be noted that this

analysis is based solely on negative ion FT-ICR-MS, and as such, has a focus for compounds that can be detected in this mode. This applies to all samples so a comparison can be made between samples in this study.

All designated formulae (11,242) contained at least one O compound due to the mixture of carboxyl and hydroxyl functional groups such as ketones, aldehydes, unsaturated ethers and alcohols found within DOM (Thurman, 2012). The masses detected across the range of samples fall into four main compound classes, outlined in Figure 6.4: (1) carbon, hydrogen and oxygen only, CHO (49 - 55%), (2) nitrogen containing compounds, CHON (24 - 37%), (3) sulphur containing compounds, CHOS (9.5 - 13%), (4) phosphorus-containing compounds, CHOP (2.5 - 5%) and to a lesser degree S- and N- containing compounds, CHONS (0.1 - 1.5%).

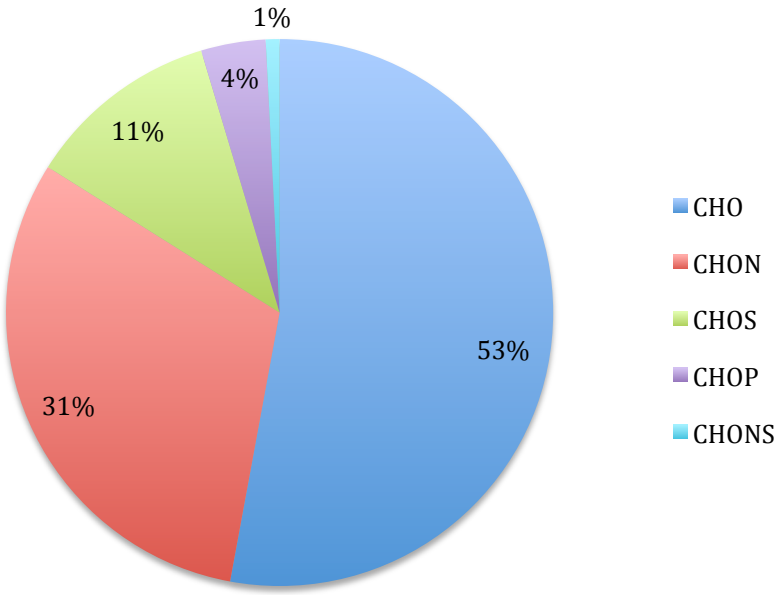

Figure 6.4: A pie chart outlining the relative abundance of compound classes (CHO, CHON, CHOS, CHOP, CHONS) in SGD endmember, measured at Kinvara Springs in September 2014.

A typical mass spacing of 14.0156 Da was observed, which spanned the entire spectra. This mass difference is derived from an increasing number of -CH_2- groups in a homologous series. Therefore, the composition of coastal DOM in Kinvara Bay was not completely random but instead exhibited a high degree of order (Appendix J). Molecules were a part of a chemically related family of compounds. This mass spacing has been observed in other studies (e.g. Koch et al., 2005).

The signal intensities exhibit a high dominance of odd over even neutral nominal masses, which reflects the relatively low N content (<40% in this study) and low relative abundance of ^{13}C in natural OM (Koch et al., 2007). Marine DOM is chemically distinct from freshwater DOM (Benner et al., 1992; Hedges et al., 1992). The differences in chemical composition of fresh and marine DOM arise due to differences in sources and formation processes in the two environments (Repeta

et al., 2002). Freshwater DOM is isotopically light, has a high C:N ratio (40 - 50), is rich in aliphatic, aromatic and carboxyl carbon (Hedges et al., 1992), and has strong absorption in the near UV (Stedmon and Bro, 2008). In contrast, seawater DOM has been shown to be isotopically heavier, has a low C:N ratio (15 - 20), is rich in alkoxy carbon and has weak absorption in the near UV. Nonetheless, 2,248 of assigned compounds were common to all samples, representing about 20%. Therefore a fraction of freshwater DOM is indistinguishable from seawater DOM; this has been seen in high molecular weight (HMW)DOM previously (Repeta et al., 2002).

6.5.4.1 Seasonal SGD-borne DOM loading

During winter, the number of compounds transported via SGD increases and there was an additional 2,212 formulae identified compared to autumn (313 unique formulae). Using only formulae exclusive to both autumn and winter, the O/C and H/C ratios decreased from 0.5 and 1.1 in winter samples to 0.3 and 0.9, respectively, in autumn samples. The average AI_{mod} for autumn was 0.5, indicating high aromaticity. This decreased to 0.37 during winter, indicating dilution with less aromatic compounds considering all nominal masses. However, the AI_{mod} for both was approximately 0.3, which was similar to seawater samples. The DBE was 12 for both seasons suggesting that there was a very high level of unsaturation under both flow regimes. Therefore, there was a high degree of recalcitrance.

The largest proportion of assigned formulae in all sample groups was classified as CHO compounds. At the Castle SGD site, these compounds consisted of 55% of all assigned formulae during autumn, which was higher than the winter samples of 46%. This may be due to the slower motion of water through the subsurface during autumn, which may result in greater absorption capacity within the aquifer. The longer residence time within the aquifer allows for greater adsorption of aquifer solids. The proportion of charge-to-mass ratio values, m/z, assigned to CHON compounds was 32% in autumn and 37% in winter. This agrees well with other studies of groundwater (e.g. Longnecker and Kujawinski, 2011) which highlighted the fact that this level was higher than values recorded in marine and riverine samples (Kujawinski et al., 2009) and from inland riverine samples (Sleighter et al., 2009). Elevated levels of CHON suggest anthropogenic terrestrial contamination coupled with limited microbial remediation within the aquifer, which may be amplified due to the relatively fast flow of groundwater through this karstic aquifer (Gill et al., 2013; McCormack et al., 2014).

Black carbon (BC) was the most abundant unique DOM compound group in the SGD samples (Castle) accounting for just under half (49.5 %) of all unique compounds during autumn. However, during winter highly unsaturated compounds were the most abundant (62.5%), while BC accounted for only 8% of the unique compounds. BC accounted for 4 - 5 % of total DOM content in SGD at the Castle site and 12% at the Arch site. Higher temperatures and longer residence time, therefore,

increased the BC content and the refractory nature of DOM. BC is a continuum of terrestrial C compounds, rather than one particular compound and/or group of compounds and has low mass and high DBE values (Nguyen and Lehmann, 2009). The chemical structures of these compounds consist of multitudes of condensed aromatic rings, and fundamentally, are carbon-rich and hydrogen-poor (Goldberg, 1985; Kim et al., 2004). Therefore, these compounds may contribute to the humic-like components in EEMF-PARAFAC analysis as humic and fulvic acids are present. FT-ICR-MS allows BC to be distinguished from humic substances. Little evidence exists for the presence of black carbon in groundwater as its aqueous solubility is low (Kim et al., 2004). Kim et al., (2004) explained that hydroxyl groups can be substituted onto BC, which can then be oxidised to quinones or carboxylic acids. The addition of the polar group (hydroxyl) made it more soluble and allowed it to accumulate in SGD. The formation of this BC soluble entity removes carbon and oxygen that cycles through plant and animal biomass ordinarily (Goldberg, 1985; Kim et al., 2004). BC is relatively biochemically inert representing a significant sink as it accounts for an important fraction of carbon buried in soils and sediments (Schmidt and Noack, 2000). Turnover of BC occurs but at a much slower rate than that of other soil organic matter (Nguyen and Lehmann, 2009). Decomposition transpires through microbial degradation (Baldock and Smernik, 2002) and abiotic oxidation (Cheng et al., 2006).

6.5.4.2 Molecular ratios

Van Krevelen plots illustrated the O:C molar ratio of the x-axis and the H:C molar ratio on the y-axis. Major biogeochemical compound classes exhibited characteristic H:C and/or O:C ratios (Baldock and Smernik, 2002; Kim et al., 2004). Therefore, plotting these against one another allowed for visual examination of these ratios and for certain compound classes to be distinguished (Kim et al., 2003; Kujawinski et al., 2009). Van Krevelen plots must be interpreted with caution as ratios may vary within particular compound classes and the literature (Bhatia et al., 2010). However, they remain a useful tool as thousands of peaks identified in mass spectra can be visually depicted. Well defined trend lines have been established in the literature to explain reaction pathways among molecules and chemical transformations, such as methylation, hydrogenation, hydration, within DOM (Kim et al., 2003).

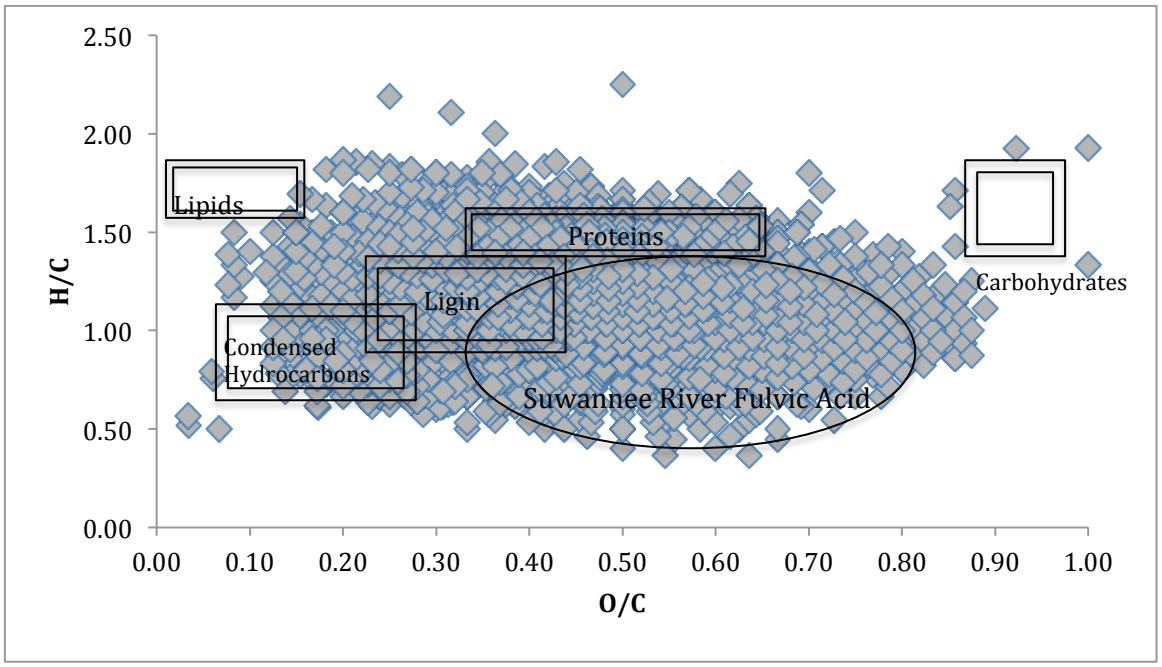

Figure 6.5: Van Krevelen plot of DOM, presenting molecules identified in the SGD endmember (n = 2), taken from Kinvara Springs September 2014.

The presence of proteins in the SGD-DOM signature suggests that SGD transports labile materials to the coastal ocean, albeit at low concentrations.

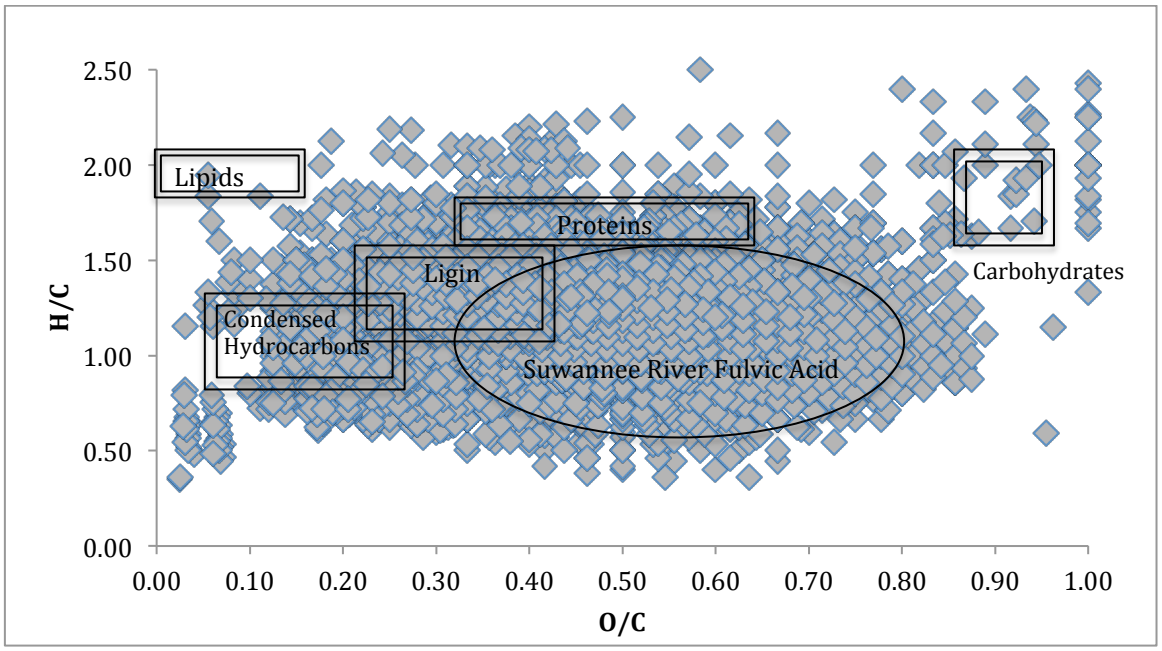

Figure 6.6: Van Krevelen plot of DOM, presenting molecules identified in seawater samples only (n = 4), in September 2014.

From a visual comparison of the two samples, it can be seen that there were a greater number of DOM molecules with greater variability in seawater samples. Variability represents the diverse sources contributing to the oceanic DOM pool due to many sources within Galway Bay including seawater, SGD, riverine flows and runoff from many different inlets (Smith and Cave, 2012; Schubert et al., 2015).

The relatively narrow range of O:C and H:C ratios of identified molecules in SGD reflect the absence of labile components such as lipids, proteins and carbohydrates (Figure 6.5). The H:C ratios span a larger range of ratios reaching as high as 2.5 in seawater samples. Higher H:C ratios represent greater unsaturation within the molecules. Therefore, molecules may be more biologically available. Bhatia et al., (2010) analysed fulvic acid from the Suwannee River and concluded that this was represented by H:C ratios of 0.5 to 1.5. Therefore, the bulk of the cloud in the middle of both endmembers represented humic substances transported from land and is predominately refractory in nature.

The region of O:C ratios of 0.25 - 0.5 and H/C ratios of 1.0 - 1.5 illustrated in the above Van Krevelen plots (Figures 6.5 and 6.6) represents lignin-type molecules (Kim et al., 2004). Lignin is an important tracer for terrestrial DOM as it is a plant-derived component. These are complex macromolecules consisting of phenylpropanoid which is randomly linked to each other by a variety of carbon-carbon and ether bonds (Nebbioso and Piccolo, 2012). Lignin may have entered groundwater through leaching from soil, and subsequently been delivered to the coastal zone via SGD. This branched macromolecular network provides chemical stability to lignin causing it to resist microbial degradation (Nebbioso and Piccolo, 2012). As this compound is solely land-derived, it confirms that these compounds are highly recalcitrant in the flow path as this compound is present in seawater at high tide. Therefore, SGD-derived carbon is contributing to oceanic carbon storage. This may have important implications for the C cycle as land-based C stocks may relocate to the ocean. Baldock and Smernik, (2002) reported charred wood samples (thermally-altered) had O/C ratios of 0.32 - 0.61 and H/C ratios of 0.46 -1.02. These types of compounds were evident in the groundwater of this region and therefore supported the findings that BC was present in SGD and was transported to the coastal ocean via this route. Condensed hydrocarbons are deficient in both oxygen and hydrogen and often contain aromatic ring structures. These may originate from BC-like molecules (Kim et al., 2004). Labile materials include proteins and lipids, which are derived from microbial activity (Bhatia et al., 2010). Higher microbial activity found in the seawater samples was likely derived from photosynthetic algae and bacteria communities present in the open ocean (Koch et al., 2008).

6.5.4.3 Organic nutrients

While compounds containing only C, H and O were the most prevalent elemental formula assigned in this study, 4,461 organic nitrogen compounds were also present in all samples. Management strategies of coastal zones have focused on inorganic nutrients, overlooking the potentially significant loads of nitrogen and phosphorus embedded in organic matter (Hwang et al., 2005; Santos et al., 2009; Rocha et al., 2015). Terrestrial DON sources in the region include septic tanks, human and animal wastes and organic components in fertilisers. The number of compounds

containing N in SGD during autumn was 1,644, increasing to 2,529 compounds in winter. This increasing winter trend was also observed for C, H, O, S and P compounds.

N-containing compounds in SGD accounted for 32 - 37% of assigned formulae in SGD across autumn and winter. Organic N represented a higher number of designated formulae in winter samples, agrees well with direct DON measurements determined in Chapter 2. Higher DON concentrations may be due to soil lixiviation at higher groundwater volumes during winter. DON can contain a complex mixture of compounds including lipids, lignin, polyphenols and proteins with variable chemical structures and biodegradability. Polyphenols are complex compounds containing N that comprised the second most abundant compound class in SGD. DON associated with soil lixiviation is often thought of as refractory as DON can be present in high concentrations in lignin. However, a portion of DON has been shown to be biodegradable (Lusk and Toor, 2016). Labile DON is present in lipid and protein-like structures. DON is a potential source of reactive N in aquatic ecosystems (Seitzinger et al., 2002; Bradley et al., 2010; Jørgensen et al., 2014). DON can be rapidly recycled within Kinvara Bay into bioavailable forms. This has been shown to contribute up to 48% of local biological N fixation (Chapter 2; Rocha et al., 2015). Tight coupling of the DON pool between production and consumption may result in large fluxes in and out of the DON pool leading to constancy in concentration (Bronk et al., 2007). Therefore, the constancy in concentration is not necessarily due to a refractory nature of DON. Instead, there may be a bioavailable fraction. Seitzinger et al., (2002) showed that up to 73% of DON could be utilised by estuarine plankton. Agriculture is the dominant land use practice in this catchment and DON associated with this source had a proportion of about 30% being bioavailable.

CHOP accounted for approximately 3% of assigned formulae. As TDP concentrations were very low across all seasons (Chapter 2), it can be concluded that inorganic P is not significant within SGD. P acts as the limiting nutrient in the bay as levels are very small, often close to the detection limit (Chapters 2 and 3). SGD was the principal source of carbon and nutrients to Kinvara Bay and was thus the primary driver for productivity within the bay. Therefore, N budgets based on DIN only may underestimate bioavailable N loading. In areas of high SGD, DON may constitute a significant portion of the total N flux and may represent a bioavailable pool.

6.5.4.4 Incubation differences

As shown above, SGD transported organic nutrients to the coastal ocean as well as high concentrations of inorganic nutrients (Burnett et al., 2003; Slomp and Van Cappellen, 2004; Rocha et al., 2015). Incubation experiments were conducted to determine the relative contribution of photo- and bio- degradation processes on allochthonous SGD within the coastal zone. Allochthonous humic DOC has been shown to be more photoreactive than algal DOC (Bertilsson and Tranvik, 2000).

Comparing the light and dark incubated samples yielded 531 unique formulae for the dark samples and 709 unique formulae for the light samples. Although, the unique formulae accounted for less than 15% of the original sample and the differences between these samples are small, comparison of these groups allows for distinctions between light and dark incubation. The average O:C and H:C ratios were very similar between light and dark samples, 0.4 and 1.2 for dark samples, respectively, compared to 0.4 and 1.0, respectively for the light samples. Lower H:C ratios resulted in lower saturated compounds. Al_{mod} also differed between the two groups, with 0.32 observed for dark samples and 0.41 for light samples. The light samples had a higher abundance of unsaturated compounds in all groups 1 through 3. Dark samples were consistently greater in the saturated compounds of groups 4 through 7. The light samples had a higher abundance of unsaturated compounds (50.3%) compared to dark samples (42.1%); this was also the case for polyphenols, where they accounted for 22.6% of the light samples, compared to 13.7% of the dark samples.

Degradation processes for SGD transported through Kinvara Bay resulted in highly saturated, refractory compounds. Highly saturated, aromatic molecules exhibit greater recalcitrance compared to molecules with low aromaticities and high unsaturation, which can contribute to productivity within the bay and therefore are labile. Highly degraded DOM in the deep ocean resists further degradation and may age to several thousand years (Koch and Dittmar, 2006). Highly unsaturated compounds comprised the vast majority (73%) of all common compound groups whereas, labile materials (saturated fatty acids, sugars and peptides) accounted for less than 1%. Therefore, SGD may contribute to transferring the carbon store on land to oceanic storage.

All terrestrially-derived samples reflected this, including the incubated samples, as labile materials accounted for less than 1% of all assigned formulae, with the order of the most abundant samples being highly unsaturated compounds > polyphenols > black carbon.

6.6 Fate of terrestrial DOM

FT-ICR-MS is capable of resolving thousands of molecules associated with SGD-borne DOM. These analyses further confirmed that SGD-borne DOM transported through the Gort-Kinvara karstic aquifer was predominately refractory in nature, as highly unsaturated compounds, polyphenols, unsaturated aliphatics and black carbon accounted for more than 95% of compounds in SGD.

H:C ratios for marine samples were relatively low, 1.3. As a result, DBE was relatively high, 8.5. The high degree of unsaturation in marine samples was surprising as marine DOM is known to have a lower proportion of aromatic carbon compared to terrestrially-derived DOM (Thurman, 1985). A small O:C ratio of 0.5 suggested that carbonyl compounds cannot explain the high level of unsaturation alone and that some degree of carbon unsaturation and non-aromatic rings must be

present. Studies showed that only about 4 - 10% of DOC in the deep-sea is of terrestrial origin (Opsahl and Benner, 1997). An important question, therefore, arises; what happens to SGD-derived DOM? The fate of SGD-borne DOM remains largely unknown. This study has shown that SGD-DOM in Kinvara was mostly composed of old refractory compounds that behaved conservatively for the most part over the transit path.

Microbial remineralisation in marine surface waters was the most dominant removal process in many regions. This has been shown in the Arctic Ocean, where 11% of the initial carbon was consumed with a turnover time of 220 days (Bussmann, 1999). The residence time 6.8 ± 1.7 days in Kinvara Bay (Rocha et al., 2015) does not allow for consumption of this highly recalcitrant DOM within the bay and timeline of this study. Photo-humification may be an important degradation pathway while photobleaching may be an important removal process in the open ocean. This was expected to be more pronounced in September 2014 due to longer sunlight hours and increased irradiance. Additionally, adsorption to particles (Hedges and Keil, 1999) may explain the removal of DOM *en route* to the ocean through the coastal zone. Another explanation may include burial of DOC in sediments or substantial reworking of the DOM material, and therefore, was no longer identified as terrestrially-derived (Hedges et al., 1992). However, the vast majority of SGD-derived DOM was transported to the ocean, which acted as a sink and may contribute to carbon storage.

The null hypothesis cannot be accepted; there is a small portion of DOM that is susceptible to degradation, but this only accounted for about 1% of identified DOM components, which is within the error of the experiment. The EEMF-PARAFAC method is not sensitive enough to detect low levels of labile components when humic substances dominate. The residence time in the coastal ocean was too short to allow for significant photo-transformations of DOM within this zone.

7. General Discussion

7.1 Karst-channelled SGD in Kinvara Bay

SGD discharge from Karst aquifer systems can be greater than from other non-karst aquifers; this is largely because karst aquifers have a higher propensity to transport large fluxes of groundwater due to large channelled flow paths created by the dissolution of calcium carbonate rock (Ford and Williams, 2007; Fleury et al. 2007). For example, the 'ojos' (eyes, in Spanish) along the karstic Yucatan Peninsula (Mexico) coastline have been reported to discharge groundwater into the Gulf of Mexico on the order of 308 m^3 d^{-1} m^{-1} with peak discharge volumes of 568 m^3 d^{-1} m^{-1} (Null et al. 2014). Gonneea et al., (2014) estimated, using radium tracer balances, that SGD rates from the Yucatan Peninsula amounted to a more conservative 40 - 95 m^3 d^{-1} m^{-1}, however, even the most conservative value -40 $m^3d^{-1}m^{-1}$, as estimated by Gonneea et al., (2014), is still high relative compared to non-karst aquifers. Kinvara Bay and its associated catchment are relatively small in area with a total zone of contribution of 483.41 km^2 compared to the Yucatan Peninsula (165,000 km^2). However, the SGD discharge rates were still elevated, reaching up to 15 m^3 d^{-1} m^{-1} over the course of this study (Chapter 2) and may be attributed to the influence of meteoric recharge in combination with preferential flow paths in karst regions. Thus, this research provides further support for the capacity of karst aquifers to transport large fluxes of SGD to receiving water bodies.

Kinvara Bay on the west coast of Ireland can be thought of as a natural laboratory for the evaluation of the effects of watershed inputs via SGD on nutrient and carbon cycles of coastal zones for the following reasons. High regional precipitation rates, well-drained soils (Finch et al. 1971) and the absence of significant rivers or streams flowing into Kinvara Bay could render SGD the primary contributor of freshwater and associated materials to the coastal zone (Schubert et al. 2015). This was confirmed by results of the present study using combined ^{222}Rn and water and salt budgets to identify the loading of freshwater into the bay from all potential pathways as well as individual source contribution. During the high rainfall periods (i.e., January 2015), SGD accounted for 68% of freshwater discharge to the bay, but this increased to 100% during the summer low rainfall months (July 2013 and June 2015). Low variability of salinity was recorded over the full tidal cycle at the SGD springs in March 2015, indicating that the recycled seawater fraction in the SGD was low (between 0-6 ppt, *c.f.* Appendix E). A number of studies of groundwater discharge from karst systems have similarly observed a higher fraction of freshwater in SGD compared to non-karst systems. For example, fresh SGD accounted for 71 - 85 % of total SGD in a karstic coastal spring in Castello, Spain (Garcia-Solsona et al. 2010) and 75 ± 25% of the total SGD volume in Yucatan Peninsula, Mexico (Gonneea et al. 2014). Therefore, reactions with recirculated seawater within the subterranean estuary (Moore, 1999) are minimised and solutes may be transported directly to the coastal zone.

7.2 SGD-derived nutrient loading

Nitrate (NO_3^-) represents one of the most influential contaminants in karstic and porous groundwater systems (Einsiedl et al., 2010; Rocha et al., 2015). NO_3^- was the dominant DIN species in SGD in each of the four sampling campaigns conducted over a two-year period in Kinvara Bay, overwhelming other nutrient delivery pathways, such as sewage and atmospheric deposition. During the survey period, the NO_3^- concentration in the fresh groundwater endmember ranged from 62 μmol L^{-1} to 157 μmol L^{-1}, being lower during summer and higher during winter campaigns. These data add to research conducted by Rocha et al., (2015) and Cave and Henry, (2010), who also analysed nutrient levels in both Kinvara Bay and the groundwater endmember. As suggested by Smith and Cave (2012), the higher NO_3^- levels in groundwater during winter may be due to soil lixiviation under higher precipitation rates whilst a higher NO_3^- removal rate within the aquifer would explain the lower concentrations found in summer campaigns.

SGD as the primary source of allochthonous DIN loading to Kinvara Bay is in line with observations from other locations throughout the globe. For instance, Tait et al., (2014) conducted a nitrogen budget analysis of a tropical reef lagoon to assess the contribution arising from SGD, concluding that it accounted for the largest source of DIN to the lagoon, accounting for 81% of inputs. On a larger scale, Moore, (2010) shows how terrigenous NO_3^- delivered via SGD might be responsible for 56% of total N inputs to the Atlantic Ocean, making it larger than the combined contributions from atmospheric deposition, surface water discharge and runoff. Based on time-series monitoring at Parkmore Pier, the majority of allochthonous DIN was retained within the bay over all campaigns. SGD-borne DIN was thus intensively circulated on an annual basis. Sediment incubation experiments conducted in July 2013 in Kinvara Bay indicate that a significant proportion of the oxidised nitrogen may have been recycled through the benthos and released back into the water column in the reduced form, ammonia, via DNRA (Rocha et al., 2015). The results obtained in this current study for summer and winter campaigns are in line with this observation as less than 1% of the allochthonous loads were exported to the wider Galway Bay. However, sediment incubation experiments were not conducted in the winter campaigns. The sediment activity would differ between summer and winter due to lower temperatures and oxygen levels and shorter days (Porubsky et al., 2009; Giblin et al., 2013). Therefore, further characterisation of the biogeochemical status of Kinvara Bay should include sediment studies from each season.

The relationship between nutrients in solution (DRSi:N:P stoichiometric ratio) is important in ecological processes and greatly influences the structure, functioning and evolution of aquatic ecosystems (Turner et al., 1998; Sardans et al., 2012; Null et al., 2014). Variability in the stoichiometry of nutrient supply and the biological demand of a system are critical determinants of nutrient limitation for primary producers (Moore et al., 2013). Whether N or P is the limiting nutrient in the marine environment has been the subject of much debate (Smith, 1984; Howarth and

Marine, 2006). Some authors state that nitrogen is the limiting nutrient in marine primary productivity and is thus of great concern regarding eutrophication (Nixon, 1995; Gattuso et al., 1998; Howarth & Marino, 2006). Other authors allude to phosphorus being potentially the limiting nutrient for marine primary productivity in systems affected by large SGD inputs (Slomp and Van Cappellen, 2004). However, coastal systems differ significantly from deep marine waters due to the supply of terrestrial organic matter and nutrients (Buddemeier et al., 2002). Coastal systems that have been heavily loaded with nutrients can display P limitation, N limitation or co-limitation (Conley et al., 2009).

In areas of karst-channelled SGD, P limitation of primary production in receiving water bodies can occur due to the high absorption affinity of P for calcium carbonate (Slomp & Van Cappellen 2004), while inorganic nitrogen travels through aquifers with minimal physical retention, particularly through well-oxygenated karst aquifers, where the dominant N species are nitrate and nitrite (Capone & Bautista, 1985; Slomp & Van Cappellen, 2004). In coastal zones where SGD is important, groundwater-borne nutrient inputs can enhance variability of nutrient resource ratios made available to phytoplankton significantly, as the solute N:P ratios in watershed inputs are very dynamic in time and space. Not only did SGD introduce high nutrient loads into Kinvara bay, but also significantly changed the nutrient availability ratios in the receiving watermass because of the high fluxes of both N and Si and correspondingly low P fluxes. Since this study was conducted, plans to treat sewage to drinking water standards have come into effect in Kinvara Bay (as of 2017). Raw sewage accounted for 72% of allochthonous TDP inputs during this study, and hence, removal of the main allochthonous P source may further drive Kinvara Bay into a state of P limitation. This is in line with research in other karst systems (e.g. Garcia-Solsona et al., 2010), such as the aquifer to the Messiniakos Gulf, SE Ionian Sea (Pavlidou et al., 2014). Kim et al., (2011) measured high and variable N:P ratios in SGD delivered to coastal embayments of Hwasun Bay and Bangdu Bay, Korea.

Nutrient enrichment may lead to altered biogeochemical functioning and biological community structure of coastal waters (Cloern, 2001) as high nutrient loading favours growth of phytoplankton that are capable of assimilating these nutrients efficiently. The biodiversity shift promotes the growth of opportunistic pelagic macroalgae, such as *Enteromorpha*. The dominance of algae can accumulate as thick mats over the sessile community or sediment surface which suppresses light availability to the underlying community (McGlathery et al., 2007). Low diversity algal or cyanobacterial blooms can then form which results in surface water hypoxia and release of toxic compounds. Therefore, there is a community shift to a lower number of tolerant species (Erisman et al., 2013). Mass accumulations of macroalgae have characteristic bloom and die-off cycles (Board et al., 2000). Eutrophication lowers the availability of Si, which results in a loss of diatoms from the community (Conley et al., 1993). The loss of diatoms has a profound effect on energy

flow through the food web (Turner et al., 1998). This biodiversity shift from benthic to pelagic primary production introduces significant diurnal variations in oxygen concentration in the water column (Herbert 1999) and is known to suffocate bivalves and cause die-off due to depleted oxygen levels (Dennison et al., 1993). As the solute and species composition of coastal ecosystems change, the biogeochemical function will also be altered. Nutrient limitation can eventually lead to growth constraints in the phytoplankton community and stoichiometric changes in phytoplankton biomass (Klausimeier et al., 2004). Thus, this would reduce the net retention and buffering capacity of the bay allowing more N to be transported downstream to the wider Galway Bay. Many studies have shown that a reduction in P has led to eutrophication problems downstream (Conley et al., 2009). The consequences of removing the main allochthonous source of P in Kinvara Bay without concomitant N reduction in SGD on the makeup and structure of the autotrophic populations thus are not yet known (Rocha et al., 2015).

In this study, nitrogen loading to Kinvara Bay was coupled with increased primary producer biomass at the SGD sites and may indicate early signs of the onset of eutrophication (Chapters 2 and 5). As seen from the future scenarios (Chapter 5) an increase in macroalgae abundance may also result in larger fluxes of bioavailable CDOM effluxed to the water column from the benthos and the macroalgae itself. Combining this with N enrichment through SGD may have significant implications on the productivity within the bay. As eutrophication progresses, toxic algal blooms, in particular of dinoflagellates would likely increase in Kinvara Bay (Rocha et al., 2015). The accumulation of HAB-derived toxins may have serious adverse consequences on the shellfish harvested within the bay. This could have detrimental effects to the fishermen in Kinvara Bay who rely on shellfish farms for their livelihood. In order to protect the coastal zone, the appropriate nutrient management strategy must be developed. N and P are most often selected for dual-nutrient management strategies as they are both required to support plant growth and are key limiting nutrients (Howarth and Marino, 2006; Paerl, 2009). Dual-nutrient management strategies have been called for in the EU Water Framework Directive and for many coastal systems in the United States (NRC, 2000).

7.3 Carbon inputs and circulation in Kinvara Bay

SGD can export substantial carbon loads into receiving waters; for example, Dorsett et al., (2011) estimated that SGD associated with karst and other carbonate systems accounts for 7 - 11% of global coastal water DIC. However, this facet is frequently neglected by marine scientists (Porubsky et al., 2014). The current study aimed to contribute to the current knowledge of carbon cycle dynamics by closing a data gap in understanding the impact of SGD on the carbon cycle of a small coastal embayment in Ireland that lacks significant surface water inputs. In Kinvara Bay, SGD accounted for more than 90% of allochthonous DOC and DIC inputs and was thus the dominant source of carbon into the system. DIC concentrations were elevated in groundwater

compared to seawater, but DOC levels were comparable, in line with observations in similar systems elsewhere (e.g. Cai & Wang 1998; Cai et al., 2003; Porubsky et al., 2014). Karst aquifers often have a higher porosity compared to non-karst aquifers due to calcium carbonate dissolution (Fleury et al., 2007). Dissolution from the low pH SGD causes elevated DIC loads associated with SGD from carbonate aquifers. As groundwater flows through the zone of contribution (483.41 km^2) of the Gort-Kinvara aquifer, groundwater is in contact with the carbonate aquifer allowing for accumulation of DIC materials. Thus, higher DIC concentration in groundwater in Kinvara can be attributed to the karst geology of the Gort-Kinvara aquifer, as shown in other karst systems (e.g. Liu et al., 2014; Szymczycha et al., 2014).

Anthropogenic loading of CO_2 in the context of global warming has become a major concern in oceanic studies as the open ocean has been shown to act as a C sink (Doney et al., 2009). The rate of current and projected atmospheric CO_2 increase is about 100 times faster than has occurred over the past 650,000 years and the rising atmospheric CO_2 levels are irreversible on human timescales (Royal Society, 2005). Ireland ranks second in the E.U. and thirty-seventh in the world rankings of highest CO_2 emission per capita (C.S.O., 2012). The first Land Ocean Interactions in the Coastal Zone (LOICZ) report asserted that whether coastal seas were net CO_2 sinks or sources could not be determined (Kempe, 1995). Net ecosystem metabolism was shown to be a net CO_2 sink through primary production in coastal zones worldwide (Smith and Hollibaugh, 1993), while organic matter discharging into the coastal zone may lead to increased respiration, acting as a net CO_2 source (Hung and Kuo, 2002). There is now evidence supporting the theory that the open ocean is a net sink for CO_2 (Chen and Borges 2009), while most estuaries and near-shore coastal areas are a net source of CO_2 (Fagan and Mackenzie, 2007; Chen and Borges, 2009). On average, inner estuaries are said to be net heterotrophic and account for 0.36 Pg C yr^{-1} of CO_2 emissions worldwide (Chen and Borges, 2009). However, the heterogeneity of the coastal ocean makes global estimates difficult and these often contain significant errors (Smith and Hollibaugh, 1993). Kinvara Bay was net heterotrophic during the wettest sampling campaign (January 2015) but net autotrophic for all other sampling periods reported on here. Most near-shore ecosystems act as CO_2 sources due to the degradation of organic carbon (Gattuso et al., 1998). However, OM inputs associated with SGD were largely refractory during this study. The net heterotrophy during the January 2015 campaign may have been sustained by elevated loading of dissolved organic matter (DOM) (Chen and Borges, 2009) associated with the highest fluxes of SGD (Chapter 4). However, anthropogenic pressure may cause an increased proportion of labile material to be incorporated in SGD-borne DOM (Ibánhez et al., 2017), which could switch Kinvara Bay to a heterotrophic dominated system. However, Ver et al., (1999) showed that DOM inputs may drive further production and storage, shifting the system to autotrophy. Thus, carbon cycle dynamics in Kinvara Bay may thus shift rapidly in terms of the autotrophy-heterotrophy pattern, which is in agreement with other study sites (Borges et al., 2010).

Groundwater is enriched in CO_2 due to organic carbon degradation within the aquifer (Gagan et al., 2002). The difference between atmospheric pCO_2 and groundwater pCO_2 may be in part due to DIC redistribution with CO_2 degassing, CO_2 trapping by carbonate mineral precipitation and other aquifer solids precipitation adjusting the pH (Macpherson, 2009). The pH of SGD in Kinvara Bay (7.07 – 7.47; Chapter 3) was consistently lower than oceanic pH, which allowed a greater potential for pCO_2 efflux from this source. Due to the large temporal and spatial variations of pCO_2, this study acts as a time stamp of the current impact of SGD on the carbon cycle under these sampling campaigns. Longer-term modelling of Kinvara Bay would be required to better constraint the carbon cycle.

An increase of CO_2 dissolved in the ocean may lower the pH, decrease the availability of carbonate ions and lower the saturation state of shell forming carbonate minerals, in a process known as ocean acidification (OA) (Kleypas et al., 2005). Studies conducted to date have opposing views on the effects of SGD on the acidification of coastal surface waters into which they discharge (Lee & Kim 2015; Liu et al., 2017). SGD delivers large quantities of DIC which may drive ocean acidification (Cyronak et al., 2014), although, this is in tandem with large fluxes of total alkalinity (TAlk), which buffer against acidification (Cyronak et al., 2013). Studies that monitor OA parameters in Irish estuarine and coastal waters and the likely effects of OA on local environments and ecosystems, as well as contribute to the global pool of inorganic carbon data are limited (McGrath et al., 2015). As Kinvara Bay hosts shellfish farms, a significant source of revenue to the local community, the importance of carbonate system studies cannot be overstated. The SGD-DIC flux was lower than the total alkalinity (TAlk) flux in each sampling campaign (Chapter 3) in Kinvara Bay, which indicates that SGD may act as a buffer against acidification in this system (Liu et al., 2017).

Coastal phytoplankton blooms can modify pH significantly (Dai et al., 2008) while benthic microbial processes influence pH and alkalinity through sediment-water exchange in coastal zones (Cyronak et al., 2013). Eutrophication, due to high nutrient loading, enhances the growth of opportunistic algae. Algal beds draw down CO_2, potentially offsetting the impacts of ocean acidification by increasing the pH (Anthony et al., 2011). Large inputs of nutrients from SGD impacted productivity within Kinvara Bay classifying the bay as mesotrophic. Rocha et al., (2015), however, classified the bay as eutrophic during their four summer campaigns due to higher N loads associated with their study. A linear relationship between TAlk and DIC showed that the biological to geochemical ratio of DIC flux was 2.03 and that metabolism accounted for 65% of DIC removal during the June 2015 campaign. Thus, pH increases in Kinvara Bay can be explained by biological production enhanced by SGD-driven DIN during this campaign, as observed by Lee and Kim, (2015) in Hwasun Bay, Korea. Other studies have also shown that metabolic activity plays a significant role in controlling the pH of coastal systems (Gattuso et al., 1998; Anthony et al., 2011)

as carbon can be cycled by means of the so-called "biological pump" (Kempe, 1996). Changes in the nutrient loading associated with SGD may thus lead to long-term changes in CO_2 sequestration. Studies that incorporate both nutrient and carbon studies are required to provide a full picture of the impact of SGD on the carbon cycle.

This study shows that during high SGD flows the pH in Kinvara Bay waters was lower due to the greater influence of low pH associated with SGD. As climate change will bring wetter seasons, SGD rates into Kinvara Bay are expected to increase, which may have important implications for the future evolution of the whole-system metabolism of Kinvara Bay and may have serious consequences on the economic value of the bay. Under wetter conditions, SGD may lower the pH of the bay during the growing season of summer and have a detrimental impact on shellfish growing here. Furthermore, the DIC in surface water may increase due to climate change (feely et al., 2004), causing further increases in DIC fluxes in karst regions such as Kinvara bay, which may lower the buffering potential of SGD. This may cause a decrease in $CaCO_3$ saturation state, which may lead to carbonate shell dissolution, which is a serious consequence of acidification in a shellfish region, such as Kinvara Bay.

Gazeau et al., (2007) studied calcification rates of shellfish; the edible mussel (*Mytilus edulis*) and Pacific Oyster (*Crassostrea gigas*), collected in the Scheldt estuary over a range of present and reduced pH conditions of 7.46 – 8.13. The calcification rates of these shellfish exhibited a strong decline as a function of decreasing pH, increasing pCO_2 and decreasing $[CO_3^{2-}]$. They concluded that mussels dissolve at pCO_2 values exceeding 1,800 ppmV and that the calcification rates of mussels would decrease by 25% and of oysters of 10% under the IPCC IS92a future scenario of 740 ppmV by 2100. Small changes in pH could have large impacts on the shellfish harvested in Kinvara Bay. In general, mussels and oysters are an important part of coastal ecosystems governing energy and nutrient flows (Gazeau et al., 2007). Thus, in order to assess the potential socio-economic and ecological impacts of acidification within Kinvara Bay it is urgent to investigate the adaptive response of the Blue mussel (*Mytilus edulis*), the non-native Pacific oyster (*Crassostrea gigas*), the European flat oyster (*Ostrea edulis*) and clam (*Ruditapes philippinarum*), grown commercially in the bay, to long-term CO_2 enrichment. A decline in these species may have serious consequences on Kinvara Bay in terms of coastal biodiversity and ecosystem functioning. This study informs coastal zone managers that monitoring of the pH level of the bay is a serious concern. This research suggests that it may be necessary for coastal zone managers to assess the current status of bays worldwide and the projected implications of global warming to implement meaningful carbon management strategies.

7.4 Further studies

SGD acts as a link between the marine and terrestrial eco-compartments and understanding the current state of this transport link is vital to better evaluate CNP budgets in order to mitigate anthropogenic pressures in coastal zones. As karst and carbonate coastal systems constitute up to 25% of the world's coastline (Williams and Ford, 2006), particular focus should be given to karst-channelled SGD in the future. The remedial action of the aquifer is minimised due to the rapid transport afforded by these systems, and therefore studies of these systems are critical.

7.4.1 CNP budgets

There are many processes within the aquifer influencing the chemical makeup of SGD in terms of DIC and TAlk. Combining DIC concentration fluxes with stable isotope data would allow greater inference about the processes occurring *en route* to the coast that may influence the chemical makeup of SGD. In particular, sulphide reduction is known to increase TAlk concentrations (Wolf-Gladrow et al., 2007). The uncoupling of sulphate reduction from sulphide oxidation would generate carbonate alkalinity with a depleted $\delta^{13}C$ value due to the organic C source, perhaps accounting for the depleted $\delta^{13}C$ DIC values found in the groundwater (Ku et al., 1999). Thus, isotope analysis may better elucidate carbon cycling in groundwater within the flow path. The relative contributions of DIC and TAlk to groundwater can determine the impact of SGD on acidification within the coastal zone.

The budgets presented in this study were based on the two primary flow regimes characteristic of karst systems, which correspond to summer and winter. Obtaining quantitative budgets for the four seasons would provide information on the changes in land use and its impact on the composition of SGD. Agricultural activities increase during spring and summer, and fertiliser runoff may occur in autumn due to the higher precipitation rates. As highlighted in Chapter 4, labile materials in the form of protein-like components were transported to Kinvara Bay via SGD during late spring. An annual analysis would be appropriate to fully understand the effects of SGD-borne carbon and nutrients on the coastal zone.

7.4.2 Component identification

Black carbon (BC) has been shown to be a major compound group in groundwater of Kinvara Bay as it comprises 4 - 5% of SGD at the Castle and 12% at the Arch discharge sites measured using FT-ICR-MS in September 2014. Little evidence exists for the presence of BC in groundwaters worldwide; this may be due to difficulty in identification. Fourier-transform ion cyclotron resonance mass spectrometry (FT-ICR-MS) is a powerful technique that allows for elemental fingerprinting. However, EEMF-PARAFAC is the more common method used for CDOM analysis. Identification of the chromophoric properties regarding its peak position in EEMF would allow future studies to determine its presence in coastal zones globally more readily. Black carbon

is known to be a major sink in the C cycle. Therefore, it is essential that C cycle studies incorporate this compound group.

Understanding the removal mechanisms for refractory carbon within the oceans is an important question globally. This pool is known to have longer residence times and be removed more slowly, the mechanisms of which are still unresolved (Kempe 1996). The residence time of SGD in Kinvara Bay is 6.8 ± 1.7 days (Rocha et al. 2015), and thus, these mechanisms may not occur during the transit path. Longer incubation studies under different natural conditions may elucidate degradation pathways of SGD-DOM in the ocean.

7.4.3 Future CDOM scenarios

Future scenarios outlined in this thesis highlight the importance of global warming and land use change on the functionality and quality of SGD within the coastal zone. In these future scenarios, more labile components may be released to the coast. Therefore, analysis and continual monitoring of Kinvara Bay and coastal zones worldwide are essential to prevent eutrophication and algal blooms. The *Fucus* treatment released more DOC than the *Enteromorpha* treatment but *Enteromorpha* released more CDOM. Therefore, it was concluded that a larger portion of the DOC released from Fucus was non-fluorescing. FT-ICR-MS analyses could be implemented in future scenario studies to determine how the type of DOC effluxed could be impacted.

7.4.4 FT-ICR-MS

This study focused on the impact of SGD within the coastal zone through *in-situ* sampling and incubation studies. Although the transport time through the aquifer is short, approximately one week (McCormack et al. 2014), studies of groundwater in transit may better elucidate the DOM components contained in SGD. During this study, some labile materials were present in peaty areas of the catchment. Studying groundwater in transit will determine if their removal is due to dilution or processes occurring along the flow path.

Seasonally variability due to temperature and land use changes would allow precise identification of the annual processes impacting Kinvara Bay. EEMF-PARAFAC analysis showed that there are protein-like peaks in EEMs in late spring; this was attributed to fertiliser runoff. FT-ICR-MS of samples collected during this time would allow for identification of fertiliser peaks, which could be used as pointers for productivity within the bay as these labile components are quickly consumed and/or diluted as such peaks are not present at any time of the year at the exit point.

References

Abril, G., Etcheber H., Borges A.V. and Frankignoulle, M., 2000. Excess atmospheric carbon dioxide transported by rivers into the Scheldt estuary. *Comptes Rendus de l'Académie des Sciences - Series IIA - Earth and Planetary Science*, *330*(11), pp.761–768.

Abril, G. and Frankignoulle, M., 2001. Nitrogen–alkalinity interactions in the highly polluted scheldt basin (belgium). *Water Research*, *35*(3), pp.844–850.

Abril, G., Nogueira, M., Etcheber, H., Lemaire, E. and Brogueira, M.J., 2002. Behaviour of organic carbon in nine contrasting European estuaries. *Estuarine, Coastal and Shelf Science*, *54*(2), pp.241–262.

Abril, G. and Borges, A.V., 2005. Carbon dioxide and methane emissions from estuaries. In *Greenhouse Gas Emissions—Fluxes and Processes*. (pp. 187-207). Springer Berlin Heidelberg.

Aherne, J. and Farrell, E.P., 2002. Deposition of sulphur, nitrogen and acidity in precipitation over Ireland: chemistry, spatial distribution and long-term trends. *Atmospheric Environment*, *36*(8), pp.1379–1389.

Ahmad, S.R. and Reynolds, D.M., 1999. Monitoring of water quality using fluorescence technique: prospect of on-line process control. *Water Research*, *33*(9), pp.2069–2074.

Algesten, G., Brydsten, L., Jonsson, P., Kortelainen, P., Löfgren, S., Rahm, L., Räike, A., Sobek, S., Tranvik, L., Wikner, J. and Jansson, M., 2006. Organic carbon budget for the Gulf of Bothnia. *Journal of Marine Systems*, *63*(3–4), pp.155–161.

Almeida, C. and Silva, M.L., 1987. Incidence of agriculture on water quality at Campina de Faro (south Portugal). In *IV Simposio de Hidrogeología de la Asociación Española de Hidrología Subterránea, Palma de Mallorca* (Vol 5).

Andersen, C.M. and Bro, R., 2003. Practical aspects of PARAFAC modeling of fluorescence excitation-emission data. *Journal of Chemometrics*, *17*(4), pp.200–215.

Amado, A. M., Farjalla, V. F., Esteves, F. D. A., Bozelli, R. L., Roland, F., and Enrich-Prast, A., 2006. Complementary pathways of dissolved organic carbon removal pathways in clear-water Amazonian ecosystems: photochemical degradation and bacterial uptake. *FEMS Microbiology Ecology*, *56*(1), pp.8–17.

Andersson, A.J. and Gledhill, D., 2013. Ocean Acidification and Coral Reefs: Effects on Breakdown, Dissolution, and Net Ecosystem Calcification. *Annual Review of Marine Science*, *5*(1), pp.321–348.

Andrady, A.L., 2011. Microplastics in the marine environment. *Marine Pollution Bulletin*, *62*(8), pp.1596–1605.

Anesio, A.M., Granéli, W., Aiken, G.R., Kieber, D.J. and Mopper, K., 2005. Effect of humic substance photodegradation on bacterial growth and respiration in lake water. *Applied and environmental microbiology*, *71*(10), pp.6267-6275.

Anthony, K.R.N., Kleypas, A. J. and Gattuso, J.-P., 2011. Coral reefs modify their seawater carbon chemistry – implications for impacts of ocean acidification. *Global Change Biology*, *17*(12), pp.3655–3666.

Arnott, D.L. and Vanni, M.J., 1996. Nitrogen and phosphorus recycling by the zebra mussel (Dreissena polymorpha) in the western basin of Lake Erie. *Canadian Journal of Fisheries and Aquatic Sciences*, *53*(3), pp.646-659.

Arstegui, J. & Harrison, W.G., 2002. Decoupling of primary production and community respiration in the ocean: implications for regional carbon studies. *Aquatic Microbial Ecology*, *29*(2), pp.199–209.

Artinger, R., Buckau, G., Geyer, S., Fritz, P., Wolf, M., and Kim, J. I., 2000. Characterization of groundwater humic substances: influence of sedimentary organic carbon. *Applied Geochemistry*, *15*(1), pp.97–116.

Atekwana, E.A. and Krishnamurthy, R.V., 1998. Seasonal variations of dissolved inorganic carbon and δ13C of surface waters: application of a modified gas evolution technique. *Journal of Hydrology*, *205*(3–4), pp.265–278.

Atkins, M.L., Santos I.R., Ruiz-Halpem, and Maher, D.T., 2013. Carbon dioxide dynamics driven by groundwater discharge in a coastal floodplain creek. *Journal of Hydrology*, *493*, pp.30–42.

Atkinson, M.J. and Smith, S.V., 1983. C: N: P ratios of benthic marine plants. *Limnology and Oceanography*, *28*(3), pp.568–574.

Azam, F., Fenchel, T., Field, J.G., Gray, J.S., Meyer-Reil, L.A. and Thingstad, F., 1983. The ecological role of water-column microbes in the sea. *Marine ecology progress series*, pp.257-263.

Baghoth, S. A., Maeng, S. K., Rodriguez, S. S., Ronteltap, M., Sharma, S., Kennedy, M., and Amy, G. L., 2008. An urban water cycle perspective of natural organic matter (NOM): NOM in drinking water, wastewater effluent storm water, and seawater. *Water Science & Technology: Water Supply*, *8*(6). pp. 701-707

Baker, A. and Spencer, R.G.M., 2004. Characterization of dissolved organic matter from source to sea using fluorescence and absorbance spectroscopy. *Science of The Total Environment*, *333*(1–3), pp.217–232.

Baker, A., Inverarity, R., Charlton, M., and Richmond, S., 2003. Detecting river pollution using fluorescence spectrophotometry: case studies from the Ouseburn, NE England. *Environmental Pollution*, *124*(1), pp.57–70.

Baker, A., 2002. Spectrophotometric discrimination of river dissolved organic matter. *Hydrological Processes*, *16*(16), pp.3203–3213.

Baker, A. and Spencer, R.G.M., 2004. Characterization of dissolved organic matter from source to sea using fluorescence and absorbance spectroscopy. *Science of The Total Environment*, *333*(1–3), pp.217–232.

Baker, A. and Genty, D., 1999. Fluorescence wavelength and intensity variations of cave waters. *Journal of Hydrology*, *217*(1–2), pp.19–34.

Baldock, J.A. and Smernik, R.J., 2002. Chemical composition and bioavailability of thermally altered Pinus resinosa (Red pine) wood. *Organic Geochemistry*, *33*(9), pp.1093–1109.

Barnes, D. K., Galgani, F., Thompson, R. C., and Barlaz, M., 2009. Accumulation and fragmentation of plastic debris in global environments. *Philosophical Transactions of the Royal Society B: Biological Sciences*, *364*(1526), pp.1985–1998.

Basterretxea, G., Tovar-Sanchez A., Beck A.J. and Masque P., 2010. Submarine groundwater discharge to the coastal environment of a Mediterranean island (Majorca, Spain): ecosystem and biogeochemical significance. *Ecosystems*, *13*(5), pp.629–643.

Bates, N. R., Best, M.H.P., Neely, K., Garley, R., Dickson, A.G. and Johnson, R.J., (2012) 'Detecting anthropogenic carbon dioxide uptake and ocean acidification in the North Atlantic Ocean', *Biogeosciences*, 9(7), pp. 2509–2522.

Bauer, J.E., Cai, W.J., Raymond, P.A., Bianchi, T.S., Hopkinson, C.S. and Ragnier, P., 2013. The changing carbon cycle of the coastal ocean. *Nature*, *504*(7478), pp.61–70.

Becher, G., Moghissl, A.A., Senesi, N., Sakellarladou, F., Bishop, K., Pettersson, C., Allard, B., Lee, Y.H., Hargitai, L., Akerback, N. and Holmbom, B., 1994. The Fourth Nordic Symposium on Humic Substances Degradation of humic substances by UV irradiation. *Environment International*, *20*(1), pp.97–101.

Beck, A. J., Tsukamoto, Y., Tovar-Sanchez, A., Huerta-Diaz, M., Bokuniewicz, H. J., and Sanudo-Wilhelmy, S. A. 2007. Importance of geochemical transformations in determining submarine groundwater discharge-derived trace metal and nutrient fluxes. *Applied Geochemistry*, *22*(2), pp.477–490.

Beck, A.J., Cochran, J.K. and Sañudo-Wilhelmy, S.A., 2010. The distribution and speciation of dissolved trace metals in a shallow subterranean estuary. *Marine Chemistry*, *121*(1), pp.145–156.

Benner, R., Chin-Leo, G., Gardner, W., Eadie, B., and Cotner, J. 1992. The fates and effects of riverine and shelf-derived DOM on Mississippi River plume/Gulf shelf processes. *Nutrient Enhanced Coastal Ocean Productivity. Publication Number TAMU-SG-92-109, Sea Grant Program, Texas A&M University, Galveston, Texas*, pp.84–94.

Benner, R. and Kaiser, K., 2011. Biological and photochemical transformations of amino acids and lignin phenols in riverine dissolved organic matter. *Biogeochemistry*, 1*02*(1-3), pp.209–222.

Benner, R., 2002. Chemical Composition and Reactivity. In *Hansell DA, Carlson CA, editors. Biogeochemistry of Marine Organic Matter*. Academic Press, pp. 56–90.

Bergström, L., 2005. *Macroalgae in the Baltic Sea: responses to low salinity and nutrient enrichment in Ceramium and Fucus*. PhD Thesis. Ekologi och geovetenskap.

Berner, R.A., 2004. *The Phanerozoic carbon cycle: CO2 and O2*, Oxford University Press Oxford.

Berner, R.A., 1992. Weathering, plants, and the long-term carbon cycle. *Geochimica et Cosmochimica Acta*, *56*(8), pp.3225–3231.

Berner, R.A., Lasaga, A.C. and Garrels, R.M., 1983. The carbonate-silicate geochemical cycle and its effect on atmospheric carbon dioxide over the past 100 million years. *American Journal of Science*, *283*(7), pp.641–683.

Bertilsson, S. and Jones, J.B., 2003. Supply of dissolved organic matter to aquatic ecosystems: autochthonous sources. *Aquatic ecosystems: interactivity of dissolved organic matter*, pp.3–24.

Bertilsson, S. and Tranvik, L.J., 2000. Photochemical transformation of dissolved organic matter in lakes. *Limnology and Oceanography*, *45*(4), pp.753–762.

Bertuzzi, A., Faganeli, J., Welker, C. and Brambati, A., 1997. Benthic fluxes of dissolved inorganic carbon, nutrients and oxygen in the Gulf of Trieste (Northern Adriatic). *Water, Air, and Soil Pollution*, *99*(1-4), pp.305-314.

Bhatia, M. P., Das, S. B., Longnecker, K., Charette, M. A., and Kujawinski, E. B., 2010. Molecular characterization of dissolved organic matter associated with the Greenland ice sheet. *Geochimica et Cosmochimica Acta*, *74*(13), pp.3768–3784.

Bidle, K.D. and Azam, F., 1999. Accelerated dissolution of diatom silica by marine bacterial assemblages. *Nature*, *397*(6719), pp.508–512.

Bieroza, M., Baker, A. and Bridgeman, J., 2012. Exploratory analysis of excitation–emission matrix fluorescence spectra with self-organizing maps—A tutorial. *Education for Chemical Engineers*, *7*(1), pp.e22–e31.

BIM—Bord Iascaigh Mhara., 2012. Environmental impact statement (EIS) for deep sea fish farm development in Galway Bay. Co. Galway, Galway, p 324

Björnsäter, B. R., and Wheeler, P. A., 1990. 'EFFECT OF NITROGEN AND PHOSPHORUS SUPPLY ON GROWTH AND TISSUE COMPOSITION OF ULVA FENESTRATA AND ENTEROMORPHA INTESTINALIS (ULVALES, CHLOROPHYTA)', *Journal of Phycology*, 26(4), pp. 603–611. doi: 10.1111/j.0022-3646.1990.00603.

Blackburn, T. H., and Blackburn, N. D., 1992. 'Model of nitrification and denitrification in marine sediments', *FEMS Microbiology Letters*, 100(1–3), pp. 517–521. doi: 10.1111/j.1574-6968.1992.tb14086.x.

Board, O. S., Council, N. R. and others (2000) Clean coastal waters: understanding and reducing the effects of nutrient pollution. National Academies Press.

Borges, A.V. and Abril, G., 2010. Carbon dioxide and methane dynamics in estuaries. In *EGU General Assembly Conference Abstracts*. (Vol. 12 p. 10812. 2010)

Borges, A.V., Alin, S.R., Chavez, F.P., Vlahos, P., Johnson, K.S., Holt, J.T., Balch, W.M., Bates, N., Brainard, R., Cai, W.J. and Chen, C.T.A., 2010. A global sea surface carbon observing system: inorganic and organic carbon dynamics in coastal oceans.

Boehm, A. B., Paytan, A., Shellenbarger, G. G., and Davis, K. A., 2006. Composition and flux of groundwater from a California beach aquifer: Implications for nutrient supply to the surf zone. *Continental Shelf Research*, *26*(2), pp.269–282.

Bousquet, P., Gaudry, A., Ciais, P., Kazan, V., Monfray, P., Simmonds, P.G., Jennings, S.G. and O'Connor, T.C., 1996. Atmospheric CO2 concentration variations recorded at Mace Head, Ireland, from 1992 to 1994. *Physics and Chemistry of the Earth*, *21*(5-6), pp.477-481.

Bouwman, A.F., Beusen, A.H.W. and Billen, G., 2009. Human alteration of the global nitrogen and phosphorus soil balances for the period 1970–2050. *Global Biogeochemical Cycles*, *23*(4), p.GB0A04.

Bown, P. R., Lees, J. A. and Young, J. R., 2004. 'Calcareous nannoplankton evolution and diversity through time', in Thierstein, H. R. and Young, J. R. (eds) *In: Thierstein, HR and Young, JR, (eds.) UNSPECIFIED (481 - 508). SPRINGER-VERLAG BERLIN (2004)*. SPRINGER-VERLAG BERLIN, pp. 481–508.

Bradley, P.B., Lomas, M.W. and Bronk, D.A., 2010. Inorganic and Organic Nitrogen Use by Phytoplankton Along Chesapeake Bay, Measured Using a Flow Cytometric Sorting Approach. *Estuaries and Coasts*, *33*(4), pp.971–984.

Brandes, M., 1978. Characteristics of Effluents from Gray and Black Water Septic Tanks. *Journal (Water Pollution Control Federation)*, *50*(11), pp.2547–2559.

Brewer, P. G. and Goldman, J. C., 1976. 'Alkalinity changes generated by phytoplankton growth1', *Limnology and Oceanography*, 21(1), pp. 108–117. doi: 10.4319/lo.1976.21.1.0108.

Bricaud, A., Morel, A. and Prieur, L., 1981. 'Absorption by dissolved organic matter of the sea (yellow substance) in the UV and visible domains', *Limnology and oceanography*, 26(1), pp. 43–53.

Bricker, S.B., Longstaff, B., Dennison, W., Jones, A., Boicourt, K., Wicks, C. and Woerner, J., 2008. Effects of nutrient enrichment in the nation's estuaries: a decade of change. *Harmful Algae*, *8*(1), pp.21-32.

Brinkmann, T., Hörsch, P., Sartorius, D., and Frimmel, F. H., 2003. Photoformation of Low-Molecular-Weight Organic Acids from Brown Water Dissolved Organic Matter. *Environmental Science & Technology*, *37*(18), pp.4190–4198.

Bronk, D. A., See, J. H., Bradley, P., and Killberg, L., 2007. DON as a source of bioavailable nitrogen for phytoplankton. *Biogeosciences*, *4*(3), pp.283–296.

Brunet, F., Gaiero, D., Probst, J. L., Depetris, P. J., Gauthier Lafaye, F., and Stille, P., 2005. δ13C tracing of dissolved inorganic carbon sources in Patagonian rivers (Argentina). *Hydrological processes*, *19*(17), pp.3321–3344.

Brzezinski, M. A., Dickson, M. L., Nelson, D. M., and Sambrotto, R. 2003. Ratios of Si, C and N uptake by microplankton in the Southern Ocean. *Deep Sea Research Part II: Topical Studies in Oceanography*, *50*(3), pp.619–633.

Bulger, A. J., Hayden, B. P., Monaco, M. E., Nelson, D. M., and McCormick-Ray, M. G., 1993. Biologically-based estuarine salinity zones derived from a multivariate analysis. *Estuaries*, *16*(2), pp.311–322.

Burnett, W. C., Peterson, R., Moore, W. S., and de Oliveira, J., 2008. Radon and radium isotopes as tracers of submarine groundwater discharge – Results from the Ubatuba, Brazil SGD assessment intercomparison. *Estuarine, Coastal and Shelf Science*, *76*(3), pp.501–511.

Burnett, W.C., Aggarwal, P.K., Aureli, A., Bokuniewicz, H., Cable, J.E., Charette, M.A., Kontar, E., Krupa, S., Kulkarni, K.M., Loveless, A. and Moore, W.S., 2006. Quantifying submarine groundwater discharge in the coastal zone via multiple methods. *Science of the Total Environment*, *367*(2), pp.498–543.

Burnett, W.C. and Dulaiova, H., 2003. Estimating the dynamics of groundwater input into the coastal zone via continuous radon-222 measurements. *Journal of Environmental Radioactivity*, *69*(1–2), pp.21–35.

Burnett, W.C., Bokuniewicz, H., Huettel, M., Moore, W.S. and Taniguchi, M., 2003. Groundwater and pore water inputs to the coastal zone. *Biogeochemistry*, *66*(1-2), pp.3–33.

Burnett, W.C., Taniguchi, M. and Oberdorfer, J., 2001. Measurement and significance of the direct discharge of groundwater into the coastal zone. *Journal of Sea Research*, *46*(2), pp.109–116.

Burnett, W., Kim, G. and Lane-Smith, D., 2001. A continuous monitor for assessment of 222Rn in the coastal ocean. *Journal of Radioanalytical and Nuclear Chemistry*, *249*(1), pp.167–172.

Bushaw-Newton, K.L., Kreeger, D.A., Doaty, S. and Velinsky, D.J., 2008. Utilization of Spartina- and Phragmites-derived dissolved organic matter by bacteria and ribbed mussels (Geukensia demissa) from Delaware Bay salt marshes. *Estuaries and Coasts*, *31*(4), pp.694–703.

Bushaw-Newton, K.L. and Moran, M.A., 1999. Photochemical formation of biologically available nitrogen from dissolved humic substances in coastal marine systems. *Aquatic Microbial Ecology*, *18*(3), pp.285–292.

Bussmann, I., 1999. Bacterial utilization of humic substances from the Arctic Ocean. *Aquatic microbial ecology*, *19*(1), pp.37–45.

Cadée, G.C., 1982. Tidal and seasonal variation in particulate and dissolved organic carbon in the western dutch Wadden Sea and Marsdiep tidal inlet. *Netherlands Journal of Sea Research*, *15*(2), pp.228–249.

Cai, W.J., Hu, X., Huang, W.J., Murrell, M.C., Lehrter, J.C., Lohrenz, S.E., Chou, W.C., Zhai, W., Hollibaugh, J.T., Wang, Y. and Zhao, P., 2011. Acidification of subsurface coastal waters enhanced by eutrophication. *Nature Geoscience*, *4*(11), pp.766–770.

Cai, W.-J., 2011. Estuarine and Coastal Ocean Carbon Paradox: CO2 Sinks or Sites of Terrestrial Carbon Incineration? *Annual Review of Marine Science*, *3*(1), pp.123–145.

Cai, W.-J.,Wang Y., Krest J. and Moore W.S., 2003. The geochemistry of dissolved inorganic carbon in a surficial groundwater aquifer in North Inlet, South Carolina, and the carbon fluxes to the coastal ocean. *Geochimica et Cosmochimica Acta*, *67*(4), pp.631–639.

Cai, W-J., Guo X., Chen C.-T.A, Dai M., Zhang L., Zhai W., Lohrenz S.E., Yin K., Harrison P.J. and Wang Y., 2008. A comparative overview of weathering intensity and HCO3 flux in the world's major rivers with emphasis on the Changjiang, Huanghe, Zhujiang (Pearl) and Mississippi Rivers. *Continental Shelf Research*, *28*(12), pp.1538–1549.

Cai W-J. and Wang Y., 1998. The chemistry, fluxes, and sources of carbon dioxide in the estuarine waters of the Satilla and Altamaha Rivers, Georgia. , *43*(4), pp.657–668.

Cao, L. and Caldeira, K., 2008. Atmospheric CO2 stabilization and ocean acidification. *Geophysical Research Letters*, *35*(19), p.L19609.

Cammack, W.L., Kalff, J., Prairie, Y.T. and Smith, E.M., 2004. Fluorescent dissolved organic matter in lakes: relationships with heterotrophic metabolism. *Limnology and Oceanography*, *49*(6), pp.2034–2045.

Capone, D.G., Bronk, D.A., Mulholland, M.R. and Carpenter, E.J. eds., 2008. *Nitrogen in the marine environment*. Academic Press.

Capriulo, G.M., Smith, G., Troy, R., Wikfors, G.H., Pellet, J. and Yarish, C., 2002. The planktonic food web structure of a temperate zone estuary, and its alteration due to eutrophication. In *Nutrients and eutrophication in estuaries and coastal waters* (pp. 263-333). Springer Netherlands.

Carlson, C.A. and Ducklow, H.W., 1996. Growth of bacterioplankton and consumption of dissolved organic carbon in the Sargasso Sea. *Aquatic Microbial Ecology*, *10(*1), pp.69–85.

Cauwet, G., 2002. Chapter 12 - DOM in the Coastal Zone - In. Hansell, D.A. and. Carlson C.A., eds., 2014 *Biogeochemistry of Marine Dissolved Organic Matter*. San Diego: Academic Press, pp. 579–609.

Cave, R.R. and Henry, T., 2011. Intertidal and submarine groundwater discharge on the west coast of Ireland. *Estuarine, Coastal and Shelf Science*, *92*(3), pp.415–423.

Charette, M.A. and Buesseler, K.O., 2004. Submarine groundwater discharge of nutrients and copper to an urban subestuary of Chesapeake Bay (Elizabeth River). *Limnology and Oceanography*, *49(*2), pp.376–385.

Chávez-Sánchez, T., Piñón-Gimate, A., Serviere-Zaragoza, E., López-Bautista, J.M. and Casas-Valdez, M., 2018. Ulva blooms in the southwestern Gulf of California: Reproduction and biomass. *Estuarine, Coastal and Shelf Science*, *200*, pp.202-211.

Chen, C.-T.A., Huang, T.-H., Fu, Y.-H., Bai, Y. and He, X., 2012. Strong sources of CO2 in upper estuaries become sinks of CO2 in large river plumes. *Current Opinion in Environmental Sustainability*, *4*(2), pp.179–185.

Chen, M., Price, R. M., Yamashita, Y., and Jaffé, R., 2010. Comparative study of dissolved organic matter from groundwater and surface water in the Florida coastal Everglades using multi-dimensional spectrofluorometry combined with multivariate statistics. *Applied Geochemistry*, *25*(6), pp.872–880.

Chen, C.-T.A. and Borges, A.V., 2009. Reconciling opposing views on carbon cycling in the coastal ocean: Continental shelves as sinks and near-shore ecosystems as sources of atmospheric CO2. *Deep Sea Research Part II: Topical Studies in Oceanography*, *56*(8–10), pp.578–590.

Chen, C. T. A., Wang, S. L., Chou, W. C., and Sheu, D. D., 2006. Carbonate chemistry and projected future changes in pH and $CaCO_3$ saturation state of the South China Sea. *Marine Chemistry*, *101*(3), pp.277–305.

Chen, J., LeBoeuf, E. J., Dai, S., and Gu, B., 2003. Fluorescence spectroscopic studies of natural organic matter fractions. *Chemosphere*, *50*(5), pp.639–647.

Chen, R.F. and Bada, J.L., 1992. The fluorescence of dissolved organic matter in seawater. *Marine Chemistry*, *37*(3), pp.191–221.

Chen, M. and Jaffé, R., 2014. Photo-and bio-reactivity patterns of dissolved organic matter from biomass and soil leachates and surface waters in a subtropical wetland. *Water Research*, *61,* pp. 181-190.

Cheng, C. H., Lehmann, J., Thies, J. E., Burton, S. D., and Engelhard, M. H., 2006. Oxidation of black carbon by biotic and abiotic processes. *Organic Geochemistry*, *37*(11), pp.1477–1488.

Choi, T. S., Kang, E. J., Kim, J. H., and Kim, K. Y., 2010. Effect of salinity on growth and nutrient uptake of Ulva pertusa (Chlorophyta) from an eelgrass bed. *ALGAE*, *25*(1), pp.17–26.

Chou, W. C., Gong, G. C., Sheu, D. D., Jan, S., Hung, C. C., and Chen, C. C., 2009. Reconciling the paradox that the heterotrophic waters of the East China Sea shelf act as a significant CO2 sink during the summertime: Evidence and implications. *Geophysical Research Letters*, *36*(15), p.L15607.

Ciaran Cannon, 2010. http://www.kildarestreet.com/sendebates/?id=2010-12-01.675.0. *http://www.kildarestreet.com/sendebates/?id=2010-12-01.675.0*.

Cifuentes, L.A. and Eldridge, P.M., 1998. A mass- and isotope-balance model of DOC mixing in estuaries. *Limnology and Oceanography*, *43*(8), pp.1872–1882.

Cioni, R., Gambardella, B. and Marini, L., 2007. Field determination of total dissolved inorganic carbon (TDIC) in natural waters using an IR analyzer: I. Preliminary laboratory tests. *Geothermics*, *36*(1), pp.47–62.

Claessens, M., De Meester, S., Van Landuyt, L., De Clerck, K., and Janssen, C. R., 2011. Occurrence and distribution of microplastics in marine sediments along the Belgian coast. *Marine Pollution Bulletin*, *62*(10), pp.2199–2204.

Clayton, C.A., Hines, J.W. and Elkins, P.D., 1987. Detection limits with specified assurance probabilities. *Analytical Chemistry*, *59*(20), pp.2506–2514.

Cloern, J.E., 2001. Our evolving conceptual model of the coastal eutrophication problem. *Marine Ecology Progress Series*, *210*, pp.223–253.

Coble, P.G., Del Castillo, C.E. and Avril, B., 1998. Distribution and optical properties of CDOM in the Arabian Sea during the 1995 Southwest Monsoon. *Deep Sea Research Part II: Topical Studies in Oceanography*, *45*(10), pp.2195–2223.

Coble, P.G., 1996. Characterization of marine and terrestrial DOM in seawater using excitation-emission matrix spectroscopy. *Marine Chemistry*, *51*(4), pp.325–346.

Coble, P. G., Green, S. A., Blough, N. V., and Gagosian, R. B., 1990. Characterization of dissolved organic matter in the Black Sea by fluorescence spectroscopy. *Nature, 348*(6300), pp. 432-435

Coble, P.G., Schultz, C.A. and Mopper, K., 1993. Fluorescence contouring analysis of DOC intercalibration experiment samples: a comparison of techniques. *Marine Chemistry*, *41*(1–3), pp.173–178.

Cole, J.J., Prairie, Y.T., Caraco, N.F., McDowell, W.H., Tranvik, L.J., Striegl, R.G., Duarte, C.M., Kortelainen, P., Downing, J.A., Middelburg, J.J. and Melack, J., 2007. Plumbing the Global Carbon Cycle: Integrating Inland Waters into the Terrestrial Carbon Budget. *Ecosystems*, *10*(1), pp.172–185.

Cole, J. J., and Caraco, N. F., 2001. Carbon in catchments: connecting terrestrial carbon losses with aquatic metabolism. *Marine and Freshwater Research*, *52*(1), pp.101–110.

Conley, D.J. and Malone, T.C., 1992. Annual cycle of dissolved silicate in Chesapeake Bay: implications for the production and fate of phytoplankton biomass. *Marine ecology progress series. Oldendorf*, *81*(2), pp.121–128.

Conley, D. J., Schelske, C. L. and Stoermer, E. F., 1993. 'Modification of the biogeochemical cycle of silica with eutrophication', *Marine Ecology Progress Series*, pp. 179–192.

Conley, D.J., Paerl, H.W., Howarth, R.W., Boesch, D.F., Seitzinger, S.P., Havens, K.E., Lancelot, C. and Likens, G.E., 2009. Controlling eutrophication: nitrogen and phosphorus. *Science*, *323*(5917), pp.1014-1015.

Cook, P. G., Wood, C., White, T., Simmons, C. T., Fass, T., and Brunner, P., 2008. Groundwater inflow to a shallow, poorly-mixed wetland estimated from a mass balance of radon. *Journal of Hydrology*, *354*(1), pp.213–226.

Cory, R.M. and McKnight, D.M., 2005. Fluorescence Spectroscopy Reveals Ubiquitous Presence of Oxidized and Reduced Quinones in Dissolved Organic Matter. *Environmental Science & Technology*, *39*(21), pp.8142–8149.

Costa Jr., O.S., Nimmo, M. and Attrill, M.J., 2008. Coastal nutrification in Brazil: A review of the role of nutrient excess on coral reef demise. *Journal of South American Earth Sciences*, *25*(2), pp.257–270.

Coxon, C. and Drew, D., 1998. Interaction of surface water and groundwater in Irish karst areas: implications for water resource management. *Gambling with Groundwater-Physical, Chemical, and Biological Aspects of Aquifer-Stream Relations*, pp.161–168.

Coxon, C., 2011. Agriculture and karst. In *Karst Management*. (pp. 103–138) Springer Netherlands.

Coxon, C. and Drew, D., 2000. Interdependence of groundwater and surface water in lowland karst areas of western Ireland: management issues arising from water and contaminant transfers. *Geological Society, London, Special publications*, *182*(1), pp.81–88.

Crain, C.M., Kroeker, K. and Halpern, B.S., 2008. Interactive and cumulative effects of multiple human stressors in marine systems. *Ecology Letters*, *11*(12), pp.1304–1315.

Crook, E.D., Potts, D., Rebolledo-Vieyra, M. and Paytan, A., 2012. Calcifying coral abundance near low-pH springs: implications for future ocean acidification. *Coral Reefs*, *31*(1), pp.239–245.

C.S.O.,2012a.
http://www.cso.ie/en/media/csoie/census/documents/census2011vol1andprofile1/Table,5.pdf.

C.S.O.,2012b.
http://www.cso.ie/en/media/csoie/census/documents/census2011vol1andprofile1/Table,6.pdf.

Cyronak, T., Santos, I.R., Erler, D.V., Maher, D.T. and Eyre, B.D., 2014. Drivers of pCO2 variability in two contrasting coral reef lagoons: The influence of submarine groundwater discharge. *Global Biogeochemical Cycles*, *28*(4), p.2013GB004598.

Cyronak, T., Santos I.R., Erler D.V. and Eyre B.D., 2013. Groundwater and porewater as major sources of alkalinity to a fringing coral reef lagoon (Muri Lagoon, Cook Islands). *Biogeosciences*, *10*(4), pp.2467–2480.

Cyronak, T., Schulz, K. G., Santos, I. R., and Eyre, B. D., 2014. Enhanced acidification of global coral reefs driven by regional biogeochemical feedbacks. *Geophysical Research Letters*, *41*(15), p.2014GL060849.

Cyronak, T., 2013. The changing carbonate chemistry of coral reefs : ocean acidification, submarine groundwater discharge, and calcium carbonate $CaCO_3$ sediment dissolution. *PhD thesis, Southern Cross University, Lismore, NSW*. Available at: http://epubs.scu.edu.au/theses/378.

Dai, M., Yin, Z., Meng, F., Liu, Q., and Cai, W. J., 2012. Spatial distribution of riverine DOC inputs to the ocean: an updated global synthesis. *Current Opinion in Environmental Sustainability*, *4*(2), pp.170–178.

Dai, M., Zhai W., Cai W-J., Callahan J., Huang B., Shang S., Huang T., Li X., Lu Z., Chen W. and Chen Z., 2008. Effects of an estuarine plume-associated bloom on the carbonate system in the lower reaches of the Pearl River estuary and the coastal zone of the northern South China Sea. *Continental Shelf Research*, *28(*12), pp.1416–1423.

Dalsgaard, T. and Krause-Jensen, D., 2006. Monitoring nutrient release from fish farms with macroalgal and phytoplankton bioassays. *Aquaculture*, *256*(1–4), pp.302–310.

Deakin, J., 2000. Groundwater protection zone delineation at a large karst spring in western Ireland. *Geological Society, London, Special Publications*, *182*(1), pp.89–98.

Delincé, G., 2013. *The Ecology of the Fish Pond Ecosystem: with special reference to Africa* (Vol. 72). Springer Science & Business Media.

Del Castillo, C. E. and Miller, R. L., 2008. 'On the use of ocean color remote sensing to measure the transport of dissolved organic carbon by the Mississippi River Plume', *Remote Sensing of Environment*, 112(3), pp. 836–844. doi: 10.1016/j.rse.2007.06.015.

DeMaster, D.J., 1981. The supply and accumulation of silica in the marine environment. *Geochimica et Cosmochimica Acta*, *45*(10), pp.1715–1732.

Denning, A.S., Oren, R., McGuire, D., Sabine, C., Doney, S., Paustian, K., Torn, M., Dilling, L., Heath, L., Tans, P. and Wofsy, S., 2005. Science implementation strategy for the North American carbon program. *Report of the NACP Implementation Strategy Group of the US Carbon Cycle Interagency Working Group. US Carbon Cycle Science Program, Washington, DC*, p.68.

Dennison, W.C., Orth, R.J., Moore, K.A., Stevenson, J.C., Carter, V., Kollar, S., Bergstrom, P.W. and Batiuk, R.A., 1993. Assessing water quality with submersed aquatic vegetation. *BioScience*, *43*(2), pp.86–94.

Derraik, J.G.B., 2002. The pollution of the marine environment by plastic debris: a review. *Marine Pollution Bulletin*, *44*(9), pp.842–852.

Determann, S., Reuter, R., Wagner, P. and Willkomm, R., 1994. Fluorescent matter in the eastern Atlantic Ocean. Part 1: method of measurement and near-surface distribution. *Deep Sea Research Part I: Oceanographic Research Papers*, *41*(4), pp.659–675.

Dickson, A. G. and Riley, J. P. (1978) 'The effect of analytical error on the evaluation of the components of the aquatic carbon-dioxide system', *Marine Chemistry*, 6(1), pp. 77–85. doi: 10.1016/0304-4203(78)90008-7.

Dickson, A.G. and Millero, F.J., 1987. A comparison of the equilibrium constants for the dissociation of carbonic acid in seawater media. *Deep Sea Research Part A. Oceanographic Research Papers*, *34*(10), pp.1733–1743.

Dickson, A.G., 2010. The carbon dioxide system in seawater: Equilibrium chemistry and measurements.

Dittmar, T., Koch, B., Hertkorn, N. and Kattner, G., 2008. A simple and efficient method for the solid-phase extraction of dissolved organic matter (SPE-DOM) from seawater. *Limnology and Oceanography: Methods*, *6*(6), pp.230–235.

Dobson, M. and Laming, D., 1999. Field meeting: western Ireland, 9–17 May, 1998. *Proceedings of the Geologists' Association*, *110*(4), pp.335–348.

Doney, S., Balch W.M., Fabry V.J. and Feely R.A., 2009. Ocean Acidification: A Critical Emerging Problem for the Ocean Sciences. *Oceanography*, *22*(4), pp.16–25.

Doney, S.C., Lindsay, K., Caldeira, K., Campin, J.M., Drange, H., Dutay, J.C., Follows, M., Gao, Y., Gnanadesikan, A., Gruber, N. and Ishida, A., 2004. Evaluating global ocean carbon

models: The importance of realistic physics. *Global Biogeochemical Cycles*, *18*(3), p.GB3017.

Dorsett A., Cherrier J., Martin J.B. and Cable J.E., 2011. Assessing hydrologic and biogeochemical controls on pore-water dissolved inorganic carbon cycling in a subterranean estuary: A 14C and 13C mass balance approach. *Marine Chemistry*, *127*(1), pp.76–89.

Drew, D.P 1990. The Hydrology of the Burren, County Clare. *Irish Geography*, *23*(2), pp.69–89.

Drew, D.P., 2008. Hydrogeology of lowland karst in Ireland. *Quarterly Journal of Engineering Geology and Hydrogeology*, *41*(1), pp.61–72.

Drew D.P., Doerfliger N.and Formentin K., 1997. The use of bacteriophages for multi-tracing in a lowland karst aquifer in western ireland. In *Tracer Hydrology 97*. Balkema Publishers, pp. 33–37.

Drew D.P., 2003. The Hydrology of the Burren and of the Clare and Galway Lowlands. In *Caves of County Clare and South Galway*. Bristol, United Kingdom: University of Bristol Spelaelogical Society.

Drew, D.P., 1996. Agriculturally induced environmental changes in the Burren Karst, Western Ireland. *Environmental Geology*, *28*(3), pp.137–144.

Drew, D.P. and Coxon, C.E., 1988. The effects of land drainage on groundwater resources in karstic areas of Ireland. In *Proceedings of the 21st IAH Congress, Geological Publishing House, Beijing, China*. pp., 204–209.

Drew, D.P. and Jones, G.L., 2000. Post-Carboniferous pre-Quaternary karstification in Ireland. *Proceedings of the Geologists' Association*, *111*(4), pp.345–353.

Duarte, C.M., 1995. Submerged aquatic vegetation in relation to different nutrient regimes. *Ophelia*, *41*(1), pp.87–112.

Duarte, C.M, Hendriks IE, Moore TS, Olsen YS, Steckbauer A, Ramajo L, Carstensen J, Trotter JA and McCulloch 2013. Is Ocean Acidification an Open-Ocean Syndrome? Understanding Anthropogenic Impacts on Seawater pH. *Estuaries and Coasts*, *36*(2), pp.221–236.

Dulaiova, H., Burnett, W.C., Chanton, J.P., Moore, W.S., Bokuniewicz, H.J., Charette, M.A. and Sholkovitz, E., 2006. Assessment of groundwater discharges into West Neck Bay, New York, via natural tracers. *Continental Shelf Research*, *26(*16), pp.1971–1983.

Dulaiova, H., Gonneea, M.E., Henderson, P.B. and Charette, M.A., 2008. Geochemical and physical sources of radon variation in a subterranean estuary — Implications for groundwater radon activities in submarine groundwater discharge studies. *Marine Chemistry*, *110*(1–2), pp.120–127.

Dürr, H.H., Meybeck, M., Hartmann, J., Laruelle, G.G. and Roubeix, V., 2011. Global spatial distribution of natural riverine silica inputs to the coastal zone. *Biogeosciences*, *8*(3), pp.597–620.

Egleston, E.S., Sabine, C.L. and Morel, F.M.M., 2010. Revelle revisited: Buffer factors that quantify the response of ocean chemistry to changes in DIC and alkalinity. *Global Biogeochemical Cycles*, *24(*1), p.GB1002.

Einsiedl, F., Radke, M. and Maloszewski, P., 2010. Occurrence and transport of pharmaceuticals in a karst groundwater system affected by domestic wastewater treatment plants. *Journal of contaminant hydrology*, *117*(1), pp.26–36.

Einsiedl, F., 2005. Flow system dynamics and water storage of a fissured-porous karst aquifer characterized by artificial and environmental tracers. *Journal of Hydrology*, 312(1–4), pp.312–321.

Einsiedl, F., 2012. Sea-water/groundwater interactions along a small catchment of the European Atlantic coast. *Applied Geochemistry*, *27*(1), pp.73–80.

Éireann, M., Met Éireann - The Irish Weather Service. Available at: http://www.met.ie/

Eisenreich, S.J., Bannerman, R.T. and Armstrong, D.E., 1975. A Simplified Phosphorus Analysis Technique. *Environmental Letters*, *9*(1), pp.43–53.

Elementar, 2014. Vario TOC Cube.

E.P.A., 2008 Water Quality in Ireland 2006: Key Indicators of the Aquatic Environment. *Environmental Protection Agency (EPA)*. Available at: http://www.epa.ie/pubs/reports/water/waterqua/waterqualityinireland2006.html#.Vkcky-lPyIl

E.P.A., 2010. Application for wastewater discharge licence by Galway County Council for Kinvara, pop. Equivalent 1270. http://www.epa.ie/licences/lic_eDMS/090151b28028deed.pdf

E.P.A., 2011. *Water Framework Directive Groundwater Monitoring Programme*, Environmental Protection Agency.

E.P.A., 2013 Water Quality in Ireland 2010 - 2012. *Environmental Protection Agency (EPA)*. Available at: http://www.epa.ie/pubs/reports/water/waterqua/wqr20102012/#.Vkcpl-lPyIl.

Erisman, J.W., Galloway, J.N., Seitzinger, S., Bleeker, A., Dise, N.B., Petrescu, A.R., Leach, A.M. and de Vries, W., 2013. Consequences of human modification of the global nitrogen cycle. *Philosophical Transactions of the Royal Society B: Biological Sciences*, 368(1621), p.20130116.

Erler, D.V., Santos, I.R., Zhang, Y., Tait, D.R., Befus, K.M., Hidden, A., Li, L. and Eyre, B.D., 2014. Nitrogen transformations within a tropical subterranean estuary. *Marine Chemistry*, *164,* pp.38–47.

European Communities Environmental Objectives (Groundwater) Regulations 2010. S.I. No. 9/2010

EUROPEAN COMMUNITIES (QUALITY OF SHELLFISH WATERS) REGULATIONS 2006 S.I. No. 268 of 2006

European Parliament and the Council of the European Union, 2000 European Parliament and the Council of the European Union **Directive 2000/60/EC of the European Parliament and of the Council Establishing a Framework for the Community Action in the Field of Water Policy** (2000)

European Parliament and the Council of the European Union, 2006 European Parliament and the Council of the European Union Directive 2006/113/EC of the European Parliament and of the Council of 12 December 2006 on the quality required of shellfish waters, 2006

Fabry, V.J., Seibel, B.A., Feely, R.A. and Orr, J.C., 2008. Impacts of ocean acidification on marine fauna and ecosystem processes. *ICES Journal of Marine Science*, *65*(3), pp.414-432.

Fagan, K.E. and Mackenzie, F.T., 2007. Air–sea CO2 exchange in a subtropical estuarine-coral reef system, Kaneohe Bay, Oahu, Hawaii. *Marine Chemistry*, *106*(1–2), pp.174–191.

Farjalla, V.F., Amado, A.M., Suhett, A.L. and Meirelles-Pereira, F., 2009. DOC removal paradigms in highly humic aquatic ecosystems. *Environmental Science and Pollution Research*, *16*(5), pp.531–538.

Feely, R.A., Sabine, C.L., Lee, K., Berelson, W., Kleypas, J., Fabry, V.J. and Millero, F.J., 2004. Impact of Anthropogenic CO2 on the CaCO3 System in the Oceans. *Science*, *305*(5682), pp.362–366.

Feely, R.A. and Doney, S.C., 2011. Ocean Acidification: The Other CO2 Problem. *ASLO Web Lectures*, *3*(1), pp.1–59.

Fellman, J.B., Hood, E., Edwards, R.T. and D'Amore, D.V., 2009. Changes in the concentration, biodegradability, and fluorescent properties of dissolved organic matter during stormflows in coastal temperate watersheds. *Journal of Geophysical Research: Biogeosciences*, *114*(G1), p.G01021.

Fellman, J.B., Hood, E. and Spencer, R.G., 2010. Fluorescence spectroscopy opens new windows into dissolved organic matter dynamics in freshwater ecosystems: A review. *Limnology and Oceanography*, *55*(6), pp.2452–2462.

Ferrari, G. M., Dowell, M. D., Grossi, S., and Targa, C., 1996. Relationship between the optical properties of chromophoric dissolved organic matter and total concentration of dissolved organic carbon in the southern Baltic Sea region. *Marine Chemistry*, *55*(3–4), pp.299–316.

Ferrari, G. M., 2000. 'The relationship between chromophoric dissolved organic matter and dissolved organic carbon in the European Atlantic coastal area and in the West Mediterranean Sea (Gulf of Lions)', *Marine Chemistry*, 70(4), pp. 339–357. doi: 10.1016/S0304-4203(00)00036-0.

Fiebig, D.M., 1995. Groundwater discharge and its contribution of dissolved organic carbon to an upland stream. *Archiv für Hydrobiologie*, *134*(2), pp.129–155.

Fimmen, R. L., Cory, R. M., Chin, Y. P., Trouts, T. D., and McKnight, D. M., 2007. Probing the oxidation–reduction properties of terrestrially and microbially derived dissolved organic matter. *Geochimica et Cosmochimica Acta*, *71*(12), pp.3003–3015.

Finch, T.F., Culleton, E. and Diamond, S., 1971. *Soils of County Clare*, Dublin: An Foras Talúntais.

Fish, J. D. and Fish, S., 2011. *A Student's Guide to the Seashore*. Cambridge University Press.

Fleury, P., Bakalowicz, M. and de Marsily, G., 2007. Submarine springs and coastal karst aquifers: A review. *Journal of Hydrology*, *339*(1–2), pp.79–92.

Fong, P., Fong, J. J. and Fong, C. R., 2004. 'Growth, nutrient storage, and release of dissolved organic nitrogen by Enteromorpha intestinalis in response to pulses of nitrogen and phosphorus', *Aquatic Botany*, 78(1), pp. 83–95. doi: 10.1016/j.aquabot.2003.09.006.

Forja, J.M. and Gómez-Parra, A., 1998. Measuring nutrient fluxes across the sediment-water interface using benthic chambers. *Marine Ecology Progress Series,* pp.95-105.

Fortes, M. D. and Lüning, K., 1980. 'Growth rates of North Sea macroalgae in relation to temperature, irradiance and photoperiod', *Helgoländer Meeresuntersuchungen*, 34(1), p. 15.

Fourqurean, J.W., Jones, R.D. and Zieman, J.C., 1993. Process Influencing Water Column Nutrient Characteristics and Phosphorus Limitation of Phytoplankton Biomass in Florida Bay, FL,

USA:Inferences from Spatial Distributions. *Estuarine, Coastal and Shelf Science*, *36*(3), pp.295–314.

Frankignoulle, M., Abril, G., Borges, A., Bourge, I., Canon, C., Delille, B., Libert, E. and Théate, J.M., 1998. Carbon dioxide emission from European estuaries. *Science*, *282*(5388), pp.434–436.

Gagan, M.K., Ayliffe, L.K., Opdyke, B.N., Hopley, D., Scott-Gagan, H. and Cowley, J., 2002. Coral oxygen isotope evidence for recent groundwater fluxes to the Australian Great Barrier Reef. *Geophysical research letters*, *29*(20).

Gall, S.C. and Thompson, R.C., 2015. The impact of debris on marine life. *Marine Pollution Bulletin*, *92*(1–2), pp.170–179.

Gallagher, D., Mara, C. and Hannigan, M., 2010. Submission to Galway County Council on the Review of Kinvara Local Area Plan.

Galloway, J.N. Asner, G.P., Cleveland, C.C., Green, P.A., Holland, E.A., Karl, D.M., Michaels, A.F., Porter, J.H., Towsend, A.R. and Vorosmarty, C.J., 2004. Nitrogen cycles: past, present, and future. *Biogeochemistry*, *70*(2), pp.153–226.

Galloway, J.N., 1998. The global nitrogen cycle: changes and consequences. *Environmental pollution*, *102*(1), pp.15–24.

Galway County Council, 2012. http://www.galway.ie/en/Business/WestRegionalAuthority/ProfileoftheRegion/. *http://www.galway.ie/en/Business/WestRegionalAuthority/ProfileoftheRegion/*.

Galway Couty Council, 2013. KINVARA SEWERAGE SCHEME STAGE 1.

Gan, S., Wu, Y. and Zhang, J., 2016. Bioavailability of dissolved organic carbon linked with the regional carbon cycle in the East China Sea. *Deep Sea Research Part II: Topical Studies in Oceanography*, *124*, pp.19–28.

Garcia-Solsona, E., Garcia-Orellana, J., Masqué, P., Rodellas, V., Mejías, M., Ballesteros, B. and Domínguez, J.A., 2010. Groundwater and nutrient discharge through karstic coastal springs (Castelló, Spain). *Biogeosciences*, *7(*9), pp.2625–2638.

Gattuso J.P., Pichon M., Delesalle B., Canon C. and Frankignoulle M., 1996. Carbon fluxes in coral reefs. I. Lagrangian measurement of community metabolism and resulting air-sea CO2 disequilibrium. *Marine Ecology Progress Series*, *145*, pp.109–121.

Gattuso, J.-P., Frankignoulle, M. and Wollast, R., 1998. Carbon and Carbonate Metabolism in Coastal Aquatic Ecosystems. *Annual Review of Ecology and Systematics*, *29*(1), pp.405–434.

Ghinaglia, L.T., Herrera-Silveira, J.A. and Comín, F.A., 2004. Structural variations of phytoplankton in the coastal seas of Yucatan, Mexico. *Hydrobiologia*, *519*(1-3), pp.85–102.

Giblin, A.E. and Gaines, A.G., 1999. Nitrogen inputs to a marine embayment: the importance of groundwater. *Biogeochemistry*, *10*(3), pp.309–328.

Giblin, A.E., Tobias, C.R., Song, B., Weston, N., Banta, G.T. and H. RIVERA-MONROY, V.I.C.T.O.R., 2013. The importance of dissimilatory nitrate reduction to ammonium (DNRA) in the nitrogen cycle of coastal ecosystems. *Oceanography*, *26*(3), pp.124-131.

Gill, L.W., Naughton, O., Johnston, P.M., 2013. Characterisation of hydrogeological connections in a lowland karst network using time series analysis of water levels in ephemeral groundwater-fed lakes (turloughs). *Journal of Hydrology, 499,* pp.289-302.

Gill, L.W., Naughton, O. and Johnston, P.M., 2013. Modeling a network of turloughs in lowland karst. *Water Resources Research*, *49*(6), pp.3487–3503.

Goldberg, E., 1985. Black carbon in the environment. United States: Wiley and Sons, New York, NY.

Gonfiantini, R. and Zuppi, G.M., 2003. Carbon isotope exchange rate of DIC in karst groundwater. *Chemical Geology*, *197*(1–4), pp.319–336.

Goñi, M.A. and Gardner, I.R., 2003. Seasonal dynamics in dissolved organic carbon concentrations in a coastal water-table aquifer at the forest-marsh interface. *Aquatic Geochemistry*, *9*(3), pp.209–232.

Goñi, M.A., Teixeira, M.J. and Perkey, D.W., 2003. Sources and distribution of organic matter in a river-dominated estuary (Winyah Bay, SC, USA). *Estuarine, Coastal and Shelf Science*, *57*(5), pp.1023–1048.

Gonneea, M.E., Charette, M.A., Liu, Q., Herrera-Silveira, J.A. and Morales-Ojeda, S.M.,2014. Trace element geochemistry of groundwater in a karst subterranean estuary (Yucatan Peninsula, Mexico). *Geochimica et Cosmochimica Acta*, *132*, pp.31–49.

González, F.U.T., Herrera-Silveira, J.A. & Aguirre-Macedo, M.L., 2008. Water quality variability and eutrophic trends in karstic tropical coastal lagoons of the Yucatán Peninsula. *Estuarine, Coastal and Shelf Science*, *76*(2), pp.418–430.

Goodwillie, R., 2003. 'Vegetation of turloughs', *Wetlands of Ireland. Distribution, ecology, uses and economic value*, pp. 135–144.

Gordon, D.C., Boudreau, P.R., Mann, K.H., Ong, J.E., Silvert, W.L., Smith, S.V., Wattayakorn, G., Wulff, F. and Yanagi, T., 1996. *LOICZ biogeochemical modelling guidelines*, LOICZ Core Project, Netherlands Institute for Sea Research.

Graiff, A., Liesner, D., Karsten, U. and Bartsch, I., 2015. Temperature tolerance of western Baltic Sea *Fucus* vesiculosus–growth, photosynthesis and survival. *Journal of experimental marine biology and ecology*, *471*, pp.8-16.

Green, S.A. and Blough, N.V., 1994. Optical absorption and fluorescence properties of chromophoric dissolved organic matter in natural waters. *Limnology and Oceanography*, *39*(8), pp.1903–1916.

Green, T.R., Taniguchi, M., Kooi, H., Gurdak, J.J., Allen, D.M., Hiscock, K.M., Treidel, H. and Aureli, A., 2011. Beneath the surface of global change: Impacts of climate change on groundwater. *Journal of Hydrology*, *405*(3-4), pp.532-560.

Grøn, C., Tørsløv, J., Albrechtsen, H. J., and Jensen, H. M., 1992. Biodegradability of dissolved organic carbon in groundwater from an unconfined aquifer. *Science of the total environment*, *117*, pp.241–251.

Gu, B., Schelske, C.L. and Hodell, D.A., 2004. Extreme^ 1^ 3C enrichments in a shallow hypereutrophic lake: Implications for carbon cycling. *Limnology and Oceanography*, *49,* pp.1152–1159.

Green, S.A. and Blough, N.V., 1994. Optical absorption and fluorescence properties of chromophoric dissolved organic matter in natural waters. *Limnology and Oceanography*, *39*(8), pp.1903–1916.

Green, D. S., Boots, B., Blockley, D. J., Rocha, C., and Thompson, R., 2015. Impacts of discarded plastic bags on marine assemblages and ecosystem functioning. *Environmental science & technology*, *49*(9), pp.5380–5389.

Gregory, M.R., 2009. Environmental implications of plastic debris in marine settings—entanglement, ingestion, smothering, hangers-on, hitch-hiking and alien invasions. *Philosophical Transactions of the Royal Society of London B: Biological Sciences*, *364*(1526), pp.2013–2025.

Grime, J.P., 1979. Competition and the struggle for existence. *Population dynamics,.(Eds RM Anderson, BD Turner, LR Taylor)* pp.123-139.

Guillemette, F., McCallister, S.L. and Giorgio, P.A., 2013. Differentiating the degradation dynamics of algal and terrestrial carbon within complex natural dissolved organic carbon in temperate lakes. *Journal of Geophysical Research: Biogeosciences*, *118*(3), pp.963–973.

Guo, W., Stedmon, C. A., Han, Y., Wu, F., Yu, X., and Hu, M., 2007. The conservative and non-conservative behavior of chromophoric dissolved organic matter in Chinese estuarine waters. *Marine Chemistry*, *107*(3), pp.357–366.

Guo, W., Xu, J., Wang, J., Wen, Y., Zhuo, J., and Yan, Y., 2010. Characterization of dissolved organic matter in urban sewage using excitation emission matrix fluorescence spectroscopy and parallel factor analysis. *Journal of Environmental Sciences*, *22*(11), pp.1728–1734.

Guzman, A., Janik, H. and Kosakowska, A., 2010. Preliminary Testing of the Influence of Modified Polycaprolactones on Anabaena Variabilis Growth in Seawater. *Journal of Polymers and the Environment*, *18*(4), pp.679–684.

Gyllenhammar, A. and Håkanson, L., 2005. Environmental consequence analyses of fish farm emissions related to different scales and exemplified by data from the Baltic – a review. *Marine Environmental Research*, *60*(2), pp.211–243.

De Haan, H., 1993. Solar UV-light penetration and photodegradation of humic substances in peaty lake water. *Limnology and Oceanography*, *38*(5), pp.1072–1076.

Häder, D. P., Kumar, H. D., Smith, R. C., and Worrest, R. C., 2007. Effects of solar UV radiation on aquatic ecosystems and interactions with climate change. *Photochemical & Photobiological Sciences*, *6*(3), pp.267–285.

Hagedorn, B. and Cartwright, I., 2010. The CO2 system in rivers of the Australian Victorian Alps: CO2 evasion in relation to system metabolism and rock weathering on multi-annual time scales. *Applied Geochemistry*, *25*(6), pp.881–899.

Hagström, A., Azam, F., Andersson, A., Wikner, J., and Rassoulzadegan, F., 1988. Microbial loop in an oligotrophic pelagic marine ecosystem: possible roles of cyanobacteria and nanoflagellates in the organic fluxes. *Marine ecology progress series. Oldendorf*, *49*(1), pp.171–178.

Hejzlar, J., Dubrovský, M., Buchtele, J., and Růžička, M., 2003. The apparent and potential effects of climate change on the inferred concentration of dissolved organic matter in a temperate stream (the Malše River, South Bohemia). *Science of The Total Environment*, *310*(1–3), pp.143–152.

Hansell, D.A., 2002. DOC in the global ocean carbon cycle. *Biogeochemistry of marine dissolved organic matter*, *298*(5600), pp.685–715.

Hansell, D.A., 2013. Recalcitrant Dissolved Organic Carbon Fractions. *Annual Review of Marine Science*, *5*(1), pp.421–445.

Hansell, D.A. and Carlson, C.A., 2014. *Biogeochemistry of Marine Dissolved Organic Matter*, Academic Press.

Hedges, J. I., Hatcher, P. G., Ertel, J. R., and Meyers-Schulte, K. J., 1992. A comparison of dissolved humic substances from seawater with Amazon River counterparts by 13C-NMR spectrometry. *Geochimica et Cosmochimica Acta*, *56*(4), pp.1753–1757.

Hedges, J.I. and Keil, R.G., 1999. Organic geochemical perspectives on estuarine processes: sorption reactions and consequences. *Marine Chemistry*, *65*(1–2), pp.55–65.

Hedges, J.I. and Prahl, F.G., 1993. Early Diagenesis: Consequences for Applications of Molecular Biomarkers. In M. H. Engel & S. A. Macko, eds. *Organic Geochemistry*. Topics in Geobiology. Springer US, pp. 237–253. Springer US.

Hedges, J.I., Keil, R.G. and Benner, R., 1997. What happens to terrestrial organic matter in the ocean? *Organic Geochemistry*, *27*(5–6), pp.195–212.

Hélie, J.-F., Hillaire-Marcel, C. and Rondeau, B., 2002. Seasonal changes in the sources and fluxes of dissolved inorganic carbon through the St. Lawrence River—isotopic and chemical constraint. *Chemical Geology*, *186*(1), pp.117–138.

Helms, J. R., Stubbins, A., Ritchie, J. D., Minor, E. C., Kieber, D. J., and Mopper, K., 2008. Absorption spectral slopes and slope ratios as indicators of molecular weight, source, and photobleaching of chromophoric dissolved organic matter. *Limnology and Oceanography*, *53*(3), p.955.

Helms, J. R., Stubbins, A., Perdue, E. M., Green, N. W., Chen, H., and Mopper, K., 2013. Photochemical bleaching of oceanic dissolved organic matter and its effect on absorption spectral slope and fluorescence. *Marine Chemistry, 155*, pp.81–91.

Henze, M., 2008. *Biological Wastewater Treatment: Principles, Modelling and Design*, IWA Publishing.

Her, N., Amy, G., McKnight, D., Sohn, J., and Yoon, Y., 2003. Characterization of DOM as a function of MW by fluorescence EEM and HPLC-SEC using UVA, DOC, and fluorescence detection. *Water Research*, *37*(17), pp.4295–4303.

Herbert, R.A., 1999. Nitrogen cycling in coastal marine ecosystems. *FEMS Microbiology Reviews*, *23*(5), pp.563–590.

Hessen, D.O., 1998. *Aquatic Humic Substances: Ecology and Biogeochemistry*. (Vol. 133) Springer Science & Business Media.

Holmén, K., 2000. 11 - The Global Carbon Cycle. In R. J. C., Henning Rodhe and Gordon H. Orians Michael C. Jacobson, ed. *International Geophysics*. Earth System ScienceFrom Biogeochemical Cycles to Global Change. Academic Press, pp. 282–321.

Houghton, R.A., 2001 Counting Terrestrial Sources and Sinks of Carbon. *Climatic Change*, *48*(4), pp.525–534.

Howarth, R.W. and Marino, R., 2006. Nitrogen as the limiting nutrient for eutrophication in coastal marine ecosystems: Evolving views over three decades. *Limnology and Oceanography*, *51*(1part2), pp.364–376.

Howland, R.J., Tappin, A.D., Uncles, R.J., Plummer, D.H. and Bloomer, N.J., 2000. Distributions and seasonal variability of pH and alkalinity in the Tweed Estuary, UK. *Science of The Total Environment*, *251–252*, pp.125–138.

Hudson, N., Baker, A. and Reynolds, D., 2007. Fluorescence analysis of dissolved organic matter in natural, waste and polluted waters—a review. *River Research and Applications*, *23*(6), pp.631–649.

Hwang, D., Lee, Y.-W. and Kim, G., 2005. Large submarine groundwater discharge and benthic eutrophication in Bangdu Bay on volcanic Jeju Island, Korea. *Limnology and Oceanography*, *50*(5), pp.1393–1403.

Hwang, D. W., Kim, G., Lee, W. C., and Oh, H. T., 2010. The role of submarine groundwater discharge (SGD) in nutrient budgets of Gamak Bay, a shellfish farming bay, in Korea. *Journal of Sea Research*, *64*(3), pp.224–230.

Iavorivska, L., Boyer, E.W. and DeWalle, D.R., 2016. Atmospheric deposition of organic carbon via precipitation. *Atmospheric Environment*, *146,* pp.153–163.

Ibánhez, J.S.P., Leote, C. and Rocha, C., 2011. Porewater nitrate profiles in sandy sediments hosting submarine groundwater discharge described by an advection–dispersion-reaction model. *Biogeochemistry*, *103*(1-3), pp.159–180.

Ibánhez, J.S.P., Leote, C. and Rocha, C., 2013. Seasonal enhancement of submarine groundwater discharge (SGD)-derived nitrate loading into the Ria Formosa coastal lagoon assessed by 1-D modeling of benthic NO_3^- profiles. *Estuarine, Coastal and Shelf Science*, *132*, pp.56–64.

Ibánhez, J.S.P. and Rocha, C., 2014. Effects of recirculation of seawater enriched in inorganic nitrogen on dissolved organic carbon processing in sandy seepage face sediments. *Marine Chemistry*, *166*, pp.48–58.

Ibánhez, J. S. P. Arévalo, E., Kelly, T., Papaspyrou, S., Rocha, C. and Nicolaidou, A., 2017. 'Unraveling the dispersion and environmental impact of anthropogenic discharges in transitional water ecosystems', *Estuarine, Coastal and Shelf Science*.

Imhof, H. K., Schmid, J., Niessner, R., Ivleva, N. P., and Laforsch, C., 2012. A novel, highly efficient method for the separation and quantification of plastic particles in sediments of aquatic environments. *Limnology and Oceanography: Methods*, *10*(7), pp.524–537.

IPCC, 2007. *Climate change 2007: The physical science basis. Contribution of Working Group I to the Fourth Assessment Report of the Intergovernmental Panel on Climate Change*, *Agenda*, *6*(07) p.333

IPCC, 2014: Climate Change 2014: Synthesis Report. Contribution of Working Groups I, II and III to the Fifth Assessment Report of the Intergovernmental Panel on Climate Change [Core Writing Team, R.K. Pachauri and L.A. Meyer (eds.)]. IPCC, Geneva, Switzerland, 151 pp.

Ivar do Sul, J. A. and Costa, M. F., 2014. 'The present and future of microplastic pollution in the marine environment', *Environmental Pollution*, 185(Supplement C), pp. 352–364. doi: 10.1016/j.envpol.2013.10.036.

Jackson, G.A. and Williams, P.M., 1985. Importance of dissolved organic nitrogen and phosphorus to biological nutrient cycling. *Deep Sea Research Part A. Oceanographic Research Papers*, *32*(2), pp.223–235.

Jambeck, J. R., Geyer, R., Wilcox, C., Siegler, T. R., Perryman, M., Andrady, A., Narayan, R. and Law, K. L., 2015. Plastic waste inputs from land into the ocean. *Science*, *347*(6223), pp.768–771.

Jahnke, R., Richards, M., Nelson, J., Robertson, C., Rao, A. and Jahnke, D., 2005. Organic matter remineralization and porewater exchange rates in permeable South Atlantic Bight continental shelf sediments. *Continental Shelf Research*, *25*(12-13), pp.1433-1452.

Jarvie, H.P., Whitton, B.A. & Neal, C., 1998. Nitrogen and phosphorus in east coast British rivers: Speciation, sources and biological significance. *Science of The Total Environment*, 210–*211*, pp.79–109.

Jennings O'Donovan & Partners (2011). Engineering Proposals for the Reinstatement of Culverts on the N18 and the Provision of New Culverts on Minor Roads at Kiltartan / Feasibility of an Overland Channel from Coole to Kinvarra:. Review of the South Galway Flood Studies Report. Office of Public Works, Galway.

Jerlov, N. G., 2014. *Optical oceanography*. Elsevier.

Jessen, C., Bednarz, V. N., Rix, L., Teichberg, M., and Wild, C., 2015. Marine Eutrophication. In R. H. Armon & O. Hänninen, eds. *Environmental Indicators*. pp. 177–203. Springer Netherlands.

Ji, T., Du, J., Moore, W. S., Zhang, G., Su, N., and Zhang, J., 2013. Nutrient inputs to a Lagoon through submarine groundwater discharge: The case of Laoye Lagoon, Hainan, China. *Journal of Marine Systems*, 111–112, pp.253–262.

Jiao, N., Herndl, G.J., Hansell, D.A., Benner, R., Kattner, G., Wilhelm, S.W., Kirchman, D.L., Weinbauer, M.G., Luo, T., Chen, F. and Azam, F., 2010. Microbial production of recalcitrant dissolved organic matter: long-term carbon storage in the global ocean. *Nature Reviews Microbiology*, *8(*8), pp.593–599.

Jiao, N. and Azam, F., 2011. Microbial carbon pump and its significance for carbon sequestration in the ocean. *Microbial Carbon Pump in the Ocean*, *10,* pp.43–45.

Jiang, L. Q., Cai, W. J., and Wang, Y., 2008. A comparative study of carbon dioxide in river- and marine-dominated estuaries. *Limnology and Oceanography*, *53*(6), pp.2603–2615.

Johannes, 1980. The Ecological Significance of the Submarine Discharge of Groundwater. *Marine Ecology - Progress Series*, *3*, pp.365–373.

Johannes, R. E. and Hearn, C. J., 1985. 'The effect of submarine groundwater discharge on nutrient and salinity regimes in a coastal lagoon off Perth, Western Australia', *Estuarine, Coastal and Shelf Science*, 21(6), pp. 789–800. doi: 10.1016/0272-7714(85)90073-3.

Jørgensen, L., Markager, S. and Maar, M., 2014. On the importance of quantifying bioavailable nitrogen instead of total nitrogen. *Biogeochemistry*, *117*(2-3), pp.455–472.

Kačaroğlu, F., 1999. Review of Groundwater Pollution and Protection in Karst Areas. *Water, Air, and Soil Pollution*, *113*(1-4), pp.337–356.

Kähler, P., Bjornsen, P. K., Lochte, K., and Antia, A., 1997. Dissolved organic matter and its utilization by bacteria during spring in the Southern Ocean. *Deep Sea Research Part II: Topical Studies in Oceanography*, *44*(1), pp.341–353.

Kalle, K., 1938. 'Zum Problem der Meer Wasserfarbe', *Ann. Hydrol. Mar. Mitt.*, 66, pp. 1–13.

Kalle, K., 1949. 'Fluoreszenz und gelbstoff im bottnischen und finnischen meerbusen', *Ocean Dynamics*, 2(4), pp. 117–124.

Kamermans, P., Hemminga, M., Mateo, M. A., Marba, N., Stapel, J., and Mtolera, M., 2002. Groundwater effects on diversity and abundance of lagoonal seagrasses in Kenya and on Zanzibar Island (East Africa). *Marine Ecology Progress Series, 231,* pp.75-83

Karst Working Group, 2000. *The Karst of Ireland: Limestone Landscapes, Caves and Groundwater Drainage Systems*,

Katsoyiannis, A. and Samara, C., 2007. The fate of dissolved organic carbon (DOC) in the wastewater treatment process and its importance in the removal of wastewater contaminants. *Environmental Science and Pollution Research-International*, *14*(5), pp.284–292.

Kempe, S., 1996. *Coastal seas: a net source or sink of atmospheric carbon dioxide?*, LOICZ, Texel, The Netherlands.

Kilroy, G. and Coxon, C., 2005. Temporal variability of phosphorus fractions in Irish karst springs. *Environmental Geology*, *47*(3), pp.421–430.

Kim, J. I., Buckau, G., Li, G. H., Duschner, H., and Psarros, N., 1990. Characterization of humic and fulvic acids from Gorleben groundwater. *Fresenius' Journal of Analytical Chemistry*, *338*(3), pp.245–252.

Kim, G., Lee, K. K., Park, K. S., Hwang, D. W., and Yang, H. S., 2003. Large submarine groundwater discharge (SGD) from a volcanic island. *Geophysical Research Letters*, *30*(21), p.2098.

Kim, G., Ryu, J. W., Yang, H. S., and Yun, S. T., 2005. Submarine groundwater discharge (SGD) into the Yellow Sea revealed by 228Ra and 226Ra isotopes: Implications for global silicate fluxes. *Earth and Planetary Science Letters*, *237*(1–2), pp.156–166.

Kim, T. H., Kwon, E., Kim, I., Lee, S. A., and Kim, G. 2013. Dissolved organic matter in the subterranean estuary of a volcanic island, Jeju: Importance of dissolved organic nitrogen fluxes to the ocean. *Journal of Sea Research*, *78,* pp.18–24.

Kim, T. H., Waska, H., Kwon, E., Suryaputra, I. G. N., and Kim, G. 2012. Production, degradation, and flux of dissolved organic matter in the subterranean estuary of a large tidal flat. *Marine Chemistry, 142,* pp.1-10.

Kim, S., Simpson, A. J., Kujawinski, E. B., Freitas, M. A., and Hatcher, P. G., 2003. High resolution electrospray ionization mass spectrometry and 2D solution NMR for the analysis of DOM extracted by C18 solid phase disk. *Organic Geochemistry*, *34*(9), pp.1325–1335.

Kim, S., Kaplan, L. A., Benner, R., and Hatcher, P. G., 2004. Hydrogen-deficient molecules in natural riverine water samples—evidence for the existence of black carbon in DOM. *Marine Chemistry*, *92*(1–4), pp.225–234.

Kimble, J.M., Follett, R.F. and Stewart, B.A., 2000. *Assessment Methods for Soil Carbon* (No. 631.41 A846a). Boca Raton, US: CRC Press.

Kirk, J. T. O., 1976. 'Yellow substance (gelbstoff) and its contribution to the attenuation of photosynthetically active radiation in some inland and coastal south-eastern Australian waters', *Marine and Freshwater Research*, 27(1), pp. 61–71.

Klausmeier, C.A., Litchman, E., Daufresne, T. and Levin, S.A., 2004. Optimal nitrogen-to-phosphorus stoichiometry of phytoplankton. *Nature*, *429*(6988), pp.171–174.

Kleypas, J. A., Feely, R. A., Fabry, V. J., Langdon, C., Sabine, C. L., and Robbins, L. L., 2005. Impacts of ocean acidification on coral reefs and other marine calcifiers: a guide for future research. In *Report of a workshop held*. (Vol. 18 p. 20).

Klug, J.L. and Cottingham, K.L., 2001. Interactions among environmental drivers: community responses to changing nutrients and dissolved organic carbon. *Ecology*, *82*(12), pp.3390–3403.

Koch, B. P., Ludwichowski, K. U., Kattner, G., Dittmar, T., and Witt, M., 2008. Advanced characterization of marine dissolved organic matter by combining reversed-phase liquid chromatography and FT-ICR-MS. *Marine Chemistry*, *111*(3–4), pp.233–241.

Koch, B. P., Witt, M., Engbrodt, R., Dittmar, T., and Kattner, G. 2005. Molecular formulae of marine and terrigenous dissolved organic matter detected by electrospray ionization Fourier transform ion cyclotron resonance mass spectrometry. *Geochimica et Cosmochimica Acta*, *69*(13), pp.3299–3308.

Koch, B.P., Dittmar, T., Witt, M., and Kattner, G., 2007. Fundamentals of Molecular Formula Assignment to Ultrahigh Resolution Mass Data of Natural Organic Matter. *Analytical Chemistry*, *79*(4), pp.1758–1763.

Koch, B.P. and Dittmar, T., 2006. From mass to structure: an aromaticity index for high-resolution mass data of natural organic matter. *Rapid Communications in Mass Spectrometry*, *20*(5), pp.926–932.

Kokya, B.A. and Kokya, T.A., 2008. Proposing a formula for evaporation measurement from salt water resources. *Hydrological Processes*, *22*(12), pp.2005–2012.

Koch, B. P., Dittmar, T., Witt, M., and Kattner, G., 2005. Characterization of chromophoric dissolved organic matter (CDOM) in the Baltic Sea by excitation emission matrix fluorescence spectroscopy. *Marine Chemistry*, *96*(3–4), pp.273–292.

Kowalczuk, P., Durako, M. J., Young, H., Kahn, A. E., Cooper, W. J., and Gonsior, M., 2009. Characterization of dissolved organic matter fluorescence in the South Atlantic Bight with use of PARAFAC model: Interannual variability. *Marine Chemistry*, *113*(3), pp.182–196.

Kristensen, E., Ahmed, S.I. & Devol, A.H., 1995. Aerobic and anaerobic decomposition of organic matter in marine sediment: Which is fastest? *Limnology and Oceanography*, *40*(8), pp.1430–1437.

Kroeger, K.D. and Charette, M.A., 2008. Nitrogen biogeochemistry of submarine groundwater discharge. *Limnology and Oceanography*, *53*(3), pp.1025–1039.

Kujawinski, E. B., Longnecker, K., Blough, N. V., Del Vecchio, R., Finlay, L., Kitner, J. B., and Giovannoni, S. J., 2009. Identification of possible source markers in marine dissolved organic matter using ultrahigh resolution mass spectrometry. *Geochimica et Cosmochimica Acta*, *73*(15), pp.4384–4399.

Kujawinski, E. B., Freitas, M. A., Zang, X., Hatcher, P. G., Green-Church, K. B., and Jones, R. B., 2002. The application of electrospray ionization mass spectrometry (ESI MS) to the

structural characterization of natural organic matter. *Organic Geochemistry*, *33*(3), pp.171–180.

Kujawinski, E.B., 2011. The Impact of Microbial Metabolism on Marine Dissolved Organic Matter. *Annual Review of Marine Science*, *3*(1), pp.567–599.

LACHAT, 2014. LACHAT QuikChem 8500FIA System Manual.

Lakowicz, J.R., 2006. *Principles of Fluorescence Spectroscopy*. *Journal of Biomedical Optics*, *13*(2), p.029901.

Lakowicz, J.R., 1983. Protein Fluorescence. In *Principles of Fluorescence Spectroscopy*. (pp. 341–381). Springer US.

Lambert, M.J. and Burnett, W.C., 2003. Submarine groundwater discharge estimates at a Florida coastal site based on continuous radon measurements. *Biogeochemistry*, *66*(1-2), pp.55–73.

Lancelot, C., Fasham, M., Legendre, L., Radach, G., Scott, M., and Kirchman, D. L., 1993. Dissolved Organic Matter in Biogeochemical Models of the Ocean. In G. T. Evans and M. J. R. Fasham, eds. *Towards a Model of Ocean Biogeochemical Processes*. NATO ASI Series. (pp., 209–225).. Springer Berlin Heidelberg.

Lane, R.R., Day, J.W., Justic, D., Reyes, E., Marx, B., Day, J.N. and Hyfield, E., 2004. Changes in stoichiometric Si, N and P ratios of Mississippi River water diverted through coastal wetlands to the Gulf of Mexico. *Estuarine, Coastal and Shelf Science*, *60*(1), pp.1–10.

Lange, H.J.D., Morris, D.P. and Williamson, C.E., 2003. Solar ultraviolet photodegradation of DOC may stimulate freshwater food webs. *Journal of Plankton Research*, *25*(1), pp.111–117.

Langer, G., Geisen, M., and Baumann, KH., 2006. 'Species-specific responses of calcifying algae to changing seawater carbonate chemistry', *Geochemistry, Geophysics, Geosystems*, 7(9), p. Q09006. doi: 10.1029/2005GC001227.

Lapworth, D. J., Gooddy, D. C., Morris, B. L., and Butcher, A., 2007. Investigating groundwater movement and pathogen transport in sandstone aquifers using intrinsic fluorescence spectroscopy.

Lapworth, D. J., Gooddy, D. C., Butcher, A. S., and Morris, B. L., 2008. Tracing groundwater flow and sources of organic carbon in sandstone aquifers using fluorescence properties of dissolved organic matter (DOM). *Applied Geochemistry*, *23*(12), pp.3384–3390.

Lavery, P.S. and McComb, A.J., 2009. The Nutritional Eco-physiology of Chaetomorpha linum and Ulva rigida in Peel Inlet, Western Australia. *Botanica Marina*, *34*(3), pp.251–260.

Lawaetz, A.J. and Stedmon, C.A., 2009. Fluorescence intensity calibration using the Raman scatter peak of water. *Applied spectroscopy*, *63*(8), pp.936–940.

Lee, Y. W., Hwang, D. W., Kim, G., Lee, W. C., and Oh, H. T., 2009. Nutrient inputs from submarine groundwater discharge (SGD) in Masan Bay, an embayment surrounded by heavily industrialized cities, Korea. *Science of the total environment*, *407*(9), pp.3181–3188.

Lee, C. M., Jiao, J. J., Luo, X., and Moore, W. S., 2012. Estimation of submarine groundwater discharge and associated nutrient fluxes in Tolo Harbour, Hong Kong. *Science of the Total Environment*, *433*, pp.427–433.

Lee, J. and Kim, G., 2015. Dependence of coastal water pH increases on submarine groundwater discharge off a volcanic island. *Estuarine, Coastal and Shelf Science*, *163*, Part B, pp.15–21.

Leenheer, J.A. and Croué, J.-P., 2003. Peer reviewed: characterizing aquatic dissolved organic matter. *Environmental science & technology*, *37*(1), p.18A–26A.

Leote, C., Ibánhez, J.S. and Rocha, C., 2008. Submarine Groundwater Discharge as a nitrogen source to the Ria Formosa studied with seepage meters. *Biogeochemistry*, *88*(2), pp.185–194.

Lewis, E., Wallace, D. and Allison, L.J., 1998. *Program developed for CO2 system calculations*, Carbon Dioxide Information Analysis Center, managed by Lockheed Martin Energy Research Corporation for the US Department of Energy Tennessee.

Litchman, E. and Klausmeier, C.A., 2008. Trait-Based Community Ecology of Phytoplankton. *Annual Review of Ecology, Evolution, and Systematics*, *39,* pp.615–639.

Liu, Q., Charette, M.A., Henderson, P.B., McCorkle, D.C., Martin, W. and Dai, M., 2014. Effect of submarine groundwater discharge on the coastal ocean inorganic carbon cycle. *Limnology and Oceanography*, *59*(5), pp.1529–1554.

Liu Q., Dai, M., Chen, W., Huh, C-A., Wang, G., Li, Q. and Charette, M.A., 2012. How significant is submarine groundwater discharge and its associated dissolved inorganic carbon in a river-dominated shelf system? *Biogeosciences*, *9*(5), pp.1777–1795.

Liu, Q., Charette, M.A., Breier, C.F., Henderson, P.B., McCorkle, D.C., Martin, W. and Dai, M., 2017. Carbonate system biogeochemistry in a subterranean estuary – Waquoit Bay, USA. *Geochimica et Cosmochimica Acta*, *203*, pp.422–439.

Lønborg, C., Álvarez-Salgado, X. A., Davidson, K., Martínez-García, S., and Teira, E., 2010. Assessing the microbial bioavailability and degradation rate constants of dissolved organic matter by fluorescence spectroscopy in the coastal upwelling system of the Ría de Vigo. *Marine Chemistry*, *119*(1–4), pp.121–129.

Longnecker, K. and Kujawinski, E.B., 2011. Composition of dissolved organic matter in groundwater. *Geochimica et Cosmochimica Acta*, *75*(10), pp.2752–2761.

Lueker, T. J., Dickson, A. G. and Keeling, C. D. (2000) 'Ocean pCO2 calculated from dissolved inorganic carbon, alkalinity, and equations for K1 and K2: validation based on laboratory measurements of CO2 in gas and seawater at equilibrium', *Marine Chemistry*, 70(1–3), pp. 105–119.

Lusk, M.G. and Toor, G.S., 2016. Dissolved organic nitrogen in urban streams: Biodegradability and molecular composition studies. *Water Research*, *96*, pp.225–235.

MacCarthy, P., 2001. The principles of humic substances: An introduction to the first principle. In E. A. Ghabbour and G. Davies, eds. *Humic Substances*. Cambridge: Royal Society of Chemistry, pp., 19–30.

MacIntyre, S., Wanninkhof, R. and Chanton, J.P., 1995. Trace gas exchange across the air-water interface in freshwater and coastal marine environments. *Biogenic trace gases: Measuring emissions from soil and water*, pp.98-125.

Mackenzie, F.T., Ver, L.M. and Lerman, A., 2002. Century-scale nitrogen and phosphorus controls of the carbon cycle. *Chemical Geology*, *190*(1–4), pp.13–32.

Macpherson, G.L., 2009. CO2 distribution in groundwater and the impact of groundwater extraction on the global C cycle. *Chemical Geology*, *264*(1–4), pp.328–336.

Maher, D.T., Santos, I.R., Golsby-Smith, L., Gleeson, J. and Eyre, B.D., 2013. Groundwater-derived dissolved inorganic and organic carbon exports from a mangrove tidal creek: The missing mangrove carbon sink? *Limnology and Oceanography*, *58*(2), pp.475–488.

Maher, D.T., Cowley, K., Santos, I.R., Macklin, P. and Eyre, B.D., 2015. Methane and carbon dioxide dynamics in a subtropical estuary over a diel cycle: Insights from automated in situ radioactive and stable isotope measurements. *Marine Chemistry*, *168*, pp.69–79.

Maie, N., Yang, C., Miyoshi, T., Parish, K., and Jaffé, R., 2005. Chemical characteristics of dissolved organic matter in an oligotrophic subtropical wetland/estuarine ecosystem. *Limnology and Oceanography*, *50*(1), pp.23–35.

Maie, N., Boyer, J. N., Yang, C., and Jaffé, R., 2006. Spatial, geomorphological, and seasonal variability of CDOM in estuaries of the Florida Coastal Everglades. *Hydrobiologia*, *569*(1), pp.135–150.

Martins, I., Oliveira, J. M., Flindt, M. R., and Marques, J. C., 1999. The effect of salinity on the growth rate of the macroalgae Enteromorpha intestinalis (Chlorophyta) in the Mondego estuary (west Portugal). *Acta Oecologica*, *20*(4), pp.259–265.

Matson, P. A. Parton, WL., Power, AG., and Swift, MJ., 1997. 'Agricultural Intensification and Ecosystem Properties', *Science*, 277(5325), pp. 504–509. doi: 10.1126/science.277.5325.504.

Mayer, L.M., Schick, L.L. and Loder, T.C., 1999. Dissolved protein fluorescence in two Maine estuaries. *Marine Chemistry*, *64*(3), pp.171–179.

McCormack, T., Gill, L. W., Naughton, O., and Johnston, P. M., 2014. Quantification of submarine/intertidal groundwater discharge and nutrient loading from a lowland karst catchment. *Journal of Hydrology*, *519*, Part B, pp.2318–2330.

McCormack, T. and Naughton, O., 2016. 'Groundwater flooding in the Gort lowlands', *Irish Groundwater Newsletter*, p. 7.

McCarthy, J.J., 2001. *Climate Change 2001: Impacts, Adaptation, and Vulnerability: Contribution of Working Group II to the Third Assessment Report of the Intergovernmental Panel on Climate Change*, Cambridge University Press.

McGlathery, K. J., Sundbäck, K., and Anderson, I. C., 2007. Eutrophication in shallow coastal bays and lagoons: the role of plants in the coastal filter. *Marine Ecology Progress Series*, *348*(1), pp.1–18.

McGrath, T., McGovern, E., Cave, R.R. and Kivimäe, C., (2016) 'The Inorganic Carbon Chemistry in Coastal and Shelf Waters Around Ireland', *Estuaries and Coasts*, 39(1), pp. 27–39. doi: 10.1007/s12237-015-9950-6.

McIntyre, A.M. and Guéguen, C., 2013. Binding interactions of algal-derived dissolved organic matter with metal ions. *Chemosphere*, *90*(2), pp.620–626.

McKnight, D. M., Boyer, E. W., Westerhoff, P. K., Doran, P. T., Kulbe, T., and Andersen, D. T., 2001. Spectrofluorometric characterization of dissolved organic matter for indication of precursor organic material and aromaticity. *Limnology and Oceanography*, *46*(1), pp.38–48.

McQuatters-Gollop, A., Gilbert, A. J., Mee, L. D., Vermaat, J. E., Artioli, Y., Humborg, C., and Wulff, F. 2009. How well do ecosystem indicators communicate the effects of anthropogenic eutrophication? *Estuarine, Coastal and Shelf Science*, *82*(4), pp.583–596.

Mehrbach, C., 1973. Measurement of the apparent dissociation constants of carbonic acid in seawater at atmospheric pressure. *Limnology and Oceanography, 18(6),* pp.897-907.

Mengis, M., Gächter, R., Wehrli, B. and Bernasconi, S., 1997. Nitrogen elimination in two deep eutrophic lakes. *Limnology and Oceanography*, *42*(7), pp.1530–1543.

Miller, A.E.J., 1999. Seasonal Investigations of Dissolved Organic Carbon Dynamics in the Tamar Estuary, U.K. *Estuarine, Coastal and Shelf Science*, *49*(6), pp.891–908.

Miller and Moran, M.A., 1997. Interaction of photochemical and microbial processes in the degradation of refractory dissolved organic matter from a coastal marine environment. *Limnology and Oceanography*, *42*, pp.1317–1324.

Millero, F.J., Pierrot, D., Lee, K., Wanninkhof, R., Feely, R., Sabine, C.L., Key, R.M. and Takahashi, T., 2002. Dissociation constants for carbonic acid determined from field measurements. *Deep Sea Research Part I: Oceanographic Research Papers*, *49*(10), pp.1705–1723.

Mobed, J. J., Hemmingsen, S. L., Autry, J. L., and McGown, L. B., 1996. Fluorescence Characterization of IHSS Humic Substances: Total Luminescence Spectra with Absorbance Correction. *Environmental Science & Technology*, *30*(10), pp.3061–3065.

Møller, E.F., 2007. Production of dissolved organic carbon by sloppy feeding in the copepods Acartia tonsa, Centropages typicus, and Temora longicornis. *Limnology and Oceanography*, *52*(1), pp.79–84.

Møller, E.F., Thor, P. & Nielsen, T.G., 2003. Production of DOC by Calanus finmarchicus, C. glacialis and C. hyperboreus through sloppy feeding and leakage from fecal pellets. *Marine Ecology Progress Series*, *262*, pp.185–191.

Montluçon, D. and Sañudo-Wilhelmy, S.A., 2001. Influence of Net Groundwater Discharge on the Chemical Composition of a Coastal Environment: Flanders Bay, Long Island, New York. *Environmental Science & Technology*, *35*(3), pp.480–486.

Moore, W.S., 1999. The subterranean estuary: a reaction zone of ground water and sea water. *Marine Chemistry*, *65*(1–2), pp.111–125.

Moore, W.S., 2003. Sources and fluxes of submarine groundwater discharge delineated by radium isotopes. *Biogeochemistry*, *66*(1-2), pp.75–93.

Moore, W.S., Blanton, J.O. and Joye, S.B., 2006. Estimates of flushing times, submarine groundwater discharge, and nutrient fluxes to Okatee Estuary, South Carolina. *Journal of Geophysical Research: Oceans, 111*(C9).

Moore, W.S., Sarmiento, J.L. and Key, R.M., 2008. Submarine groundwater discharge revealed by 228Ra distribution in the upper Atlantic Ocean. *Nature Geoscience*, *1*(5), pp.309–311.

Moore, W.S., 2010. The Effect of Submarine Groundwater Discharge on the Ocean. *Annual Review of Marine Science*, *2*(1), pp.59–88.

Moore, W.S., Beck, M., Riedel, T., Van Der Loeff, M.R., Dellwig, O., Shaw, T.J., Schnetger, B. and Brumsack, H.J., 2011. Radium-based pore water fluxes of silica, alkalinity,

manganese, DOC, and uranium: A decade of studies in the German Wadden Sea. *Geochimica et Cosmochimica Acta*, *75*(21), pp.6535–6555.

Moran, M.A. and Covert, J.S., 2003. Photochemically mediated linkages between dissolved organic matter and bacterioplankton. *Aquatic ecosystems: interactivity of dissolved organic matter*, pp.243–262.

Moran, M.A. and Hodson, R.E., 1990. Bacterial production on humic and nonhumic components of dissolved organic carbon. *Limnol. Oceanogr*, *35*(8), pp.1744–1756.

Moran, M.A., Sheldon, W.M. and Zepp, R.G., 2000. Carbon loss and optical property changes during long-term photochemical and biological degradation of estuarine dissolved organic matter. *Limnology and Oceanography*, *45*(6), pp.1254–1264.

Moran, M.A. and Zepp, R.G., 1997. Invited Review Role of photoreactions in the formation of biologically labile compounds from dissolved organic matter. *Oceanography*, *42*(6). pp.1307-1316.

Moore, C.J., 2008. Synthetic polymers in the marine environment: A rapidly increasing, long-term threat. *Environmental Research*, *108*(2), pp.131–139.

Mostofa, K.M., Wu, F., Liu, C.Q., Fang, W.L., Yuan, J., Ying, W.L., Wen, L. and Yi, M., 2010. Characterization of Nanming River (southwestern China) sewerage-impacted pollution using an excitation-emission matrix and PARAFAC. *Limnology*, *11*(3), pp.217–231.

Mopper, K., Zhou, X., Kieber, R.J., Kieber, D.J., Sikorski, R.J. and Jones, R.D., 1991. Photochemical degradation of dissolved organic carbon and its impact on the oceanic carbon cycle. *Nature*, *353*(6339), pp.60–62.

Mopper, K., Kieber, D.J., Stubbins, A., Hansell, D. and Carlson, C., 2015. Marine photochemistry of organic matter: processes and impacts. *Biogeochemistry of marine dissolved organic matter*, 2, pp.389-450.

Moyle, P.B. & Leidy, R.A., 1992. Loss of biodiversity in aquatic ecosystems: evidence from fish faunas. In *Conservation biology*. pp. 127–169. Springer US.

Mucci, A., 1983. The solubility of calcite and aragonite in seawater at various salinities, temperatures, and one atmosphere total pressure. *American Journal of Science*, *283*(7), pp.780–799.

Mudarra, M., A.B. and Andreo, B., 2011. Characterisation of dissolved organic matter in karst spring waters using intrinsic fluorescence: Relationship with infiltration processes. *Science of the Total Environment*, *409*, pp.3448–3462.

Muller-Karger, F.E., Varela, R., Thunell, R., Luerssen, R., Hu, C. and Walsh, J.J., 2005. The importance of continental margins in the global carbon cycle. *Geophysical Research Letters*, *32*(1), p.L01602.

Murphy, E.M., Davis, S.N., Long, A., Donahue, D. and Jull, A.J., 1989. Characterization and isotopic composition of organic and inorganic carbon in the Milk River Aquifer. *Water Resources Research*, *25*(8), pp.1893–1905.

Murphy, K.R., Stedmon, C.A., Waite, T.D. and Ruiz, G.M., 2008. Distinguishing between terrestrial and autochthonous organic matter sources in marine environments using fluorescence spectroscopy. *Marine Chemistry*, *108*(1–2), pp.40–58.

Murphy, K.R., Butler, K.D., Spencer, R.G., Stedmon, C.A., Boehme, J.R. and Aiken, G.R., 2010. Measurement of Dissolved Organic Matter Fluorescence in Aquatic Environments: An Interlaboratory Comparison. *Environmental Science & Technology*, *44*(24), pp.9405–9412.

Murray, A.E., Arnosti, C., Christina, L., Grossart, H.P. and Passow, U., 2007. Microbial dynamics in autotrophic and heterotrophic seawater mesocosms. II. Bacterioplankton community structure and hydrolytic enzyme activities. *Aquatic Microbial Ecology*, *49*(2), pp.123-141.

Murray, C., Markager, S., Stedmon, CA., Juul-Pedersen, T., Sejr, MK. and Bruhn, A., 2015. 'The influence of glacial melt water on bio-optical properties in two contrasting Greenlandic fjords', *Estuarine, Coastal and Shelf Science*, 163(Part B), pp. 72–83. doi: 10.1016/j.ecss.2015.05.041.

Naughton, O., Johnston, P.M. and Gill, L.W., 2012. Groundwater flooding in Irish karst: The hydrological characterisation of ephemeral lakes (turloughs). *Journal of Hydrology, 470,* pp.82-97.

Nebbioso, A. and Piccolo, A., 2012. Molecular characterization of dissolved organic matter (DOM): a critical review. *Analytical and Bioanalytical Chemistry*, *405*(1), pp.109–124.

Neff, J.C., Chapin, F.S. & Vitousek, P.M., 2003. Breaks in the Cycle: Dissolved Organic Nitrogen in Terrestrial Ecosystems. *Frontiers in Ecology and the Environment*, *1*(4), pp.205–211.

Nelson, D.M., Tréguer, P., Brzezinski, M.A., Leynaert, A. and Quéguiner, B., 1995. Production and dissolution of biogenic silica in the ocean: Revised global estimates, comparison with regional data and relationship to biogenic sedimentation. *Global Biogeochemical Cycles*, *9*(3), pp.359–372.

Nelson, C.E., Donahue, M.J., Dulaiova, H., Goldberg, S.J., La Valle, F.F., Lubarsky, K., Miyano, J., Richardson, C., Silbiger, N.J. and Thomas, F.I., 2015. Fluorescent dissolved organic matter as a multivariate biogeochemical tracer of submarine groundwater discharge in coral reef ecosystems. *Marine Chemistry*, *177,* Part 2, pp.232–243.

Nelson, N.B. and Coble, P.G., 2010. Optical analysis of chromophoric dissolved organic matter. *Practical Guidelines for the Analysis of Seawater*, pp.79–96.

Newton, A., Icely, J.D., Falcão, M., Nobre, A., Nunes, J.P., Ferreira, J.G. and Vale, C., 2003. Evaluation of eutrophication in the Ria Formosa coastal lagoon, Portugal. *Continental Shelf Research*, *23*(17–19), pp.1945–1961.

Nguyen, B.T. and Lehmann, J., 2009. Black carbon decomposition under varying water regimes. *Organic Geochemistry*, *40*(8), pp.846–853.

Nielsen, S.L., Banta, G.T. and Pedersen, M.F., 2004. Decomposition of marine primary producers: consequences for nutrient recycling and retention in coastal ecosystems. In *Estuarine nutrient cycling: the influence of primary producers*. (pp. 187–216). Springer Netherlands.

Nixon, S.W., 1995. Coastal marine eutrophication: a definition, social causes, and future concerns. *Ophelia*, *41*(1), pp.199–219.

Null K.A., Knee, K.L., Crook, E.D., de Sieyes, N.R., Rebolledo-Vieyra, M., Hernandez-Terrones, L. and Paytan, A., 2014. Composition and fluxes of submarine groundwater along the Caribbean coast of the Yucatan Peninsula. *Continental Shelf Research*, *77*, pp.38–50.

Null, K.A., Dimova, N.T., Knee, K.L., Esser, B.K., Swarzenski, P.W., Singleton, M.J., Stacey, M. and Paytan, A., 2012. Submarine groundwater discharge-derived nutrient loads to San

Francisco Bay: Implications to future ecosystem changes. *Estuaries and coasts*, *35*(5), pp.1299–1315.

O'Boyle, S., Wilkes, R., McDermott, G., Longphuirt, S.N. and Murray, C., 2015. Factors affecting the accumulation of phytoplankton biomass in Irish estuaries and nearshore coastal waters: A conceptual model. *Estuarine, Coastal and Shelf Science*, *155*, pp.75–88.

O'Boyle, S., McDermott, G. and Wilkes, R., 2009. Dissolved oxygen levels in estuarine and coastal waters around Ireland. *Marine Pollution Bulletin*, *58*(11), pp.1657–1663.

O'Connor, A.E., Luek, J.L., McIntosh, H. and Beck, A.J., 2015. Geochemistry of redox-sensitive trace elements in a shallow subterranean estuary. *Marine Chemistry*, *172*, pp.70–81.

Ohno, T., 2002. Fluorescence inner-filtering correction for determining the humification index of dissolved organic matter. *Environmental science & technology*, *36*(4), pp.742–746.

Opsahl, S. and Benner, R., 1997. Distribution and cycling of terrigenous dissolved organic matter in the ocean. *Nature*, *386*(6624), pp.480–482.

Osburn, C.L. and Morris, D.P., 2003. Photochemistry of chromophoric dissolved organic matter in natural waters. In E. W. Helbling and H. Zagarese, eds. *UV Effects in Aquatic Organisms and Ecosystems*. The Royal Society of Chemistry, *1,* pp. 185–218. Available at: http://dx.doi.org/10.1039/9781847552266-00185.

Osburn, C.L., Retamal, L. and Vincent, W.F., 2009. Photoreactivity of chromophoric dissolved organic matter transported by the Mackenzie River to the Beaufort Sea. *Marine Chemistry*, *115*(1–2), pp.10–20.

Pabich, W.J., Valiela, I. and Hemond, H.F., 2001. Relationship between DOC concentration and vadose zone thickness and depth below water table in groundwater of Cape Cod, U.S.A. *Biogeochemistry*, *55*(3), pp.247–268.

Paerl, H.W., 2009. Controlling Eutrophication along the Freshwater–Marine Continuum: Dual Nutrient (N and P) Reductions are Essential. *Estuaries and Coasts*, *32*(4), pp.593–601.

Parlanti, E., Wörz, K., Geoffroy, L. and Lamotte, M., 2000. Dissolved organic matter fluorescence spectroscopy as a tool to estimate biological activity in a coastal zone submitted to anthropogenic inputs. *Organic Geochemistry*, *31*(12), pp.1765–1781.

Passow, U., De La Rocha, CL., Arnosti, C., Grossart, H-P., Murray, A. and Engel, A., 2007. 'Microbial dynamics in autotrophic and heterotrophic seawater mesocosms. I. Effect of phytoplankton on the microbial loop', *Aquatic Microbial Ecology*, 49(2), pp. 109–121. doi: 10.3354/ame01138.

Pavlidou, A., Papadopoulos, V.P., Hatzianestis, I., Simboura, N., Patiris, D. and Tsabaris, C., 2014. Chemical inputs from a karstic submarine groundwater discharge (SGD) into an oligotrophic Mediterranean coastal area. *Science of The Total Environment*, *488–489,* pp.1–13.

Paytan, A., Shellenbarger, G.G., Street, J.H., Gonneea, M.E., Davis, K., Young, M.B. and Moore, W.S., 2006. Submarine groundwater discharge: An important source of new inorganic nitrogen to coral reef ecosystems. *Limnology and Oceanography*, *51*(1), pp.343–348.

Peng, T.-H., Takahashi, T., Broecker, WS. and Olafsson, J., 1987. 'Seasonal variability of carbon dioxide, nutrients and oxygen in the northern North Atlantic surface water: observations and a model', *Tellus B: Chemical and Physical Meteorology*, 39(5), pp. 439–458. doi: 10.3402/tellusb.v39i5.15361.

Pereira, H.C., Allott, N., Coxon, C., Naughton, O., Johnston, P. and Gill, L., 2011. Phytoplankton of turloughs (seasonal karstic Irish lakes). *Journal of Plankton Research*, *33*(3), pp.385–403.

Petrunic, B., Einsiedl, F. and Duffy, G., 2012. Major Ion Chemistry in a Coastal Karstic Groundwater Resource Located in Western Ireland. *Irish Journal of Earth Sciences*,, pp.13–30.

Pierrot, D. E. Lewis,and D. W. R. Wallace. 2006. MS Excel Program Developed for CO2 System Calculations. ORNL/CDIAC-105a. Carbon Dioxide Information Analysis Center, Oak Ridge National Laboratory, U.S. Department of Energy, Oak Ridge, Tennessee. doi: 10.3334/CDIAC/otg.CO2SYS_XLS_CDIAC105a

Pitois, S., Jackson, M.H. and Wood, B.J., 2001. Sources of the eutrophication problems associated with toxic algae: an overview. *Journal of environmental Health*, *64*(5), pp.25–32.

Porubsky, W. P., Weston, N. B. and Joye, S. B., 2009. 'Benthic metabolism and the fate of dissolved inorganic nitrogen in intertidal sediments', *Estuarine, Coastal and Shelf Science*, 83(4), pp. 392–402. doi: 10.1016/j.ecss.2009.04.012.

Porubsky, W.P., Weston, N.B., Moore, W.S., Ruppel, C. and Joye, S.B., 2014. Dynamics of submarine groundwater discharge and associated fluxes of dissolved nutrients, carbon, and trace gases to the coastal zone (Okatee River estuary, South Carolina). *Geochimica et Cosmochimica Acta*, *131*, pp.81–97.

Povinec, P.P., Aggarwal, P.K., Aureli, A., Burnett, W.C., Kontar, E.A., Kulkarni, K.M., Moore, W.S., Rajar, R., Taniguchi, M., Comanducci, J.F. and Cusimano, G., 2006. Characterisation of submarine groundwater discharge offshore south-eastern Sicily. *Journal of Environmental Radioactivity*, *89*(1), pp.81–101.

Premrov, A., Coxon, C.E., Hackett, R., Kirwan, L. and Richards, K.G., 2012. Effects of over-winter green cover on groundwater nitrate and dissolved organic carbon concentrations beneath tillage land. *Science of the Total Environment*, *438*, pp.144–153.

Provoost, P., van Heuven, S., Soetaert, K., Laane, R.W.P.M. and Middelburg, J.J., 2010. Seasonal and long-term changes in pH in the Dutch coastal zone. *Biogeosciences*, *7*(11), pp.3869–3878.

Qualls, R.G. and Haines, B.L., 1991. Geochemistry of dissolved organic nutrients in water percolating through a forest ecosystem. *Soil Science Society of America Journal*, *55*(4), pp.1112–1123.

R Development Core Team, 2008. R: A language and environment for > statistical computing. R Foundation for Statistical Computing, > Vienna, Austria. ISBN 3-900051-07-0, URL http://www.R-project.org.

Rabalais, N.N., Harper, D.E. & Turner, R.E., 2001. Responses of Nekton and Demersal and Benthic Fauna to Decreasing Oxygen Concentrations. In N. N. Rabalais & R. E. Turner, eds. *Coastal Hypoxia: Consequences for Living Resources and Ecosystems*. American Geophysical Union, pp. 115–128.

Manaswi Raghurama (2015) *Changes in Macroalgal C:N:P and Nutrient Cycling by Intertial Sediments with Increasing Pollution A study in Kinvarra Bay, Ireland*. Trinity College Dublin.

Ramesh, R., Chen, Z., Cummins, V., Day, J., D'Elia, C., Dennison, B., Forbes, D.L., Glaeser, B., Glaser, M., Glavovic, B. and Kremer, H., 2015. 'Land–Ocean Interactions in the Coastal

Zone: Past, present & future', *Anthropocene*, 12(Supplement C), pp. 85–98. doi: 10.1016/j.ancene.2016.01.005.

Raymond, P.A. and Cole, J.J., 2003. Increase in the Export of Alkalinity from North America's Largest River. *Science*, *301*(5629), pp.88–91.

Raymond, P.A. and Bauer, J.E., 2000. Bacterial consumption of DOC during transport through a temperate estuary. *Aquatic Microbial Ecology*, *22*(1), pp.1–12.

Raymond, P.A., Bauer, J.E. and Cole, J.J., 2000. Atmospheric CO~ 2 evasion, dissolved inorganic carbon production, and net heterotrophy in the York River estuary. *Limnology and Oceanography*, *45*(8), pp.1707–1717.

Redfield, A.C., 1958. The Biological Control of Chemical Factors in the Environment. *American Scientist*, *46*(3), p.230A–221.

Redfield, A.C., Ketchum, B.H., Richard, F.A., 1963. The influence of organisms on the composition of seawater. *The sea*, 2, pp. 26–77.

Repeta, D.J., Quan, T.M., Aluwihare, L.I. and Accardi, A., 2002. Chemical characterization of high molecular weight dissolved organic matter in fresh and marine waters. *Geochimica et Cosmochimica Acta*, *66*(6), pp.955–962.

Rocha, C., Wilson, J., Scholten, J., and Schubert, M., 2015. Retention and fate of groundwater-borne nitrogen in a coastal bay (Kinvara Bay, Western Ireland) during summer. *Biogeochemistry*, *125*(2), 275-299.

Rocha, C., Ibanhez, J. and Leote, C., 2009. Benthic nitrate biogeochemistry affected by tidal modulation of Submarine Groundwater Discharge (SGD) through a sandy beach face, Ria Formosa, Southwestern Iberia. *Marine Chemistry*, *115*(1–2), pp.43–58.

Rochelle-Newall, E.J. and Fisher, T.R., 2002. Production of chromophoric dissolved organic matter fluorescence in marine and estuarine environments: an investigation into the role of phytoplankton. *Marine Chemistry*, *77*(1), pp.7–21.

Rodellas, V., Garcia-Orellana, J., Masqué, P., Feldman, M. and Weinstein, Y., 2015. Submarine groundwater discharge as a major source of nutrients to the Mediterranean Sea. *Proceedings of the National Academy of Sciences*, *112*(13), pp.3926–3930.

Rodellas, V., Garcia-Orellana, J., Trezzi, G., Masqué, P., Stieglitz, T.C., Bokuniewicz, H., Cochran, J.K. and Berdalet, E., 2017. Using the radium quartet to quantify submarine groundwater discharge and porewater exchange. *Geochimica et Cosmochimica Acta*, *196,* pp.58–73.

Rosenstock, B., Zwisler, W. and Simon, M., 2005. Bacterial Consumption of Humic and Non-Humic Low and High Molecular Weight DOM and the Effect of Solar Irradiation on the Turnover of Labile DOM in the Southern Ocean. *Microbial Ecology*, *50*(1), pp.90–101.

Romera-Castillo, C., Sarmento, H., Álvarez-Salgado, X.A., Gasol, J.M. and Marrasé, C., 2011. Net Production and Consumption of Fluorescent Colored Dissolved Organic Matter by Natural Bacterial Assemblages Growing on Marine Phytoplankton Exudates. *Applied and Environmental Microbiology*, *77*(21), pp.7490–7498.

Sadat-Noori, M., Maher, D.T. and Santos, I.R., 2016. Groundwater discharge as a source of dissolved carbon and greenhouse gases in a subtropical estuary. *Estuaries and Coasts*, *39*(3), pp.639–656.

Salonen, K. and Vähätalo, A., 1994. Photochemical mineralisation of dissolved organic matter in lake Skjervatjern. *Environment International*, *20*(3), pp.307–312.

Santos, I.R., Glud R.N., Maher S., Erler D. and Eyre B.D., 2011. Diel coral reef acidification driven by porewater advection in permeable carbonate sands, Heron Island, Great Barrier Reef. *Geophysical Research Letters*, *38*(3), p.L03604.

Santos, I.R., Burnett, W.C., Dittmar, T., Suryaputra, I.G. and Chanton, J., 2009. Tidal pumping drives nutrient and dissolved organic matter dynamics in a Gulf of Mexico subterranean estuary. *Geochimica et Cosmochimica Acta*, *73*(5), pp.1325–1339.

Santos, I.R., Burnett, W.C., Chanton, J., Mwashote, B., Suryaputra, I.G.N.A. and Dittmar, T., 2008. Nutrient biogeochemistry in a Gulf of Mexico subterranean estuary and groundwater-derived fluxes to the coastal ocean. *Limnology and Oceanography*, *53*(2), pp.705–718.

Santos, I.R., Maher, D.T. and Eyre, B.D., 2012. Coupling Automated Radon and Carbon Dioxide Measurements in Coastal Waters. *Environmental Science Technology*, *46*, pp.7685–7691.

Sardans, J., Rivas-Ubach, A. and Peñuelas, J., 2012. The C:N:P stoichiometry of organisms and ecosystems in a changing world: A review and perspectives. *Perspectives in Plant Ecology, Evolution and Systematics*, *14*(1), pp.33–47.

Schopka, H.H. and Derry, L.A., 2012. Chemical weathering fluxes from volcanic islands and the importance of groundwater: The Hawaiian example. *Earth and Planetary Science Letters*, *339–340,* pp.67–78.

Schimel, D.S., 1995. Terrestrial ecosystems and the carbon cycle. *Global Change Biology*, *1*(1), pp.77–91.

Schmidt, M.W.I. and Noack, A.G., 2000. Black carbon in soils and sediments: Analysis, distribution, implications, and current challenges. *Global Biogeochemical Cycles*, *14*(3), pp.777–793.

Schubert, M., Knoeller, K., Rocha, C. and Einsiedl, F., 2015. Evaluation and source attribution of freshwater contributions to Kinvarra Bay, Ireland, using 222Rn, EC and stable isotopes as natural indicators. *Environmental Monitoring and Assessment*, *187*(3), pp.1–15.

Sfriso, A., Pavoni, B., Marcomini, A. and Orio, A.A., 1992. Macroalgae, nutrient cycles, and pollutants in the Lagoon of Venice. *Estuaries*, *15*(4), pp.517–528.

Shah, A.A., Hasan, F., Hameed, A. and Ahmed, S., 2008. Biological degradation of plastics: A comprehensive review. *Biotechnology Advances*, *26*(3), pp.246–265.

Shank, G.C., Nelson, K. and Montagna, P.A., 2009. Importance of CDOM Distribution and Photoreactivity in a Shallow Texas Estuary. *Estuaries and Coasts*, *32*(4), pp.661–677.

Shaw, T.J., 2003. Biogeochemical Processes in Coastal Aquifers and Permeable Sediments. *Aquatic Geochemistry*, *9*(3), pp.165–169.

Skeffington, M.S., Moran, J., Connor, Á.O., Regan, E., Coxon, C.E., Scott, N.E. and Gormally, M., 2006. Turloughs–Ireland's unique wetland habitat. *Biological Conservation*, *133*(3), pp.265–290.

Skeffington, M. S. and Gormally, M., 2007. 'Turloughs: a Mosaic of Biodiversity and Management Systems Unique to Ireland', *Acta Carsologica*, 36(2). doi: 10.3986/ac.v36i2.190.

Sholkovitz, E.R., 1976. Flocculation of dissolved organic and inorganic matter during the mixing of river water and seawater. *Geochimica et Cosmochimica Acta*, *40*(7), pp.831–845.

Singh, S., D'Sa, E.J. and Swenson, E.M., 2010. Chromophoric dissolved organic matter (CDOM) variability in Barataria Basin using excitation–emission matrix (EEM) fluorescence and parallel factor analysis (PARAFAC). *Science of The Total Environment*, *408*(16), pp.3211–3222.

Seidel, M., Beck, M., Riedel, T., Waska, H., Suryaputra, I.G., Schnetger, B., Niggemann, J., Simon, M. and Dittmar, T., 2014. Biogeochemistry of dissolved organic matter in an anoxic intertidal creek bank. *Geochimica et Cosmochimica Acta*, *140*, pp.418–434.

Seitzinger, S.P., 1988. Denitrification in freshwater and coastal marine ecosystems: Ecological and geochemical significance. *Limnology and Oceanography*, *33*(4part2), pp.702–724.

Seitzinger, S.P., Harrison, J.A., Dumont, E., Beusen, A.H. and Bouwman, A.F., 2005. Sources and delivery of carbon, nitrogen, and phosphorus to the coastal zone: An overview of Global Nutrient Export from Watersheds (NEWS) models and their application. *Global Biogeochemical Cycles*, *19*(4), p.GB4S01.

Seitzinger, S.P. and Sanders, R.W., 1997. Contribution of dissolved organic nitrogen from rivers to estuarine eutrophication. *Marine Ecology Progress Series*, *159*, pp.1–12.

Seitzinger, S.P., Sanders, R.W. and Styles, R., 2002. Bioavailability of DON from natural and anthropogenic sources to estuarine plankton. *Limnology and Oceanography*, *47*(2), pp.353–366.

Semple, S., 1997. Algal growth on two sections of a fringing coral reef subject to different levels of eutrophication in Reunion Island. *Oceanologica Acta*, *20*(6), pp.851–861.

Senal, M.I.S., Jacinto, G.S., San Diego-McGlone, M.L., Siringan, F., Zamora, P., Soria, L., Cardenas, M.B., Villanoy, C. and Cabrera, O., 2011. Nutrient inputs from submarine groundwater discharge on the Santiago reef flat, Bolinao, Northwestern Philippines. *Marine Pollution Bulletin*, *63*(5–12), pp.195–200.

Shrivastava, A. and Gupta, V.B., 2011. Methods for the determination of limit of detection and limit of quantitation of the analytical methods. *Chronicles of Young Scientists*, *2*(1), p.21.

Simpson, J.H. and Rippeth, T.P., 1998. Non-conservative Nutrient Fluxes from Budgets for the Irish Sea. *Estuarine, Coastal and Shelf Science*, *47*(6), pp.707–714.

Sleighter, R.L. and Hatcher, P.G., 2007. The application of electrospray ionization coupled to ultrahigh resolution mass spectrometry for the molecular characterization of natural organic matter. *Journal of Mass Spectrometry*, *42*(5), pp.559–574.

Sleighter, R.L., McKee, G.A. and Hatcher, P.G., 2009. Direct Fourier transform mass spectral analysis of natural waters with low dissolved organic matter. *Organic Geochemistry*, *40*(1), pp.119–125.

Slomp, C.P. and Van Cappellen, P., 2004. Nutrient inputs to the coastal ocean through submarine groundwater discharge: controls and potential impact. *Journal of Hydrology*, *295*(1–4), pp.64–86.

Smith, S.V., 1981. Marine macrophytes as a global carbon sink. *Science*, *211*(4484), pp.838–840.

Smith, S.V. & Buddemeier, R.W., 1992. Global Change and Coral Reef Ecosystems. *Annual Review of Ecology and Systematics*, *23*(1), pp.89–118.

Smith, C. J., DeLaune, R. D. and Patrick, W. H., 1985. 'Fate of Riverine Nitrate Entering an Estuary: I. Denitrification and Nitrogen Burial', *Estuaries*, 8(1), pp. 15–21. doi: 10.2307/1352117.

Smith, A.M. and Cave, R.R., 2012. Influence of fresh water, nutrients and DOC in two submarine-groundwater-fed estuaries on the west of Ireland. *Science of the Total Environment*, *438*, pp.260–270.

Smith, S.V., 2001. Carbon-nitrogen-phosphorus fluxes in the coastal zone: the LOICZ approach to global assessment, and scaling issues with available data. *LOICZ Newsletter*, *21*, pp.1–3.

Smith, S.V. and Hollibaugh, J.T., 1997. Annual cycle and interannual variability of ecosystem metabolism in a temperate climate embayment. *Ecological Monographs*, 67(4), pp.509–533.

Smith, S.V. and Mackenzie, F.T., 1987. The ocean as a net heterotrophic system: Implications From the carbon biogeochemical cycle. *Global Biogeochemical Cycles*, *1*(3), pp.187–198.

Socolow, R., 1997. *Industrial ecology and global change* (Vol. 5). Cambridge University Press.

Sommer, U., 1994. Are marine diatoms favoured by high Si: N ratios? *Marine Ecology Progress Series*, *115*, pp.309–315.

Søndergaard, M., Stedmon, C.A. and Borch, N.H., 2003. Fate of terrigenous dissolved organic matter (DOM) in estuaries: Aggregation and bioavailability. *Ophelia*, *57*(3), pp.161–176.

Song, J.H., Murphy, R.J., Narayan, R. and Davies, G.B.H., 2009. Biodegradable and compostable alternatives to conventional plastics. *Philosophical Transactions of the Royal Society of London B: Biological Sciences*, *364*(1526), pp.2127–2139.

Southern Water Global 1998. *An investigation of the flooding problems in the Gort - Ardrahan area of south Galway.* Southern Wtaer Global and Jennings O'Donovan and Partners for the Office of Public Works.

Spalding, R.F. and Exner, M.E., 1993. Occurrence of Nitrate in Groundwater—A Review. *Journal of Environment Quality*, *22*(3), p.392.

Stedmon, C.A. and Bro, R., 2008. Characterizing dissolved organic matter fluorescence with parallel factor analysis: a tutorial. *Limnol. Oceanogr. Methods*, *6*, pp.572–579.

Stedmon, C.A., Markager, S. and Bro, R., 2003. Tracing dissolved organic matter in aquatic environments using a new approach to fluorescence spectroscopy. *Marine Chemistry*, *82*(3–4), pp.239–254.

Stedmon, C.A. and Markager, S., 2005. Resolving the variability in dissolved organic matter fluorescence in a temperate estuary and its catchment using PARAFAC analysis. *Limnology and Oceanography*, *50*(2), pp.686–697.

Stedmon, C.A. and Markager, S., 2005a. Tracing the production and degradation of autochthonous fractions of dissolved organic matter by fluorescence analysis. *Limnology and Oceanography*, *50*(5), pp.1415–1426.

Stewart, B.T., Santos, I.R., Tait, D.R., Macklin, P.A. and Maher, D.T., 2015. Submarine groundwater discharge and associated fluxes of alkalinity and dissolved carbon into Moreton Bay (Australia) estimated via radium isotopes. *Marine Chemistry*, *174*, pp.1–12.

Stenson, A.C., Landing, W.M., Marshall, A.G. and Cooper, W.T., 2002. Ionization and Fragmentation of Humic Substances in Electrospray Ionization Fourier Transform-Ion Cyclotron Resonance Mass Spectrometry. *Analytical Chemistry*, *74*(17), pp.4397–4409.

Stephens, B.M. and Minor, E.C., 2010. DOM characteristics along the continuum from river to receiving basin: a comparison of freshwater and saline transects. *Aquatic Sciences*, *72*(4), pp.403–417.

Street, J.H., Knee, K.L., Grossman, E.E. and Paytan, A., 2008. Submarine groundwater discharge and nutrient addition to the coastal zone and coral reefs of leeward Hawai'i. *Marine Chemistry*, *109*(3–4), pp.355–376.

Stuart, M.E. and Lapworth, D.J., 2016. Macronutrient status of UK groundwater: Nitrogen, phosphorus and organic carbon. *Science of The Total Environment*, *572*, pp.1543–1560.

Stubbins, A., Spencer, R.G., Chen, H., Hatcher, P.G., Mopper, K., Hernes, P.J., Mwamba, V.L., Mangangu, A.M., Wabakanghanzi, J.N. and Six, J., 2010. Illuminated darkness: Molecular signatures of Congo River dissolved organic matter and its photochemical alteration as revealed by ultrahigh precision mass spectrometry. *Limnology and Oceanography*, *55*(4), pp.1467–1477.

Stubbins, A., Niggemann, J. and Dittmar, T., 2012. Photo-lability of deep ocean dissolved black carbon. *Biogeosciences*, *9*(5), pp.1661–1670.

Sun, L., Perdue, E.M., Meyer, J.L. and Weis, J., 1997. Use of elemental composition to predict bioavailability of dissolved organic matter in a Georgia river. *Limnology and Oceanography*, *42*(4), pp.714–721.

Swaney D.P., and G. Giordani, 2011. *Proceedingsof the LOICZ Workshop on biogeochemical budget methodology and applications, Providence, Rhode Island, November 9-10, 2007*, LOICZ.

Szymczycha, B,, Maciejewska, A., Winogradow, A. and Pempkowiak, J., 2014. Could submarine groundwater discharge be a significant carbon source to the southern Baltic Sea? *Oceanologia*, *56*(2), pp.327–347.

Szymczycha, B., Maciejewska, A., Szczepanska, A. and Pempkowiak, J., 2013. The submarine groundwater discharge as a carbon source to the Baltic Sea. *Biogeosciences Discussions*, *10*(2), pp.2069–2091.

Taniguchi, M., 2002. Tidal effects on submarine groundwater discharge into the ocean. *Geophysical Research Letters*, *29*(12), pp.2–1.

Taniguchi, M., Turner, J.V. and Smith, A.J., 2003. Evaluations of groundwater discharge rates from subsurface temperature in Cockburn Sound, Western Australia. *Biogeochemistry*, *66*(1-2), pp.111–124.

Taylor, D., Nixon, S., Granger, S. and Buckley, B., 1995. Nutrient limitation and the eutrophication of coastal lagoons. *Marine ecology progress series. Oldendorf*, *127*(1), pp.235–244.

Taylor, J.R. and Cohen, E.R., 1998. An introduction to error analysis: the study of uncertainties in physical measurements. *Measurement Science and Technology*, *9*(6), p.1015.

Tedetti, M., Cuet, P., Guigue, C. and Goutx, M., 2011. Characterization of dissolved organic matter in a coral reef ecosystem subjected to anthropogenic pressures (La Réunion Island, Indian Ocean) using multi-dimensional fluorescence spectroscopy. *The Science of the total environment*, *409*(11), pp.2198–2210.

Terry, K.L., Laws, E.A. and Burns, D.J., 1985. Growth Rate Variation in the N:p Requirement Ratio of Phytoplankton1. *Journal of Phycology*, *21*(2), pp.323–329.

Tfaily, M.M., Corbett, J.E., Wilson, R., Chanton, J.P., Glaser, P.H., Cawley, K.M., Jaffé, R. and Cooper, W.T., 2015. Utilization of PARAFAC-Modeled Excitation-Emission Matrix (EEM) Fluorescence Spectroscopy to Identify Biogeochemical Processing of Dissolved Organic Matter in a Northern Peatland. *Photochemistry and Photobiology*, *91*(3), pp.684–695.

Thomsen, M., Lassen, P., Dobel, S., Hansen, P.E., Carlsen, L. and Mogensen, B.B., 2002. Characterisation of humic materials of different origin: a multivariate approach for quantifying the latent properties of dissolved organic matter. *Chemosphere*, *49*(10), pp.1327–1337.

Thurman, E.M., 1985. Amount of Organic Carbon in Natural Waters. In *Organic Geochemistry of Natural Waters*. Developments in Biogeochemistry. Springer Netherlands, pp. 7–65.

Thurman, E.M., 2012. Organic geochemistry of natural waters (vol. 2): Springer Science & Business Media. *United States Geological Survey, Denver, Colorado*, p.2.

Tobias, C.R., Anderson, I.C., Canuel, E.A. and Macko, S.A., 2001. Nitrogen cycling through a fringing marsh-aquifer ecotone. *Marine Ecology Progress Series*, *210,* pp.25–39.

Tosin, M., Weber, M., Siotto, M., Lott, C. and Degli-Innocenti, F., 2012. Laboratory Test Methods to Determine the Degradation of Plastics in Marine Environmental Conditions. *Frontiers in Microbiology*, 3.

Tréguer, P.J., 2014. The Southern Ocean silica cycle. *Comptes Rendus Geoscience*, *346*(11–12), pp.279–286.

Tréguer, P.J. and Rocha, C.L.D.L., 2013. The World Ocean Silica Cycle. *Annual Review of Marine Science*, *5*(1), pp.477–501.

Tremblay, L., Kohl, S.D., Rice, J.A. and Gagné, J.P., 2005. Effects of temperature, salinity, and dissolved humic substances on the sorption of polycyclic aromatic hydrocarbons to estuarine particles. *Marine Chemistry*, *96*(1–2), pp.21–34.

Tremblay, L.B., Dittmar, T., Marshall, A.G., Cooper, W.J. and Cooper, W.T., 2007. Molecular characterization of dissolved organic matter in a North Brazilian mangrove porewater and mangrove-fringed estuaries by ultrahigh resolution Fourier Transform-Ion Cyclotron Resonance mass spectrometry and excitation/emission spectroscopy. *Marine Chemistry*, *105*(1–2), pp.15–29.

Linh Trieu (2015) *The impact of biodegradable plastic and nutrient enrichment on benthic nutrient flux*. Trinity College Dublin.

Tse, K.C. & Jiao, J.J., 2008. Estimation of submarine groundwater discharge in Plover Cove, Tolo Harbour, Hong Kong by 222Rn. *Marine Chemistry*, *111*(3–4), pp.160–170.

Tuominen, L., Heinänen, A., Kuparinen, J. and Nielsen, L.P., 1998. 'Spatial and temporal variability of denitrification in the sediments of the northern Baltic Proper', *Marine Ecology Progress Series*, 172, pp. 13–24.

Twardowski, M.S., Boss, E., Sullivan, J.M. and Donaghay, P.L., 2004. Modeling the spectral shape of absorption by chromophoric dissolved organic matter. *Marine Chemistry*, *89*(1–4), pp.69–88.

Twilley, R.R., Kemp, W.M., Staver, K.W., Stevenson, J.C. and Boynton, W.R., 1985. Nutrient enrichment of estuarine submersed vascular plant communities. 1. Algal growth and effects on production of plants and associated communities. *Marine ecology progress series. Oldendorf*, *23*(2), pp.179–191.

Valiela, I., McClelland, J., Hauxwell, J., Behr, P.J., Hersh, D. and Foreman, K., 1997. Macroalgal blooms in shallow estuaries: Controls and ecophysiological and ecosystem consequences. *Limnology and Oceanography*, *42*(5part2), pp.1105–1118.

Valiela, I., Costa, J., Foreman, K., Teal, J.M., Howes, B. and Aubrey, D., 1990. Transport of groundwater-borne nutrients from watersheds and their effects on coastal waters. *Biogeochemistry*, *10*(3), pp.177–197.

Van Duin, E.H., Blom, G., Los, F.J., Maffione, R., Zimmerman, R., Cerco, C.F., Dortch, M. and Best, E.P., 2001. Modeling underwater light climate in relation to sedimentation, resuspension, water quality and autotrophic growth. *Hydrobiologia*, *444*(1-3), pp.25-42.

Ver, L.M.B., Mackenzie, F.T. & Lerman, A., 1999. Carbon cycle in the coastal zone: effects of global perturbations and change in the past three centuries. *Chemical Geology*, *159*(1–4), pp.283–304.

Veuger, B., Van Oevelen, D., Boschker, H.T. and Middelburg, J.J., 2006. Fate of peptidoglycan in an intertidal sediment: An in situ 13C-labeling study. *Limnology and Oceanography*, *51*(4), pp.1572–1580.

Viaroli, P., Bartoli, M., Azzoni, R., Giordani, G., Mucchino, C., Naldi, M., Nizzoli, D. and Tajé, L., 2005. Nutrient and iron limitation to Ulva blooms in a eutrophic coastal lagoon (Sacca di Goro, Italy). *Hydrobiologia*, *550*(1), pp.57–71.

Visser, S.A., 1985. Physiological action of humic substances on microbial cells. *Soil Biology and Biochemistry*, *17*(4), pp.457–462.

Vitousek, P.M., Aber, J.D., Howarth, R.W., Likens, G.E., Matson, P.A., Schindler, D.W., Schlesinger, W.H. and Tilman, D.G., 1997. Human Alteration of the Global Nitrogen Cycle: Sources and Consequences. *Ecological Applications*, *7*(3), pp.737–750.

Wakida, F.T. and Lerner, D.N., 2005. Non-agricultural sources of groundwater nitrate: a review and case study. *Water Research*, *39*(1), pp.3–16.

Wang, G., Wang, Z., Zhai, W., Moore, W.S., Li, Q., Yan, X., Qi, D. and Jiang, Y., 2015. Net subterranean estuarine export fluxes of dissolved inorganic C, N, P, Si, and total alkalinity into the Jiulong River estuary, China. *Geochimica et Cosmochimica Acta*, *149,* pp.103–114.

Wanninkhof, R., 1992. Relationship between wind speed and gas exchange over the ocean. *Journal of Geophysical Research: Oceans*, *97*(C5), pp.7373–7382.

Wanninkhof, R., 2014. Relationship between wind speed and gas exchange over the ocean revisited: Gas exchange and wind speed over the ocean. *Limnology and Oceanography: Methods*, *12*(6), pp.351–362.

Waska, H. and Kim, G., 2011. Submarine groundwater discharge (SGD) as a main nutrient source for benthic and water-column primary production in a large intertidal environment of the Yellow Sea. *Journal of Sea Research*, *65*(1), pp.103–113.

Wayland, D., Megson, D.P., Mudge, S.M., Icely, J.D. and Newton, A., 2008. Identifying the Source of Nutrient Contamination in a Lagoon System. *Environmental Forensics*, *9*(2-3), pp.231–239.

Weber, T. S. and Deutsch, C., 2010. 'Ocean nutrient ratios governed by plankton biogeography', *Nature*, 467(7315), p. 550.

Weishaar, J.L., Aiken, G.R., Bergamaschi, B.A., Fram, M.S., Fujii, R. and Mopper, K., 2003. Evaluation of specific ultraviolet absorbance as an indicator of the chemical composition and reactivity of dissolved organic carbon. *Environmental Science & Technology*, *37*(20), pp.4702–4708.

Weiss, R.F., 1974. Carbon dioxide in water and seawater: the solubility of a non-ideal gas. *Marine Chemistry*, *2*(3), pp.203–215.

Welsh, B.L., 1980. Comparative nutrient dynamics of a marsh-mudflat ecosystem. *Estuarine and Coastal Marine Science*, *10*(2), pp.143–164.

De Weys, J., Santos, I.R. & Eyre, B.D., 2011. Linking Groundwater Discharge to Severe Estuarine Acidification during a Flood in a Modified Wetland. *Environmental Science and Technology*, *45*(8), pp.3310–3316.

Williams P.W., 1964. *Aspects of the Limestone Physiography of Parts of Countieds Clare and Galway, Western Ireland*. University of Cambridge.

Wilson, J. and Rocha, C., 2012. Regional scale assessment of Submarine Groundwater Discharge in Ireland combining medium resolution satellite imagery and geochemical tracing techniques. *Remote Sensing of Environment*, *119*, pp.21–34.

Wolf-Gladrow, D.A., Zeebe, R.E., Klaas, C., Körtzinger, A. and Dickson, A.G., 2007. Total alkalinity: The explicit conservative expression and its application to biogeochemical processes. *Marine Chemistry*, *106*(1–2), pp.287–300.

Wong, G.T.F 1988. Alkalinity in the south-eastern United States continental shelf waters. *Estuarine, Coastal and Shelf Science*, *27*(5), pp.567–579.

Worrall F., Reed M., Warburton J. and Burt T., 2003. Carbon budget for a British upland peat catchment. *Science of The Total Environment*, *312*(1–3), pp.133–146.

Wu, F.C., Kothawala, D.N., Evans, R.D., Dillon, P.J. and Cai, Y.R., 2007. Relationships between DOC concentration, molecular size and fluorescence properties of DOM in a stream. *Applied Geochemistry*, *22*(8), pp.1659–1667.

Yamashita, Y., Jaffé, R., Maie, N. and Tanoue, E., 2008. Assessing the dynamics of dissolved organic matter (DOM) in coastal environments by excitation emission matrix fluorescence and parallel factor analysis (EEM-PARAFAC). *Limnology and Oceanography*, *53*(5), p.1900.

Yamashita, Y. and Tanoue, E., 2004. Chemical characteristics of amino acid-containing dissolved organic matter in seawater. *Organic Geochemistry*, *35*(6), pp.679–692.

Yang, L., Chen, C.T.A., Hong, H., Chang, Y.C. and Lui, H.K., 2015. Mixing behavior and bioavailability of dissolved organic matter in two contrasting subterranean estuaries as revealed by fluorescence spectroscopy and parallel factor analysis. *Estuarine, Coastal and Shelf Science*, *166,* Part B, pp.161–169.

Yao, X., Zhang, Y., Zhu, G., Qin, B., Feng, L., Cai, L. and Gao, G., 2011. Resolving the variability of CDOM fluorescence to differentiate the sources and fate of DOM in Lake Taihu and its tributaries. *Chemosphere*, *82*(2), pp.145–155.

Yoon, W. and Benner, R., 1992. 'Denitrification and oxygen consumption in sediments of two south Texas estuaries', *Marine Ecology Progress Series*, 90, pp. 157–167.

Zeebe, R.E. and Wolf-Gladrow, D.A., 2001. *CO2 in Seawater: Equilibrium, Kinetics, Isotopes* (No. 65). Gulf Professional Publishing.

Zepp, R.G., 2003. Solar UVR and aquatic Carbon, nitrogen, sulfur and metals cycles. In E. W. Helbling and H. Zagarese, eds. *UV Effects in Aquatic Organisms and Ecosystems*. The Royal Society of Chemistry, pp. 137–184.

Zepp, R.G., Callaghan, T.V. and Erickson, D.J., 1995. Effects of increased solar ultraviolet radiation on biogeochemical cycles. *Ambio*, *24*(3), pp.181–7.

Zhai, W., Dai M., Cai W-J., Wang Y. and Wang Z., 2005. High partial pressure of CO2 and its maintaining mechanism in a subtropical estuary: the Pearl River estuary, China. *Marine Chemistry*, *93*(1), pp.21–32.

Zhang, W.L., Tian, Z.X., Zhang, N. and Li, X.Q.,1996. Nitrate pollution of groundwater in northern China. *Agriculture, Ecosystems & Environment*, *59*(3), pp.223–231

Zhang, J. and Mandal, A.K., 2012. Linkages between submarine groundwater systems and the environment. *Current Opinion in Environmental Sustainability*, *4*(2), pp.219–226.

Zhang, D., Lee, D.-J. and Pan, X., 2012. Fluorescent quenching for biofilm extracellular polymeric substances (EPS) bound with Cu(II). *Journal of the Taiwan Institute of Chemical Engineers*, *43*(3), pp.450–454.

Zonneveld, K.A.F., Versteegh, G.J.M., Kasten, S., Eglinton, T.I., Emeis, K.C., Huguet, C., Koch, B.P., de Lange, G.J., De Leeuw, J.W., Middelburg, J.J. and Mollenhauer, G., 2010. Selective preservation of organic matter in marine environments; processes and impact on the sedimentary record.

Zsolnay, A., Baigar, E., Jimenez, M., Steinweg, B. and Saccomandi, F., 1999. Differentiating with fluorescence spectroscopy the sources of dissolved organic matter in soils subjected to drying. *Chemosphere*, *38*(1), pp.45–50

Appendix A – Important Hydrological Data - Raw Data measured *in-situ*

July 2013

Collection Date	Time	Site ID	Temperature [°C]	Dissolved Oxygen [%]	Cond [µS/cm]	Salinity [ppt]	pH
22/07/13	11.00	Castle	14.7	44.7	73.69	3.67	6.92
22/07/13	11.20	Castle	14.5	36.7	63.74	3.17	7.25
22/07/13	11.40	Castle	15.3	41.4	59.57	2.96	7.40
22/07/13	12.00	Castle	15.0	38.4	53.49	2.67	7.43
22/07/13	12.20	Castle	14.4	35.6	48.06	2.31	7.52
22/07/13	12.40	Castle	14.0	34.4	44.59	2.22	7.35
22/07/13	13.00	Castle	14.4	36.8	39.31	1.90	7.42
22/07/13	13.20	Castle	15.0	36.8	37.06	1.84	7.57
22/07/13	13.40	Castle	13.8	34.9	37.33	1.86	7.37
22/07/13	14.50	Sewage	21.3	124.1	44.42	22.2	7.57
22/07/13	15.10	Sewage	21.4	116.0	42.93	21.8	7.85
22/07/13	15.35	Sewage	21.7	108.1	41.12	20.58	7.93
22/07/13	15.50	Sewage	21.5	110.4	44.25	22.15	8.09
22/07/13	16.10	Sewage	21.1	110.9	44.05	21.9	8.18
22/07/13	16.30	Sewage	20.8	108.0	46.79	23.4	8.22
22/07/13	16.50	Sewage	21.0	107.0	46.21	23.3	8.24
22/07/13	17.05	Sewage	21.0	106.0	46.57	23.3	8.25
22/07/13	17.30	Sewage	21.1	104.9	46.66	23.36	8.28
22/07/13	13.00	PP	20.2	115.3	44.58	31.58	7.85
22/07/13	13.20	PP	20.1	123.9	45.16	32.03	7.54
22/07/13	13.40	PP	20.7	123.7	44.42	31.46	7.51
22/07/13	14.00	PP	20.5	145.5	44.89	31.82	8.03
22/07/13	14.20	PP	20.1	121.1	45.01	31.92	7.92
22/07/13	14.40	PP	20.1	123.6	45.2	32.07	7.98
22/07/13	15.00	PP	19.5	110.5	45.9	32.61	8.14
22/07/13	15.20	PP	20.5	120.3	43.98	31.11	7.94
22/07/13	15.40	PP	19.6	121.2	45.39	32.21	8.09
22/07/13	16.00	PP	20.2	111.7	45.46	32.27	8.16
22/07/13	16.20	PP	19.9	120.9	44.87	31.81	8.05
22/07/13	16.40	PP	20.1	118.6	45.16	32.03	8.16
22/07/13	17.00	PP	20.1	121.5	45.35	32.18	8.14
22/07/13	17.20	PP	19.8	123.6	43.51	30.75	8.03
22/07/13	17.40	PP	20.1	129.3	45.44	32.25	8.26
22/07/13	18.00	PP	20.8	120.5	44.89	31.82	8.11

22/07/13	18.20	PP	19.9	124.3	45.32	32.16	8.11
22/07/13	18.40	PP	19.9	120.7	44.98	31.89	8.05
22/07/13	19.00	PP	19.7	124.1	44.96	31.88	8.04
22/07/13	19.20	PP	20.1	122.8	43.79	30.97	8.05
22/07/13	19.40	PP	19.7	135.6	43.21	30.51	8.12
22/07/13	20.00	PP	19.2	119.9	44.74	31.71	8.01
22/07/13	20.20	PP	19.1	126.8	43.48	30.72	8.11
22/07/13	20.40	PP	18.9	124.4	66.00	30.60	8.04
22/07/13	21.00	PP	18.9	124.8	72.03	30.40	8.10
22/07/13	21.20	PP	19.2	121.8	44.73	31.70	8.08
22/07/13	21.40	PP	19.0	117.9	43.69	30.89	8.03
22/07/13	22.00	PP	18.7	113.1	43.03	30.37	8.01
22/07/13	22.20	PP	18.6	110.9	42.23	30.48	8.04
22/07/13	22.40	PP	18.7	109.9	44.32	31.38	8.05
22/07/13	23.00	PP	18.4	98.3	34.23	23.64	7.99
22/07/13	23.20	PP	18.6	82.9	42.47	29.94	8.05
22/07/13	23.40	PP	18.3	95.7	44.88	31.82	7.88
23/07/13	00.00	PP	17.8	64.8	44.60	31.60	7.93
23/07/13	00.20	PP	17.5	92.9	44.44	31.47	7.78
23/07/13	00.40	PP	17.8	88.5	44.29	31.35	7.87
23/07/13	01.00	PP	17.2	76.6	42.98	30.34	7.85
23/07/13	01.20	PP	17.3	99.7	43.21	30.51	7.91
23/07/13	01.40	PP	17.4	92.0	44.10	31.21	7.96
23/07/13	02.00	PP	17.5	90.7	44.05	31.17	7.98
23/07/13	02.20	PP	17.7	92.5	43.99	31.12	8.04
23/07/13	02.40	PP	17.4	101.6	44.65	31.64	8.07
23/07/13	03.00	PP	17.8	108.9	44.77	31.73	8.14
23/07/13	03.20	PP	17.8	105.0	44.66	31.64	8.19
23/07/13	03.40	PP	17.7	110.8	44.72	31.69	8.21
23/07/13	04.00	PP	17.6	107.7	44.66	31.64	8.23
23/07/13	04.20	PP	17.5	110.9	45.61	32.39	8.25
23/07/13	04.40	PP	17.4	110.8	45.24	32.10	8.24
23/07/13	05.00	PP	17.5	107.4	44.97	31.89	8.25
23/07/13	05.20	PP	17.6	109.1	44.64	31.63	8.26
23/07/13	05.40	PP	17.6	110.6	44.54	31.55	8.26
23/07/13	06.00	PP	17.7	108.2	44.73	31.70	8.26
23/07/13	06.20	PP	17.6	109.8	44.98	31.89	8.27

23/07/13	06.40	PP	17.8	111.2	44.51	31.53	8.25
23/07/13	07.00	PP	17.9	108.7	44.49	31.51	8.26
23/07/13	07.20	PP	17.9	111.0	44.61	31.60	8.26
23/07/13	07.40	PP	17.9	112.3	44.62	31.61	8.26
23/07/13	08.00	PP	17.8	112.5	44.52	31.53	8.26
23/07/13	08.20	PP	17.9	113.1	44.54	31.55	8.26
23/07/13	08.40	PP	18.0	108.4	44.48	31.50	8.25
23/07/13	09.00	PP	18.0	110.8	45.21	32.07	8.28
23/07/13	09.20	PP	17.8	112.1	43.81	30.98	8.25
23/07/13	09.40	PP	17.8	110.0	44.58	31.58	8.25
23/07/13	10.00	PP	18.0	107.0	44.31	31.37	8.26
23/07/13	10.20	PP	17.9	110.8	43.53	30.76	8.21
23/07/13	10.40	PP	17.9	108.7	44.39	31.43	8.18
23/07/13	11.00	PP	18.0	107.2	43.48	30.72	8.17
23/07/13	11.20	PP	18.0	110.5	43.18	30.49	8.17
23/07/13	11.40	PP	18.1	102.6	43.68	30.88	8.11
23/07/13	12.00	PP	18.6	110.6	43.95	31.09	8.12
23/07/13	12.20	PP	19.1	115.9	43.7	30.90	8.16
23/07/13	12.40	PP	19.2	115.1	47.87	34.16	8.15

January 2015

Collection Date	Time	Site ID	Temperature [°C]	Dissolved Oxygen [%]	Cond [µS/cm]	Salinity [ppt]	pH
31/01/15	08.40	Castle	7.3	80.6	562	0.52	7.13
31/01/15	09.00	Castle	6.9	83.8	565	0.52	7.41
31/01/15	09.20	Castle	6.7	80.5	566	0.52	7.12
31/01/15	09.40	Castle	6.7	80.4	561	0.52	7.38
31/01/15	10.00	Castle	7.3	75.9	560	0.52	7.47
31/01/15	10.20	Castle	7.5	77.7	562	0.52	7.52
31/01/15	10.40	Castle	7.4	82.9	561	0.52	7.60
31/01/15	11.00	Castle	7.8	72.0	566	0.52	7.47
31/01/15	11.20	Castle	7.6	83.5	565	0.52	7.85
31/01/15	11.40	Castle	7.5	79.4	647	0.60	7.85
31/01/15	12.00	Castle	8.6	67.6	557	0.52	7.37
31/01/15	15.00	Sewage	7.2	92.7	700	0.65	7.76
31/01/15	15.20	Sewage	7.3	92.1	660	0.62	7.82
31/01/15	15.40	Sewage	7.3	94.0	747	0.70	7.70
31/01/15	16.00	Sewage	6.6	91.2	1578	1.54	7.70
31/01/15	16.20	Sewage	8.3	91.0	887	0.84	7.72
31/01/15	16.40	Sewage	8.5	84.4	642	0.60	7.64
31/01/15	17.00	Sewage	7.5	89.6	963	0.91	7.76
31/01/15	17.20	Sewage	7.5	85.7	903	0.85	7.62
31/01/15	17.40	Sewage	7.9	74.2	966	0.92	7.44
01/02/15	10.00	PP	5.6	95.0	4960	3.03	7.84
01/02/15	10.30	PP	6.0	93.0	6510	4.05	7.85
01/02/15	11.00	PP	6.1	96.5	17230	11.49	7.68
01/02/15	11.30	PP	6.9	97.0	16600	11.03	7.93
01/02/15	12.00	PP	7.5	96.1	24200	16.59	7.79
01/02/15	12.30	PP	7.6	98.9	24700	16.96	7.73
01/02/15	13.00	PP	7.0	101.1	27900	19.36	7.96
01/02/15	13.30	PP	7.0	98.7	28500	19.81	8.10
01/02/15	14.00	PP	7.0	113.8	26600	18.38	8.32
01/02/15	14.30	PP	7.4	98.1	29300	20.42	8.19
01/02/15	15.00	PP	6.7	108.8	29500	20.57	8.29
01/02/15	15.30	PP	6.6	106.7	29500	17.58	8.32
01/02/15	16.00	PP	6.5	91.7	21500	14.59	8.21
01/02/15	16.30	PP	5.6	95.2	23700	16.22	8.22

01/02/15	17.00	PP	5.3	95.2	26800	18.53	8.17
01/02/15	17.30	PP	4.5	89.1	6960	4.35	8.13
01/02/15	18.00	PP	4.5	88.9	7390	4.63	8.12
01/02/15	18.30	PP	5.7	93.3	10100	6.47	7.82
01/02/15	19.00	PP	6.1	89.3	11780	7.63	8.06
01/02/15	19.30	PP	5.9	88.1	10770	6.93	7.99
01/02/15	20.00	PP	6.6	86.9	10720	6.90	7.84
01/02/15	20.30	PP	6.4	86.6	11950	7.75	7.77
01/02/15	21.00	PP	8.3	84.9	11910	7.72	7.62
01/02/15	21.30	PP	8.3	83.7	14810	9.76	7.90
01/02/15	22.00	PP	9.3	80.9	15270	10.09	7.83
01/02/15	22.30	PP	8.9	82.1	18940	12.72	7.82
01/02/15	23.00	PP	10.4	80.5	13150	8.59	7.80
01/02/15	23.30	PP	8.6	84.7	23700	16.22	7.83
02/02/15	00.00	PP	8.5	82.5	21000	14.22	7.94
02/02/15	00.30	PP	9.1	87.6	28400	19.73	8.04
02/02/15	01.00	PP	8.9	82.8	24500	16.81	7.95
02/02/15	01.30	PP	10.9	82.9	26800	18.53	8.16
02/02/15	02.00	PP	9.2	82.9	26100	18.00	8.21
02/02/15	02.30	PP	10.3	85.2	27900	19.36	8.00
02/02/15	03.00	PP	9.2	81.4	28000	19.43	8.00
02/02/15	03.30	PP	8.3	80.9	30000	20.95	8.10
02/02/15	04.00	PP	9.1	83.2	30400	21.25	8.06
02/02/15	04.30	PP	8.4	85.8	29900	20.87	8.06
02/02/15	05.00	PP	9.1	85.6	24700	16.96	8.03
02/02/15	05.30	PP	8.1	81.8	16290	10.81	7.99
02/02/15	06.00	PP	7.5	80.1	13740	9.00	7.99
02/02/15	06.30	PP	7.8	80.5	14850	9.79	7.85
02/02/15	07.00	PP	9.0	81.2	13960	9.16	7.83
02/02/15	07.30	PP	9.6	79.9	16580	11.02	7.80
02/02/15	08.00	PP	8.9	81.8	18910	12.70	7.81
02/02/15	08.30	PP	6.8	80.6	17930	11.99	7.93
02/02/15	09.00	PP	9.2	83.6	24800	17.03	7.86
02/02/15	09.30	PP	7.9	83.5	21648	14.51	7.93

June 2015

Collection Date	Time	Site ID	Temperature [°C]	Dissolved Oxygen [%]	Conductivity [µS/cm]	Salinity [ppt]	pH
11/06/15	18.45	Castle	14.1	73.2	582	0.54	7.93
11/06/15	19.00	Castle	13.5	70.0	583	0.54	7.46
11/06/15	19.15	Castle	14.1	82.9	584	0.54	7.20
11/06/15	19.30	Castle	13.3	64.5	569	0.53	6.96
11/06/15	19.45	Castle	13.4	72.8	605	0.56	7.18
11/06/15	20.00	Castle	13.2	63.5	580	0.54	6.93
11/06/15	20.15	Castle	13.0	66.5	555	0.51	6.99
11/06/15	20.30	Castle	13.6	77.5	556	0.51	7.12
11/06/15	20.45	Castle	13.8	78.9	558	0.52	7.17
11/06/15	21.00	Castle	13.3	74.8	546	0.50	7.23
11/06/15	21.15	Castle	13.7	79.7	564	0.52	7.29
11/06/15	21.30	Castle	13.3	73.6	571	0.53	7.27
11/06/15	13.05	Sewage	17.7	119.0	10710	11.81	8.41
11/06/15	13.25	Sewage	19.3	120.5	10450	11.50	8.24
11/06/15	13.40	Sewage	18.6	136.4	10180	11.18	8.60
11/06/15	13.55	Sewage	17.9	127.6	9698	10.61	8.42
11/06/15	14.15	Sewage	18.2	125.5	9980	10.95	8.39
11/06/15	14.35	Sewage	19.5	119.3	11190	12.38	8.29
11/06/15	14.55	Sewage	18.0	137.4	10400	11.44	8.54
11/06/15	15.00	Sewage	18.1	134.8	10090	11.08	8.66
11/06/15	15.15	Sewage	17.7	121.6	10750	6.92	8.60
11/06/15	15.30	Sewage	17.8	123.1	9930	6.35	8.57
11/06/15	15.45	Sewage	17.4	124.3	10090	6.46	8.70
11/06/15	16.00	Sewage	17.2	120.6	42500	---	8.72
12/06/15	07.30	PP	16.3	98.0	40900	29.67	8.51
12/06/15	08.00	PP	14.7	100.1	40900	29.51	8.62
12/06/15	08.30	PP	14.6	102.0	40900	28.4	8.65
12/06/15	09.00	PP	14.9	101.1	43200	28.4	8.63
12/06/15	09.30	PP	14.9	101.7	44000	28.4	8.63
12/06/15	10.00	PP	14.7	101.3	46400	30.22	8.65
12/06/15	10.30	PP	15.3	98.6	45300	30.86	8.61
12/06/15	11.00	PP	15.6	100.7	46700	32.78	8.66
12/06/15	11.30	PP	16.8	100.8	47300	31.9	8.65
12/06/15	12.00	PP	17.4	102.9	47000	33.02	8.83

12/06/15	12.30	PP	18.6	105.0	47700	33.51	8.79
12/06/15	13.00	PP	17.8	109.6	47400	33.26	8.72
12/06/15	13.30	PP	18.3	103.6	47400	33.83	8.71
12/06/15	14.00	PP	18.4	113.7	48400	33.59	8.75
12/06/15	14.30	PP	17.3	115.3	48800	33.59	8.81
12/06/15	15.00	PP	18.0	108.0	49500	34.39	8.79
12/06/15	15.30	PP	15.8	105.8	49600	34.72	8.74
12/06/15	16.00	PP	15.7	108.1	48500	35.28	8.70
12/06/15	16.30	PP	15.1	108.7	49500	35.37	8.77
12/06/15	17.00	PP	15.6	107.8	49600	34.47	8.80
12/06/15	17.30	PP	15.1	110.4	49600	35.28	8.79
12/06/15	18.00	PP	15.4	108.5	48800	35.37	8.76
12/06/15	18.30	PP	15.3	102.8	48900	35.37	8.74
12/06/15	19.00	PP	15.2	103.4	47600	34.72	8.71
12/06/15	19.30	PP	14.8	105.9	46300	34.8	8.76
12/06/15	20.00	PP	14.8	104.7	44700	33.75	8.75
12/06/15	20.30	PP	14.8	104.0	45500	32.7	8.75
12/06/15	21.00	PP	14.7	104.6	45400	31.42	8.75
12/06/15	21.30	PP	14.3	104.6	46000	32.06	8.74
12/06/15	22.00	PP	14.3	103.6	46000	31.98	8.74
12/06/15	22.30	PP	14.0	101.1	47300	32.46	8.71
12/06/15	23.00	PP	13.8	100.5	46700	32.46	8.70
12/06/15	23.30	PP	13.7	99.5	47100	33.51	8.69
13/06/15	00.00	PP	13.2	96.4	48000	33.02	8.69
13/06/15	00.30	PP	13.3	98.9	48100	33.34	8.73
13/06/15	01.00	PP	13.4	99.4	48700	34.07	8.71
13/06/15	01.30	PP	13.2	93.8	49600	34.15	8.62
13/06/15	02.00	PP	13.2	96.3	49600	33.64	8.67
13/06/15	02.30	PP	13.2	97.2	49600	34.37	8.69
13/06/15	03.00	PP	13.1	98.6	49500	35.37	8.69
13/06/15	03.30	PP	13.1	98.1	49800	35.37	8.69
13/06/15	04.00	PP	13.2	102.4	49100	35.28	8.73
13/06/15	04.30	PP	13.1	101.8	49800	35.53	8.73
13/06/15	05.00	PP	13.3	101.3	48200	34.96	8.73
13/06/15	05.30	PP	13.1	115.8	48400	35.53	8.74
13/06/15	06.00	PP	13.1	116.2	48300	34.23	8.74
13/06/15	06.30	PP	12.5	115.5	47300	34.39	8.73

13/06/15	07.00	PP	12.9	119.6	47100	34.31	8.72	

January 2016

Collection Date	Time	Site ID	Temperature [°C]	Dissolved Oxygen [%]	Conductivity [µS/cm]	Salinity [ppt]	pH
30/01/16	14.00	Castle	8.6	67.5	600	0.56	6.99
30/01/16	14.15	Castle	8.5	72.6	557	0.52	6.93
30/01/16	14.30	Castle	8.7	72.7	572	0.53	7.15
30/01/16	14.45	Castle	8.6	69.8	566	0.52	7.11
30/01/16	15.00	Castle	8.8	63.9	550	0.51	7.11
30/01/16	15.15	Castle	8.8	62.6	569	0.53	7.07
30/01/16	15.30	Castle	8.8	68.4	568	0.53	7.12
30/01/16	15.45	Castle	8.9	67.9	559	0.52	7.09
30/01/16	16.00	Castle	9.2	66.3	560	0.52	7.10
30/01/16	16.15	Castle	9.0	64.4	555	0.51	7.10
30/01/16	08.00	Sewage	6.9	92.0	1213	1.16	7.34
30/01/16	08.15	Sewage	5.8	98.7	1194	1.14	7.79
30/01/16	08.30	Sewage	5.6	99.0	2150	2.13	7.78
30/01/16	08.45	Sewage	6.3	98.0	2200	2.18	7.87
30/01/16	09.15	Sewage	6.8	101.8	670	0.63	8.19
30/01/16	09.30	Sewage	7.3	99.9	573	0.53	8.07
30/01/16	09.45	Sewage	7.3	98.0	426	0.39	7.98
30/01/16	10.00	Sewage	7.3	100.0	478	0.00	7.90
30/01/16	10.15	Sewage	6.6	101.0	2360	2.35	8.09
30/01/16	10.30	Sewage	6.5	101.1	2430	2.42	8.20
30/01/16	18.15	PP	7.4	98.0	37400	34.66	8.21
30/01/16	18.45	PP	7.7	97.6	38000	35.11	8.37
30/01/16	19.15	PP	7.8	97.9	38100	35.33	8.36
30/01/16	19.45	PP	7.7	97.1	37900	35.22	8.44
30/01/16	20.15	PP	7.4	97.0	38000	35.11	8.50
30/01/16	20.45	PP	7.7	97.8	36800	33.88	8.49
30/01/16	21.15	PP	7.7	96.5	37100	34.32	8.57
30/01/16	21.45	PP	7.6	96.5	37500	34.77	8.58
30/01/16	22.15	PP	7.5	96.9	31800	31.85	8.59
30/01/16	22.45	PP	7.3	95.8	22600	21.79	8.57
30/01/16	23.15	PP	7.4	95.4	19350	18.40	8.51
30/01/16	23.45	PP	7.4	92.8	13820	12.71	8.43

31/01/16	00.15	PP	7.5	93.9	14390	13.31	8.40
31/01/16	00.45	PP	7.6	92.5	14220	13.07	8.38
31/01/16	01.15	PP	9.0	92.2	14400	13.14	8.26
31/01/16	01.45	PP	8.8	89.0	13770	12.59	8.41
31/01/16	02.15	PP	8.8	90.2	16880	15.73	8.47
31/01/16	02.45	PP	9.3	90.8	18080	16.95	8.48
31/01/16	03.15	PP	8.8	90.3	17620	16.43	8.50
31/01/16	03.45	PP	9.0	89.5	18080	16.90	8.48
31/01/16	04.15	PP	8.7	90.2	19040	17.57	8.42
31/01/16	04.45	PP	8.6	90.3	20700	18.92	8.46
31/01/16	05.15	PP	9.5	91.9	25300	23.48	8.45
31/01/16	05.45	PP	10.5	92.5	29300	27.26	8.44
31/01/16	06.15	PP	9.8	92.5	33100	30.65	8.47
31/01/16	06.45	PP	10.4	94.3	38500	36.31	8.50
31/01/16	07.15	PP	10.6	95.7	29200	27.08	8.54
31/01/16	07.45	PP	9.9	95.6	38800	34.63	8.54
31/01/16	08.15	PP	10.3	94.9	39200	35.25	8.55
31/01/16	08.45	PP	10.5	94.1	39100	33.94	8.55
31/01/16	09.15	PP	10.4	95.5	40100	35.20	8.58
31/01/16	09.45	PP	10.2	96.8	39700	34.78	8.57
31/01/16	10.15	PP	10.4	96.7	40100	36.10	8.60
31/01/16	10.45	PP	10.2	96.9	40000	34.89	8.61
31/01/16	11.15	PP	10.2	99.1	39800	34.78	8.63
31/01/16	11.45	PP	10.0	97.8	40100	35.10	8.61
31/01/16	12.15	PP	10.2	97.1	39200	34.05	8.58
31/01/16	12.45	PP	10.1	96.7	38700	33.63	8.60
31/01/16	13.15	PP	10.4	98.0	39000	33.73	8.60
31/01/16	13.45	PP	10.5	99.8	39700	34.47	8.57
31/01/16	14.15	PP	10.8	96.4	39900	34.36	8.61
31/01/16	14.45	PP	10.9	97.5	38800	33.32	8.61
31/01/16	15.15	PP	10.6	98.4	39400	34.15	8.62
31/01/16	15.45	PP	10.5	99.4	39100	35.74	8.64
31/01/16	16.15	PP	10.6	98.2	39200	35.05	8.62
31/01/16	16.45	PP	10.4	99.3	39000	35.73	8.63
31/01/16	17.15	PP	10.3	96.9	38800	36.53	8.66

Appendix B – Measured Nutrient Concentrations for Budgetary Analysis (Chapter 2) - Raw Data

July 2013

Collection Date	Time	Site ID	Salinity (ppt)	NO_3^- (μmol L^{-1})	NO_2^- (μmol L^{-1})	NH_4^+ (μmol L^{-1})	DRSi (μmol L^{-1})	TDP (μmol L^{-1}
22/07/13	11.00	Castle	3.67	60.8	5.5	0.3	51.1	N/A
22/07/13	11.20	Castle	3.17	59.3	11.3	0.4	47.7	0.9
22/07/13	11.40	Castle	2.96	57.6	9.7	0.4	48.0	0.7
22/07/13	12.00	Castle	2.67	57.4	16.2	0.4	46.3	0.7
22/07/13	12.20	Castle	2.31	58.4	11.7	0.4	46.1	0.7
22/07/13	12.40	Castle	2.22	61.9	22.5	0.6	45.5	0.7
22/07/13	13.00	Castle	1.90	60.6	22.3	0.7	46.4	0.7
22/07/13	13.20	Castle	1.84	59.4	20.8	0.3	45.5	0.7
22/07/13	13.40	Castle	1.86	59.1	14.8	0.6	46.9	0.7
22/07/13	14.50	Sewage	22.2	0.1	0.4	3.2	4.3	0.4
22/07/13	15.10	Sewage	21.8	0.5	0.4	0.5	4.8	0.2
22/07/13	15.35	Sewage	20.58	3.1	1.9	46.8	8.8	0.5
22/07/13	15.50	Sewage	22.15	1.9	0.5	14.2	5.2	0.8
22/07/13	16.10	Sewage	21.9	0.9	0.5	17.5	2.8	0.5
22/07/13	16.30	Sewage	23.4	0.1	0.4	7.6	2.1	0.2
22/07/13	16.50	Sewage	23.3	0.5	0.4	1.2	2.2	0.1
22/07/13	17.05	Sewage	23.3	2.1	0.4	2.5	2.4	0.2
22/07/13	17.30	Sewage	23.36	31.7	0.4	9.5	1.8	0.5
22/07/13	13.00	PP	31.58	3.2	0.7	2.3	5.4	0.8
22/07/13	13.20	PP	32.03	41.5	0.7	0.8	1.2	0.5
22/07/13	13.40	PP	31.46	4.6	0.7	0.8	5.7	0.4
22/07/13	14.00	PP	31.82	4.2	0.7	2.9	9.0	0.7
22/07/13	14.20	PP	31.92	4.1	0.8	1.3	8.9	0.7
22/07/13	14.40	PP	32.07	2.6	0.6	0.8	2.7	0.5
22/07/13	15.00	PP	32.61	2.9	0.7	0.9	3.2	0.4
22/07/13	15.20	PP	31.11	1.7	0.6	0.8	2.4	0.5
22/07/13	15.40	PP	32.21	1.8	0.8	0.9	2.7	0.5
22/07/13	16.00	PP	32.27	3.4	0.7	1.1	2.6	0.4
22/07/13	16.20	PP	31.81	1.7	0.6	0.8	1.8	0.4
22/07/13	16.40	PP	32.03	1.5	0.8	0.9	2.1	0.3
22/07/13	17.00	PP	32.18	0.9	0.6	0.8	1.7	0.3
22/07/13	17.20	PP	30.75	0.5	0.9	0.7	4.9	0.4
22/07/13	17.40	PP	32.25	0.1	0.8	3.2	3.1	0.2
22/07/13	18.00	PP	31.82	4.4	0.9	6.1	6.8	0.2

22/07/13	18.20	PP	32.16	1.6	1.0	5.6	4.3	0.1
22/07/13	18.40	PP	31.89	0.1	0.7	2.5	2.4	0.1
22/07/13	19.00	PP	31.88	0.1	0.8	1.6	3.6	0.2
22/07/13	19.20	PP	30.97	0.1	0.8	0.6	2.5	0.2
22/07/13	19.40	PP	30.51	0.1	0.8	0.6	2.8	0.2
22/07/13	20.00	PP	31.71	0.1	0.8	2.4	2.5	0.2
22/07/13	20.20	PP	30.72	0.2	0.8	3.1	3.0	0.2
22/07/13	20.40	PP	30.60	0.4	0.8	3.6	3.7	0.1
22/07/13	21.00	PP	30.40	0.2	0.8	3.3	4.0	0.2
22/07/13	21.20	PP	31.70	0.1	0.8	3.0	3.7	0.2
22/07/13	21.40	PP	30.89	0.2	0.8	1.0	3.2	0.1
22/07/13	22.00	PP	30.37	0.2	0.8	2.1	3.3	0.1
22/07/13	22.20	PP	30.48	0.1	0.8	3.1	3.4	0.1
22/07/13	22.40	PP	31.38	0.1	0.7	0.6	2.1	0.1
23/07/13	23.00	PP	23.64	0.2	0.7	3.9	2.1	0.4
23/07/13	23.20	PP	29.94	0.1	0.7	2.3	2.2	0.1
23/07/13	23.40	PP	31.82	0.2	0.8	4.3	2.3	0.1
23/07/13	00.00	PP	31.60	1.8	1.1	7.1	3.9	0.1
23/07/13	00.20	PP	31.47	1.3	1.1	4.2	3.0	0.1
23/07/13	00.40	PP	31.35	1.7	0.9	1.3	4.4	0.4
23/07/13	01.00	PP	30.34	1.4	0.8	2.4	2.9	0.2
23/07/13	01.20	PP	30.51	1.1	1.0	3.4	3.6	0.3
23/07/13	01.40	PP	31.21	3.5	0.8	7.2	6.1	0.8
23/07/13	02.00	PP	31.17	3.2	0.9	4.6	5.6	0.1
23/07/13	02.20	PP	31.12	3.2	0.9	0.6	5.5	0.5
23/07/13	02.40	PP	31.64	2.7	1.0	2.3	5.2	0.3
23/07/13	03.00	PP	31.73	3.0	0.8	0.7	6.2	0.3
23/07/13	03.20	PP	31.64	3.4	0.7	8.0	12.2	0.4
23/07/13	03.40	PP	31.69	1.9	0.7	0.8	6.5	0.5
23/07/13	04.00	PP	31.64	0.5	0.3	1.9	13.1	0.4
23/07/13	04.20	PP	32.39	2.7	0.5	1.8	12.4	1.2
23/07/13	04.40	PP	32.10	1.5	0.7	0.6	12.6	0.4
23/07/13	05.00	PP	31.89	2.0	0.4	0.6	17.1	0.7
23/07/13	05.20	PP	31.63	17.1	0.4	0.6	13.3	0.2
23/07/13	05.40	PP	31.55	14.0	0.5	0.5	11.5	0.2
23/07/13	06.00	PP	31.70	12.8	0.4	2.1	12.8	0.2
23/07/13	06.20	PP	31.89	6.7	0.9	4.1	8.1	0.3

23/07/13	06.40	PP	31.53	6.0	0.7	1.1	10.0	0.2
23/07/13	07.00	PP	31.51	0.5	0.8	9.2	3.1	0.1
23/07/13	07.20	PP	31.60	0.4	0.7	1.5	3.0	0.2
23/07/13	07.40	PP	31.61	0.4	0.7	1.9	3.0	0.1
23/07/13	08.00	PP	31.53	0.3	0.8	2.2	3.0	0.1
23/07/13	08.20	PP	31.55	0.4	0.9	3.9	3.0	0.1
23/07/13	08.40	PP	31.50	0.1	0.7	2.2	2.4	0.1
23/07/13	09.00	PP	32.07	0.2	0.7	2.7	2.3	0.5
23/07/13	09.20	PP	30.98	0.1	0.7	0.9	3.0	0.2
23/07/13	09.40	PP	31.58	0.2	0.6	2.5	2.4	0.2
23/07/13	10.00	PP	31.37	0.1	0.6	0.5	2.5	0.3
23/07/13	10.20	PP	30.76	0.1	0.6	1.2	2.7	0.2
23/07/13	10.40	PP	31.43	0.1	0.5	3.1	3.0	0.2
23/07/13	11.00	PP	30.72	0.4	0.6	2.8	6.9	0.2
23/07/13	11.20	PP	30.49	0.1	0.7	3.4	7.6	0.3
23/07/13	11.40	PP	30.88	0.2	0.6	3.7	10.1	0.7
23/07/13	12.00	PP	31.09	0.1	0.6	1.1	8.9	1.1
23/07/13	12.20	PP	30.90	0.1	0.6	1.0	6.0	0.2
23/07/13	12.40	PP	34.16	0.1	0.6	0.7	6.3	0.1

January 2015

Collection Date	Time	Site ID	Salinity (ppt)	NO_3^- (µmol L^{-1})	NO_2^- (µmol L^{-1})	NH_4^+ (µmol L^{-1})	DRSi (µmol L^{-1})	TDP (µmol L^{-1})
31/01/15	08.40	Castle	0.52	13.94	1.85	1.40	4.64	0.08
31/01/15	09.00	Castle	0.52	13.92	1.86	1.12	4.68	0.06
31/01/15	09.20	Castle	0.52	14.21	1.86	1.04	4.68	0.06
31/01/15	09.40	Castle	0.52	13.99	1.86	1.06	4.57	0.08
31/01/15	10.00	Castle	0.52	13.99	1.86	1.09	4.61	0.06
31/01/15	10.20	Castle	0.52	13.92	1.86	1.15	4.61	0.07
31/01/15	10.40	Castle	0.52	13.79	1.86	1.03	4.57	0.07
31/01/15	11.00	Castle	0.52	13.64	1.86	1.02	4.64	0.08
31/01/15	11.20	Castle	0.52	13.71	1.86	1.07	4.61	0.15
31/01/15	11.40	Castle	0.60	13.85	1.86	1.05	4.57	0.07
31/01/15	12.00	Castle	0.52	13.56	1.86	1.02	4.61	0.07
31/01/15	15.00	Sewage	0.65	4.01	1.86	1.13	3.61	0.27
31/01/15	15.20	Sewage	0.62	3.94	1.86	1.12	3.93	0.35
31/01/15	15.40	Sewage	0.70	4.20	1.86	1.08	3.82	0.11
31/01/15	16.00	Sewage	1.54	4.91	1.86	1.21	3.79	0.11
31/01/15	16.20	Sewage	0.84	4.22	1.86	1.06	3.68	0.22
31/01/15	16.40	Sewage	0.60	4.04	1.86	1.05	3.68	0.09
31/01/15	17.00	Sewage	0.91	4.05	1.86	1.32	3.96	0.11
31/01/15	17.20	Sewage	0.85	4.14	1.86	1.12	3.71	0.09
31/01/15	17.40	Sewage	0.92	3.94	1.86	1.15	3.64	0.08
01/02/15	10.15	PP	3.03	5.41	1.86	1.19	5.41	0.07
01/02/15	10.45	PP	4.05	5.39	1.86	1.09	5.39	0.07
01/02/15	11.15	PP	11.49	4.32	1.86	1.09	4.32	0.07
01/02/15	11.45	PP	11.03	4.28	1.86	1.09	4.28	0.07
01/02/15	12.15	PP	16.59	3.39	1.86	1.15	3.39	0.07
01/02/15	12.45	PP	16.96	3.25	1.86	1.15	3.25	0.07
01/02/15	13.15	PP	19.36	2.85	1.86	1.11	2.85	0.07
01/02/15	13.45	PP	19.81	2.81	1.85	1.14	2.81	0.07
01/02/15	14.15	PP	18.38	2.84	1.86	1.22	2.84	0.07
01/02/15	14.45	PP	20.42	2.78	1.86	1.21	2.78	0.06
01/02/15	15.15	PP	20.57	2.49	1.86	1.21	2.49	0.07
01/02/15	15.45	PP	17.58	2.34	1.86	1.33	2.34	0.11
01/02/15	16.15	PP	14.59	3.70	1.84	1.21	3.70	0.06
01/02/15	16.45	PP	16.22	3.49	1.86	1.14	3.49	0.05

01/02/15	17.15	PP	18.53	3.19	1.86	1.15	3.19	0.06
01/02/15	17.45	PP	4.35	5.03	1.86	1.12	5.03	0.05
01/02/15	18.15	PP	4.63	5.09	1.86	1.21	5.09	0.08
01/02/15	18.45	PP	6.47	4.80	1.86	1.16	4.80	0.08
01/02/15	19.15	PP	7.63	4.76	1.86	1.11	4.76	0.07
01/02/15	19.45	PP	6.93	4.63	1.86	1.16	4.63	0.07
01/02/15	20.15	PP	6.90	4.51	1.86	1.21	4.51	0.07
01/02/15	20.45	PP	7.75	4.39	1.86	1.14	4.39	0.06
01/02/15	21.15	PP	7.72	4.36	1.86	1.16	4.36	0.06
01/02/15	21.45	PP	9.76	4.06	1.87	1.23	4.06	0.08
01/02/15	22.15	PP	10.09	4.15	1.86	1.15	4.15	0.06
01/02/15	22.45	PP	12.72	4.00	1.86	1.11	4.00	0.06
01/02/15	23.15	PP	8.59	3.42	1.86	1.14	3.42	0.08
01/02/15	23.45	PP	16.22	3.22	1.86	1.08	3.22	0.08
01/02/15	00.15	PP	14.22	3.49	1.86	1.11	3.49	0.07
01/02/15	00.45	PP	19.73	2.71	1.86	1.19	2.71	0.07
01/02/15	01.15	PP	16.81	2.90	1.86	1.14	2.90	0.07
01/02/15	01.45	PP	18.53	2.79	1.86	1.15	2.79	0.14
01/02/15	02.15	PP	18.00	2.86	1.86	1.13	2.86	0.21
01/02/15	02.45	PP	19.36	2.52	1.86	1.23	2.52	0.07
01/02/15	03.15	PP	19.43	2.25	1.88	1.11	2.25	0.05
01/02/15	03.45	PP	20.95	2.26	1.86	1.10	2.26	0.06
01/02/15	04.15	PP	21.25	2.22	1.86	1.09	2.22	0.06
01/02/15	04.45	PP	20.87	2.17	1.86	1.06	2.17	0.05
01/02/15	05.15	PP	16.96	3.01	1.86	1.14	3.01	0.05
01/02/15	05.45	PP	10.81	4.29	1.86	1.56	4.29	0.10
01/02/15	06.15	PP	9.00	4.36	1.86	1.21	4.36	0.06
01/02/15	06.45	PP	9.79	4.29	1.86	1.07	4.29	0.06
01/02/15	07.15	PP	9.16	4.13	1.86	1.39	4.13	0.04
01/02/15	07.45	PP	11.02	3.90	1.86	1.27	3.90	0.06
01/02/15	08.15	PP	12.70	3.21	1.86	1.21	3.21	0.04
01/02/15	08.45	PP	11.99	3.48	1.86	1.11	3.48	0.04
01/02/15	09.15	PP	17.03	2.74	1.86	1.11	2.74	0.07
01/02/15	09.45	PP	14.51	2.41	1.78	1.40	2.41	0.05

June 2015

Collection Date	Time	Site ID	Salinity (ppt)	NO_3^- (μmol L^{-1})	NO_2^- (μmol L^{-1})	NH_4^+ (μmol L^{-1})	DRSi (μmol L^{-1})	TDP (μmol L^{-1})
11/06/15	19.00	Castle	0.54	81.43	0.20	BDL	43.57	0.28
11/06/15	19.15	Castle	0.54	80.71	0.15	BDL	43.57	0.21
11/06/15	19.30	Castle	0.53	83.57	0.26	BDL	44.29	0.22
11/06/15	19.45	Castle	0.56	82.86	0.99	BDL	43.57	0.26
11/06/15	20.00	Castle	0.54	83.57	0.18	BDL	43.57	0.24
11/06/15	20.15	Castle	0.51	84.29	0.01	BDL	44.29	0.24
11/06/15	20.30	Castle	0.51	82.86	0.04	BDL	52.50	0.23
11/06/15	20.45	Castle	0.52	85.00	0.11	BDL	44.29	0.27
11/06/15	21.00	Castle	0.50	82.86	0.20	BDL	44.29	0.24
11/06/15	21.15	Castle	0.52	82.14	0.20	BDL	45.71	0.24
11/06/15	13.25	Sewage	11.50	13.21	0.29	0.86	20.07	0.21
11/06/15	13.40	Sewage	11.18	13.29	0.82	10.21	19.71	0.15
11/06/15	13.55	Sewage	10.61	14.00	0.34	0.89	21.71	0.21
11/06/15	14.15	Sewage	10.95	14.07	0.25	2.02	21.54	0.33
11/06/15	14.35	Sewage	12.38	12.07	0.21	0.97	21.57	0.31
11/06/15	14.55	Sewage	11.44	12.36	0.32	2.85	20.21	0.27
11/06/15	15.00	Sewage	11.08	13.57	0.49	0.96	20.39	0.35
11/06/15	15.15	Sewage	6.92	9.57	0.23	1.71	20.64	0.20
11/06/15	15.30	Sewage	6.35	13.29	0.16	2.26	20.82	0.16
11/06/15	15.45	Sewage	6.46	12.01	0.22	2.14	21.75	0.63
11/06/15	07.30	PP	29.67	3.21	0.37	0.43	5.34	0.23
11/06/15	08.00	PP	29.51	3.30	0.32	1.21	5.12	0.20
11/06/15	08.30	PP	28.4	5.14	0.33	1.21	6.23	0.21
11/06/15	09.00	PP	28.4	4.47	0.31	0.74	5.91	0.18
12/06/15	09.30	PP	28.4	4.35	0.46	3.12	6.05	0.17
12/06/15	10.00	PP	30.22	4.10	0.34	2.17	5.98	0.21
12/06/15	10.30	PP	30.86	4.27	0.35	3.40	7.26	0.25
12/06/15	11.00	PP	32.78	4.59	0.43	2.86	6.62	0.25
12/06/15	11.30	PP	31.9	3.89	0.38	0.51	5.27	0.21
12/06/15	12.00	PP	33.02	2.72	0.38	2.90	4.07	0.23
12/06/15	12.30	PP	33.51	1.55	0.49	1.22	3.40	0.24
12/06/15	13.00	PP	33.26	2.08	0.49	2.43	6.19	0.27
12/06/15	13.30	PP	33.83	2.46	0.65	5.26	4.09	0.20
12/06/15	14.00	PP	33.59	2.09	0.39	1.84	4.16	0.25

12/06/15	14.30	PP	33.59	1.24	1.00	1.70	3.99	0.24
12/06/15	15.00	PP	34.39	1.13	0.52	2.59	4.37	0.21
12/06/15	15.30	PP	34.72	1.00	0.39	3.44	4.31	0.17
12/06/15	16.00	PP	35.28	0.96	0.39	1.21	4.06	0.24
12/06/15	16.30	PP	35.37	0.93	0.37	3.42	3.52	0.25
12/06/15	17.00	PP	34.47	0.82	0.50	0.56	4.28	0.20
12/06/15	17.30	PP	35.28	0.88	0.41	0.51	3.40	0.22
12/06/15	18.00	PP	35.37	0.89	0.37	0.55	3.15	0.22
12/06/15	18.30	PP	35.37	0.95	0.40	0.51	3.67	0.19
12/06/15	19.00	PP	34.72	0.90	0.44	0.51	3.50	0.17
12/06/15	19.30	PP	34.8	0.97	0.41	0.46	4.02	0.19
12/06/15	20.00	PP	33.75	1.23	0.38	1.30	3.70	0.24
12/06/15	20.30	PP	32.7	1.65	0.38	1.13	4.80	0.19
12/06/15	21.00	PP	31.42	1.79	0.53	1.13	4.09	0.17
12/06/15	21.30	PP	32.06	1.64	0.41	2.40	4.48	0.26
12/06/15	22.00	PP	31.98	1.39	0.36	0.45	5.34	0.28
12/06/15	22.30	PP	32.46	3.00	0.37	1.23	4.13	0.25
12/06/15	23.00	PP	32.46	3.11	0.44	0.61	4.63	0.61
12/06/15	23.30	PP	33.51	2.09	0.57	4.21	3.37	0.57
12/06/15	00.00	PP	33.02	1.83	0.43	0.55	3.95	0.72
12/06/15	00.30	PP	33.34	0.96	0.32	0.50	3.47	0.64
12/06/15	01.00	PP	34.07	1.44	0.40	0.51	3.91	0.72
12/06/15	01.30	PP	34.15	0.88	0.44	0.50	3.46	0.72
13/06/15	02.00	PP	33.64	1.36	0.45	1.69	3.31	0.72
13/06/15	02.30	PP	34.37	0.64	0.39	1.09	2.84	0.67
13/06/15	03.00	PP	35.37	0.72	0.41	1.09	3.09	0.72
13/06/15	03.30	PP	35.37	1.05	0.43	0.94	3.01	0.52
13/06/15	04.00	PP	35.28	1.01	0.61	1.34	3.05	0.69
13/06/15	04.30	PP	35.53	1.20	0.54	0.40	3.41	0.66
13/06/15	05.00	PP	34.96	1.15	0.42	1.42	3.63	0.49
13/06/15	05.30	PP	35.53	1.66	0.42	0.51	3.09	0.65
13/06/15	06.00	PP	34.23	1.36	0.33	0.53	3.59	0.45
13/06/15	06.30	PP	34.39	1.23	0.68	0.57	3.74	0.58

January 2016

Collection Date	Time	Site ID	Salinity (ppt)	NO_3^- (μmol L^{-1})	NO_2^- (μmol L^{-1})	NH_4^+ (μmol L^{-1})	DRSi (μmol L^{-1})	TDP (μmol L^{-1})
30/01/16	14.00	Castle	0.56	99.46	1.61	0.41	51.96	1.77
30/01/16	14.15	Castle	0.52	98.01	2.70	0.10	50.71	1.12
30/01/16	14.30	Castle	0.53	94.80	1.49	0.11	50.18	1.13
30/01/16	14.45	Castle	0.52	97.80	1.90	0.09	51.07	1.14
30/01/16	15.00	Castle	0.51	98.46	1.52	0.03	50.89	0.91
30/01/16	15.15	Castle	0.53	97.76	1.65	0.06	51.25	0.81
30/01/16	15.30	Castle	0.53	99.77	1.47	0.17	51.61	0.96
30/01/16	15.45	Castle	0.52	100.31	2.49	0.14	50.89	0.99
30/01/16	16.00	Castle	0.52	98.22	1.77	0.33	50.54	0.88
30/01/16	16.15	Castle	0.51	98.94	1.85	0.25	50.71	0.83
30/01/16	08.00	Sewage	1.16	38.05	0.45	0.17	40.98	0.28
30/01/16	08.15	Sewage	1.14	37.05	1.31	0.12	42.50	6.55
30/01/16	08.30	Sewage	2.13	34.31	1.41	10.96	40.71	4.16
30/01/16	08.45	Sewage	2.18	32.79	1.19	27.32	40.36	1.77
30/01/16	09.15	Sewage	0.63	33.14	1.57	0.22	40.71	1.55
30/01/16	09.30	Sewage	0.53	31.93	1.55	0.18	40.71	1.50
30/01/16	09.45	Sewage	0.39	32.30	1.22	0.11	40.00	1.44
30/01/16	10.00	Sewage	0.00	32.42	1.95	0.72	40.18	1.25
30/01/16	10.15	Sewage	2.35	32.09	1.34	0.15	40.54	1.15
30/01/16	10.30	Sewage	2.42	34.10	1.62	0.19	41.43	1.14
30/01/16	10.30a	Sewage	2.36	35.03	1.40	0.24	39.64	1.51
30/01/16	18.15	PP	34.66	35.18	0.90	0.31	30.77	0.82
30/01/16	18.45	PP	35.11	35.26	1.44	0.29	30.95	0.80
30/01/16	19.15	PP	35.33	31.33	1.40	0.29	31.36	0.80
30/01/16	19.45	PP	35.22	31.39	1.14	0.23	32.91	0.77
30/01/16	20.15	PP	35.11	32.06	1.17	0.32	30.86	0.77
30/01/16	20.45	PP	33.88	31.03	0.97	0.33	30.46	0.90
30/01/16	21.15	PP	34.32	32.44	0.91	0.38	30.66	0.70
30/01/16	21.45	PP	34.77	31.84	1.04	0.28	30.75	0.98
30/01/16	22.15	PP	31.85	28.20	0.99	0.64	26.84	1.02
30/01/16	22.45	PP	21.79	25.55	0.66	0.42	24.04	0.88
30/01/16	23.15	PP	18.40	20.96	0.59	0.44	22.88	0.87
31/01/16	23.45	PP	12.71	16.58	0.41	0.52	18.46	0.91

31/01/16	00.15	PP	13.31	15.39	0.93	1.72	16.91	0.81
31/01/16	01.15	PP	13.14	15.81	1.00	0.74	13.30	0.77
31/01/16	01.45	PP	12.59	15.60	0.70	2.36	12.75	0.70
31/01/16	02.15	PP	15.73	15.82	0.83	0.74	12.25	0.73
31/01/16	02.45	PP	16.95	15.87	0.43	0.79	13.11	0.78
31/01/16	03.15	PP	16.43	15.32	0.42	0.62	11.34	0.78
31/01/16	03.45	PP	16.90	15.47	0.67	0.00	10.70	0.69
31/01/16	04.15	PP	17.57	14.92	0.39	0.41	10.05	0.71
31/01/16	04.45	PP	18.92	15.36	0.57	0.41	12.73	0.74
31/01/16	05.15	PP	23.48	17.96	0.47	0.75	13.63	0.73
31/01/16	05.45	PP	27.26	15.19	0.32	0.71	13.41	0.70
31/01/16	06.15	PP	30.65	16.43	0.64	0.52	14.30	0.75
31/01/16	06.45	PP	36.31	14.41	0.92	0.68	13.88	0.71
31/01/16	07.15	PP	27.08	16.24	0.75	1.11	13.48	0.79
31/01/16	07.45	PP	34.63	15.93	0.98	1.87	11.02	1.01
31/01/16	08.15	PP	35.25	16.91	0.58	1.20	11.84	0.80
31/01/16	08.45	PP	33.94	17.63	0.43	0.75	13.11	0.76
31/01/16	09.15	PP	35.20	19.00	0.38	0.74	14.27	0.82
31/01/16	09.45	PP	34.78	18.51	0.48	0.68	15.16	0.89
31/01/16	10.15	PP	36.10	18.20	0.43	1.08	14.09	0.78
31/01/16	10.45	PP	34.89	18.67	0.42	0.77	13.07	0.82
31/01/16	11.15	PP	34.78	17.71	0.48	1.44	12.50	0.69
31/01/16	11.45	PP	35.10	17.32	0.40	0.51	12.73	1.00
31/01/16	12.15	PP	34.05	16.53	0.97	0.55	10.68	1.11
31/01/16	12.45	PP	33.63	16.07	0.58	0.57	13.13	0.93
31/01/16	13.15	PP	33.73	18.07	0.50	0.87	14.20	0.82
31/01/16	13.45	PP	34.47	18.72	0.50	0.78	15.30	0.78
31/01/16	14.15	PP	34.36	16.27	0.43	1.01	13.34	0.82
31/01/16	14.45	PP	33.32	21.15	0.39	1.87	14.61	0.94
31/01/16	15.15	PP	34.15	21.71	0.34	0.87	14.04	0.81
31/01/16	15.45	PP	35.74	30.22	0.39	0.70	15.96	0.79
31/01/16	16.15	PP	35.05	33.82	0.37	1.79	15.18	0.76
31/01/16	16.45	PP	35.73	21.49	0.39	1.28	18.79	0.82
30/01/16	17.15	PP	36.53	33.82	0.58	1.75	23.46	0.81
30/01/16	17.45	PP	34.66	32.19	1.02	0.41	29.02	0.82

Appendix C: Examples of Calculations

Water/Salt Budgets:

Table C.1: Integrated Area of Flood Example from January 2015. The change in height of the tide (m) was multiplied by the change in time (hr), this was then multiplied by the salinity to determine the associated salt flux. The flood flux is represented by positive values as the salt is entering the bay while the ebb flux is negative as the tide is leaving the bay. The integrated area of the daily ebb tide is subtracted from the daily flood to determine the net exchange of salt (g m^{-2} d^{-1}) with the open ocean.

Time	Tide Height (m)	Change in height with time (m)	Change in Time (hr)	Change in height /Change in time dh/dt (m hr^{-1})	Salinity (mg m^{-3})	Flux = Salinity * dh/dt
09.30	1.160					
10.00	1.200	0.040	0.5	0.08	3.03	0.24
10.30	1.320	0.120	0.5	0.24	4.05	0.97
11.00	1.530	0.210	0.5	0.42	11.49	4.82
11.30	1.800	0.270	0.5	0.54	11.03	5.96
12.00	2.100	0.300	0.5	0.6	16.59	9.95
12.30	2.400	0.300	0.5	0.6	16.96	10.17
13.00	2.740	0.340	0.5	0.68	19.36	13.16
13.30	3.100	0.360	0.5	0.72	19.81	14.26
14.00	3.480	0.380	0.5	0.76	18.38	13.97
14.30	3.860	0.380	0.5	0.76	20.42	15.52
15.00	4.120	0.260	0.5	0.52	20.57	10.70
15.30	4.280	0.160	0.5	0.32	17.58	5.63
16.00	4.290	0.010	0.5	0.02	14.59	0.29
16.30	4.180	-0.110	0.5	-0.22	16.22	-3.57
17.00	4.000	-0.180	0.5	-0.36	18.53	-6.67
17.30	3.750	-0.250	0.5	-0.5	4.35	-2.17
18.00	3.450	-0.300	0.5	-0.6	4.63	-2.78
18.30	3.110	-0.340	0.5	-0.68	6.47	-4.40
19.00	2.730	-0.380	0.5	-0.76	7.63	-5.80
20.00	2.340	-0.390	0.5	-0.78	6.93	-5.41
20.30	1.960	-0.380	0.5	-0.76	6.90	-5.24
21.00	1.650	-0.310	0.5	-0.62	7.75	-4.80
21.30	1.430	-0.220	0.5	-0.44	7.72	-3.40
22.00	1.290	-0.140	0.5	-0.28	9.76	-2.73
22.30	1.260	-0.030	0.5	-0.06	10.09	-0.61

Table C.2: SGD calculation from water/salt budgets from January 2015. The integrated area of the daily ebb tide is subtracted from the daily flood to determine the exchange of salt per m^2 (g m^{-2} d^{-1}) with the open ocean. This was then multiplied by the mean tidal level (m^2) to determine the total exchange of salt with the open ocean. This value was then divided by the salinity of fresh groundwater from Loughcurragh South borehole located 10 km inland from the SGD springs to determine the water flux from land. This was then multiplied by the associated FW/SGD ratio determined for that sampling point to remove freshwater runoff from the SGD value.

Flood flux mg m^{-2} A	Ebb flux mg m^{-2} B	Flood – Ebb (mg m^{-2} d^{-1}) A - B	C *MTL C * 1618 m^2 (mg d^{-1})	D/Terrestrial FW Salinity (0.43 mg m^{-3}) m^3 d^{-1}	E*FW/SGD ratio m^3 d^{-1}
(A) 219.82	(B) 135.52	(C) 84.3	(D) 136,391.1	(E) 317,187	215,687

Tidal Exchange of Nutrients:

Table C.3: Integrated Area of Flood Example from January 2015. The change in height of the tide (m) was multiplied by the change in time (hr), this was then multiplied by the nutrient concentration (mol m^{-3}) to determine the associated nutrient flux. The flood flux is represented by positive values as the salt is entering the bay while the ebb flux is negative as the tide is leaving the bay. The integrated area of the daily ebb tide is subtracted from the daily flood to determine the net exchange of nutrient (mol m^{-2} d^{-1}) with the open ocean (Parkmore Pier Tidal Exchange). This is then multiplied by the mean tidal level (MTL) to determine flux over the area (m^2) that this occurs (mol d^{-1}).

Time	Tide Height (m) A.	Change in height with time (m) B. (A2 – A1)	Change in Time (hr) C.	Change in height /Change in time dh/dt (m hr^{-1}) D = B/C	Nutrient (NO_3^-) (mol m^{-3}) E.	Flux = [Nutrient] * dh/dt mol m^{-2} h^{-1} F = D*E	mol m^{-2} h^{-1} *MTL(m^2) mol d^{-1} G = F*MTL
09.30	1.160						
10.00	1.200	0.040	0.5	0.08	0.054	0.005	8.76
10.30	1.320	0.120	0.5	0.24	0.054	0.016	26.00
11.00	1.530	0.210	0.5	0.42	0.043	0.021	33.42
11.30	1.800	0.270	0.5	0.54	0.043	0.027	43.34
12.00	2.100	0.300	0.5	0.6	0.034	0.025	40.40
12.30	2.400	0.300	0.5	0.6	0.033	0.026	42.07
13.00	2.740	0.340	0.5	0.68	0.029	0.023	37.44
13.30	3.100	0.360	0.5	0.72	0.028	0.022	35.34
14.00	3.480	0.380	0.5	0.76	0.028	0.020	31.57
14.30	3.860	0.380	0.5	0.76	0.028	0.016	25.18
15.00	4.120	0.260	0.5	0.52	0.025	0.010	15.85
15.30	4.280	0.160	0.5	0.32	0.023	0.005	7.73
16.00	4.290	0.010	0.5	0.02	0.037	0.000	0.12
16.30	4.180	-0.110	0.5	-0.22	0.035	-0.007	-11.42
17.00	4.000	-0.180	0.5	-0.36	0.032	-0.013	-20.25
17.30	3.750	-0.250	0.5	-0.5	0.050	-0.028	-45.40
18.00	3.450	-0.300	0.5	-0.6	0.051	-0.035	-56.69
18.30	3.110	-0.340	0.5	-0.68	0.048	-0.037	-60.11
19.00	2.730	-0.380	0.5	-0.76	0.048	-0.039	-62.59
20.00	2.340	-0.390	0.5	-0.78	0.046	-0.037	-59.91
20.30	1.960	-0.380	0.5	-0.76	0.045	-0.033	-53.90
21.00	1.650	-0.310	0.5	-0.62	0.044	-0.028	-44.56
21.30	1.430	-0.220	0.5	-0.44	0.044	-0.021	-33.42
22.00	1.290	-0.140	0.5	-0.28	0.041	-0.012	-19.96
22.30	1.260	-0.030	0.5	-0.06	0.042	-0.004	-7.12

Flood NO_3^- Flux – Ebb NO_3^- Flux = sum(G) = -128.1 mol per one tidal cycle.

Tidal Exchange of Nutrients:

Table C.4: Wet deposition flux example for January 2015. The cumulative 14-day precipitation (mm) was determined from www.met.ie for the closest weather stations, Athenry and Oranmore. This was converted to m and then multiplied by the surface area of the bay (m^2) to determine the volume (m^3) of precipitation. The volume of precipitation (m^3) was multiplied by the nitrate concentration (mol m^{-3}) to determine the flux of nitrate in the 14 day period. This was then divided by 14 to determine the mol d^{-1} flux.

Cumulative 14-day precipitation (mm) A.	mm converted to m B.	Rainfall*Surface Area of Bay (m^2) C. = B*Area (m^3)	NO_3^- conc (mol m^{-3}) D.	Flux = C*D mol in 14 day period	mol d^{-1} = E/14
53.2	0.05	224504	0.0075	1739.9	124.3

Primary Productivity Calculations:

Table C.5: An example of the primary productivity calculations in Chapter 3. January 2015 net retention within Kinvara Bay was measured by adding the allochthonous loading (precipitation, sewage and SGD) to the sediment fluxes and tidal exchange at Parkmore Pier and retaining the signs. This was then used to calculate the projected concentration of the measured nutrients in the water column in the absence of assimilation by primary producers by converting this to a concentration value in µmol L^{-1}. The primary producer's transfer of nutrients was then estimated as the difference between the projected concentration and the actual measured concentration of the relevant nutrient within the bay as per calculations shown in Rocha et al. (2015). This value was then converted back into a flux by reversing the calculations.

Allochthonous Loading mol d^{-1}	Sediment Fluxes mol d^{-1}	Tidal Exchange mol d^{-1}	Net Retention D = A + B +C mol d^{-1}	D*Retention time (d) mol
A. 3516	B. -19,600	C. -213.6	D. -16297	E. -110822
E/Volume at MTL (m^3) mol m^{-3}	Projected Concentration Convert to µmol L^{-1}	Actual Conc µmol L^{-1}	Difference (G-H) µmol L^{-1}	Reverse Flux calculation (E – G)
F. -0.0091	G. -9.07	H. 3.6	I. -5.47	-9830

Appendix D: Measured Carbon Species (DOC, DIC, TAlk) Concentrations for Budgetary Analysis (Chapter 3) - Raw Data

July 2013

Collection Date	Time	Site ID	Salinity (ppt)	DOC (μmol L^{-1}) n = 3	Standard Deviation (μmol L^{-1})	DIC (μmol L^{-1}) n = 3	Standard Deviation (μmol L^{-1})	TAl (μmol
22/07/13	11.00	Castle	3.67	445.77	8.53	---	---	---
22/07/13	11.20	Castle	3.17	425.08	4.61	---	---	---
22/07/13	11.40	Castle	2.96	378.26	3.77	---	---	---
22/07/13	12.00	Castle	2.67	425.41	4.04	---	---	---
22/07/13	12.20	Castle	2.31	554.86	8.97	---	---	---
22/07/13	12.40	Castle	2.22	587.45	4.34	---	---	---
22/07/13	13.00	Castle	1.90	353.52	1.23	---	---	---
22/07/13	13.20	Castle	1.84	334.34	3.80	---	---	---
22/07/13	13.40	Castle	1.86	358.39	3.26	---	---	---
22/07/13	14.50	Sewage	22.2	234.86	9.65	2,039.96	35.48	---
22/07/13	15.10	Sewage	21.8	273.13	19.43	2,193.32	9.80	---
22/07/13	15.35	Sewage	20.58	272.88	17.97	2,333.79	3.28	---
22/07/13	15.50	Sewage	22.15	209.00	7.36	2,199.90	6.21	---
22/07/13	16.10	Sewage	21.9	266.44	12.09	2,108.68	8.56	---
22/07/13	16.30	Sewage	23.4	305.59	8.53	2,050.09	7.20	---
22/07/13	16.50	Sewage	23.3	226.69	12.17	2,020.36	5.97	---
22/07/13	17.05	Sewage	23.3	178.34	3.85	2,033.02	4.64	---
22/07/13	17.30	Sewage	23.36	124.41	1.33	2,024.86	1.75	---
22/07/13	13.00	PP	31.58	249.42	24.27	1,918.92	28.35	---
22/07/13	13.20	PP	32.03	228.96	8.49	1,995.11	1.76	---
22/07/13	13.40	PP	31.46	207.31	13.36	1,997.65	6.46	---
22/07/13	14.00	PP	31.82	196.40	12.76	1,997.83	6.58	---
22/07/13	14.20	PP	31.92	198.39	8.83	1,999.76	6.35	---
22/07/13	14.40	PP	32.07	185.67	9.98	2,016.24	8.78	---
22/07/13	15.00	PP	32.61	197.99	6.83	2,003.99	6.06	---
22/07/13	15.20	PP	31.11	194.54	12.04	2,005.25	6.56	---
22/07/13	15.40	PP	32.21	196.27	5.84	1,995.85	5.10	---
22/07/13	16.00	PP	32.27	227.27	13.60	2,007.76	11.76	---
22/07/13	16.20	PP	31.81	211.82	11.10	1,976.48	27.09	---
22/07/13	16.40	PP	32.03	195.36	10.99	2,034.48	2.73	---
22/07/13	17.00	PP	32.18	215.70	16.31	2,053.86	10.16	---
22/07/13	17.20	PP	30.75	198.67	12.67	2,037.57	7.29	---
22/07/13	17.40	PP	32.25	178.05	3.98	2,066.48	1.12	---

22/07/13	18.00	PP	31.82	226.29	14.52	2,027.33	9.41	---
22/07/13	18.20	PP	32.16	262.28	13.96	2,255.18	2.47	---
22/07/13	18.40	PP	31.89	201.96	14.13	2,196.36	8.74	---
22/07/13	19.00	PP	31.88	191.53	8.20	2,289.54	5.90	---
22/07/13	19.20	PP	30.97	276.33	19.90	2,280.89	12.89	---
22/07/13	19.40	PP	30.51	326.41	15.53	2,247.43	24.51	---
22/07/13	20.00	PP	31.71	196.91	8.08	2,321.63	10.16	---
22/07/13	20.20	PP	30.72	175.28	9.21	2,223.57	9.75	---
22/07/13	20.40	PP	30.60	191.25	14.58	2,243.73	5.53	---
22/07/13	21.00	PP	30.40	189.88	0.71	2,222.76	0.82	---
22/07/13	21.20	PP	31.70	199.78	2.46	2,084.45	3.29	---
22/07/13	21.40	PP	30.89	202.13	19.61	2,124.22	17.63	---
22/07/13	22.00	PP	30.37	202.05	9.22	2,108.54	8.97	---
22/07/13	22.20	PP	30.48	183.52	0.02	2,065.48	0.56	---
22/07/13	22.40	PP	31.38	191.84	14.01	2,086.90	5.64	---
23/07/13	23.00	PP	23.64	162.21	14.83	2,009.91	27.09	---
23/07/13	23.20	PP	29.94	145.27	5.45	2,103.77	1.49	---
23/07/13	23.40	PP	31.82	140.28	2.72	2,086.49	1.23	---
23/07/13	00.00	PP	31.60	171.79	4.15	2,070.17	6.05	---
23/07/13	00.20	PP	31.47	186.33	5.36	2,082.23	2.91	---
23/07/13	00.40	PP	31.35	195.39	19.25	2,083.39	7.17	---
23/07/13	01.00	PP	30.34	135.07	16.45	2,103.06	4.48	---
23/07/13	01.20	PP	30.51	163.87	6.19	2,077.91	6.80	---
23/07/13	01.40	PP	31.21	147.27	10.35	2,089.71	4.67	---
23/07/13	02.00	PP	31.17	142.22	13.77	2,099.49	3.85	---
23/07/13	02.20	PP	31.12	169.37	9.58	2,037.28	24.13	---
23/07/13	02.40	PP	31.64	114.11	7.43	2,127.76	0.67	---
23/07/13	03.00	PP	31.73	151.74	15.12	2,196.09	8.37	---
23/07/13	03.20	PP	31.64	166.80	7.05	2,155.04	1.94	---
23/07/13	03.40	PP	31.69	179.07	2.62	2,109.63	1.91	---
23/07/13	04.00	PP	31.64	146.32	3.70	2,093.57	2.84	---
23/07/13	04.20	PP	32.39	146.74	4.66	2,062.36	2.13	---
23/07/13	04.40	PP	32.10	137.22	1.21	2,066.82	3.44	---
23/07/13	05.00	PP	31.89	142.00	4.62	2,091.44	1.38	---
23/07/13	05.20	PP	31.63	147.71	16.09	2,052.78	26.12	---
23/07/13	05.40	PP	31.55	125.34	17.36	2,127.72	6.73	---
23/07/13	06.00	PP	31.70	127.21	9.72	2,121.73	5.08	---

23/07/13	06.20	PP	31.89	146.42	7.67	2,110.76	3.25	---
23/07/13	06.40	PP	31.53	130.27	17.25	2,121.28	10.46	---
23/07/13	07.00	PP	31.51	133.90	0.57	2,140.00	0.78	---
23/07/13	07.20	PP	31.60	145.35	5.53	2,107.41	1.79	---
23/07/13	07.40	PP	31.61	134.11	1.74	2,107.48	2.24	---
23/07/13	08.00	PP	31.53	135.98	6.48	2,101.92	3.14	---
23/07/13	08.20	PP	31.55	192.09	24.27	1,918.92	28.35	---
23/07/13	08.40	PP	31.50	121.74	8.49	1,995.11	1.76	---
23/07/13	09.00	PP	32.07	122.45	13.36	1,997.65	6.46	---
23/07/13	09.20	PP	30.98	174.27	12.76	1,997.83	6.58	---
23/07/13	09.40	PP	31.58	163.85	8.83	1,999.76	6.35	---
23/07/13	10.00	PP	31.37	175.00	9.98	2,016.24	8.78	---
23/07/13	10.20	PP	30.76	183.80	6.83	2,003.99	6.06	---
23/07/13	10.40	PP	31.43	234.49	12.04	2,005.25	6.56	---
23/07/13	11.00	PP	30.72	146.18	5.84	1,995.85	5.10	---
23/07/13	11.20	PP	30.49	156.89	13.60	2,007.76	11.76	---
23/07/13	11.40	PP	30.88	184.07	11.10	1,976.48	27.09	---
23/07/13	12.00	PP	31.09	119.05	10.99	2,034.48	2.73	---
23/07/13	12.20	PP	30.90	114.88	16.31	2,053.86	10.16	---
23/07/13	12.40	PP	34.16	133.09	12.67	2,037.57	7.29	---
23/07/13	---	Marine	35.22	178.06	21.36	2,060.84	31.28	---

January 2015

Collection Date	Time	Site ID	Salinity (ppt)	DOC (μmol L^{-1}) n = 3	Std Dev (μmol L^{-1})	DIC (μmol L^{-1}) n = 3	Std Dev (μmol L^{-1})	TAlk (μmol L^{-1})
31/01/15	08.40	Castle	0.52	315.90	3.89	4,340.59	44.32	4,768.80
31/01/15	09.00	Castle	0.52	303.01	5.63	4,594.39	1.50	4,756.80
31/01/15	09.20	Castle	0.52	291.57	4.38	4,615.71	38.52	4,799.20
31/01/15	09.40	Castle	0.52	300.14	3.53	4,554.38	0.19	4,813.60
31/01/15	10.00	Castle	0.52	300.82	4.20	4,610.52	0.67	4,742.40
31/01/15	10.20	Castle	0.52	294.66	2.93	4,693.56	2.62	4,803.20
31/01/15	10.40	Castle	0.52	330.19	2.96	4,480.91	0.56	4,770.40
31/01/15	11.00	Castle	0.52	301.88	1.60	4,536.26	66.35	4,810.40
31/01/15	11.20	Castle	0.52	295.38	2.48	4,590.56	144.70	4,764.00
31/01/15	11.40	Castle	0.60	298.50	2.65	4,483.53	2.54	4,688.00
31/01/15	15.00	Sewage	0.52	640.87	4.10	1,720.73	120.77	2427.20
31/01/15	15.20	Sewage	0.65	685.87	11.83	1,859.88	1.65	2518.40
31/01/15	15.40	Sewage	0.62	647.33	2.35	1,876.13	3.99	2528.00
31/01/15	16.00	Sewage	0.70	673.84	9.19	2,001.25	1.58	2717.60
31/01/15	16.20	Sewage	1.54	642.39	5.41	1,913.03	0.72	2536.80
31/01/15	16.40	Sewage	0.84	630.95	5.31	1,890.70	2.53	2527.20
31/01/15	17.00	Sewage	0.60	653.12	2.59	1,895.23	1.47	2545.60
31/01/15	17.20	Sewage	0.91	619.57	3.69	1,833.07	2.30	2556.00
31/01/15	17.40	Sewage	0.85	642.90	0.10	1,856.87	0.66	2590.40
01/02/15	10.15	PP	3.03	520.36	3.84	2,653.45	200.83	2835.20
01/02/15	10.45	PP	4.05	516.30	4.49	2,901.10	8.53	2798.40
01/02/15	11.15	PP	11.49	444.26	4.07	2,833.73	6.22	2711.20
01/02/15	11.45	PP	11.03	446.87	5.17	2,830.21	4.49	2771.20
01/02/15	12.15	PP	16.59	395.37	1.73	2,799.30	6.97	2699.20
01/02/15	12.45	PP	16.96	380.18	3.82	2,731.43	5.21	2684.00
01/02/15	13.15	PP	19.36	362.91	1.76	2,744.72	4.37	2705.60
01/02/15	13.45	PP	19.81	374.33	1.46	2,713.76	5.46	2846.40
01/02/15	14.15	PP	18.38	395.59	5.22	2,738.03	2.79	2707.20
01/02/15	14.45	PP	20.42	353.75	8.52	2,694.30	5.09	2704.00
01/02/15	15.15	PP	20.57	290.29	55.95	2,454.88	02.11	2699.20
01/02/15	15.45	PP	17.58	451.46	47.80	2,807.57	14.67	2745.60
01/02/15	16.15	PP	14.59	384.63	3.49	2,809.16	7.34	2699.20
01/02/15	16.45	PP	16.22	376.55	7.25	2,790.60	5.82	2700.00

01/02/15	17.15	PP	18.53	342.35	6.60	2,935.94	13.46	2796.00
01/02/15	17.45	PP	4.35	495.49	8.08	2,847.96	1.58	2816.00
01/02/15	18.15	PP	4.63	555.71	4.66	2,744.68	13.16	2760.80
01/02/15	18.45	PP	6.47	101.93	10.27	2,756.55	10.67	2771.20
01/02/15	19.15	PP	7.63	674.16	11.17	2,817.65	7.22	2810.40
01/02/15	19.45	PP	6.93	539.41	8.42	2,805.26	4.73	2804.80
01/02/15	20.15	PP	6.90	520.05	4.64	2,955.79	9.88	2807.20
01/02/15	20.45	PP	7.75	514.72	7.74	2,793.00	7.64	2799.20
01/02/15	21.15	PP	7.72	506.59	4.88	2,765.94	5.76	2816.40
01/02/15	21.45	PP	9.76	312.85	52.57	2,784.55	7.22	2841.60
01/02/15	22.15	PP	10.09	574.06	37.46	1,985.32	63.07	2736.80
01/02/15	22.45	PP	12.72	485.06	5.76	2,031.16	2.33	2720.00
01/02/15	23.15	PP	8.59	425.66	6.06	2,071.29	3.51	2723.20
01/02/15	23.45	PP	16.22	402.18	10.89	1,954.50	5.92	2700.00
01/02/15	00.15	PP	14.22	428.73	1.65	1,978.07	4.08	2685.60
01/02/15	00.45	PP	19.73	380.00	5.84	2,009.19	1.32	2720.00
01/02/15	01.15	PP	16.81	404.60	6.32	2,021.87	1.44	2792.80
01/02/15	01.45	PP	18.53	433.76	5.66	1,972.91	2.13	2707.20
01/02/15	02.15	PP	18.00	430.62	5.93	1,994.28	0.11	2680.00
01/02/15	02.45	PP	19.36	406.59	11.52	1,945.19	68.10	2666.40
01/02/15	03.15	PP	19.43	464.57	2.65	1,979.83	1.01	2696.80
01/02/15	03.45	PP	20.95	427.98	7.31	1,974.96	1.29	2639.20
01/02/15	04.15	PP	21.25	388.71	0.51	1,987.58	0.75	2681.60
01/02/15	04.45	PP	20.87	376.97	3.07	2,162.29	9.27	2623.20
01/02/15	05.15	PP	16.96	421.48	1.92	2,089.92	2.15	2854.40
01/02/15	05.45	PP	10.81	553.65	5.36	2,166.82	2.87	2835.20
01/02/15	06.15	PP	9.00	562.12	5.94	2,090.89	1.75	2798.40
01/02/15	06.45	PP	9.79	527.92	2.87	2,107.96	2.67	2711.20
01/02/15	07.15	PP	9.16	616.46	3.50	2,012.85	7.01	2771.20
01/02/15	07.45	PP	11.02	544.58	4.60	2,039.31	4.48	2699.20
01/02/15	08.15	PP	12.70	520.10	3.69	1,954.52	4.91	2684.00
01/02/15	08.45	PP	11.99	501.96	5.41	1,938.97	1.67	2705.60
01/02/15	09.15	PP	17.03	467.49	3.40	2,653.45	200.83	2846.40
01/02/15	09.45	PP	14.51	474.06	2.73	2,901.10	8.53	2707.20

June 2015

Collection Date	Time	Site ID	Salinity (ppt)	DOC (μmol L^{-1}) n = 3	Standard Deviation (μmol L^{-1})	DIC (μmol L^{-1}) n = 3	Standard Deviation (μmol L^{-1})	TAlk (μmol L^{-1})
11/06/15	19.00	Castle	0.54	355.28	12.43	3,789.43	108.69	4,601.60
11/06/15	19.15	Castle	0.54	373.05	10.46	4,103.66	7.16	4,535.20
11/06/15	19.30	Castle	0.53	366.32	5.01	4,148.68	416.70	4,518.40
11/06/15	19.45	Castle	0.56	381.62	14.60	4,069.80	400.44	4,557.60
11/06/15	20.00	Castle	0.54	385.81	10.63	4,042.80	404.14	4,509.60
11/06/15	20.15	Castle	0.51	375.34	16.47	3,986.21	1.94	4,598.40
11/06/15	20.30	Castle	0.51	379.40	7.33	4,020.40	400.14	4,536.80
11/06/15	20.45	Castle	0.52	378.51	8.49	3,947.12	401.76	4,554.40
11/06/15	21.00	Castle	0.50	380.59	6.55	4,123.20	8.71	4,549.60
11/06/15	21.15	Castle	0.52	366.88	8.17	4,064.95	402.56	4,552.00
11/06/15	13.25	Sewage	11.50	588.00	7.17	2,649.94	1.17	2,860.80
11/06/15	13.40	Sewage	11.18	526.66	8.65	2,623.27	0.69	2,863.20
11/06/15	13.55	Sewage	10.61	533.80	6.36	2,651.08	1.11	2,860.80
11/06/15	14.15	Sewage	10.95	498.76	10.11	2,644.05	1.74	2,852.80
11/06/15	14.35	Sewage	12.38	477.48	5.45	2,621.22	1.22	2,809.60
11/06/15	14.55	Sewage	11.44	490.96	5.91	2,656.50	1.54	2,872.80
11/06/15	15.00	Sewage	11.08	479.29	3.72	2,644.92	2.52	2,878.40
11/06/15	15.15	Sewage	6.92	490.21	11.20	2,745.48	0.83	2,859.20
11/06/15	15.30	Sewage	6.35	495.49	1.10	2,718.65	1.03	2,856.80
11/06/15	15.45	Sewage	6.46	485.41	1.68	2,627.81	1.36	2,842.40
11/06/15	07.30	PP	29.67	211.71	8.78	2,432.91	82.24	2,468.80
11/06/15	08.00	PP	29.51	357.98	8.22	2,338.37	3.96	2,480.00
11/06/15	08.30	PP	28.4	283.93	4.15	2,381.85	0.88	2,521.60
11/06/15	09.00	PP	28.4	282.12	3.41	2,366.93	2.92	2,524.80
12/06/15	09.30	PP	28.4	294.82	17.93	2,383.40	0.46	2,528.00
12/06/15	10.00	PP	30.22	270.13	2.55	2,361.63	1.81	2,496.00
12/06/15	10.30	PP	30.86	311.85	21.96	2,351.20	1.73	2,498.40
12/06/15	11.00	PP	32.78	227.10	28.13	2,300.68	0.92	2,299.60
12/06/15	11.30	PP	31.9	227.24	21.41	2,285.03	2.46	2,464.80
12/06/15	12.00	PP	33.02	306.10	20.44	2,220.35	0.62	2,376.80
12/06/15	12.30	PP	33.51	230.48	1.00	2,083.74	68.91	2,402.40
12/06/15	13.00	PP	33.26	283.61	10.30	2,190.75	1.35	2,433.60
12/06/15	13.30	PP	33.83	349.25	8.46	2,208.28	1.46	2,424.00

12/06/15	14.00	PP	33.59	317.28	13.87	2,187.98	1.81	2,387.20
12/06/15	14.30	PP	33.59	305.29	10.08	2,152.38	1.42	2,395.20
12/06/15	15.00	PP	34.39	232.78	20.66	2,124.77	3.50	2,375.20
12/06/15	15.30	PP	34.72	220.12	8.27	2,162.90	1.46	2,320.80
12/06/15	16.00	PP	35.28	213.32	6.67	2,131.57	1.73	2,342.40
12/06/15	16.30	PP	35.37	210.74	10.37	2,125.80	0.42	2,304.00
12/06/15	17.00	PP	34.47	188.79	0.60	2,113.30	1.58	2,347.20
12/06/15	17.30	PP	35.28	310.62	4.72	2,010.83	63.49	2,345.60
12/06/15	18.00	PP	35.37	248.91	4.45	2,151.05	1.77	2,333.60
12/06/15	18.30	PP	35.37	196.76	3.22	2,148.93	2.23	2,342.00
12/06/15	19.00	PP	34.72	207.15	2.72	2,173.55	3.77	2,350.40
12/06/15	19.30	PP	34.8	189.82	2.49	2,140.07	0.85	2,351.20
12/06/15	20.00	PP	33.75	244.09	6.37	2,219.89	1.58	2,370.40
12/06/15	20.30	PP	32.7	237.86	3.28	2,237.82	0.12	2,432.80
12/06/15	21.00	PP	31.42	256.24	0.90	2,290.11	0.35	2,454.40
12/06/15	21.30	PP	32.06	262.78	2.08	2,279.02	2.34	2,440.80
12/06/15	22.00	PP	31.98	271.20	10.35	2,311.90	2.65	2,442.40
12/06/15	22.30	PP	32.46	193.64	1.82	2,171.45	1.11	2,459.20
12/06/15	23.00	PP	32.46	188.54	3.43	2,129.47	70.87	2,440.80
12/06/15	23.30	PP	33.51	181.30	1.82	2,166.28	1.66	2,420.80
12/06/15	00.00	PP	33.02	198.00	6.97	2,233.16	1.71	2,516.00
12/06/15	00.30	PP	33.34	178.34	9.08	2,117.74	3.59	2,427.20
12/06/15	01.00	PP	34.07	171.38	2.69	2,121.65	1.42	2,345.20
12/06/15	01.30	PP	34.15	244.49	13.29	2,102.21	2.67	2,362.40
13/06/15	02.00	PP	33.64	212.32	0.81	2,111.26	1.60	2,357.60
13/06/15	02.30	PP	34.37	186.76	17.06	2,049.79	0.50	2,308.00
13/06/15	03.00	PP	35.37	188.07	15.89	2,069.16	1.63	2,323.20
13/06/15	03.30	PP	35.37	162.85	1.62	1,952.14	57.00	2,308.00
13/06/15	04.00	PP	35.28	168.01	1.81	2,043.44	2.25	2,333.60
13/06/15	04.30	PP	35.53	181.12	8.36	2,054.76	2.38	2,332.80
13/06/15	05.00	PP	34.96	189.79	7.50	2,058.20	0.72	2,343.20
13/06/15	05.30	PP	35.53	186.86	9.29	2,062.24	2.06	2,336.80
13/06/15	06.00	PP	34.23	265.07	7.17	2,088.12	1.45	2,384.80
13/06/15	06.30	PP	34.39	337.30	11.26	2,112.53	1.04	2,367.20
13/06/15	07.00	PP	34.31	188.19	2.68	2,109.57	0.94	2,352.80
13/06/15	---	Marine	36.93					

January 2016

Collection Date	Time	Site ID	Salinity (ppt)	DOC (μmol L^{-1}) n = 3	Standard Deviation (μmol L^{-1})	DIC (μmol L^{-1}) n = 3	Standard Deviation (μmol L^{-1})	TAlk (μmol L^{-1})
30/01/16	14.00	Castle	0.56	258.42	1.46	4771.86	3.53	5148.80
30/01/16	14.15	Castle	0.52	267.44	2.75	4858.03	12.36	5099.20
30/01/16	14.30	Castle	0.53	263.89	3.59	4863.70	0.71	5192.00
30/01/16	14.45	Castle	0.52	255.15	3.57	4880.77	6.71	5146.67
30/01/16	15.00	Castle	0.51	240.24	5.63	4940.63	18.13	---
30/01/16	15.15	Castle	0.53	260.98	6.46	4847.54	14.84	---
30/01/16	15.30	Castle	0.53	266.61	0.83	4849.17	31.26	---
30/01/16	15.45	Castle	0.52	258.59	1.25	4909.24	12.95	---
30/01/16	16.00	Castle	0.52	268.94	1.52	4807.95	1.47	---
30/01/16	16.15	Castle	0.51	270.55	0.98	4431.06	8.36	---
30/01/16	08.00	Sewage	1.16	489.12	0.79	2708.45	11.25	3063.20
30/01/16	08.15	Sewage	1.14	473.44	1.81	2728.56	1.30	2887.20
30/01/16	08.30	Sewage	2.13	476.55	5.71	2735.35	20.08	2967.20
30/01/16	08.45	Sewage	2.18	484.10	7.37	2743.96	1.18	---
30/01/16	09.15	Sewage	0.63	485.51	4.49	2708.99	4.12	---
30/01/16	09.30	Sewage	0.53	485.12	3.13	2705.45	2.18	---
30/01/16	09.45	Sewage	0.39	479.60	1.98	2729.27	0.53	---
30/01/16	10.00	Sewage	0.00	532.56	4.37	2603.66	13.42	---
30/01/16	10.15	Sewage	2.35	491.95	8.00	2689.22	1.71	---
30/01/16	10.30	Sewage	2.42	446.79	5.37	3096.71	3.24	---
30/01/16	18.15	PP	34.15	359.09	3.51	2421.52	8.65	2626.40
30/01/16	18.45	PP	34.66	370.86	2.04	2661.20	19.43	---
30/01/16	19.15	PP	35.11	350.76	4.34	2568.61	0.94	2711.20
30/01/16	19.45	PP	35.33	364.53	9.55	2575.19	0.47	---
30/01/16	20.15	PP	35.22	348.49	2.79	2420.44	2.65	2684.30
30/01/16	20.45	PP	35.11	331.67	7.51	2518.36	0.41	---
30/01/16	21.15	PP	33.88	343.19	10.48	2454.75	9.36	2602.40
30/01/16	21.45	PP	34.32	321.09	4.43	2538.43	12.78	---
30/01/16	22.15	PP	34.77	325.28	7.46	2495.05	2.88	2669.60
30/01/16	22.45	PP	31.85	318.15	4.77	1961.87	13.07	---
30/01/16	23.15	PP	21.79	304.30	4.36	2095.09	5.30	---
30/01/16	23.45	PP	18.40	246.60	6.26	2156.24	12.19	2692.00

31/01/16	00.15	PP	12.71	225.78	5.65	2182.51	177.57	---
31/01/16	00.45	PP	13.31	199.44	0.65	1715.32	3.77	2644.80
31/01/16	01.15	PP	13.07	204.02	5.17	1859.99	44.45	---
31/01/16	01.45	PP	13.14	216.79	0.34	2337.93	3.36	2966.40
31/01/16	02.15	PP	12.59	206.47	3.15	1752.75	2.06	---
31/01/16	02.45	PP	15.73	199.47	3.90	2019.36	2.18	2690.40
31/01/16	03.15	PP	16.95	212.99	3.57	2148.42	7.24	---
31/01/16	03.45	PP	16.43	207.16	6.83	2244.50	1.59	2581.60
31/01/16	04.15	PP	16.90	204.14	1.58	2177.23	10.19	---
31/01/16	04.45	PP	17.57	297.72	7.92	2157.08	7.12	2611.20
31/01/16	05.15	PP	18.92	193.70	2.72	2212.74	1.88	---
31/01/16	05.45	PP	23.48	203.41	0.58	1942.55	1.18	2722.40
31/01/16	06.15	PP	27.26	197.14	1.37	2011.12	3.00	---
31/01/16	06.45	PP	30.65	235.14	2.62	2042.55	47.69	2795.20
31/01/16	07.15	PP	36.31	203.83	6.42	2152.41	7.71	---
31/01/16	07.45	PP	27.08	194.28	1.20	2180.60	0.24	2928.00
31/01/16	08.15	PP	34.63	197.70	1.67	2184.93	0.24	---
31/01/16	08.45	PP	35.25	189.68	3.60	2175.02	0.59	2597.60
31/01/16	09.15	PP	33.94	200.92	1.14	2198.17	2.24	---
31/01/16	09.45	PP	35.20	243.85	7.19	2191.59	0.71	3091.20
31/01/16	10.15	PP	34.78	210.52	1.63	2255.70	15.78	---
31/01/16	10.45	PP	36.10	339.72	1.86	2271.90	21.02	3045.60
31/01/16	11.15	PP	34.89	227.34	14.84	2390.01	9.07	---
31/01/16	11.45	PP	34.78	199.50	5.13	2195.63	0.53	2648.80
31/01/16	12.15	PP	35.10	205.66	0.36	2038.22	2.12	---
31/01/16	12.45	PP	34.05	191.45	1.97	2078.18	8.01	2614.00
31/01/16	13.15	PP	33.63	239.80	2.31	2127.73	12.25	---
31/01/16	13.45	PP	33.73	214.10	1.20	2122.61	14.42	2501.60
31/01/16	14.15	PP	34.47	230.78	0.42	2035.89	13.31	0.82
31/01/16	14.45	PP	34.36	251.48	3.25	2147.17	1.71	2887.20
31/01/16	15.15	PP	33.32	252.48	3.58	2229.98	82.54	---
31/01/16	15.45	PP	34.15	321.12	3.48	2350.00	1.24	3076.00
31/01/16	16.15	PP	35.74	351.62	5.85	2537.39	13.19	---
31/01/16	16.45	PP	35.05	359.09	3.51	2670.65	7.71	2488.40
31/01/16	17.15	PP	35.73	370.86	2.04	2421.52	8.65	---
31/01/16	17.45	PP	36.53	350.76	4.34	2661.20	19.43	2901.60
31/01/16	---	Marine	34.66	208.94	13.57	2084.68	12.75	2,369.60

Appendix E: CDOM 3-Component Model for Kinvara Bay (Chapter 4) – DOC Concentration, CDOM Scores and Indicator Parameters, where recorded.

The below tables detail the CDOM and DOC results, where recorded, for the model described in Chapter 4. --- represents data not recorded and SUVA254 was not recorded in many campaigns, this column has been removed from the relevant tables.

October 2012: DOC not measured during October 2012 sampling campaign.

Sample I.D.	Salinity (ppt)	CDOM Score	FI	HIX
GW 24	0.33	0.677	1.54	0.90
Castle	0.25	0.134	1.52	0.94
GW KR	0.00	0.968	1.42	0.97
GW1	0.20	0.237	1.30	0.95
GW10	0.29	0.324	1.78	0.90
GW12	0.30	0.170	1.76	0.86
GW13	0.32	0.212	1.89	0.90
GW14	0.31	0.081	2.02	0.72
GW15	0.29	0.033	2.29	0.83
GW16	0.33	1.073	2.37	0.94
GW18	0.31	0.526	1.61	0.80
GW19	0.09	1.076	1.25	0.96
GW20	0.23	0.055	1.53	0.94
GW21	0.11	0.014	1.48	0.96
GW22	0.31	1.226	1.59	0.74
GW23	0.28	0.411	1.46	0.81
GW25	0.23	0.407	1.25	0.94
GW26	0.26	0.901	1.45	0.96
GW27	0.21	0.407	1.37	0.89
GW28	0.24	0.597	1.77	0.96
HT SGD	1.15	0.206	1.29	0.95
Marine	29.80	0.264	1.39	0.91
Bay Water Upper	30.00	0.442	1.62	0.78
Bay Water Lower	24.30	0.840	1.66	0.84
Sewage	1.95	0.780	1.32	0.95
Castle	0.25	0.801	1.34	0.93

March 2013:

Sample I.D.	Salinity (ppt)	Abs (360nm)	FI	HIX	SUVA 254	CDOM Score	DOC (µmol L^{-1})	Standard Deviation (µmol L^{-1}) n = 3
Owenshree Upper	0.01	---	1.27	0.96	---	0.669	733.97	29.03
Forest	0.03	---	1.30	0.95	---	0.993	864.59	45.97
Peat	0.03	---	1.17	0.97	---	0.911	1,066.00	17.59
Ballycahill River Upper	0.14	---	1.21	0.96	---	0.330	1,034.97	23.40
GW3	0.23	---	1.31	0.90	---	1.181	476.63	23.63
GW7	0.29	---			---	0.324	511.13	32.81
Caherglassan	0.12	---	1.32	0.95	---	0.795	818.26	30.30
Garryland	0.04	---	1.35	0.94	---	0.174	677.85	33.87
Coole	0.11	---	1.43	0.95	---	1.237	931.97	21.17
Coole GWS	0.30	---	1.82	0.88	---	1.074	796.03	24.05
Lydacan	0.17	---	1.39	0.86	---	1.137	647.40	67.92
BH11	0.25	---	1.42	0.81	---	0.308	551.24	24.20
Ballinduff	0.21	---	1.43	0.90	---	0.936	724.76	69.13
Coy	0.14	---	1.28	0.96	---	1.038	798.78	7.38
Skehannagh	0.01	0.31	1.67	0.89	---	0.079	909.94	79.73
Blackrock	0.11	---	1.41	0.96	---	1.055	756.70	44.42
Ballycahrun River	0.21	---	1.24	0.96	---	0.638	848.63	21.74
Derrywee	0.02	---	1.24	0.97	---	0.136	1,131.09	3.49
Derrywee Lower	0.03	---	1.37	0.97	---	0.839	976.77	7.13
Pollhoish	0.04	0.14	1.61	0.91	---	0.361	581.96	25.08
Loughcurragh South	0.20	0.62	1.31	0.95	---	0.576	684.04	38.67
GW10	0.29	---	1.40	0.92	---	0.324	611.27	123.19
GW12	0.30	---	1.49	0.92	---	0.170	807.99	28.82
GW15	0.29	---	1.57	0.87	---	0.033	794.95	7.79
GW22	0.31	---		0.93	---	1.226	380.29	29.82
Farm GW20	0.39	---	1.47	0.90	---	0.923	599.64	47.65
Castle	0.29	---	1.32	0.92	---	1.349	725.73	32.82
Arch	1.67	---			---	0.772	664.70	13.96
S3	0.29	0.71	1.35	0.93	---		482.10	17.99
GW16	0.35	0.42	1.74	0.91	---	0.648	748.49	58.44

July 2013:

Sample I.D.	Salinity (ppt)	Abs (360nm)	FI	HIX	SUVA 254	DOC (µmol L^{-1})	Standard Deviation (µmol L^{-1}) n = 3	CDOM Score
Castle	3.67	0.07	1.44	0.96	---	454.59	16.43	0.663
1100	3.17	0.08	1.44	0.95	---	425.06	3.26	0.659
1120	2.96	0.08	1.42	0.95	---	382.12	7.20	0.673
1140	2.67	0.08	1.30	0.96	---	432.85	13.21	0.614
1200	2.31	0.08	1.51	0.96	---	567.13	22.17	0.611
1220	2.22	0.07	1.28	0.96	---	599.93	21.83	0.644
1240	1.90	0.08	1.57	0.95	---	360.05	11.34	0.630
1300	1.84	0.08	1.43	0.96	---	336.94	5.25	0.619
1320	1.86	0.08	1.06	0.96	---	363.22	8.68	0.774
1340	1.91	0.06	1.29	0.94	---	372.51	14.58	0.209
Sewage								
1520	20.58	0.07	1.30	0.87	---	260.84	9.32	0.406
1540	22.15	0.07	1.34	0.87	---	291.69	2.31	0.395
1600	21.9	0.07	1.32	0.86	---	347.41	4.05	0.198
1620	23.4	0.07	1.38	0.83	---	255.89	6.72	0.249
1640	23.3	0.07	1.55	0.87	---	212.71	2.65	0.138
1700	23.3	0.08	1.45	0.85	---	310.88	3.21	0.249
1720	23.36	0.07	1.64	0.83	---	340.14	7.96	0.169
1740	3.67	0.07	1.41	0.83	---	225.11	5.22	0.163
1800	3.17	0.07	1.57	0.87	---	280.54	6.53	0.240
PP 1300	31.46	0.02	1.99	0.85	---	249.42	0.78	0.120
1320	30.30	0.02	1.28	0.83	---	228.96	2.62	0.242
1340	28.90	0.02	1.29	0.84	---	207.31	8.48	0.170
1400	31.32	0.02	1.39	0.85	---	196.40	4.12	0.221
1420	31.17	0.01	1.63	0.85	---	198.39	5.86	0.122
1440	33.31	0.02	1.13	0.92	---	185.67	0.66	0.229
1500	32.86	0.02	1.05	0.82	---	197.99	2.21	0.157
1520	33.14	0.01	1.65	0.82	---	194.54	1.40	0.237
1540	33.21	0.01	1.28	0.83	---	196.27	0.25	0.164
1600	31.58	0.01	1.38	0.85	---	227.27	3.82	0.267
1620	32.03	0.01	1.92	0.87	---	211.82	20.00	0.236
1640	31.46	0.00	1.41	0.85	---	195.36	1.62	0.263
1700	31.82	0.01	1.31	0.83	---	215.70	2.74	0.213
1720	31.92	0.01	1.34	0.80	---	198.67	0.22	0.198
1740	32.07	0.00	1.08	0.84	---	178.05	1.05	0.134
1800	32.61	0.01	1.29	0.84	---	226.29	0.86	0.231
1820	31.11	0.01	1.42	0.82	---	262.28	1.37	0.314
1840	32.21	0.01	1.54	0.83	---	201.96	1.98	0.450
1900	32.27	0.01	1.28	0.83	---	191.53	2.08	0.155
1920	31.81	0.01	1.16	0.79	---	276.33	2.67	0.248
1940	32.03	0.01	1.28	0.84	---	326.41	3.27	0.228
2000	32.18	0.02	1.63	0.81	---	196.91	0.82	0.363
2020	30.75	0.02	1.53	0.83	---	175.28	3.72	0.201
2040	32.25	0.02	1.41	0.83	---	191.25	2.86	0.213
2100	31.82	0.02	1.16	0.80	---	189.88	4.21	0.154
2120	32.16	0.03	1.29	0.75	---	199.78	0.22	0.285
2140	31.89	0.02	1.27	0.79	---	202.13	2.82	0.271
2200	31.88	0.04	1.22	0.83	---	202.05	3.19	0.288

2220	30.97	0.03	1.60	0.80	---	183.52	0.76	0.306
2240	30.51	0.04	1.72	0.77	---	191.84	2.97	0.287
2300	31.71	0.04	0.95	0.81	---	162.21	0.17	0.214
2320	30.72	0.03	1.12	0.83	---	145.27	1.45	0.243
2340	48.86	0.02	1.18	0.85	---	140.28	1.74	0.146
0000	53.91	0.04	1.43	0.83	---	171.79	9.95	0.228
0020	31.70	0.04	1.86	0.84	---	186.33	0.78	0.223
0040	30.89	0.03	1.29	0.84	---	195.39	2.62	0.250
0120	30.37	0.04	1.28	0.84	---	135.07	8.48	0.253
0140	29.66	0.02	1.30	0.87	---	163.87	4.12	0.197
0200	31.38	0.02	1.57	0.89	---	147.27	5.86	0.153
0220	23.64	0.02	1.57	0.88	---	142.22	0.66	0.342
0240	29.94	0.02	1.60	0.87	---	169.37	---	0.174
0300	31.82	0.01	1.17	0.87	---	114.11	---	0.202
0320	31.60	0.03	1.41	0.85	---	151.74	---	0.185
0340	31.47	0.02	1.04	0.84	---	166.80	---	0.191
0400	31.35	0.01	1.73	0.84	---	179.07	---	0.313
0420	30.17	0.02	1.36	0.82	---	146.32	---	0.168
0440	30.34	0.02	1.64	0.82	---	146.74	---	0.140
0500	30.51	0.01	1.74	0.84	---	137.22	---	0.232
0520	31.21	0.02	1.45	0.80	---	142.00	---	0.123
0540	31.17	0.01	1.13	0.82	---	147.71	---	0.206
0600	31.12	0.02	1.31	0.79	---	125.34	---	0.140
0620	31.64	0.02	1.24	0.85	---	127.21	---	0.242
0640	31.73	0.02	1.61	0.83	---	146.42	---	0.112
0700	31.64	0.02	1.30	0.82	---	130.27	---	0.187
0720	31.69	0.02	1.20	0.84	---	133.90	---	0.222
0740	31.64	0.01	1.30	0.82	---	145.35	---	0.339
0800	32.39	0.02	1.69	0.81	---	134.11	---	0.223
0900	32.10	0.03	1.43	0.79	---	135.98	---	0.311
0920	31.89	0.05	0.97	0.83	---	192.09	---	0.225
0940	31.63	0.04	1.35	0.82	---	121.74	---	0.201
1040	31.55	0.04	1.32	0.84	---	122.45	---	0.164
1100	31.70	0.03	1.27	0.86	---	174.27	---	0.265
1120	31.89	0.02	1.38	0.84	---	163.85	---	0.168
1140	31.53	0.01	1.04	0.83	---	175.00	---	0.198
1200	31.51	0.02	1.34	0.84	---	183.80	---	0.118
1220	31.60	0.01	1.41	0.84	---	234.49	---	0.801
1240	31.61	0.01	1.35	0.85	---	146.18	---	0.987
1300	31.53	0.00	1.34	0.86	---	156.89	---	0.816
Arch		---	1.33	0.90	---	---	---	0.799
Ballycahalan		---	1.14	0.95	---	---	---	---
Ballycahill		---			---	---	---	---
Upper			1.27	0.98				
Coole GWS		---	1.64	0.91	---	---	---	---
Coole		---	1.32	0.96	---	---	---	---
Coy		---	1.15	0.98	---	---	---	---
Derrywee		---	1.23	0.96	---	---	---	---
Forest		---	1.18	0.97	---	---	---	---
Garryland		---	1.51	0.95	---	---	---	---
GW10		---	1.77	0.88	---	174.68	12.3	---
GW16		---	1.66	0.90	---	---	---	---
GW20		---	1.22	0.82	---	181.93	24.8	---
GW15		---	1.94	0.85	---	201.81	10.0	---

Lydacan	---	1.28	0.94	---	---	---	---
OL	---	1.23	0.98	---	---	---	---
Pollhoish	---	1.52	0.90	---	161.93	32.6	---
S3	---	1.35	0.96	---	---	---	---
SGD HT	---	1.34	1.21	---	---	---	---
Skehannagh	---	1.29	0.91	---	---	---	---

May 2014: DOC Concentrations measured *in-situ* at Kinvara Springs

Sample I.D.	Salinity (ppt)	Abs (360nm)	FI	HIX	SUVA 254	DOC (µmol L^{-1})	Standard Deviation (µmol L^{-1}) n = 3	CDOM Score
Castle 1130	0.22	0.100	1.33	0.95	13.48	784.72	3.06	0.865
1145	0.20	0.083	1.27	0.96	14.80	719.39	8.19	0.804
1200	0.20	0.079	1.40	0.96	14.32	688.32	16.13	0.836
1215	0.20	0.096	1.36	0.96	14.59	734.14	14.95	0.809
1240	0.19	0.079	1.15	0.96	19.58	771.53	10.33	0.182
1300	0.20	0.083	1.34	0.96	10.22	748.13	13.93	0.185
1315	0.19	0.092	1.08	0.96	13.76	855.32	5.02	0.386
1330	0.19	0.079	1.19	0.96	22.45	716.31	13.62	0.300
1345	0.19	0.086	1.27	0.96	20.36	830.79	14.76	0.221
1400	0.18	0.078	1.39	0.96	18.29	705.37	14.98	0.174
Arch	0.32	0.062	1.33	0.93	7.93	600.30	13.54	0.254

September 2014 DOC Concentrations measured *in-situ* at Kinvara Springs

Sample I.D.	Salinity (ppt)	Abs (360nm)	FI	HIX	SUVA 254	DOC (µmol L^{-1})	Standard Deviation (µmol L^{-1}) n = 3	CDOM Score
Castle 0740	7.49	0.048	1.34	0.94	13.69	267.36	5.74	0.704
Castle 0755	7.72	0.043	1.27	0.96	14.99	217.61	3.82	0.731
Castle 0805	7.62	0.045	1.28	0.94	14.68	266.52	9.37	0.706
Castle 0820	7.29	0.041	1.45	0.96	16.55	223.49	37.51	0.767
Castle 0840	7.19	0.049	1.31	0.96	17.07	210.60	43.63	0.720
Castle 0900	7.53	0.043	1.55	0.95	11.39	330.29	48.25	0.760
Castle 0915	7.12	0.045	1.32	0.95	17.73	282.89	89.73	0.705
Castle 0930	7.34	0.062	1.36	0.95	15.86	139.23	25.85	0.899
Castle 0940	7.30	0.047	1.31	0.94	7.58	167.67	61.44	0.344
Castle 0955	7.33	0.041	1.45	0.96	12.07	167.74	19.61	0.477
Castle 1005	6.24	0.040	1.40	0.95	22.04	432.39	51.83	0.704
Arch	8.83	0.047	1.50	0.95	15.86	257.62	6.94	0.757
Loughcurragh South	0.22	0.062	1.38	0.96	7.03	587.63	61.11	0.388
Seawater (Low tide)	32.9	0.007	1.70	0.75	3.59	7.86	0.00	0.356
Seawater (High tide)	35.5	0.005	1.48	0.74	3.34	14.11	0.51	0.336
Parkmore Pier	33.1	0.014	1.35	0.85	3.86	19.85	4.63	0.310

January 2015:

Sample I.D.	Salinity (ppt)	Abs (360nm)	FI	HIX	SUVA 254	DOC (µmol L^{-1})	Standard Deviation (µmol L^{-1}) n = 3	CDOM Score
0830	0.52	0.033	1.32	0.96	8.32	445.77	3.89	0.663
0850	0.52	0.032	1.18	0.95	8.29	291.57	5.63	0.659
0910	0.52	0.030	1.50	0.96	8.42	300.14	4.38	0.673
0930	0.52	0.033	1.38	0.96	8.43	300.82	3.53	0.614
0950	0.52	0.037	1.62	0.96	8.10	294.66	4.20	0.611
1020	0.52	0.033	1.25	0.95	7.87	330.19	2.93	0.644
1040	0.52	0.032	1.38	0.96	7.09	301.88	2.96	0.630
1100	0.60	0.038	1.47	0.96	8.19	295.38	1.60	0.619
1130	0.58	0.034	1.44	0.94	8.57	302.48	2.48	0.774
1145	---	0.038	1.33	0.95	8.17	298.50	2.65	0.827
Sewage 1450	0.65	0.091	1.31	0.94	8.95	640.87	4.10	0.738
1510	0.62	0.100	1.38	0.95	9.42	685.87	11.83	0.755
1535	0.70	0.094	1.24	0.99	9.03	647.33	2.35	0.761
1550	1.54	0.091	1.17	0.95	8.25	673.84	9.19	0.769
1610	0.84	0.099	1.49	0.96	9.01	642.39	5.41	0.761
1635	0.60	0.101	0.90	0.94	9.36	630.95	5.31	0.292
1650	0.91	0.099	1.18	0.98	8.78	653.12	2.59	0.751
1705	0.85	0.100	1.55	0.99	9.41	619.57	3.69	0.763
1730	0.92	0.095	1.28	0.97	9.25	642.90	0.10	0.262
PP 0000	3.03	0.048	1.42	0.94	7.96	428.73	1.65	0.268
0030	4.05	0.049	1.37	0.95	6.51	380.00	5.84	0.290
0100	11.49	0.048	1.15	0.91	6.73	404.60	6.32	0.398
0130	11.03	0.051	1.57	0.89	6.19	433.76	5.66	0.402
0200	16.59	0.044	1.17	0.93	6.28	430.62	5.93	0.311
0230	16.96	0.051	1.33	0.93	6.41	406.59	11.52	0.385
0300	19.36	0.046	1.32	0.91	5.53	464.57	2.65	0.279
0330	19.81	0.052	1.37	0.92	6.18	427.98	7.31	0.374
0400	18.38	0.040	1.23	0.91	6.27	388.71	0.51	0.286
0430	20.42	0.038	1.22	0.93	6.15	376.97	3.07	0.325
0500	20.57	0.045	1.17	0.92	6.92	421.48	1.92	0.291
0530	17.58	0.066	1.21	0.90	6.72	553.65	5.36	0.301
0600	14.59	0.074	1.57	---	7.37	562.12	5.94	0.254
0630	16.22	0.069	1.16	---	7.70	527.92	2.87	0.422
0700	18.53	0.070	1.18	---	6.56	616.46	3.50	0.312
0730	4.35	0.065	1.42	---	7.01	544.58	4.60	0.365
0800	4.63	0.054	1.24	0.95	6.45	520.10	3.69	0.383
0830	6.47	0.059	1.25	0.94	7.33	501.96	5.41	0.376
0900	7.63	0.046	1.42	0.96	6.28	467.49	3.40	0.290
0930	6.93	0.043	1.36	0.93	10.21	474.06	2.73	0.287
1000	6.90	0.083	1.38	0.96	9.69	520.36	3.84	0.234
1030	7.75	0.082	1.37	0.94	9.71	516.30	4.49	0.360
1100	7.72	0.061	1.50	0.94	9.27	444.26	4.07	0.165
1130	9.76	0.068	1.58	---	9.31	446.87	5.17	0.261
1200	10.09	0.049	1.58	---	8.93	395.37	1.73	0.304
1230	12.72	0.052	1.06	---	6.55	380.18	3.82	0.307
1300	8.59	0.032	1.52	0.93	6.81	362.91	1.76	0.337
1330	16.22	0.049	1.48	0.91	6.93	374.33	1.46	0.236

1400	14.22	0.044	1.61	0.94	6.72	395.59	5.22	0.359
1430	19.73	0.043	0.95	0.94	6.60	353.75	8.52	0.307
1500	16.81	0.042	1.39	0.93	5.35	290.29	55.95	0.314
1530	18.53	0.045	1.45	0.94	8.08	451.46	47.80	0.318
1600	18.00	0.047	1.56	0.94	8.05	384.63	3.49	0.293
1630	19.36	0.042	1.37	0.92	9.02	376.55	7.25	0.302
1700	19.43	0.083	1.79	0.96	9.83	342.35	6.60	0.276
1730	20.95	0.076	1.24	0.95	9.18	495.49	8.08	0.338
1800	21.25	0.077	1.38	0.95	9.41	555.71	4.66	0.259
1830	20.87	0.067	1.59	---	6.60	101.93	10.27	0.308
1900	16.96	0.075	1.19	---	8.14	674.16	11.17	0.292
1930	10.81	0.068	1.48	---	8.59	539.41	8.42	0.222
2000	9.00	0.066	1.23	0.95	8.08	520.05	4.64	0.289
2030	9.79	0.070	1.13	---	8.59	514.72	7.74	0.658
2100	9.16	0.066	1.66	---	7.20	506.59	4.88	0.803
2130	11.02	0.065	1.23	---	6.95	312.85	52.57	0.347
2200	12.70	0.053	1.21	0.94	8.46	574.06	37.46	0.402
2230	11.99	0.061	1.24	---	7.57	485.06	5.76	0.367
2300	17.03	0.038	1.18	---	6.72	425.66	6.06	0.723
2330	14.51	0.048	1.34	0.94	10.21	402.18	10.89	0.262

March 2015: Full Tidal Cycle at Kinvara Springs

Sample I.D.	**Salinity (ppt)**	**Abs (360nm)**	**FI**	**HIX**	**DOC (µmol L^{-1})**	**Standard Deviation (µmol L^{-1}) n = 3**	**CDOM Score**
1200	0.21	---	1.34	0.94	316.59	5.12	0.438
1240	0.25	---	1.41	0.96	277.39	72.69	0.324
1320	0.24	---	1.39	0.93	536.52	14.79	0.471
Arch	0.29	---	1.36	0.95	525.85	14.11	0.305
1400	0.46	---	1.43	0.94	338.40	9.13	0.468
1430	0.45	---	1.53	0.96	369.83	4.00	0.307
1450	0.69	---	1.53	0.92	246.28	7.01	0.491
1510	0.43	---	1.48	0.92	315.80	3.41	0.357
1545	0.64	---	1.55	0.93	285.52	3.56	0.471
1615	0.55	---	1.40	0.93	479.21	2.09	0.240
1625	0.68	---	1.35	0.93	726.49	13.48	0.492
1625	0.80	---	1.65	0.92	406.41	9.96	0.505
1635	1.21	---	1.27	0.95	423.92	4.36	0.199
1650	0.53	---	1.37	0.94	463.53	4.26	0.478
1710	1.01	---	1.59	0.94	376.05	5.19	0.657
1720	1.20	---	1.43	0.95	325.99	6.18	0.430
1735	1.35	---	1.16	0.95	313.56	5.73	0.385
1745	1.39	---	1.33	0.95	268.12	6.06	0.628
1800	1.53	---	1.19	0.93	267.67	4.30	0.307
1810	2.51	---	1.27	0.94	388.38	6.02	0.725
1820	2.43	---	1.47	0.94	417.20	3.50	0.706
1830	1.73	---	1.46	0.94	490.00	6.40	0.557
1840	1.86	---	1.42	0.94	417.16	8.13	0.526
1910	2.50	---	1.41	0.94	410.74	5.11	0.342
1925	3.62	---	1.38	0.94	737.87	6.72	0.510
1935	3.30	---	1.30	0.93	455.84	8.49	0.436
1945	3.39	---	1.39	0.93	495.04	17.92	0.436

1955	2.92	---	1.41	0.93	562.92	5.83	0.433
2015	6.21	---	1.52	0.93	350.44	20.23	0.426
2025	5.38	---	1.29	0.93	332.56	3.73	0.421
2035	3.11	---	1.44	0.93	244.48	5.81	0.445
2045	1.70	---	1.51	0.93	454.72	4.74	0.453
2050	0.98	---	1.41	0.93	241.42	6.90	0.437
2100	0.76	---	1.53	0.93	274.80	6.94	0.271
2105	0.62	---	1.36	0.93	227.46	3.49	0.371
2115	0.63	---	1.58	0.93	295.11	5.30	0.760
2130	0.49	---	1.46	0.93	233.77	5.38	0.785
2200	0.46	---	1.28	0.93	232.54	6.06	0.794
2230	0.46	---			236.57	2.66	0.757
Pier		---			367.54	11.39	
Bay 1	34.78	---	1.31	0.90	287.08	8.52	0.370
Bay 2	34.04	---	1.53	0.90	464.99	3.43	0.315
Bay 3	33.14	---	1.36	0.91	406.93	6.67	0.261
Bay 4	10.44	---	1.50	0.91	546.01	7.77	0.444
Bay 5	31.78	---	1.21	0.85	427.50	3.35	0.434
Bay 6	36.84	---	1.36	0.74	316.32	12.20	0.469
Bay 7	35.31	---	1.21	0.75	317.40	6.49	0.468
Bay 8	36.71	---	1.43	0.84	306.98	5.62	0.447
Shoreline	33.67	---	1.26	0.93	307.43	6.17	0.752

June 2015:

Sample I.D.	**Salinity (ppt)**	**Abs (360nm)**	**FI**	**HIX**	**DOC (µmol L^{-1})**	**Standard Deviation (µmol L^{-1}) n = 3**	**CDOM Score**
Castle	0.54	0.049	1.35	0.95	355.28	12.43	0.728
Castle	0.54	0.042	1.31	0.95	373.05	10.46	0.713
Castle	0.54	0.048	1.29	0.95	366.32	5.01	0.310
Castle	0.53	0.044	1.24	0.96	381.62	14.60	0.775
Castle	0.56	0.042	1.44	0.95	385.81	10.63	0.828
Castle	0.54	0.044	1.80	0.95	375.34	16.47	0.792
Castle	0.51	0.054	1.23	0.96	379.40	7.33	0.847
Castle	0.51	0.058	1.32	0.96	378.51	8.49	0.809
Castle	0.52	0.058	1.41	---	380.59	6.55	0.807
Castle	0.50	0.055	1.37	---	366.88	8.17	0.793
Castle	0.52	0.049	1.35	---	377.46	5.06	0.808
Castle	0.53	0.048	1.53	0.94	355.28	12.43	0.797
Sewage	11.81	0.069	1.34	0.94	588.00	7.17	0.831
Sewage	11.50	0.072	1.32	0.94	526.66	8.65	0.798
Sewage	11.18	0.073	1.31	0.94	533.80	6.36	0.845
Sewage	10.61	0.071	1.30	0.94	498.76	10.11	0.813
Sewage	10.95	0.073	1.50	---	477.48	5.45	0.831
Sewage	12.38	0.073	1.22	---	490.96	5.91	0.798
Sewage	11.44	0.073	1.39	---	479.29	3.72	0.845
Sewage	11.08	0.073	1.35	---	490.21	11.20	0.813
Sewage	6.92	0.080	1.37	---	495.49	1.10	0.831
Sewage	6.35	0.074	1.17	---	485.41	1.68	0.798
Sewage	6.46	0.081	1.32	---	499.17	4.95	0.845
Sewage	30.67	0.074	1.28	---	583.01	1.19	0.813
PP07.30	29.40	0.021	1.64	0.88	211.71	8.78	---

08.00	29.40	0.031	1.59	0.89	357.98	8.22	---
08.30	29.40	0.022	1.14	0.91	283.93	4.15	---
09.00	31.22	0.024	1.58	0.90	282.12	3.41	---
09.30	31.86	0.023	1.35	0.89	294.82	17.93	---
10.00	33.78	0.032	1.31	0.92	270.13	2.55	---
10.30	32.90	0.024	1.22	0.91	311.85	21.96	---
11.00	34.02	0.020	1.07	0.88	227.10	28.13	---
11.30	34.51	0.021	1.39	0.92	227.24	21.41	---
12.00	34.26	0.021	1.53	0.87	306.10	20.44	---
12.30	34.83	0.008	1.47	---	230.48	1.00	---
13.00	34.59	0.007	1.30	---	283.61	10.30	---
13.30	34.59	0.009	1.15	0.86	349.25	8.46	---
14.00	35.39	0.028	1.20	---	317.28	13.87	---
14.30	35.72	0.006	1.25	---	305.29	10.08	---
15.00	36.28	0.010	1.23	0.86	232.78	20.66	---
15.30	36.37	0.017	1.22	0.78	220.12	8.27	---
16.00	35.47	0.002	1.89	---	213.32	6.67	---
16.30	36.28	0.025	1.69	---	210.74	10.37	---
17.00	36.37	0.013	1.04	0.87	188.79	0.60	---
17.30	36.37	0.005	1.86	---	310.62	4.72	---
18.00	35.72	0.008	2.14	0.79	248.91	4.45	---
18.30	35.80	0.009	1.15	0.82	196.76	3.22	---
19.00	34.75	0.020	1.26	0.80	207.15	2.72	---
19.30	33.70	0.023	1.46	---	189.82	2.49	---
20.00	32.42	0.037	1.37	---	244.09	6.37	---
20.30	33.06	0.035	1.49	---	237.86	3.28	---
21.00	32.98	0.035	1.66	0.83	256.24	0.90	---
21.30	33.46	0.023	1.35	---	262.78	2.08	---
22.00	33.46	0.026	1.33	---	271.20	10.35	---
22.30	34.51	0.017	1.15	0.88	193.64	1.82	---
23.00	34.02	0.020	1.55	---	188.54	3.43	---
23.30	34.34	0.018	1.36	---	181.30	1.82	---
00.00	35.07	0.013	1.25	0.87	198.00	6.97	---
00.30	35.15	0.014	1.51	---	178.34	9.08	---
01.00	35.64	0.019	1.01	---	171.38	2.69	---
01.30	36.37	0.020	1.39	0.80	244.49	13.29	---
02.00	36.37	0.009	1.39	---	212.32	0.81	---
02.30	36.37	0.014	1.67	---	186.76	17.06	---
03.00	36.28	0.025	1.92	0.76	188.07	15.89	---
03.30	36.53	0.024	1.40	---	162.85	1.62	---
04.00	35.96	0.013	1.12	---	168.01	1.81	---
04.30	36.53	0.019	1.01	0.84	181.12	8.36	---
05.00	35.96	0.028	1.37	0.87	189.79	7.50	---
05.30	35.23	0.026	1.25	0.88	186.86	9.29	---
06.00	35.39	0.011	1.28	0.84	188.19	2.68	---
06.30	35.31	0.025	1.41	---	196.74	10.00	---
07.00	34.51	0.021	1.36	---	265.07	7.17	---

Appendix F: EEMF-PARAFAC 3-Component Model for Kinvara Bay, n = 333

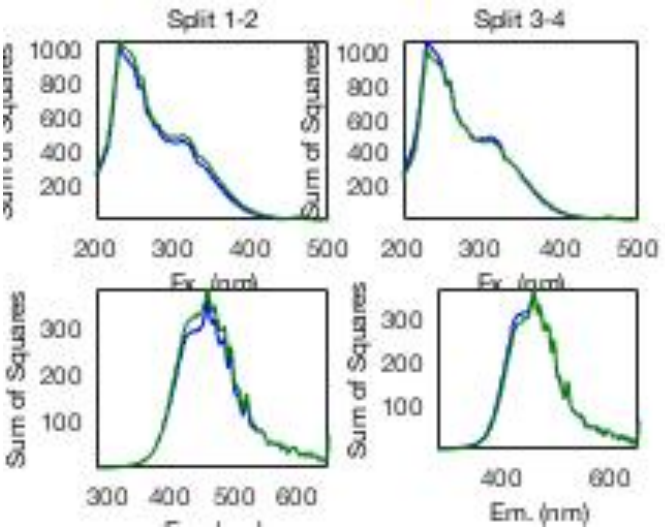

Figure F1: Split half validation of 3-component model shows that the sum of squares of the excitation and emission wavelengths split equally and therefore, the 3-componet model is validated.

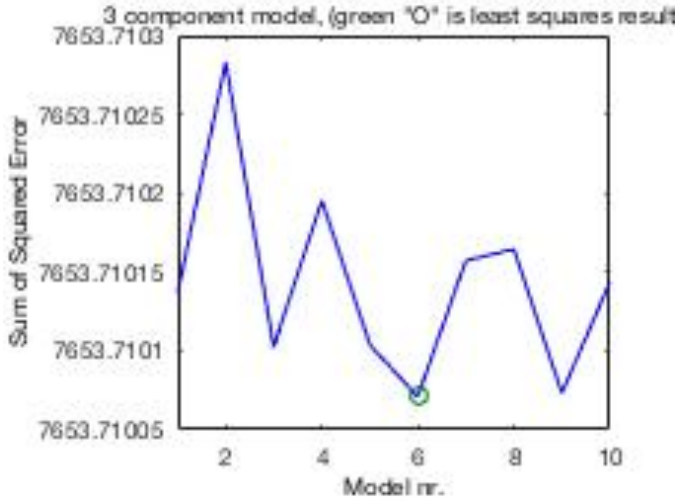

Figure F2: Least squares result of 10 Random Initialisation of 3-component model. Green 'O' represents the least square result. Thus, it is a true minima

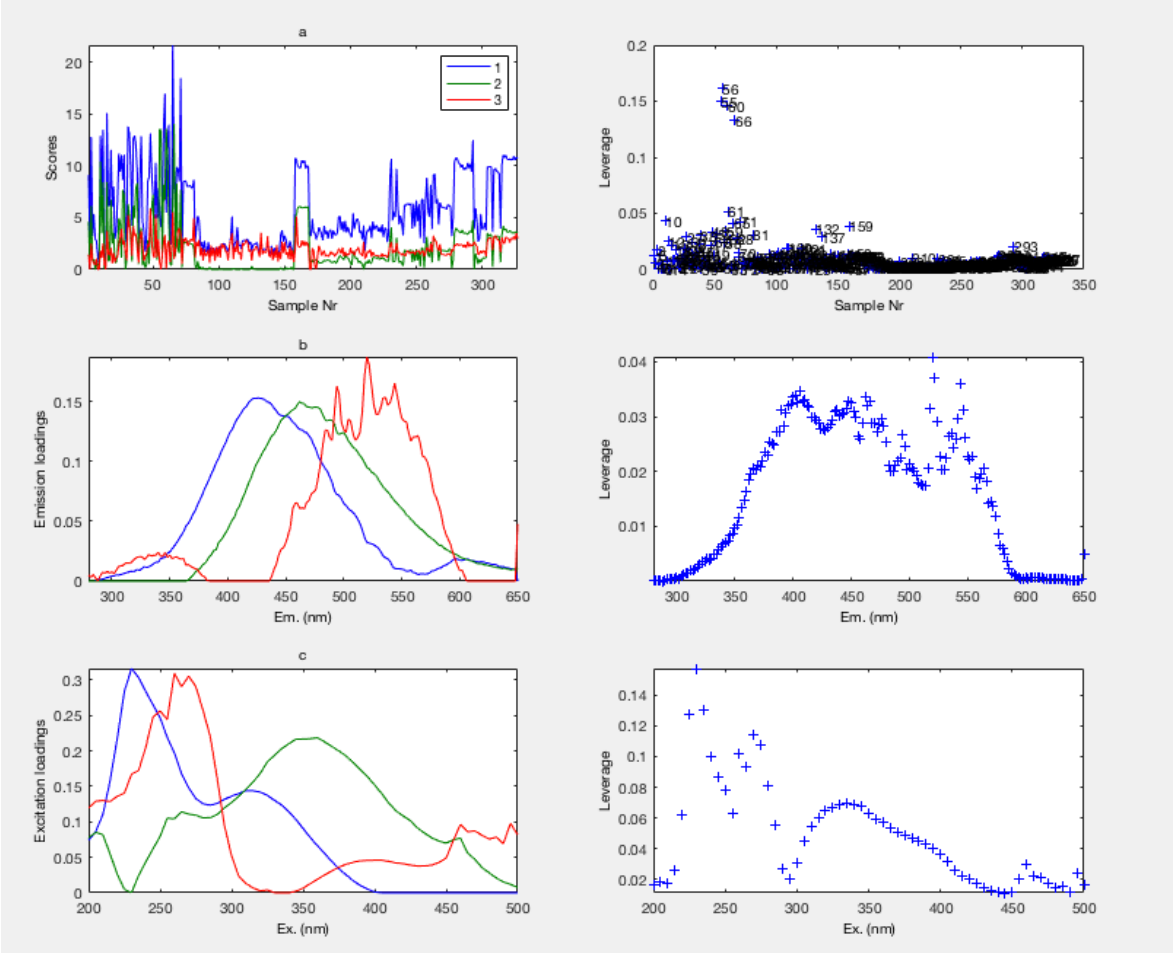

Figure F3: Scores, Excitation and Emission Leverage and Loadings of 3-component model in Kinvara Bay. EEMs with high leverage were examined and deemed representative of the 3-component model.

Appendix G: EEMF-PARAFAC 5-Component Model for Kinvara Bay Sediment Incubation Experiment, n = 338

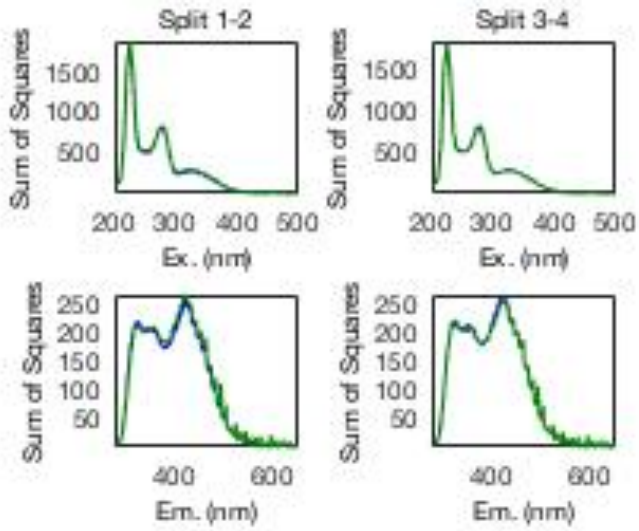

Figure G1: Split half validation of 5-component model shows that the sum of squares of the excitation and emission wavelengths split equally and therefore, the 5-componet model is validated.

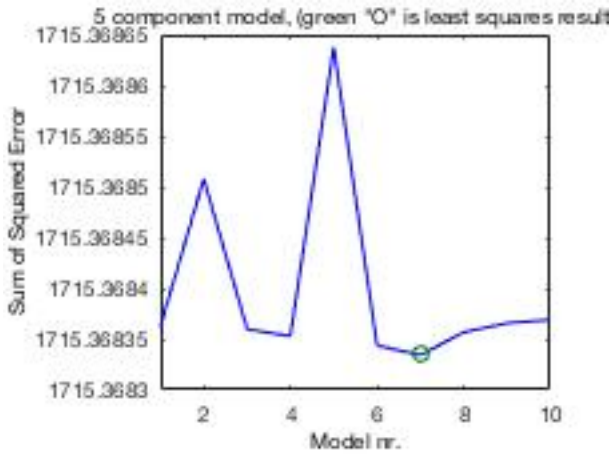

Figure G2: Least squares result of 10 Random Initialisation of the 5-component model. Green 'O' represents the least square result. Thus, it is a true minima

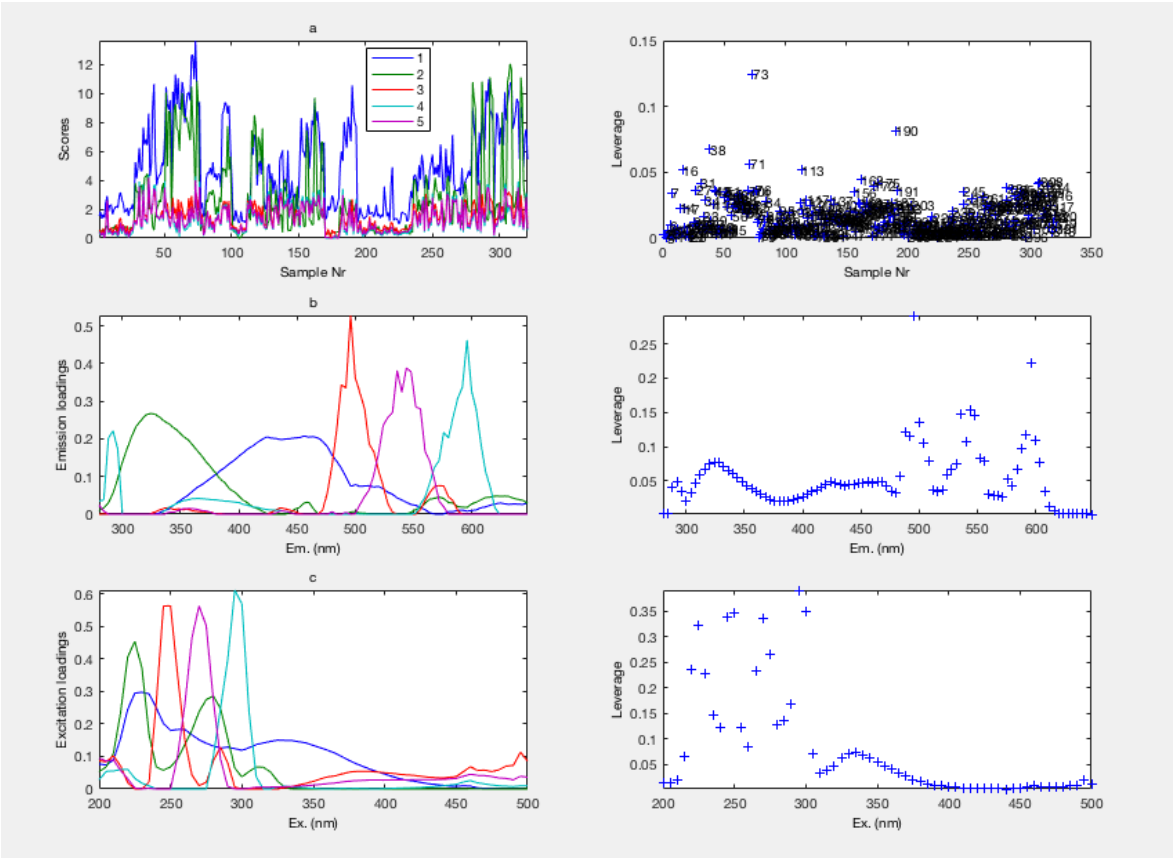

Figure G3: Scores, Excitation and Emission Leverage and Loadings of 5-component model in Kinvara Bay. EEMs with high leverage were examined and deemed representative of the 5-component model.

Appendix H: Whole Core Sediment Incubation DOC fluxes

C = Control, CMP = Addition of microplastics, MA = Addition of Macroalgae A (*Fucus vesiculosus*), MAMP = Addition of Macroalgae A and microplastics, MB = Addition of Macroalgae B (*Enteromorpha intestinalis*), MBMP = Addition of Macroalgae B and microplastics

Sample Name	DOC ($\mu mol\ L^{-1}$)	Standard Deviation (n=3) ($\mu mol\ L^{-1}$)	CDOM (a350)
C1 13 1600	241.64	1.98	0.007
C1 13 1800	247.15	0.52	0.009
C1 13 2000	237.80	1.98	0.009
C2 13 2000	258.45	6.22	0.009
C1 13 2200	228.44	0.62	0.007
C2 13 2200	233.63	6.00	0.012
C3 13 2200	210.99	0.85	0.013
C3 14 0800	221.79	0.17	0.008
C2 14 0800	253.33	6.52	0.007
C1 14 0800	262.68	3.58	0.007
C3 14 1400	196.06	1.08	0.005
C2 14 1400	217.10	2.64	0.006
C1 14 1400	195.79	2.50	0.006
C1 14 2200	229.20	0.28	0.005
C3 14 2200	218.67	3.73	0.008
C1 14 0000	224.20	3.42	0.005
C2 14 0000	214.48	0.09	0.012
C3 14 0000	188.31	1.87	0.012
C2 15 0600	236.46	0.58	0.009
C1 15 0600	191.77	2.31	0.006
C2 15 2200	188.38	0.80	0.009
C1 15 2200	195.20	1.47	0.005
C3 16 0600	209.54	1.65	0.013
C2 16 0600	235.55	14.59	0.009
C1 16 0600	191.96	2.05	0.008
C2 16 2200	220.93	2.36	0.018
C1 16 2200	217.15	1.56	0.007
C3 16 2200	213.10	0.27	0.001
C2 17 0600	212.47	3.91	0.013
C3 17 0600	220.42	1.82	0.009
C1 17 0600	173.66	35.48	0.015
C2MP 13 1600	195.73	1.37	0.008
C2MP 13 1800	257.58	10.70	0.01
C2MP 13 2000	188.91	1.73	0.006
C3MP 13 2000	197.94	2.40	0.011
C3MP 13 2200	193.66	0.71	0.005
C2MP 13 2200	204.20	1.91	0.008
C1 MP 13 2200	269.99	3.42	0.019
C1MP 14 0200	305.62	2.03	0.009
C1MP 14 0400	259.56	10.15	0.005
C3MP 14 0600	248.33	2.12	0.012
C2MP 14 0800	237.73	3.54	0.010
C3MP 14 0800	217.05	0.48	0.007
C1MP 14 1000	369.30	0.86	0.012
C2MP 14 1000	252.66	4.62	0.007
C2MP 14 1200	248.65	4.48	0.007

C3MP 14 1200	210.43	0.38	0.006
C1MP 14 1400	205.53	1.08	0.005
C3MP 14 1400	240.58	0.85	0.012
C2MP 14 1400	257.47	2.64	0.007
C2MP 14 2200	227.60	1.82	0.013
C3MP 14 2200	237.60	0.93	0.008
C1MP 14 2200	237.71	1.79	0.007
C1MP 14 0000	238.70	0.53	0.024
C3MP 14 0000	206.30	0.62	0.010
C2MP 14 0000	212.18	0.04	0.009
C2MP 15 0600	261.25	1.02	0.010
C3MP 15 0600	185.20	1.91	0.009
C3 MP 15 2200	212.84	1.33	0.011
C2MP 15 2200	290.02	1.16	0.012
C3MP 16 0600	204.16	1.42	0.012
C2MP 16 0600	298.61	2.27	0.019
C1MP 16 0600	212.66	4.27	0.025
C1MP 16 2200	243.16	3.02	0.023
C2MP 16 2200	295.21	1.82	0.028
C3MP 16 2200	214.20	4.05	0.028
C1MP 17 0600	237.31	1.87	0.018
MA3 13 1600	3519.26	16.97	0.043
MA3 13 1800	3611.13	67.50	0.050
MA3 13 2000	3687.28	2.19	0.059
MA2 14 0200	3989.23	30.09	0.066
MA2 14 0400	4307.01	29.26	0.063
MA1 14 0800	2594.19	45.18	0.038
MA3 14 0800	2273.02	35.73	0.044
MA2 14 1000	2929.03	33.49	0.031
MA3 14 1200	4598.64	31.26	0.044
MA3 14 1200	318.43	64.87	0.028
MA3 14 1400	1278.56	54.89	0.022
MA2 14 1400	2157.83	10.53	0.031
MA1 14 1400	1695.25	15.33	0.043
MA1 14 2200	2290.33	44.64	0.029
MA2 14 2200	2580.46	64.86	0.021
MA1MP 14 1400	2934.81	25.93	0.023
MA3MP 14 0200	3906.93	35.65	0.052
MA3MP 14 0400	3583.11	107.40	0.063
MA2MP 14 0600	2932.45	38.38	0.054
MA1MP 14 0600	3740.15	18.71	0.058
MA1MP 14 0800	3444.64	8.11	0.042
MA2MP 14 1200	2569.12	38.46	0.032
MA1MP 14 1200	3226.49	69.02	0.031
MA3MP 14 1200	2733.16	79.80	0.042
MA3MP 14 1400	2641.42	10.94	0.028
MA2MP 14 1400	2301.34	53.18	0.023
MA2MP 14 2200	772.17	13.77	0.031
MA1MP 14 2200	917.12	10.35	0.042
MA3MP 14 2200	1438.47	32.94	0.039
MA1MP 15 0600	1468.51	29.26	0.035
MA2MP 15 0600	916.03	1.37	0.050
MA1MP 15 2200	1605.44	49.37	0.045

MB1 13 2000	1724.46	23.60	0.061
MB3 14 0800	905.00	9.01	0.051
MB2 14 0800	830.85	9.81	0.057
MB1 14 0800	880.85	2.64	0.077
MB2 14 1200	676.47	47.74	0.026
MB1 14 1200	637.56	7.35	0.024
MB3 14 1200	685.14	4.12	0.024
MB1 14 1400	646.88	7.44	0.032
MB2 14 1400	656.71	7.53	0.036
MB3 14 1400	647.00	7.95	0.026
MB3 14 2200	667.00	3.05	0.037
MB1 14 2200	863.83	32.59	0.064
MB2 14 2200	806.02	8.62	0.077
MB1MP 13 1600	1045.33	55.46	0.049
MB2MP 13 1600	1045.26	41.80	0.056
MB3MP 13 1600	901.57	72.98	0.078
MB1MP 13 1800	1966.11	29.17	0.053
MB3MP 13 1800	1975.67	31.83	0.063
MB2MP 13 2000	1082.29	3.94	0.034
MB3MP 14 0600	1165.56	39.04	0.062
MB2MP 14 0600	1470.46	3.88	0.052
MB1MP 14 0600	1408.54	7.26	0.044
MB1MP 14 0800	1053.36	28.26	0.060
MB2MP 14 0800	1159.37	4.73	0.055
MB3MP 14 0800	936.29	7.14	0.056
MB3MP 14 1200	1061.62	45.18	0.020
MB2MP 14 1200	1030.88	40.80	0.020
MB1MP 14 1200	1113.19	12.58	0.028
MB3MP 14 1400	719.86	18.43	0.032
MB2MP 14 1400	889.80	12.54	0.033
MB1MP 14 1400	878.73	19.26	0.021
MB3MP 14 2200	569.18	3.61	0.034
MB3MP 14 2200	1398.65	35.69	0.031
MB2MP 14 2200	731.56	92.20	0.026
MB1MP 14 2200	774.30	89.52	0.034
MB3MP 14 0000	1135.83	51.44	0.049
MB2MP 15 0600	581.95	46.20	0.033
MB1MP 15 0600	537.19	5.65	0.029
MB3MP 15 0600	471.26	11.20	0.040
MB2MP 15 2200	522.24	4.40	0.044
MB3MP 15 2200	499.62	1.88	0.042
MB1MP 15 2200	609.86	17.46	0.047
MB1MP 16 0600	722.27	106.41	0.028
MB1MP 16 2200	629.75	2.81	0.041
MB3MP 17 0600	888.43	71.96	0.030
MB1MP 17 0600	760.27	2.08	0.046
MB1MP 17 2200	671.20	21.28	0.055

Appendix I: Sediment Incubation Setup

Figure I1: Experimental cores (Inner diameter = 6.4 cm, height = approx. 50 cm). Aeration was achieved with a pump and air stone. The funnel was to prevent evaporation. Cores were placed by a large window to simulate real conditions.

Appendix J: FT-ICR-MS Spectrum of SGD

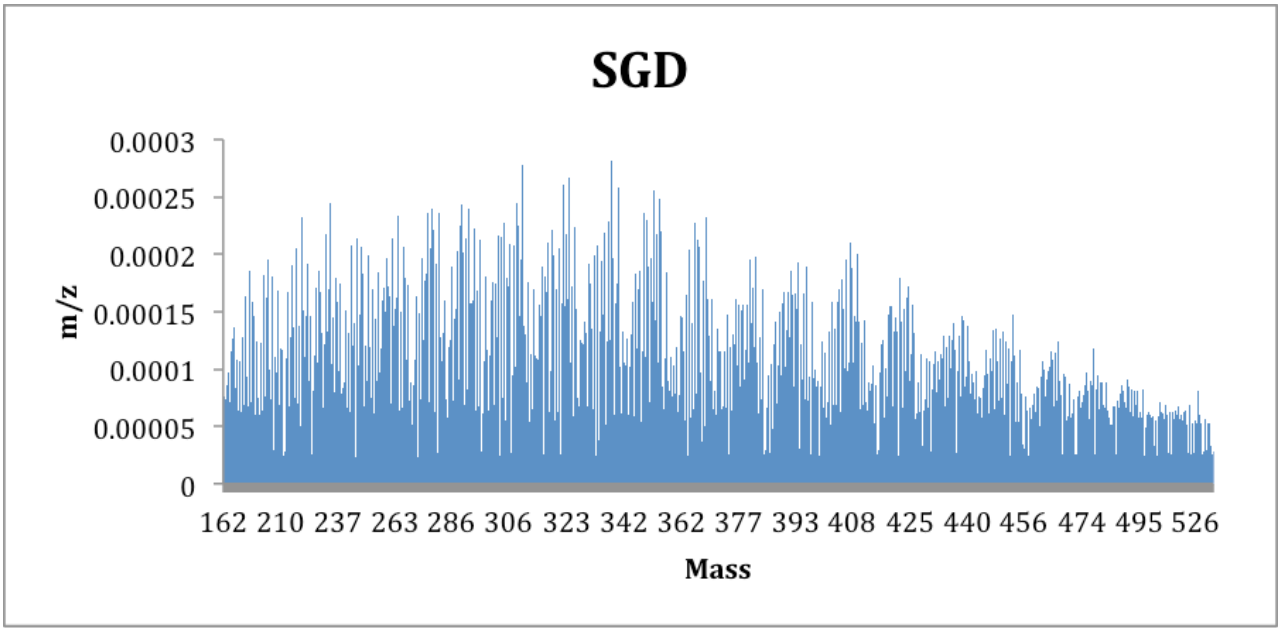

Figure J1: FT-ICR-MS Spectrum of SGD collected at Kinvara Springs in September 2014, n = 2. m/z is the mass to charge ratio